Abordaje multidimensional de la infección por el virus de la hepatitis E (HEV): ecología viral, caracterización, análisis de la respuesta celular *in vitro* y estudio de resistencia a la ribavirina

MSc. Florencia Cancela D'Angelo

Tesis de Doctorado en Ciencias Biológicas

Programa de Desarrollo de las Ciencias Básicas (PEDECIBA)

Área Biología

Orientación Biología Molecular y Celular

Sección Virología, Facultad de Ciencias, Universidad de la República

Laboratorio de Ecología Viral y Virus Zoonóticos, Departamento de Bacteriología y Virología, Instituto de Higiene, Facultad de Medicina, Universidad de la República

Orientador:

Dr. Santiago Mirazo

Co-orientador:

Dr. Juan Arbiza

Montevideo, Uruguay

2023

Cancela D'Angelo, Florencia

Abordaje multidimensional de la infección por el virus de la hepatitis E (HEV): ecología viral, caracterización, análisis de la respuesta celular *in vitro* y estudio de resistencia a la ribavirina / Florencia Cancela. –

Montevideo: Universidad de la República, Facultad de Ciencias, Instituto de Higiene, 2023.

Director:

Santiago Mirazo

Codirector:

Juan Arbiza

Tesis de Doctorado – Universidad de la República, Programa de Desarrollo de las Ciencias Básicas, 2023.

Referencias bibliográficas: p. 79.

1. Hepatitis E, 2. Hospederos, 3. Caracterización genética, 4. Estudios *in silico*, 5. Resistencia a ribavirina.

TRIBUNAL DE DEFENSA DE TESIS

Dra. Adriana Delfraro

Dr. Gonzalo Moratorio

Dra. María Belén Pisano

COMISIÓN DE ADMISIÓN Y SEGUIMIENTO (CAS)

Dr. Gonzalo Moratorio

Dr. Andrés Iriarte

Dr. Otto Pritsch†

AGRADECIMIENTOS

Muy especialmente a Santiago por su excelente disposición, invaluables enseñanzas, escuchando y aconsejándome, por sus palabras de aliento y, sobre todo, por siempre confiar en mí e impulsarme y apoyarme a seguir mis ideas!

A Juan por haberme abierto las puertas al mundo de la Virología y permitirme formarme en un área que me terminó apasionando.

A la Comisión de Admisión y Seguimiento (CAS): Dres. Gonzalo Moratorio y Andrés Iriarte.

A los miembros del tribunal, Dres. Adriana Delfraro, Gonzalo Moratorio y María Belén Pisano por aceptar evaluar esta Tesis.

A la Comisión Académica de Posgrado (CAP), UdelaR por la Beca de Doctorado otorgada.

A la Comisión Sectorial de Investigación Científica (CSIC I+D) por la financiación de este proyecto.

A todos los integrantes y compañeros de Viro de Facultad de Ciencias que me acompañaron todos estos años, compartiendo experiencias y siempre dispuestos a ayudar.

A mis nuevos compañeros del Dpto. de Bacteriología y Virología del Instituto de Higiene.

A la Dra. Yanina Panzera por haberme permitido realizar una pasantía en la Plataforma Genómica de Fcien y formarme en el mundo del NGS y por su gran apoyo en los análisis bioinformáticos.

A Santi y Caro de Colombia por haberme introducido en el mundo in silico, compartiendo todos sus conocimientos con muy buena onda, sin quienes esos estudios no habrían sido posibles.

A los Dres. Andrés Cabrera y Rodrigo Puentes por brindarnos amablemente las muestras de los animales de cautiverio.

A Andrés Iriarte por su generosas colaboración en la secuenciación de los genomas completos de HEV.

A la Dra. Alexandra Cravino por su contribución con los resultados de fototrampeo en fauna silvestre.

A los cazadores Pablo González y Federico Bentancor (Dosel S.A.) y a los dueños y capataces de estancias por el aporte de las muestras.

Al Programa de Trasplante Hepático del Hospital Militar por permitirnos tener acceso a muestras clínicas a través del convenio de colaboración establecido.

Al Dr. Reimar Johne del German Federal Institute for Risk Assessment Berlín-Alemania, por cedernos amablemente la línea celular A549/D3 y la cepa de HEV.

Al Dr. Donald B. Smith por asesorarnos en la clasificación del nuevo subtipo de HEV3.

A Karina Cabrera de la AUPC por brindarnos las muestras de cerdos utilizadas en esta Tesis.

A mis amigos por estar siempre presentes a lo largo de este proceso.

A mi familia, no alcanzan las palabras para agradecer su inmenso amor y comprensión, su apoyo incondicional, por siempre creer en mí y acompañarme a lo largo de este camino, y por enseñarme que con determinación y motivación el cielo es el límite…

"La ciencia y la vida cotidiana no pueden ni deben estar separadas"

- Rosalind Franklin -

INDICE

LISTA DE ABREVIATURAS

°C	Grados Celsius
aa	Aminoácidos
ACLF	Falla hepatica *Acute-on-chronic*
ALT	Alanina aminotransferasa
ARN ss+	ARN simple hebra polaridad positiva
ARN	Ácido ribonucleico
CARDs	Dominio de activación de caspasas
CC50%	concentración citotóxica 50%
CRE	Elementos reactivos en *cis*
CO_2	Dióxido de carbono
DAPI	4',6-Diamidino-2'-fenilindol
dPCR	*Digital* PCR
Dpi	Días post-infección
E	Eficiencia
EID	Enfermedades infecciosas emergentes
eHEV	Partícula "cuasi-envuelta" del virus de hepatitis E
ESCRT	Complejo endosomal requerido para transporte
FFU	Unidades formadoras de foco
GTP	Guanosina trifosfato
HEL	Helicasa
HEV	Virus de hepatitis E
HEVc	Hepatitis crónica
HEVa	Hepatitis aguda
HEV-SOT	Hepatitis E en transplantados de órganos sólidos
HEV1-HEV8	Genotipos 1 al 8 de HEV
HIV-1	Virus de la inmunodeficiencia humana tipo 1
HVR	Hipervariable
HSPGs	Proteoglicanos de heparán sulfato
IC50	Concentración inhibitoria 50
ICTV	Comité Internacional de Taxonomía Viral
IFI	Inmunofluorescencia indirecta
ISGs	Genes estimulados por interferón
MAVS	proteína de señalización antiviral mitocondrial
MEM	Medio mínimo esencial
MDS	Simulación de dinámica molecular
min	Minutos

MT	Metiltransferasa
MTT	3-(4,5-dimetiltiazol-2-il)-2,5-difenil tetrazolio
NAT	Amplificación de ácidos nucleicos
NGS	Secuenciación masiva
nm	Nanómetros
nt	Nucleótidos
OMS	Organización Mundial de la Salud
PAMPs	Reconocimiento de patrones moleculares asociados a patógenos
PCP	Cisteín-proteasa tipo papaína
PRO	Región rica en prolina
PRR	Receptores de reconocimiento de patrones
rNTPs	Ribonucleótidos trifosfato
R^2	Coeficiente de determinación
RBV	Ribavirina
RBVD	Ribavirina difosfato
RBVM	Ribavirina monofosfato
RBVT	Ribavirina trifosfato
RdRp	ARN polimerasa ARN-dependiente
RLRs	Receptores de tipo gen inducible por ácido retinoico I
RPM	Revoluciones por minuto
RT	Retrotranscripción
SBDD	Diseño de drogas basado en estructura
seg	Segundos
SFB	Suero fetal bovino
SOT	Trasplante de órganos sólidos
TH	Trasplante de hígado
TLRs	Receptores tipo-*Toll*
VP13	Proteína de ORF3
VLP	*Virus-like particle*
X	Dominio X
Y	Dominio Y
µg	Microgramo
µl	Microlitro
µM	Micromolar
ml	Mililitro

RESUMEN

La infección con el virus de la hepatitis E (HEV) es una de las principales causas de hepatitis aguda a nivel mundial. La presentación clínica de hepatitis E se manifiesta principalmente como una enfermedad aguda y autolimitada, aunque se han reportado frecuentemente casos crónicos con manifestaciones extrahepáticas en pacientes trasplantados e individuos inmunocomprometidos, en los cuales el tratamiento con ribavirina (RBV) es la única terapia disponible.

HEV pertenece a la familia *Hepeviridae*, dentro de la cual encontramos la especie *Paslahepevirus balayani* que se divide en 8 genotipos (HEV1-HEV8) y en subtipos, y la especie *Paslahepevirus alci* que consiste en cepas de HEV provenientes principalmente de alces de Suecia (*Alces alces*), denominadas HEV-*moose*. HEV presenta un genoma ARN simple hebra de polaridad positiva de aproximadamente 7,2 Kb conteniendo tres marcos abiertos de lectura (ORF1-3) parcialmente solapados.

HEV3 se transmite mayoritariamente por vía zoonótica en países industrializados a través del contacto directo con animales infectados o por el consumo de carne contaminada, particularmente por sus principales reservorios, el cerdo doméstico y el jabalí, aunque presenta un rango de hospedero en constante expansión, dónde se incluyen ciervos, ratas y conejos, entre otros.

En 2011 se reportaron en Uruguay los primeros casos de infección aguda por HEV3 en humanos y los estudios de caracterización genética mostraron que no era posible asignarlos a ningún subtipo conocido. Además, recientemente por medio de un estudio serológico en donantes de sangre, se detectó una tasa de seroprevalencia de HEV de un 10% (10 veces mayor que el último análisis hace 20 años) y se reportó el primer caso de infección crónica, siendo uno de los pocos países de la región, permitiendo, por lo tanto, avanzar en el estudio de su epidemiología molecular y específicamente en la caracterización y clasificación de las cepas de HEV3, para lo cual se requiere obtener genomas completos. Por otro lado, se identificó también la presencia de anticuerpos anti-HEV en jabalíes, ARN de HEV3 en cerdos y se reportaron las primeras evidencias de que los pecaríes de cuello blanco (*Pecari tajacu*) son susceptibles a la infección por HEV3.

En este contexto, se estima que HEV circula en Uruguay de forma principalmente asintomática y a través de mecanismos de transmisión no identificados, planteando la necesidad de estudiar más en profundidad este punto y llevando a plantearse qué otras especies animales podrían estar contribuyendo a la diseminación viral.

A su vez, se desconocen los mecanismos moleculares y virológicos que llevan a la cronificación de hepatitis E, por lo que resulta importante avanzar en los estudios de su biología viral y resistencia antiviral mediante aproximaciones *in vitro* e *in silico* (ya que solamente hay estructuras cristalográficas disponibles para ORF2), especialmente para las variantes que circulan en Uruguay.

Debido a los limitados conocimientos sobre la circulación de HEV en Uruguay y Sudamérica, en esta Tesis se llevó a cabo un amplio relevamiento serológico y molecular en distintas especies animales para comprender con un enfoque de Una Salud, la situación epidemiológica de HEV en el país.

Los resultados obtenidos demuestran, por primera vez, la presencia de anticuerpos anti-HEV en ciervos Axis (*Axis axis*) silvestres con una tasa del 11,1% (6/54) y la co-circulación de cepas zoonóticas HEV3 y variantes *moose* HEV-*like* en esta especie. Asimismo, se detectaron anticuerpos anti-HEV en 10,5% (2/19) de venados, 20% (2/10) de pecaríes y 0,73% (1/137) de ovinos. Si bien más estudios son necesarios, estos resultados sugieren que esta especie de ciervos podría agregarse a lista de reservorios de HEV.

A su vez, se obtuvieron los primeros genomas completos de HEV3 para el país y la región, correspondientes a un caso de infección crónica y a un suino (HEV_C1_Uy y HEV-8_uy), lo que permitió implementar estudios de clasificación más robustos.

Los análisis filogenéticos y de p-distancia revelaron que todas las secuencias de HEV3 detectadas en el país en humanos, cerdos y ciervos Axis forman un *cluster* monofilético, con una importante divergencia con el resto de los subtipos de HEV3 conocidos. Por lo tanto, proponemos clasificar al *cluster* de secuencias identificadas en el país como subtipo 3o.

Estos datos ponen de manifiesto la activa circulación de HEV entre animales silvestres y la población humana en Uruguay.

Por otro lado, a partir de la cepa HEV_C1_Uy se generó un modelo *in silico* 3D de la proteína ARN polimerasa (RdRp) y se identificó el posible sitio de unión de RBV a esta proteína, brindando información sobre la interacción entre la RdRp de subtipo 3o y la droga.

Además, fue posible aislar en células A549/D3 la cepa HEV_C1_Uy. Estudios *in vitro* realizados a partir de este aislamiento mostraron ausencia de resistencia a RBV (con un aumento en el valor de IC50) y una expresión diferencial de proteínas de apoptosis, citoquinas y de la vía NFκB, con respecto a una cepa europea del subtipo 3c de infección persistente (HEV_47832c) y a células sin infectar.

En conclusión, esta Tesis contribuye a profundizar aspectos poco explorados de la epidemiología molecular en Uruguay, así como en la respuesta celular ante la infección por HEV, derivando en nuevas posibles líneas de investigación.

Estos resultados podrían brindar herramientas para el diseño de potenciales políticas sanitarias para la prevención de la transmisión e infección por HEV.

Palabras claves: Hepatitis E; Hospederos; Caracterización genética; Estudios *in silico*; Resistencia a ribavirina

1. INTRODUCCIÓN

1.1 Virus de la Hepatitis E (HEV)

La infección por el virus de la hepatitis E (HEV) es actualmente reconocida como una importante causa de hepatitis aguda viral globalmente. HEV es endémico en países en desarrollo, y desde hace unos años ha cobrado gran relevancia en países desarrollados no-endémicos. A nivel mundial, se han reportado unos 20 millones de infecciones y 70.000 decesos anuales por HEV [1, 2].

La primera epidemia por hepatitis E documentada ocurrió en India en 1955 proveniente de agua contaminada [3], el cual fue atribuido inicialmente a hepatitis A y no fue hasta la década de los 80 que se confirmó la presencia de un nuevo agente viral, con la obtención de su genoma completo años después [3, 4].

1.2. Virología molecular y estructura

HEV es un virus pequeño de simetría icosaédrica que se encuentra en el torrente sanguíneo y cultivo celular como una partícula asociada a membrana cubierta en lípidos denominada "cuasi-envuelta" (eHEV) con un diámetro de ~40 nm, mientras que en materia fecal y bilis pierde su envoltura detectándose como una partícula desnuda de 32-34 nm (Fig. 1) [5].

Hasta el momento, solo se ha descrito la estructura cristalográfica para la *virus-like particle* de HEV (VLP) T=1 (PDB ID: 3HAG [6]), existiendo solamente modelos que representan el ensamblaje de la cápside nativa T=3 [6].

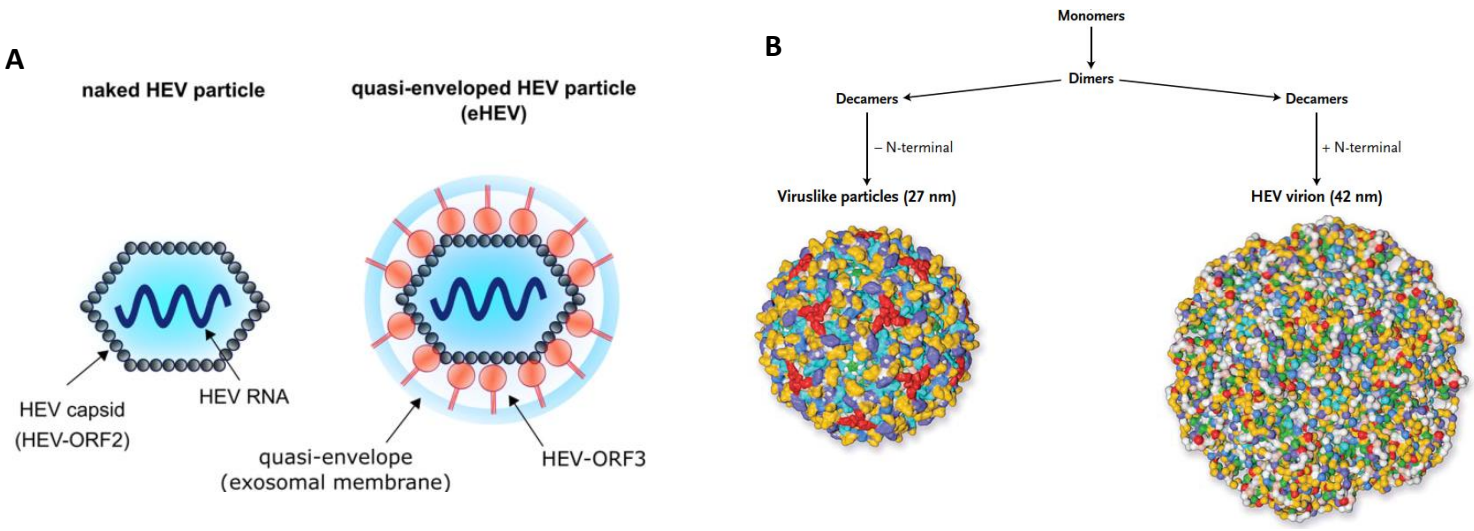

Fig 1. Morfología de la partícula de HEV. A. Representación esquemática de las formas desnudas y "cuasi-envuelta" (eHEV) de HEV. La proteína de ORF3 (VP13) se une a la superficie de eHEV interaccionando con componentes de la maquinaria celular ESCRT para facilitar la liberación de las partículas. **B**. Modelo de ensamblaje de la partícula de HEV, comenzando con los monómeros de cápside (ORF2) que se auto-ensamblan en dímeros y subsecuentemente en decámeros. Los decámeros carentes de la región N-terminal de ORF2 se ensamblan en VLPs T=1. Los decámeros completos encapsidan el ARN viral para formar los viriones nativos T=3 [146, 147]. Extraído y adaptado de [147, 148].

1.2.1. Organización genómica y proteínas virales

En el marco de este punto se publicó una revisión actualizada con el propósito de profundizar la información sobre los principales aspectos estructurales de las proteínas de HEV y sus funciones, la cual se puede encontrar completa al final de la sección *Introducción*.

Brevemente, HEV pertenece al alfavirus-*like* supergrupo III de virus ARN simple hebra de polaridad positiva (ARN ss+), cuyos miembros codifican una helicasa (HEL) tipo 1, un dominio de metiltransferasa (MT) tipo 1 y un dominio de ARN polimerasa ARN-dependiente (RdRp) tipo 3 [7]. Los virus animales de este supergrupo incluyen miembros de los géneros *Alphavirus*, *Rubivirus* y de la subfamilia *Orthohepevirinae* correspondientes a las familias *Togaviridae*, *Matonaviridae* y *Hepeviridae*, respectivamente. Sin embargo, a pesar de que HEV puede circular como eHEV, no presenta glicoproteínas de superficie, difiriendo en ese aspecto de los virus envueltos animales alfa-*like* [7, 8]. Interesantemente, los alfavirus tienen

una organización genómica similar a los virus de planta pertenecientes a los géneros *Tobamovirus*, *Tobravirus*, *Hordeivirus* y *Furovirus.*

HEV presenta un genoma ARN ss+ de aproximadamente 7,2 Kb con una caperuza de metil-guanosina en el extremo 5´ y una cola poli-A en el extremo 3´, conteniendo tres marcos abiertos de lectura (ORF1-3) parcialmente solapados [9].

El ORF1 codifica para una poliproteína no-estructural de 5082 nt (1693 aa) con 8 dominios funcionales. Desde el extremo N-terminal hasta el extremo C-terminal los dominios putativos son: MT, dominio Y (Y), cisteín-proteasa tipo papaína (PCP), región hipervariable (HVR), región rica en prolina (PRO), dominio X (X), HEL y RdRp [10]. Se desconoce si esta poliproteína requiere un procesamiento posterior en dominios individuales o si es capaz de funcionar como una única unidad, ya que se han obtenido resultados contradictorios [11–14].

El dominio de RdRp es de particular interés para esta Tesis (*Capítulo 3*), por lo cual se enfatizará en la misma. Esta proteína de HEV junto con la del virus de la rubéola (*Rubivirus*) y del virus de la vena necrótica amarilla de la remolacha (*Benyviridae*) conforman un *cluster* filogenético cercano. En este supergrupo se han identificado ocho motivos conservados (I-VIII), donde en el motivo VI de la RdRp de HEV se encuentra la secuencia GDD altamente conservada, la cual cumple un rol crucial en la actividad catalítica [15].

El ORF2 de 1983 nt y 660 aa codifica para la proteína de cápside, identificándose tres dominios: S, M y P conocido como E2s, el cual representa el mínimo dominio antigénico capaz de inducir respuesta de anticuerpos neutralizantes anti-HEV [16].

El ORF3 es el ORF más pequeño del genoma de HEV, es traducido a partir de un ARN subgenómico y se solapa al ORF2 por 300 nt en un marco diferente, produciendo una fosfoproteína de 113-115 aa (VP13). Esta región de solapamiento corresponde a la región más conservada entre numerosas cepas de HEV [10]. VP13 actúa como un viroporina de canal iónico requerida para la liberación de las partículas virales y también es capaz de unirse a la superficie viral formando la partícula eHEV [17].

Hasta el momento, solamente están disponibles las estructuras cristalográficas para la HEV-VLP (PDB ID: 3HAG) y para la región E2s, región mínima antigénica dentro de la ORF2 (PDB ID: 3GGQ).

1.3. Clasificación filogenética y epidemiología

Según la clasificación actualizada del ICTV 2022, HEV pertenece a la familia *Hepeviridae* y se divide actualmente en dos subfamilias: *Orthohepevirinae* y *Parahepevirinae*. La subfamilia *Orthohepevirinae* se clasifica a su vez en cuatro géneros: *Avihepevirus* (aves)*, Chirohepevirus* (murciélagos)*, Paslahepevirus* (humanos, cerdos, jabalíes, ciervos, alces, etc) y *Rocahepevirus* (ratas, hurones, visones) (Fig. 2) [18]. Estudios de identidad entre cepas de HEV de aves, ratas y humanos revelaron un rango de valor de 45%-57% a nivel nucleotídico y de 20%-55% a nivel aminoacídico [19].

En esta Tesis nos enfocaremos particularmente en la especie *Paslahepevirus balayani* y *Paslahepevirus alci* dentro del género *Paslahepevirus.*

La especie *P. alci* consiste en cepas de HEV inicialmente descritas en alces de Suecia (*Alces alces*), denominadas HEV-*moose,* para las cuales se ha reportado una identidad nucleotídica de 37%-63% y una identidad aminoacídica de 45%-70% con respecto a las secuencias pertenecientes a las subfamilias *Orthohepevirinae* y *Parahepevirinae* [20].

Por otro lado, la especie *P. balayani*, comprende 8 genotipos (HEV1-HEV8) [21], de los cuales HEV1-4 y HEV7 infectan humanos [22], dividiéndose a su vez en subtipos [21].

Según la distribución geográfica y transmisión de los genotipos se han identificado dos perfiles epidemiológicos preponderantes correspondientes a HEV1-HEV2 y a HEV3-HEV4, que se describen a continuación.

Los genotipos HEV1 (subtipos 1a-1g) y HEV2 (subtipos 2a y 2b) son considerados antroponóticos, es decir que infectan sólo humanos y simios superiores, asociados a brotes o epidemias en regiones de menores recursos como Asia y África consideradas altamente endémicas (Fig. 3), transmitiéndose a través del consumo de agua contaminada (Tabla 1).

Los genotipos HEV3 (subtipos 3a-3n) y HEV4 (subtipos 4a-4i) tienen características epidemiológicas muy similares entre sí (Tabla 1), se transmiten por vía zoonótica con un amplio rango de hospederos y dan lugar a casos esporádicos de hepatitis aguda, así como también pueden producir cuadros de hepatitis crónica con manifestaciones extrahepáticas, siendo el HEV3 más prevalente en estos casos [23]. Sin embargo, HEV3 se encuentra distribuido mundialmente y HEV4 es predominante en Asia, detectándose en algunos países de Europa (Fig. 3) [23].

Para estos cuatro genotipos se estima un rango de seroprevalencia promedio de 1%-52% en los países industrializados y de 4%-94% en los países en desarrollo, reportándose que aproximadamente 1/8 de la población mundial (> 900 millones de individuos) ha cursado la infección por HEV en algún momento de la vida [24].

Por otro lado, los genotipos HEV5 y HEV6 solo han sido identificados en jabalíes mayoritariamente de Japón, y HEV7 y HEV8 se encuentran restringidos a camellos dromedarios y bactrianos de Medio Oriente y África. No obstante, recientemente fue detectado un caso de infección por HEV7 en un paciente con trasplante de hígado consumidor de carne y leche de camello [25].

A pesar de que existe una alta heterogeneidad y variabilidad entre las cepas de HEV, sólo existe un único serotipo [26], posiblemente debido a una gran conservación a nivel aminoacídico en la región antigénica de la cápside viral [27].

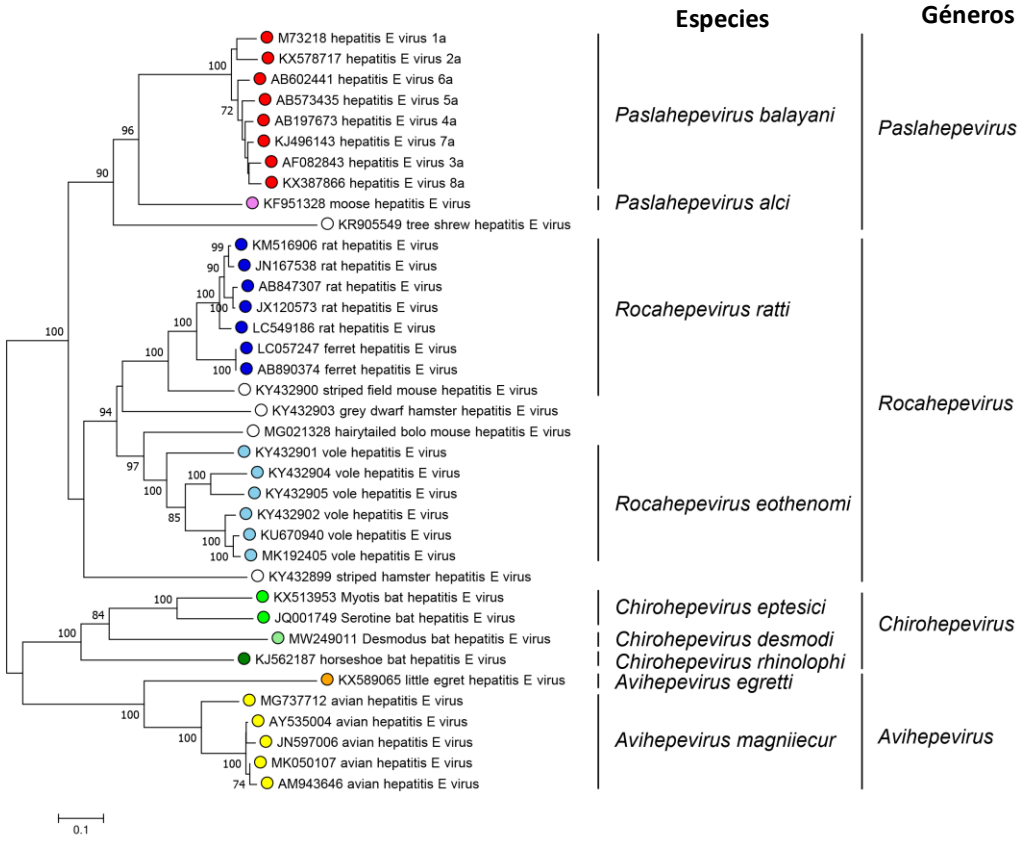

Fig.2. Árbol filogenético de la subfamilia *Orthohepevirinae* basado en la región MT de ORF1. Los círculos en las ramas están coloreados por especie. Los círculos blancos indican secuencias sin clasificar. Extraído y adaptado de ICTV Global Report *Hepeviridae* [18].

Tabla 1. Resumen de las características epidemiológicas de los genotipos HEV1-4 *P.balayani*.

Genotipo	Hospedero	Distribución genotipos	Distribución subtipos*	Transmisión principal	Presentación clínica
HEV1	Humanos, Chimpancés	Regiones de bajos recursos (Asia, Cuba, África, Uruguay)	**1a**: India, Pakistán, Reino Unido, Birmania **1b:** Pakistán, Cuba **1c:** India **1d**: Marruecos **1e**: Chad **1f:** Bangladesh, India, Reino Unido **1g**: India, Mongolia, Pakistán, Japón, Reino Unido	Fecal-oral	Brotes epidémicos (Hepatitis aguda, mayor gravedad en embarazadas)
HEV2	Humanos, Chimpancés	Regiones de bajos recursos (México, África)	**2a:** México **2b:** Nigeria	Fecal-oral	Brotes epidémicos (Hepatitis aguda)
HEV3	Humanos, cerdos, jabalíes, ciervos y otros mamíferos	Global	**3a**: Japón, Estados Unidos, Reino Unido, Alemania, Canadá, Singapur, China, México, Tailandia, Corea del Sur **3b:** Japón, China, Canadá **3c:** Países Bajos, Francia, Alemania, Suecia, Reino Unido, Tailandia, Canadá **3e**: Francia, España, Alemania, Reino Unido, Italia, Japón, Hungría **3f:** Alemania, Reino Unido, Francia, España, Suecia, Dinamarca, Tailandia, Japón, Singapur **3g:** Kirguistán **3h**: Francia, Suiza, Mongolia **3i:** Suecia, Alemania **3j**: Canadá **3k**: Japón **3l:** Francia, Italia **3m**: Francia, España **3n:** Italia	Zoonótica	Casos esporádicos (Hepatitis aguda, crónica y manifestaciones extrahepáticas) Más frecuente en hombres > 40 años
HEV4	Humanos, cerdos, jabalíes, ciervos y otros mamíferos	Asia y algunos países de Europa	**4a**: China, Mongolia, Taiwán, Corea del Sur **4b**: Taiwán, China, Camboya, Japón **4c**: Japón **4d**: China **4e**: India **4f:** Japón **4g**: China, Japón **4h**: China **4i:** China, Japón	Zoonótica	Casos esporádicos (Hepatitis aguda, crónica y manifestaciones extrahepáticas)

*Se describe la distribución geográfica de los subtipos para las cepas que presentan genoma completo disponible [28].

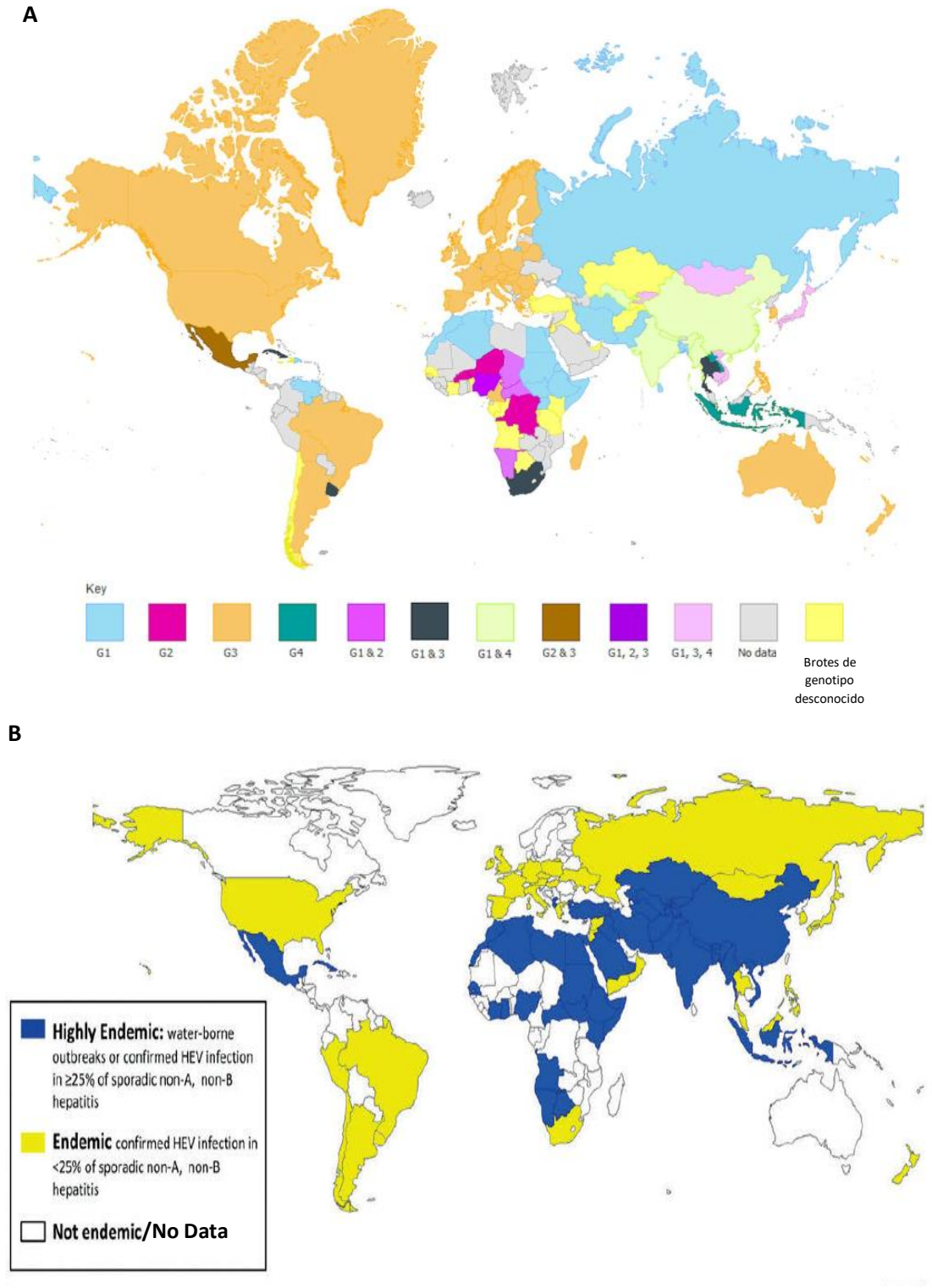

Fig.3. Distribución mundial de la infección por HEV. A. Distribución geográfica de los genotipos HEV1-HEV4. El mapa indica los genotipos de HEV identificados para cada país. Extraído y adaptado de [29]. **B.** Epidemiología de hepatitis E clasificada en regiones endémicas, altamente endémicas y no endémicas o sin datos registrados. Extraído y adaptado de [30].

1.4. Ecología viral de HEV3

Esta Tesis se centrará principalmente en el genotipo HEV3 dentro de *P. balayani,* el cual se describe más en detalle a continuación.

HEV3 se encuentra ampliamente distribuido entre cerdos domésticos (*Sus scrofa domesticus*) y jabalíes (*Sus scrofa*), considerados sus principales reservorios animales. Asimismo, este genotipo (el de mayor diversidad genética) ha sido detectado en un amplio rango de hospedadores domésticos y silvestres (Tablas 2, 3 y Fig. 4) que se encuentra en constante expansión, entre ellos ciervos, ganado, ratas y conejos, por lo que el espectro completo de especies reservorios de HEV o susceptibles a la infección permanece aún desconocido [23].

Entre los animales domésticos, se ha identificado HEV3 en varios rumiantes importantes desde el punto de vista agro-productivo como vacas, ovejas y cabras [31]. Además, se ha reportado seroprevalencia de HEV en mascotas de compañía, pero hasta el momento no ha sido posible detectar ARN viral, por lo que el genotipo no ha podido ser identificado [32].

Por otro lado, HEV ha sido detectado en numerosos miembros de la familia *Cervidae*, de la familia *Bovidae,* así como también en cetáceos [31].

En Uruguay, se reportó una tasa de prevalencia de anticuerpos de HEV en cerdos y jabalíes de 46,8% y 22,1%, respectivamente [33] y un 16,6% de ARN viral en hígados de cerdo faenados correspondiente a HEV3 (Fig. 4). Asimismo, en 2020 nuestro grupo reportó las primeras evidencias de que los pecaríes de cuello blanco (*Pecari tajacu*) son susceptibles a la infección por HEV3 presentando una seroprevalencia de 24,7% (Fig. 4) [34].

Tabla 2. Lista de animales domésticos descritos como hospederos para HEV3 y HEV4 y el rango de seroprevalencia reportado [31].

Especie animal	Nombre científico	Seroprevalencia (%)
Cerdo	*Sus scrofa domesticus*	2,9–89
Conejo	*Oryctolagus cuniculus*	36–50
Ganado	*Bos taurus*	0–51,6
Perro	*Canis lupus*	0,8-56,6
Gato	*Felis catus*	0-32,6
Burro	*Equus asinus*	12,3
Visón	*Mustela lutreola*	9
Cabra	*Capra aegagrus hircus*	0-46,7
Caballo	*Equus caballus*	18,2
Oveja	*Ovis aries*	2,1-35,2

Tabla 3. Lista de animales silvestres descritos como hospederos para HEV3 y HEV4 y el rango de seroprevalencia reportado [31].

Especie animal	Nombre científico	Seroprevalencia (%)
Jabalí	*Sus scrofa*	1–56
Ratón de cuello amarillo	*Apodemus flavicollis*	0,2
Delfín nariz de botella	*Tursiops truncatus*	16,1-32,2
Mangosta Japonesa	*Herpestes auropunctatus*	8,1-21
Liebre	*Lepus europaeus*	2,2
Mapache	*Procyon lotor*	53,8
Lince Ibérico	*Lynx pardinus*	7,4-33,6
Ciervo Rojo	*Cervus elaphus*	0-13,9
Reno de bosque	*Rangifer tarandus*	3,2-23,1
Alce	*Alces alces*	5,9-19,5
Corzo	*Capreolus capreolus*	0-6,8
Ciervo Sika	*Cervus nippon*	3,13-6,73
Ciervo Yezo	*Cervus nippon yesoensis*	34,8
Yak	*Bos grunniens*	3,3
Ciervo de cola blanca	*Odocoileus virginianus*	8,8
Ciervo mulo	*Odocoileus hemionus*	4,5

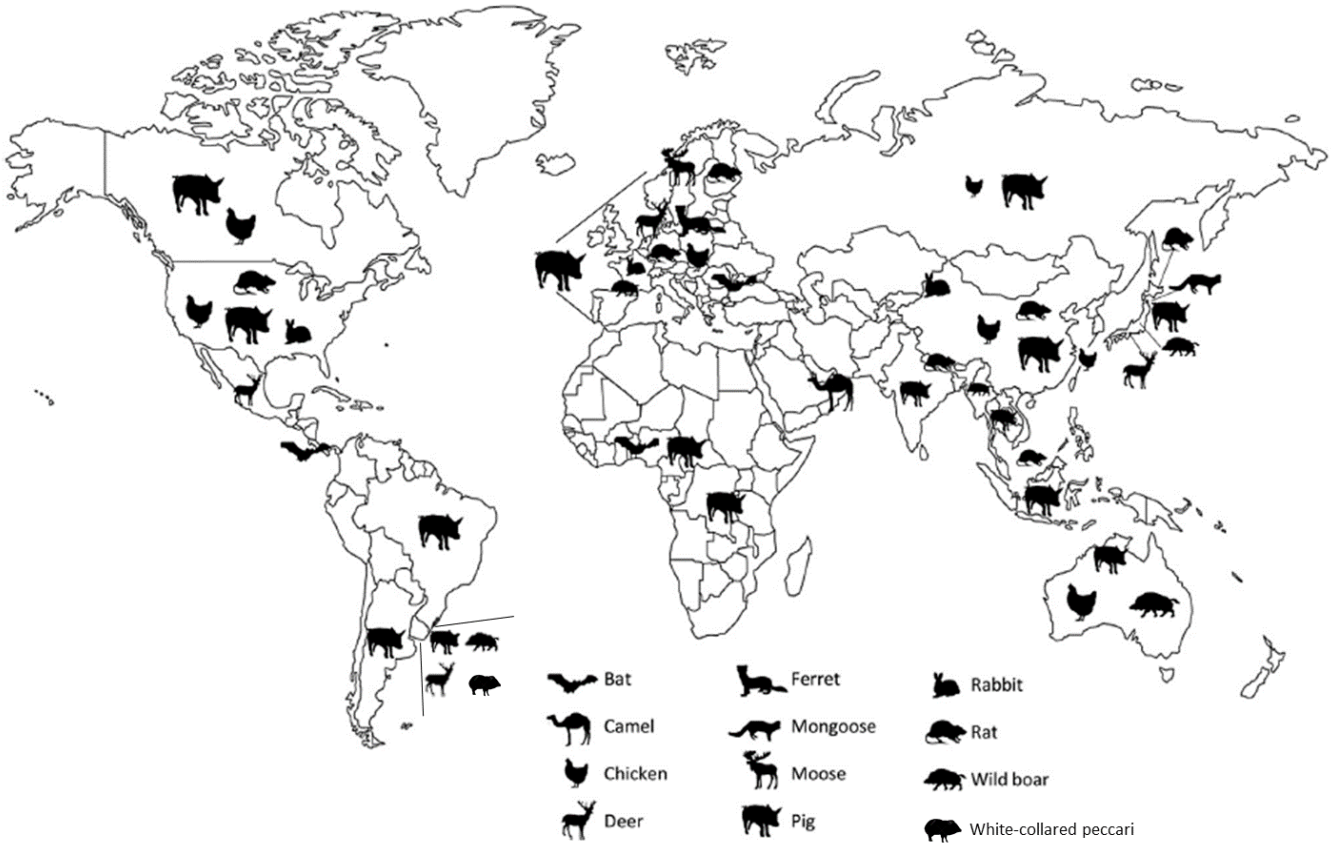

Fig. 4. Distribución geográfica de cepas HEV3, HEV4 y variantes HEV-*like* en animales terrestres. El rol de los visones, ratas y conejos en la transmisión zoonótica de HEV es aún desconocido. Extraído y adaptado de [35].

1.5. Transmisión

HEV se consideraba, hasta hace algunos años, sólo endémico en países en desarrollo de bajos recursos, no obstante, la presencia de casos autóctonos ha sido ampliamente confirmada en países económicamente desarrollados que se creían no-endémicos [29].

De hecho, reportes recientes detectaron un 21% y un 6,3% de ARN de HEV en cerdos de matadero en Reino Unido [36] y Estados Unidos [37], respectivamente.

En países en desarrollo y desarrollados, dónde HEV3-HEV4 son prevalentes, las vías de transmisión reportadas son: zoonótica (principal vía), por transfusión sanguínea y por trasplante de órganos. En dicho contexto, la transmisión zoonótica se relaciona mayormente al consumo de carne contaminada cruda o poco cocida como embutidos o chacinados proveniente de los animales reservorios o mediante el contacto directo con estas especies a partir de animales infectados [23], así como también se ha asociado a riesgo ocupacional por exposición entre veterinarios, cazadores, granjeros o trabajadores en contacto cercano con animales, ya que en estos animales reservorios la infección se presenta de forma asintomática, pasando de esta manera inadvertida [38–41].

Sin embargo, en países en desarrollo dónde HEV1-HEV2 son prevalentes, las vías de transmisión reportadas son: la ruta fecal-oral por agua contaminada (principal vía), de persona a persona, vertical y por transfusión sanguínea.

HEV es excretado en las heces, por lo tanto, las partículas virales pueden alcanzar las fuentes de agua, moluscos bivalvos y los cultivos por irrigación (Fig. 5). Como se mencionó anteriormente, la transmisión fecal-oral se ha relacionado a grandes brotes por agua contaminada debido a malas condiciones sanitarias [23].

No obstante, también se ha reconocido la contaminación de fuentes de agua por HEV3-HEV4 como consecuencia del escurrimiento de los desechos de las granjas de cerdos hacia aguas superficiales (Fig. 5) [23].

Por otra parte, si bien la transmisión parenteral de este virus no es la ruta principal de diseminación, HEV ha sido reconocido como un agente transmisible por transfusiones, significando un potencial riesgo para los bancos de sangre [42]. De todas formas, se estima que la infectividad de HEV en productos sanguíneos es un 50%, dependiendo de la carga viral [43, 44]. En algunos países de Europa se han implementado programas de *screening* de ARN de HEV en bancos de sangre pero en Sudamérica no es actualmente realizado [45].

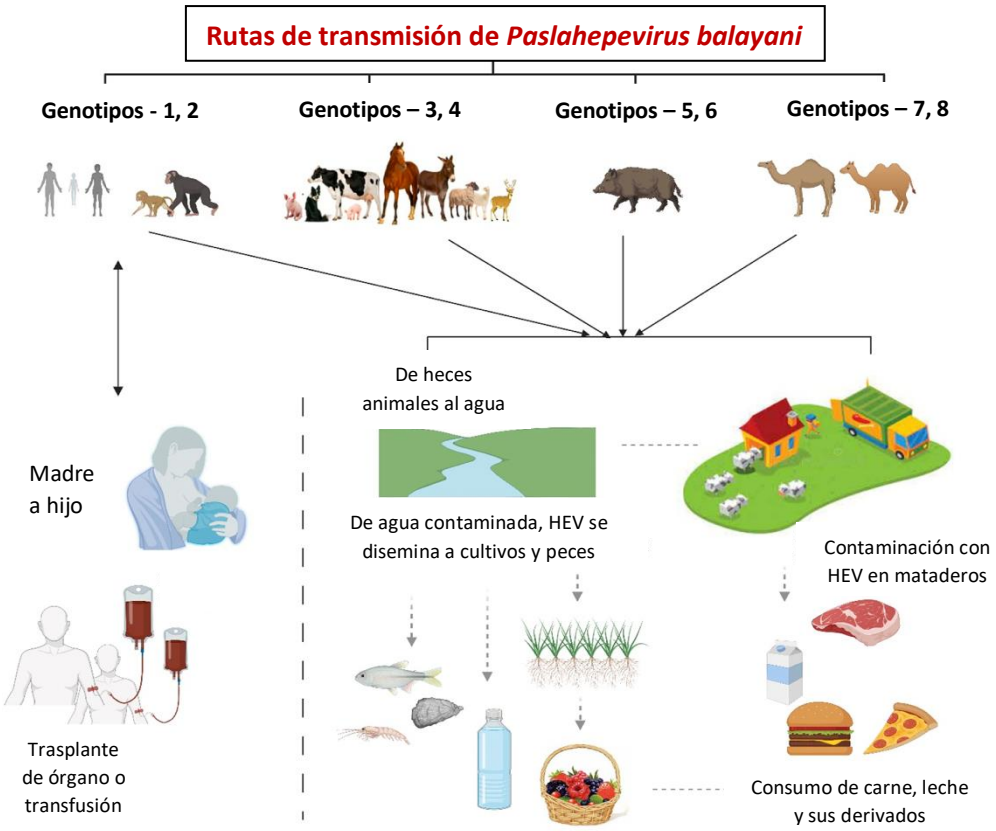

Fig.5. Rutas de transmisión de HEV. Se muestran en la figura de transmisión de HEV para los distintos genotipos de *Paslahepevirus balayani.* Extraído y adaptado de [31].

1.6. Presentación clínica

Las infecciones por HEV se presentan desde cuadros asintomáticas hasta hepatitis aguda (HEVa) auto-limitada en la población general con una tasa de letalidad menor al 4% [46]. En estos casos los principales síntomas son fiebre, ictericia, vómitos, alteración de las transaminasas hepáticas y mialgias, presentándose en un 5-30% de los infectados por HEV [47].

Particularmente, la infección con HEV3 puede causar hepatitis crónica (HEVc) con un rápido progreso a cirrosis, especialmente en pacientes receptores de transplante de órganos sólido (SOT) u oncológicos e individuos inmunocomprometidos con linfoma, leucemia e infección por el virus de la inmunodeficiencia humana (HIV) [3].

La infección por HEV1 cobra gran relevancia especialmente en mujeres embarazadas, ya que presenta una elevada tasa de letalidad de hasta un 20-30% debido al desarrollo de falla hepática fulminante. Además, puede causar importantes complicaciones clínicas como defectos congénitos, eclampsia, parto prematuro y abortos [3].

1.6.1. Infección crónica por HEV3

HEVc es la manifestación clínica de mayor preocupación asociada a la infección por HEV3 en 20-50% de los pacientes inmunocomprometidos o pacientes SOT que hayan recibido trasplante de hígado o riñón, pudiendo derivar en cirrosis y falla hepática en un 10% de los individuos [3].

En pacientes con enfermedad hepática previa, puede ocurrir la manifestación conocida como falla hepática-*acute-on-chronic* (ACLF) incluyendo complicaciones clínicas como ascitis, encefalopatía hepática, coagulopatía y falla multiorgánica asociada al síndrome de respuesta inflamatoria severa [3, 48]. Los casos de ACLF están vinculados a una elevada mortalidad, cercana al 70% [3].

Además, la hepatitis crónica, así como los casos agudos están frecuentemente relacionados con manifestaciones extrahepáticas severas, entre ellas, el síndrome de Guillan-Barre, trombocitopenia, pancreatitis, glomerulonefritis, etc. [3].

1.7. Biología viral

Si bien la infección por HEV ha sido reconocida como un serio problema de salud pública desatendido y notoriamente sub-diagnosticado [49], es muy escasa la información disponible sobre los aspectos básicos del ciclo de vida viral y los mecanismos moleculares y bioquímicos con respecto a la patogénesis viral y la relación virus-hospedero, fundamentalmente debido a que no existe un sistema eficiente y estandarizado de aislamiento de HEV en cultivos celulares [50]. Hasta el momento, la línea celular humana A549 (células epiteliales de carcinoma pulmonar) ha sido considerada como uno de los modelos más adecuados para la propagación de HEV *in vitro* [51, 52].

Interesantemente, a pesar de que la recombinación inter- e intra-genómica es muy infrecuente en HEV, se ha reportado que algunas cepas obtenidas de casos de HEVc presentan

variantes recombinantes virus-hospedador en la región HVR (ORF1) [53], lo cual se ha propuesto que le podría conceder una ventaja replicativa *in vitro* [54].

Particularmente, se reportó para la cepa 47832 una inserción de 186 nt en la región HVR proveniente de otras regiones dentro de la ORF1 [55].

Asimismo, para la cepa Kernow-C1 aislada de un paciente con hepatitis crónica portador de HIV-1, se reportó una inserción de 171 nt en la región HVR proveniente del gen ribosomal humano S17, que demostró conferirle una mejor adaptación al crecimiento *in vitro* y la capacidad de infectar un mayor rango de especies *in vitro* (humanos, cerdos y ciervos), sugiriendo que el prolongado período de infección crónica (2 años en este caso) en un individuo inmunocomprometido pudo favorecer la mutación del virus generando un alto título viral y una mayor variabilidad de cuasiespecies, demostrando que la infección crónica por HEV puede tener importantes implicancias para la evolución de este agente [53, 56].

En los últimos años, se han reportado diversas aproximaciones metodológicas con el objetivo de estudiar la replicación y patogénesis de HEV. Particularmente, se han constatado diferencias significativas en la expresión génica de citoquinas para monos *Rhesus* infectados con HEV3 o HEV1 [57] y para la infección *in vitro* de HEV1 en células A549 [104].

En este sentido, se han implementado además análisis ómicos (transcriptómicos, proteómicos y metabolómicos) [58–60].

Por un lado, se han reportado estudios de transcriptómica en células Huh-7 transfectadas con un replicón de HEV1 [61] y en células HepG2 transfectadas con un lentivirus recombinante del ORF3-HEV suino [62], los cuales mostraron hallazgos muy interesantes que colaboraron a la compresión de la biología viral de HEV en un comienzo, pero en ningún caso se emplearon partículas de HEV completamente infectivas.

A su vez, estudios de la respuesta celular a la infección por HEV4 suino en células A549 mediante proteómica reportaron 31 proteínas diferencialmente expresadas, sin embargo, no fue posible identificar las proteínas que tienen un rol determinante en la infección por HEV [58] En esta misma línea, se reportó un estudio de proteómica comparativa entre hígados porcinos infectados experimentalmente con cepas de HEV3 de distintos subtipos (3c, 3e y 3f), observándose diferencias para los procesos de síntesis de colesterol, metabolismo lipídico y respuesta inflamatoria [59].

Por otra parte, a través de análisis metabolómicos del suero de pacientes infectados, se observó que la presencia de metabolitos específicos puede utilizarse como marcadores para diferenciar los casos de falla hepática de los de hepatitis aguda [60].

1.8. Diagnóstico

El período de incubación de HEV dura entre 2-9 semanas para los casos agudos y generalmente, el ARN puede ser detectado en suero por 2-6 semanas posteriores a la infección y en heces por hasta 2 semanas más (Fig. 6).

Los anticuerpos IgM anti-HEV se presentan en circulación a las 3-4 semanas luego de la infección y persisten hasta por 4-6 semanas. Por otro lado, los anticuerpos IgG pueden permanecer por varios años luego de la recuperación [23].

La detección de HEV se realiza de forma indirecta mediante test serológicos comerciales para IgM e IgG anti-ORF2 HEV o mediante la amplificación de ácidos nucleicos (NAT) por RT-PCR, RT-nested PCR y/o PCR en Tiempo Real [23].

Recientemente, la guía de la Asociación Europea de Estudio del Hígado recomendó utilizar una combinación de tests serológicos y moleculares para el correcto diagnóstico de la infección por HEV (Fig.7) [3].

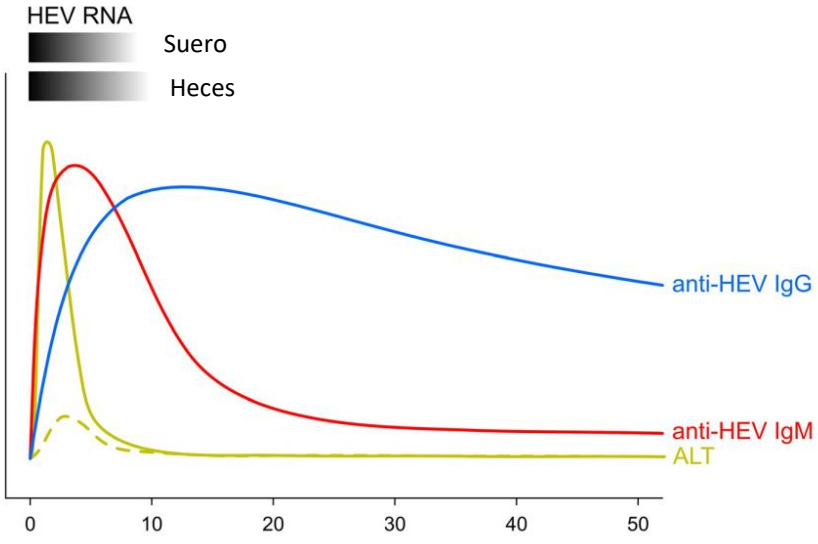

Fig. 6. Curso de la infección por HEV. Se representa la concentración de ARN de HEV en suero y heces en forma de gradiente. Se indican los marcadores bioquímicos de la enzima alanina aminotransferasa (ALT) y marcadores serológicos (IgM, IgG). La línea punteada muestra los patrones más comunes de ALT en pacientes con un aumento moderado de la enzima. Extraído y adaptado de [23].

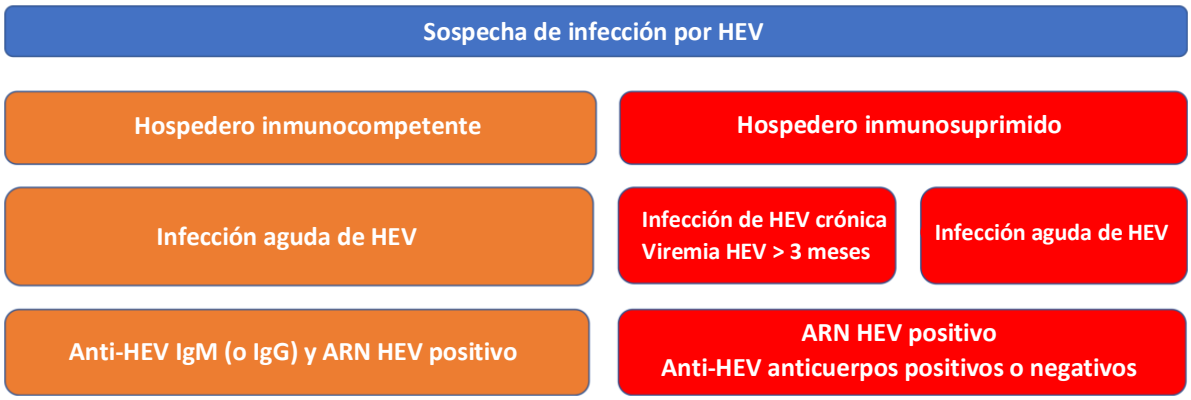

Fig. 7. Algoritmo diagnóstico para infección por HEV. Para el diagnóstico de hepatitis aguda en pacientes inmunocompetentes, se deben usar ambos tests serológicos y moleculares en combinación. Sin embargo, los tests serológicos no son confiables para pacientes inmunocomprometidos. En casos dónde el ARN de HEV se detecta por más de 3 meses, se considera hepatitis crónica. Extraído y adaptado de [3].

1.9. Tratamiento

En la mayoría de los cuadros agudos y auto-limitados de hepatitis E no se requiere tratamiento. No obstante, en casos de hepatitis crónica y ACLF dónde el ARN permanece detectable por al menos 3-6 meses, no existe un tratamiento antiviral específico aprobado. La primera opción terapéutica consiste en disminuir la terapia inmunosupresora (en los pacientes trasplantados), la cual es exitosa en solo el 30% de los casos [63].

Si bien para el tratamiento de la hepatitis crónica podría emplearse Interferón-α pegilado, el mismo está contraindicado en pacientes trasplantados por incrementar el riesgo a rechazo [3].

Por lo tanto, en los casos dónde no se logra el *clearance* viral, se recurre a la administración de 1200 mg/día de ribavirina (RBV) durante 3 meses, presentando en general buenos resultados [64, 65]. Sin embargo, se ha comprobado que el tratamiento con esta droga falla en algunos casos debido al desarrollo de resistencia antiviral de HEV posiblemente asociada a las sustituciones G1634R, Y1320H y K1383N en la RdRp [66].

El tratamiento con RBV puede causar efectos secundarios como anemia hemolítica y reacciones dérmicas y está contraindicado en mujeres embarazadas, a su vez, en pacientes con función renal alterada la concentración de RBV a administrar debe ser cuidadosamente ajustada [67].

Recientemente, varios autores han sugerido que la hepatitis E debería ser considerada como una enfermedad desatendida [68, 69], debido a que el impacto producido por enfermedades emergentes constituye un problema de creciente preocupación desde el punto de vista sanitario y clínico, sumado al hecho de que hasta el momento el único tratamiento existente para estos casos es la monoterapia con RBV.

1.10. Antecedentes y situación en Uruguay

En 2011 se reportaron en Uruguay los primeros casos de infección aguda por HEV en humanos, asociados a HEV3 [70], los cuales formaron un *cluster* monofilético que no agrupó con los subtipos conocidos. Recientemente, por medio de un estudio serológico en donantes de sangre de Uruguay, se obtuvo una tasa de seroprevalencia de HEV de un 10% (10 veces mayor que el último análisis hace 20 años) [71]. Además, en 2014 se identificó un caso de una cepa autóctona asociada a HEV1 [72].

Estos valores de seropositividad de HEV en donantes de sangre y en reservorios animales (*Sección 1.4*) indican la presencia de una intensa circulación viral a nivel poblacional con probablemente una gran proporción de casos asintomáticos. De hecho, a pesar de que la hepatitis E es de notificación obligatoria en el país, sólo 30 casos han sido reportados entre 2015-2020 [73]. Algunos de esos casos detectados fueron reportados por nuestro grupo y corresponden a hepatitis con complicaciones y manifestaciones extrahepáticas asociadas a falla hepática fulminante y hepatitis crónica [74, 75].

A partir de muestras de suero de estos casos clínicos de hepatitis E aguda, en el marco de mi Tesis de Maestría PEDECIBA (*Aproximación al estudio de la replicación in vitro del Virus de la Hepatitis E (HEV) a través de análisis proteómicos y transcriptómicos*) y Proyecto CSIC I+D 2016, se implementó un sistema de aislamiento en A549 (habiéndose también evaluado la línea HepG2 y cultivo primario de hepatocitos de rata neonata). Como resultado, se aislaron cepas de HEV3 *in vitro* en A549 [76], a partir de los cuales se realizaron estudios transcriptómicos, obteniéndose una expresión diferencial de 1089 genes sobre-regulados y 1083 sub-regulados. Se observó que la infección puede dar lugar a una desregulación simultánea de los procesos de metabolismo, sistema inmune, proliferación celular, apoptosis y organización del citoesqueleto. Si bien en mi Tesis de Maestría se logró desarrollar un

sistema de aislamiento de HEV, éste resultó ser poco reproducible y requerir mucho tiempo para desarrollar la infección.

1.11. Fundamentación de la investigación de esta Tesis

Se estima que HEV circula en Uruguay de forma principalmente asintomática y a través de mecanismos de transmisión no identificados aún. Por lo tanto, esto plantea la necesidad de estudiar más en profundidad los posibles mecanismos implicados y debido en parte a la limitada información epidemiológica en el país, concretamente de la fauna silvestre, es pertinente preguntarse qué otras especies animales, podrían llegar a estar contribuyendo a la diseminación viral. Este enfoque está siendo actualmente complementado mediante el relevamiento de HEV en aguas residuales y mascotas de compañía de Uruguay en el marco de una Tesina de Grado de la Licenciatura en Ciencias Biológicas de la estudiante Romina Icasuriaga, bajo la orientación del Dr. Santiago Mirazo y la co-orientación de MSc. Florencia Cancela.

Si bien HEV circula en forma críptica con casos mayormente asintomáticos, el desarrollo de esta línea de investigación en el laboratorio ha permitido construir alianzas con el sector de la salud, llevando a la detección de casos clínicos (no usual en la región) y por tanto, ofreciendo la oportunidad de indagar en el estudio de los mismos. En este contexto, debido a que Uruguay es uno de los pocos países de América que ha reportado casos crónicos de hepatitis E, esto permite avanzar en el estudio de su epidemiología molecular y específicamente en la caracterización y clasificación de las cepas de HEV3, para lo cual se requiere obtener genomas completos.

A su vez, se desconocen los mecanismos moleculares y virológicos que llevan a la cronificación de hepatitis E, por lo que se justifica la necesidad de avanzar en los estudios de biología viral y resistencia antiviral mediante aproximaciones *in vitro* e *in silico.* Particularmente, debido a que las cepas de HEV3 identificadas en Uruguay pertenecen a un único subtipo de circulación exclusiva, resulta interesante profundizar en el estudio de la biología viral para variantes de este subtipo.

Estos aspectos pretenden ser abordados a lo largo de esta Tesis.

1.12. Cancela et al., 2022. Structural aspects of hepatitis E virus

Las *Secciones 1.2.* y *1.2.1*. de esta Introducción están basadas en una revisión publicada en el marco de la actual Tesis de Doctorado conteniendo información actualizada sobre las proteínas de HEV y sus propiedades biológicas con especial énfasis en sus funciones y características estructurales, la cual se adjunta a continuación:

Cancela F, Noceti O, Arbiza J, Mirazo S. Structural aspects of hepatitis E virus. Arch Virol. 2022 Dec;167(12):2457-2481. doi: 10.1007/s00705-022-05575-8. Epub 2022 Sep 13.

Archives of Virology
https://doi.org/10.1007/s00705-022-05575-8

REVIEW

Structural aspects of hepatitis E virus

Florencia Cancela[1] · Ofelia Noceti[2] · Juan Arbiza[1] · Santiago Mirazo[1,3,4]

Received: 30 March 2022 / Accepted: 4 June 2022

Abstract

Hepatitis E virus (HEV) is a leading cause of acute hepatitis worldwide. Hepatitis E is an enterically transmitted zoonotic disease that causes large waterborne epidemic outbreaks in developing countries and has become an increasing public-health concern in industrialized countries. In this setting, the infection is usually acute and self-limiting in immunocompetent individuals, although chronic cases in immunocompromised patients have been reported, frequently associated with several extrahepatic manifestations. Moreover, extrahepatic manifestations have also been reported in immunocompetent individuals with acute HEV infection. HEV belongs to the alphavirus-like supergroup III of single-stranded positive-sense RNA viruses, and its genome contains three partially overlapping open reading frames (ORFs). ORF1 encodes a nonstructural protein with eight domains, most of which have not been extensively characterized: methyltransferase, Y domain, papain-like cysteine protease, hypervariable region, proline-rich region, X domain, Hel domain, and RNA-dependent RNA polymerase. ORF2 and ORF3 encode the capsid protein and a multifunctional protein believed to be involved in virion release, respectively. The novel ORF4 is only expressed in HEV genotype 1 under endoplasmic reticulum stress conditions, and its exact function has not yet been elucidated. Despite important advances in recent years, the biological and molecular processes underlying HEV replication remain poorly understood, primarily due to a lack of detailed information about the functions of the viral proteins and the mechanisms involved in host-pathogen interactions. This review summarizes the current knowledge concerning HEV proteins and their biological properties, providing updated detailed data describing their function and focusing in detail on their structural characteristics. Furthermore, we review some unclear aspects of the four proteins encoded by the ORFs, highlighting the current key information gaps and discussing potential novel experimental strategies for shedding light on those issues.

Keywords Hepatitis E virus · Structural biology · Review

Introduction

Hepatitis E virus (HEV) infection is currently regarded as the major cause of acute viral hepatitis in the world. It is endemic in developing countries and is now becoming recognized in industrialized countries, with 20 million HEV infections and 70,000 deaths annually [Sayed and Meuleman, 2019; Webb and Dalton, 2019].

HEV is present in feces and bile as a non-enveloped particle of 32–34 nm, while in circulating blood and culture supernatants, HEV can be found as a membrane-associated particle covered in lipids, named "quasi-enveloped" HEV with a diameter of ~ 40 nm [Ji et al., 2021].

HEV is a member of the family *Hepeviridae*, subfamily *Orthohepevirinae* [Smith et al., 2014], and has a single-stranded positive-sense RNA genome (RNA ss+) of approximately 7.2 kb [Kumar et al., 2013]. According to

Handling Editor Michael A. Purdy

✉ Santiago Mirazo
smirazo@fcien.edu.uy

1 Sección Virología, Facultad de Ciencias, Universidad de la República, Montevideo, Uruguay

2 Programa Nacional de Trasplante Hepático y Unidad Docente Asistencial Centro Nacional de Tratamiento Hepatobiliopancreatico. Hospital Central de las Fuerzas Armadas, Montevideo, Uruguay

3 Departamento de Bacteriología y Virología, Instituto de Higiene, Facultad de Medicina, Universidad de la República, Montevideo, Uruguay

4 Av. Alfredo Navarro 3051, PC 11600 Montevideo, Uruguay

Published online: 13 September 2022

phylogenetic analysis, HEV strains can be divided into eight distinct genotypes (HEV1-HEV8) and subtypes [Smith et al., 2014]. HEV1 and HEV2 anthroponotic strains are known to cause large waterborne epidemic outbreaks in developing countries [Kumar et al., 2013], whereas HEV3 and HEV4 are zoonotic and have recently become an increasing public-health issue in developed countries. Infections with these genotypes have been associated with the consumption of raw or undercooked food, particularly pork meat and liver sausages [Colson and Decoster, 2019].

Acute HEV infection is generally self-limiting in the general population, with a case fatality rate < 4%. Nonetheless, in pregnant women infected with HEV1, this rate may increase to 20%, as infection can evolve to fulminant liver failure [Chandra et al., 2008b; Kumar et al., 2013].

Chronic HEV infections can lead to liver failure in some cases, or to acute-on-chronic liver failure in patients with previous liver disease [Horvatits et al., 2019]. Recently, chronic and acute-on-chronic hepatitis E have been considered clinical manifestations of major concern related to HEV3 infection in individuals receiving liver and kidney transplants as well as immunocompromised HIV, lymphoma, and leukemia patients [Fang and Han, 2017; Gerolami et al., 2008; Pischke et al., 2010]. Furthermore, chronic hepatitis E is frequently associated with severe extrahepatic manifestations [Narayanan et al., 2019]. However, extrahepatic manifestations such as neurological disorders, have also been reported in immunocompetent individuals with acute HEV infection [Mendoza-Lopez et al., 2020; Wu et al., 2021].

The HEV genome has a methyl guanosine cap (m7G) at the 5'end and a polyA tail at the 3' end, and it contains three partially overlapping open reading frames (ORFs) [Kumar et al., 2013].

The HEV Sar55 strain (GenBank accession number AF444002) was used as a reference for the nucleotide and amino acid positions mentioned throughout the following text.

Briefly, ORF1 encodes a non-structural polyprotein, ORF2 encodes a capsid protein, and ORF3 encodes a multifunctional protein. Two short untranslated regions (NCRs) at the 5' and 3' ends have also been described, with lengths of 27 and 68 nt, respectively [Nan and Zhang, 2016]. In addition, the viral genome contains four *cis*-reactive elements (CREs), one of which overlaps the 3' carboxy-terminal sequence of ORF2 and the 3' NCR and plays an essential role in viral replication by binding to the RNA-dependent RNA polymerase (RdRp). The second one is located in the intergenic region between ORF1 and ORF3 and forms a stem-loop structure, which has been suggested to be the site of initiation of synthesis of a 2.2-kb capped subgenomic bicistronic mRNA [Cao et al., 2010; Parvez, 2015a]. The other two highly conserved CREs are located at the start of ORF1 and at the end of ORF2 [Ju et al., 2020].

The bicistronic mRNA encodes the ORF2 and ORF3 proteins, the latter of which substantially overlaps the 5' region of ORF2 in different reading frames [Graff et al., 2006].

In addition, HEV1 strains contain an additional ORF (ORF4, nt 2835–3308), with an internal ribosome entry site (IRES)-like (nt 2701–2787) translation initiation site [Nair et al., 2016]. This short-lived ORF4 protein (20 kDa) is expressed under endoplasmic reticulum (ER) stress conditions, and its expression is likely induced by the antiviral response of the host. The N-terminal region of the ORF4 product interacts with multiple viral and host proteins in order to generate a replication complex with RdRp, Hel, and eukaryotic elongation factor 1 isoform-1 (eEF1α1), stimulating RdRp activity [Nair et al., 2016].

Here, we present a thorough update of the main structural characteristics of the HEV proteins (Figs. 1–4) and their functions, discussing current issues and proposing potential experimental strategies.

HEV viral proteins

HEV belongs to the alphavirus-like supergroup III of RNA ss + viruses, whose members encode a type 1 helicase (Hel), a type 1 methyltransferase domain (MT), and a type 3 RdRp domain. They also produce capped genomic RNAs and subgenomic RNAs encoding the structural protein and have a polyA tail [van der Heijden and Bol, 2002]. Animal viruses from this supergroup include members of the genera *Alphavirus* and *Rubivirus* and the subfamily *Orthohepevirinae* of the families *Togaviridae, Matonaviridae*, and *Hepeviridae*, respectively. Although HEV can circulate as a "quasi-enveloped" particle, it lacks surface glycoproteins, thereby differing from enveloped animal alpha-like viruses [van der Heijden and Bol, 2002; Yin et al., 2016]. Furthermore, members of these viral families have a conserved X domain, whose function remains unknown [Koonin and Dolja, 1993]. Interestingly, alphaviruses have a genome organization similar to the one seen in plant viruses belonging to the genera *Tobamovirus, Tobravirus, Hordeivirus*, and *Furovirus*. However, the structural proteins have at least three different origins, resulting in viruses with very divergent structures [Strauss and Strauss, 1994].

ORF1

ORF1 is the largest open reading frame in the HEV genome, with 5082 nucleotides (nt), encoding a polyprotein 1693 amino acid (aa) in length, containing eight putative functional domains. These domains include, from the N-terminal

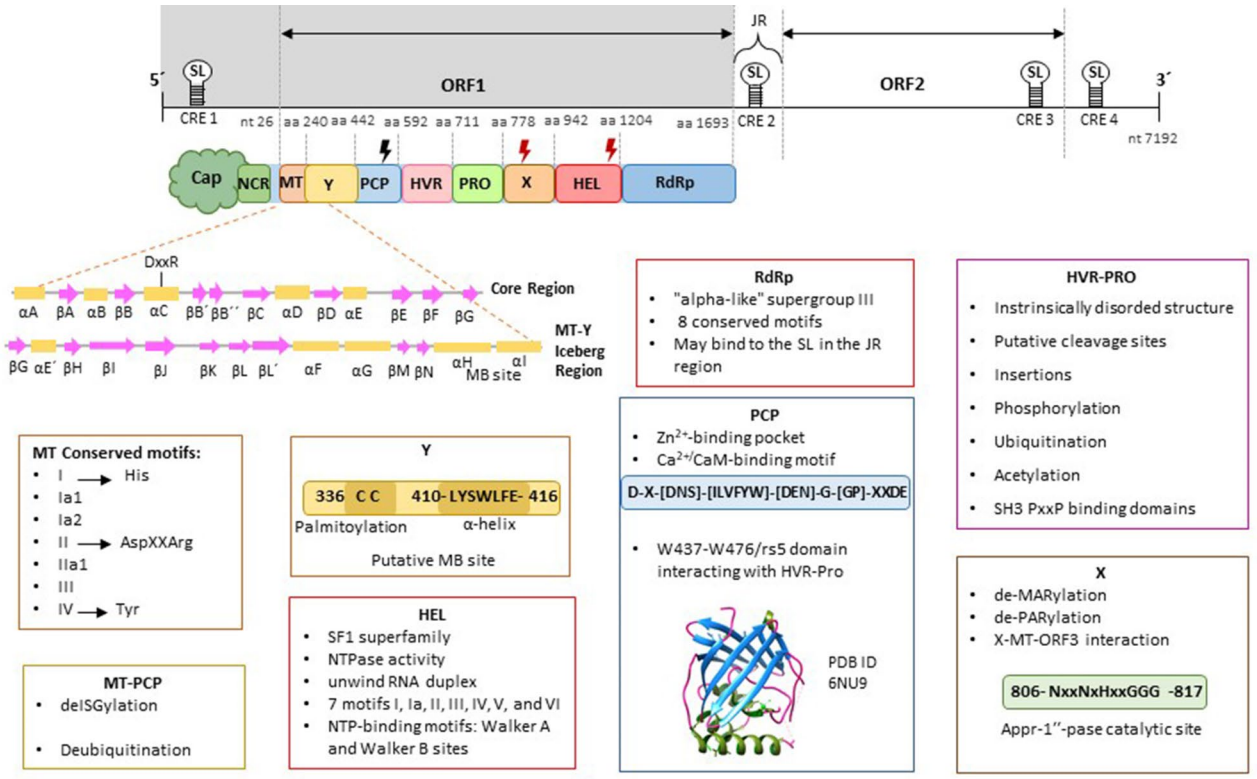

Fig. 1 Schematic representation of ORF1 of HEV. The HEV genome is approximately 7.2 kb in length, with a methyl guanosine cap (Cap) at the 5' end and a polyA at the 3' end, containing two untranslated regions (NCRs) at the 5' and 3' ends. HEV contains three partially overlapping open reading frames (ORFs). ORF1 includes eight putative domains: Y domain (Y), papain-like cysteine protease (PCP), hypervariable region (HVR), proline-rich region (PRO), X domain (X), helicase (HEL), and RNA-dependent RNA polymerase (RdRp). Four *cis*-reactive elements (CRE) with a stem-loop structure (SL) are indicated, the second of which is located in the junction region (JR). The black lightning bolt symbol represents the cleavage site for the serine protease cellular factor Xa, and the red lightning bolt symbols represent cleavage sites for the serine protease thrombin in ORF1. "MB" indicates the membrane-binding site in the MT-Y iceberg region. The nucleotide and amino acid positions are according to HEV strain Sar55 (GenBank accession number AF444002).

to the C-terminal end: MT, Y domain (Y), papain-like cysteine protease (PCP), hypervariable region (HVR), proline-rich region (Pro), X domain (X), Hel domain, and RdRp [Nan and Zhang, 2016].

The non-structural ORF1 protein of HEV shares the most sequence similarity with rubi-like viruses of the genera *Rubivirus*, *Betatetravirus*, *Benyvirus*, and *Omegatetravirus* as well as Sclerotinia sclerotiorum debilitation-associated virus [Batts et al., 2011; Liu et al., 2009].

Localization studies of the ORF1-encoded protein in human cell lines have shown that it is associated with the cell membrane in the perinuclear region, particularly in the ER and the ER-Golgi intermediate compartment [Perttilä et al., 2013].

Whether the ORF1 polyprotein needs to be further processed into single domains or can function as a single unit is still unclear, as contradictory results have been obtained [Paliwal et al., 2014; Parvez, 2013; Perttilä et al., 2013; Suppiah et al., 2011].

So far, although several studies have demonstrated the proteolytic processing of the ORF1 polyprotein in vaccinia virus, baculovirus, and eukaryotic expression systems, it is not yet clear whether this proteolysis occurs due to viral or host proteases [Sehgal et al., 2006]. It has been hypothesized that the HEV ORF1 polyprotein is processed by the cellular factor Xa (in the PCP domain) and thrombin (in the X domain) [Palta et al., 2014], and this processing seems to be essential for viral replication [Kanade et al., 2018]. These cellular serine proteases are involved in the blood coagulation cascade [Palta et al., 2014] and are first synthesized in the liver as precursor proenzymes (prothrombin and factor X, respectively), after which prothrombin is cleaved into active thrombin by factor X in the plasma [Wood et al., 2011]. In contrast, ORF1 expression in cell-free and prokaryotic systems does not result in polyprotein processing [Ansari et al., 2000].

Recently, in order to study the polyprotein processing of HEV ORF1, a novel BacMam strategy was employed in which a complete HEV3 genome (GenBank accession

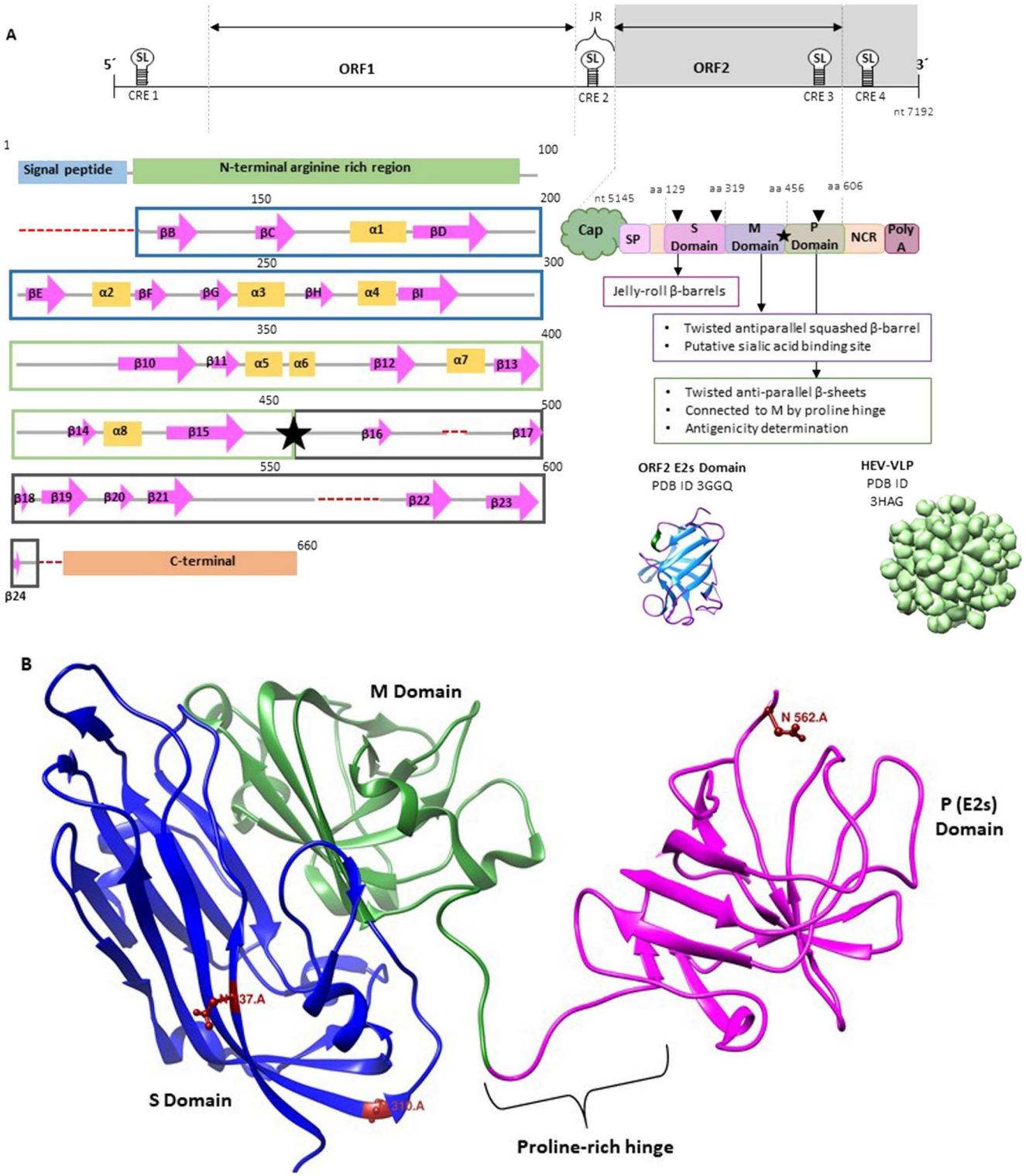

Fig. 2 Summary of ORF2 structure and characteristics. (A) ORF2 contains a signal peptide (SP) and three domains: the shell domain (S), middle domain (M), and protruding domain (P). The black triangles indicate the glycosylation sites in ORF2 (N137, N310, and N562), and the black star indicates the proline-rich hinge between the M and P domains. The secondary structure of the HEV3 capsid protein (PDB ID 2ZTN) is displayed. S, M, and P domains are shown in blue, green, and black, respectively. α-Helices, β-sheets, and loops are represented by yellow rectangles, pink arrows, and grey thick lines. Red dashed lines indicate the disordered regions. The nucleotide and amino acid positions are according to HEV strain Sar55 (GenBank accession number AF444002). (B) 3D structure of the capsid protein (HEV3 PDB ID 2ZTN). N-linked glycosylation sites (N137 and N310 in the S domain and N562 in the P domain) are indicated in red.

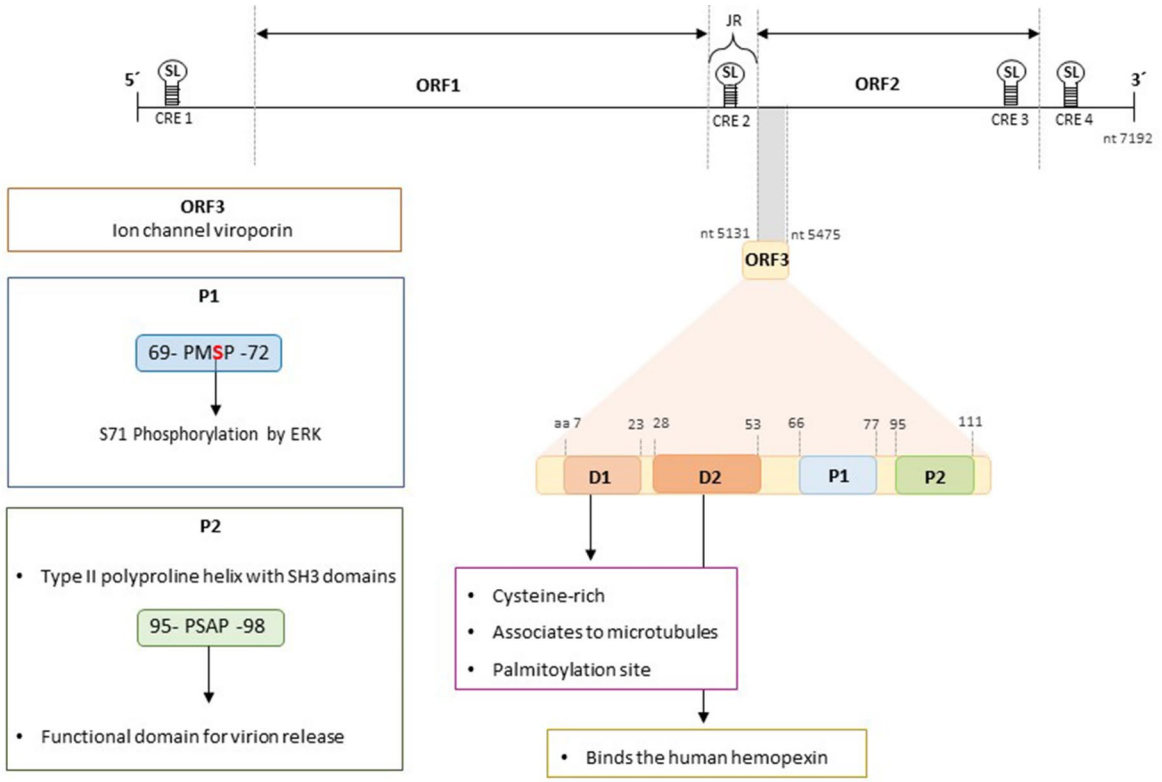

Fig. 3 Major features and motifs of ORF3. The two hydrophobic domains (D1 and D2) and the two proline-rich domains (P1 and P2) are shown.

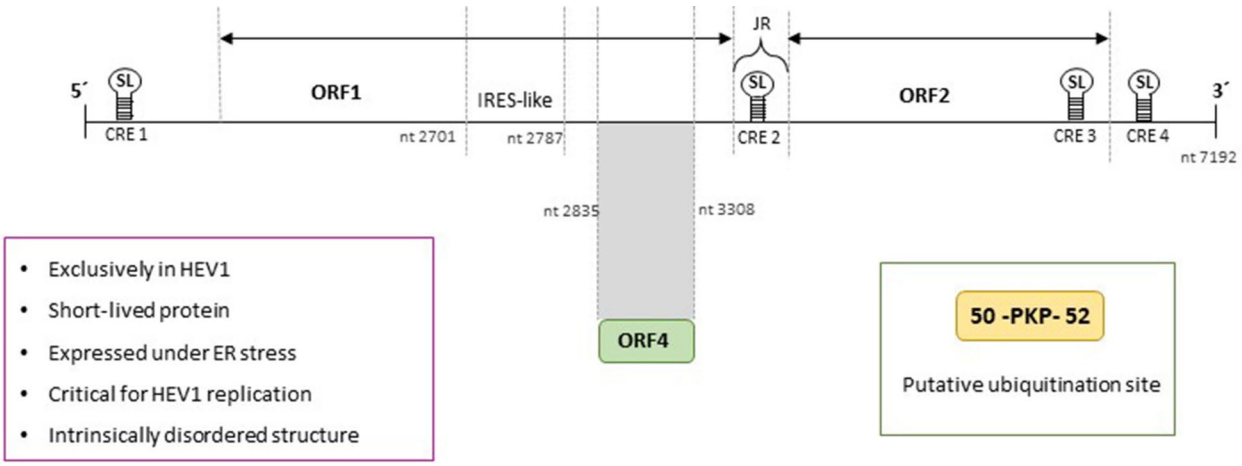

Fig. 4 Novel ORF4, present only in HEV1. The IRES-like element (nt 2701–2787) and ORF4 protein (overlapping ORF1), with its putative ubiquitination site, are shown.

number AY575859) was cloned into a BacMam vector. Huh7 cells were infected with the recombinant baculovirus containing the HEV genome, and fragments of 18, 35, 37, 56 kDa were obtained, corresponding to PCP, MT, RdRp, and ORF2, respectively, suggesting that proteolytic processing had occurred. Additionally, MT activity was confirmed [Kumar et al., 2020].

Methyltransferase domain

Early studies revealed the expression of a 110-kDa HEV protein (P110) and an 80-kDa putative proteolytic product in insect cells [Nan and Zhang, 2016]. These proteins were shown to participate in the synthesis of the 5' cap of the viral RNA through their guanine-7-methyltransferase and guanylyltransferase (GT) activity [Nan and Zhang, 2016],

which are essential for the infectivity of HEV [Emerson et al., 2004]. The MTs of the alphavirus supergroup use an unconventional capping pathway [Decroly et al., 2011] in which the P110 polyprotein product first methylates GTP to produce m^7GTP and then transfers it to the 5′ end of the mRNA to form a covalent enzyme-m^7GTP complex, releasing pyrophosphate [Magden et al., 2001]. In alphavirus-like togaviruses, the methyl group is retrieved from S-adenosyl-L-methionine [Decroly et al., 2011]. In addition, HEV P110 was found to be strongly bound to a membrane, like an integral membrane protein, but it lacks nonpolar amino acid sequences typical of transmembrane segments [Magden et al., 2001]. Also, through *in silico* predictive approaches, a putative Zn^{2+} finger domain was identified around position 73–94 [Karpe and Lole, 2011].

Sequence analysis of the MT "alto"-group within the alphavirus supergroup (alphaviruses, orthohepeviruses, piscihepeviruses, tricornaviruses, tobamoviruses, tobraviruses, and hordeiviruses) has shown that they have a core region of 200 aa comprised of nine interspersed α-helices and β-strands, αA to αE and βA to βD, followed by three β-strands, βE to βG [Ahola and Karlin, 2015]. The HEV MT domain resembles those of alfalfa mosaic virus, brome mosaic virus, and cucumber mosaic virus of the family *Bromoviridae* [van der Poel et al., 2001], containing seven conserved motifs (I, Ia1, Ia2, II, IIa1, III, and IV) with invariant H, DxxR, and Y residues (at the beginning of βG) in I, II, and IV, respectively [Rozanov et al., 1992]. The histidine residue has been shown to be necessary for the GT reaction but not for MT activity in alphavirus-like togaviruses [Decroly et al., 2011]. The conserved DxxR motif in αC is believed to be part of the binding site for the methyl donor substrate S-adenosyl-l-methionine.

Subsequently, sequence analysis of members of over 50 genera of viruses (including HEV) demonstrated that MT has a region of conserved secondary structure downstream of the core region, named the "iceberg region". In particular, the "iceberg region" in the "alto" group within the alphavirus supergroup, which includes HEV, is composed of six to seven predicted β-strands (βG to βL'), followed by four to five α-helices (αF to αJ), with the insertion of a helix (αE') between βG and βH, and of two strands (βM and βN) between helices αG and αH, unlike the members of the "tymo" group (order *Tymovirales*) within the alphavirus supergroup [Ahola and Karlin, 2015]. The "iceberg region" in the "alto"group has three conserved or semi-conserved positions, H at the end of strand βG, D/E in the middle of strand βI, and G/A/S in the loop between βM and βN [Ahola and Karlin, 2015]. According to several studies, the "iceberg region" is crucial for MT and GT functionality, strongly suggesting that it plays an important role in binding the methyl acceptor substrate GTP [Ahola and Karlin, 2015]. The "iceberg" C-terminus region in the "alto" group contains proven membrane-binding amphipathic helices composed of a hydrophobic segment followed by polar positively charged residues in αH. In the adjacent region, additional membrane-binding amphipathic helices within αI have been predicted [Ahola and Karlin, 2015].

Recently, a study showed that D29N and V27A substitutions in the MT sequence were associated with a more severe outcome in patients with HEV-associated acute liver failure, whereas the H105R mutation was associated with low HEV viremia, suggesting that this region might be a potential antiviral drug target [Borkakoti et al., 2017].

An HEV-host protein-protein interaction network study revealed that the PSMB4 protein (component of the 20S proteasome) interacts directly with MT, presumably altering the processing of the major histocompatibility complex (MHC) class I peptides [Subramani et al., 2018; Wißing et al., 2021].

Furthermore, an MT from a cell-culture-adapted HEV strain (47832c) expressed in HEK293T cells was reported to prevent interferon regulatory factor 3 and the p65 subunit of NF-κB from phosphorylation and activation in a dose-dependent manner [Myoung et al., 2019]. Moreover, HEV MT was demonstrated to strongly inhibit pattern recognition receptor (PRR) melanoma differentiation-associated protein 5 (MDA5)-mediated induction of the IFN-β promoter [Myoung et al., 2019] as well as RIG-I-induced activation of type 1 interferons (IFNs) [Kang et al., 2018]. MDA5 and RIG-I are PRRs that sense cytoplasmic double-stranded RNA [Kang and Myoung, 2017a, 2017b; Loo et al., 2008; Takeuchi and Akira, 2010]. Interestingly, this effect was not observed for other HEV strains analyzed (Sar-55, Mex-14, ZJ-1, or Kernow-C1), which suggests that blockage of IFN-β signaling may be necessary for adaptation of HEV to cell culture. Notably, the MT of strain 47832c lacks the C-terminal Y domain-iceberg region, which is present in the other strains and is now considered an integral part of the MT protein (see section 2.1.2), suggesting that the presence or absence of the Y domain might alter the functional activity of MT. [Myoung et al., 2019]. MT interferes with ferritin secretion to decrease the inflammatory response and acts on retinoic-acid-inducible gene I (RIG-I) and MDA5 to reduce IFN production [Li et al., 2019]. As an acute-phase protein, ferritin is abundantly secreted in HEV-infected patients and is associated with the inflammatory response. Thus, it has been proposed that this domain inhibits the host immune response by preventing ferritin secretion [Li et al., 2019; Yadav and Kenney, 2021]. This seems to occur through interaction with the light chain of human ferritin [Lhomme et al., 2020a].

Y domain

This second domain, which spans from aa 216 to 442, seems to be unique to HEV, rubella virus (RubV), and the plant virus beet necrotic yellow vein virus (BNYVV) within the alpha-like supergroup, and it shows the highest sequence similarity to that of RubV [Koonin et al., 1992].

Notably, analysis of alphavirus-like superfamily sequences has suggested that the Y domain might be an extension of the C-terminal MT domain [Ahola and Karlin, 2015]. In fact, it was observed that the N-terminus of the Y domain in HEV and RubV overlapped the conserved motif III of the MT domain [Koonin et al., 1992]. However, no specific function for this region has been assigned yet.

Sequence analysis of HEV and related alphaviruses has also identified a potential palmitoylation site (C_{336}-C_{337}) that is highly conserved in genotypes HEV1-4. These amino acids, together with W_{413}, are important for HEV replication and are possibly involved in membrane binding in intracellular replication complexes [Parvez, 2017a]. Tryptophan is known to be a key hydrophobic residue for α-helical protein folding for protein-protein interactions [Parvez, 2017a].

In addition, an α-helix segment consisting of $L_{410}Y_{411}S_{412}W_{413}L_{414}F_{415}E_{416}$ has been shown to be conserved in HEV and to be involved in cytoplasmic membrane binding [Parvez, 2017a].

Furthermore, in terms of RNA secondary structure, three stable hairpins/stem-loops at nt 788–856, 857–925 and 926–994 have been shown to be indispensable for HEV replication and infectivity [Parvez, 2017a].

PCP domain

The main difference in the organization of the functional domains in the genome of members of the alpha-like supergroup lies in the protease region. The proteases of RubV and other alphaviruses show a relocation in relation to the putative PCP domain of HEV, whereas BNYVV completely lacks it. Nonetheless, a region of the HEV PCP exhibits moderate similarity to the one of RubV [Koonin et al., 1992].

The PCP domain is a putative chymotrypsin-like protease that can process both ORF1 and ORF2 [Paliwal et al., 2014]. Six highly conserved cysteine residues (C457, C459, C471, C472, C481, and C483) and three histidine residues (H443, H497, and H590) in PCP have been found to be critical for HEV-Sar55 replicon replication in S10-3 cells, possibly belonging to the enzyme active site [Parvez, 2013].

An *in silico* 3D model of HEV PCP was constructed by homology modelling using RubV p150, and the presence of a predicted "papain-like β-barrel fold" confirmed its classification as protease [Parvez and Khan, 2014]. Based on homology to RubV, residues C434 and H443 were identified as the putative catalytic dyad [Parvez and Khan, 2014], rather than C434 and H590, as had been proposed previously [Koonin et al., 1992]. In another study using 3D modelling, a catalytic triad consisting of C483, H590, and N591 was predicted to be part of the active site between the N-terminal helical domain and the C-terminal β-sheet domain, which is the main characteristic of papain-like cysteine proteases [Saraswat et al., 2019].

Furthermore, a Zn^{2+}-binding pocket coordinated by C457-H458-C459 and C481-C483 was recognized within the β-barrel fold of HEV. Structural Zn^{2+}-binding sites are commonly coordinated by four cysteines and a histidine as ligands [Zhou et al., 2009]. Based on homology modeling, putative Ca^{2+}-dependent association of the calmodulin (CaM) binding site signature "D-X-[DNS]-[ILVFYW]-[DEN]-G-[GP]-XXDE" was identified. Among the different Ca^{2+}-binding motifs found in living systems, the most common one consists of a "helix-loop-helix" structure, called the "EF-hand". Viral EF-hand Ca^{2+}-binding motifs have also been reported in the rotavirus VP7 protein, the HIV-1 gp41 protein, the polyomavirus VP1 protein, and the RubV nonstructural p150 [Zhou et al., 2007]. The presence of essential active cysteines in the overlapping putative Ca^{2+}/CaM-binding motif of HEV suggests the formation of three intramolecular disulfide bridges that might structurally enable the orientation of the EF-hand towards Ca^{2+} binding.

One of the best-known small protein modules that specifically interacts with proline-rich motifs of regulatory proteins consists of a "WW-domain" or "rsp5-domain", with two distantly located tryptophan residues. Although these modules have not been reported in viral proteins so far, in the HEV protease model, a putative W437-W476/rs5 domain has been identified and proposed to interact with the proline-rich hypervariable region in HEV ORF1.

The proposed model suggests then that the putative catalytic dyad and divalent metal-binding motifs are essential for the structural integrity of the HEV protease and for polyprotein processing and RNA replication [Parvez and Khan, 2014].

On the other hand, a recent computational analysis of the complete ORF1 polyprotein identified an uncharacterized ordered secondary structure region involving residues 510–619, surrounded by two disordered regions (residues 492–509 and 692–779). The crystal structure of this protein was determined by X-ray diffraction (PDB code 6NU9), and no similar amino acid sequences were found in the RCSB Protein Data Bank (PDB). The structure consists of 10 β-strands and four α-helices. β-Strands 1 to 10 are arranged in two antiparallel sheets that form a sandwich-like fold. α-Helices 1 and 2 are located between β-strands 1 and 2, and α-helices 3 and 4 are positioned at the C-terminus of the

protein, with α-helix 4 situated between the two antiparallel β-sheets. Furthermore, this protein exhibited significant structural similarity to multiple fatty-acid-binding domains and was found to contain a bound zinc ion coordinated by residues H671, E673, and H686. Whether this coordinated zinc plays a catalytic or structural role remains unknown. Therefore, this protein was associated with possible zinc metalloprotease activity, previously believed to be located at aa 433–592 [Proudfoot et al., 2019].

Detailed studies have suggested that the highly conserved residue E583, located between β-strands 5 and 6, might act as the catalytic residue. However, the crystal structure showed that the geometry of the zinc-binding motif was not ideal for executing a proteolytic reaction. Hence, the authors proposed that the binding of a fatty acid, which would be readily available in the liver, or another endogenous ligand between the two β-sheets could shift α-helices 3 and 4, reorienting the zinc-coordinating amino acids into a catalytically active position [Proudfoot et al., 2019].

HEV PCP has been suggested to process ORF1, due to the presence of LXGG cleavage site motifs, which are commonly found in plus-sense RNA viruses at aa 664 (between the PCP and X domains), and at aa 1205 (between Hel and RdRp), and also to possess deubiquitinating activity [Karpe and Lole, 2011], which is known to require a Zn^{2+}–binding finger [Reyes-Turcu et al., 2009], which, as discussed above, is present in the MT region.

Ubiquitination (Ub) is the process of protein tagging for selective degradation in proteasomes. There are also some small ubiquitin-like molecules (UBLs) that are expressed in eukaryotes and conjugated to target proteins to modulate their stability and function [d'Azzo et al., 2005; Haglund and Dikic, 2005; Welchman et al., 2005]. Conversely, deubiquitinating enzymes are proteases that cleave Ub or UBLs from target proteins. The deubiquitinating activity of HEV MT-PCP was tested *in vitro* employing fluorogenic UBL substrates (Ub-AMC, ISG15-AMC, Nedd8-AMC, and SUMO-AMC), and deISGylation of interferon-stimulated gene 15 (ISG-15)-conjugated cellular proteins was demonstrated [Karpe and Lole, 2011]. UBL ISG-15 is expressed and conjugated to targets, a process known as ISGylation, in response to infection and INF-α or INF-β expression, thus inhibiting entry, replication, or release of intracellular pathogens [Villarroya-Beltri et al., 2017]. Therefore, HEV MT-PCP deISGylation might play a role in evasion of cellular antiviral pathways [Karpe and Lole, 2011]. This is supported by the observation that other viral proteases, such as PCP of porcine reproductive and respiratory syndrome virus, have been found to inhibit host innate immunity through their deubiquitinase activity [Li et al., 2010; Sun et al., 2010].

Notably, the PCP domain has been demonstrated to have deubiquitinase activity for RIG-1 and TBK-1 a downstream molecule activated by mitochondrial antiviral signaling due to RIG-1. These proteins require ubiquitination for their activation in an experimental model in which IFN is induced in hepatoma cells by polyinosinic polycytidylic acid, a double-stranded RNA homologue [Nan et al., 2014b]. Indeed, it has been observed that the HEV PCP strongly downregulates MDA5-mediated activation of INF-β induction and consequently severely decreases the level of phosphorylation of interferon regulatory factor 3 (IRF3). For full induction of INF-β expression, both IRF3 and NF-κB need to be activated and translocated into the nucleus. Hence, this study supports the notion that the HEV PCP is an antagonist and regulator of the antiviral state of type 1 IFN through IRF3 and NF-κB [Kim and Myoung, 2018].

Furthermore, the entire amino-terminal region of HEV3 ORF1 (MT-Y-PCP) has been shown to inhibit IFN-stimulated response element promoter activation and the expression of several IFN-stimulated genes in response to INF-β. These regions were also found to interfere with INF-β-induced STAT1 nuclear translocation and phosphorylation, indicating that MT-Y-PCP targets the JAK/STAT pathway. This inhibitory role seemed to be genotype-dependent, as it was not seen with HEV1 [Bagdassarian et al., 2018].

An intraviral interactome analysis revealed that the PCP domain is able to self-interact and to interact with other viral proteins, including MT, RdRp, and ORF3, suggesting that it might participate not only in cleavage of the ORF1 polyprotein but also in the assembly of replication complexes, along with ORF3 [Osterman et al., 2015].

Currently, the data regarding the structure and function of the HEV protease in ORF1 processing are not fully consistent, and further investigations are needed, especially since it could be considered a potential target for antiviral drugs.

HVR and Pro domain

There is still some debate regarding the nomenclature of these two regions, since, generally, they are not discriminated as different domains and their function is currently unknown.

At first, the HVR and Pro segments were considered part of the same hypervariable region because of the extreme sequence divergence around nt 2011–2325 (aa 662–766) in the HEV-Sar55 strain [Nan and Zhang, 2016]. Later, a section overlapping the HVR at aa 712–778 was identified as a proline-rich region due to the large number of proline residues. The Pro region contains only a few bulky hydrophobic amino acids (I, M, F, W, and Y) and a high amount of polar and charged amino acids (A, G, P, and S).

The Pro region in HEV1-4 is flanked at the N- and C-terminal end by the conserved sequences TLYTRTWS and RRLLXTYPDG, respectively [Purdy et al., 2012]. Recently, the HVR region was shown to be located in an intermediate region flanked by the Pro N- and C-terminal regions [Muñoz-Chimeno et al., 2020].

Moreover, the HVR has been recognized as a hinge between the X domain and the upstream sections, with inherent flexibility resulting from the multiple "disorder-promoting" proline residues, which might lead to an unstable tertiary structure [Dunker et al., 2008; Koonin et al., 1992; Tsai et al., 2001] with incomplete folding [Campen et al., 2008; Radivojac et al., 2007; Williams et al., 2001]. It has been suggested that the Pro region might be an essential part or modulator of the helicase or protease domains [Gouvea et al., 1998]. Indeed, researchers have demonstrated that certain proteins lack a fixed structure under physiological conditions and that this unstructured state is important for their function [Dunker et al., 2008].

Interestingly, it has been suggested that the high genetic heterogeneity of the HVR and the X domain might be associated, with the persistence of the virus in the acute phase of HEV infection, which could be explained by the appearance of mutants capable of overcoming the host immune response. Furthermore, a study has revealed that the complexity and heterogeneity of the Pro and X domains are correlated, indicating that they could have evolved together, since the ORF1 product might not undergo cleavage [Lhomme et al., 2014b].

Previously, the hypervariability of the Pro region was believed to result from the high rate of insertions and deletions, but a study showed that the rate in this region is similar to that in the rest of ORF1. The difference likely lies in the tolerance of mutations in the first and second codon positions, possibly because of its intrinsically disordered structure. This variability allows a shift in codon usage towards codons containing cytosine residues, which in turn produces more proline, alanine, serine, and threonine residues, which favor formation of disordered proline-rich structures [Purdy, 2012]. In contrast, Smith et al. have proposed that the requirement for certain amino acids in this region gives rise to the increased frequency of cytosines rather than being a consequence of it. Thorough analysis has shown that the evolution of the HEV Pro region is shaped by pressures leading to increased proline content with a consequent decreased frequency of aromatic amino acids [Lhomme et al., 2014b].

It has also been observed that the carboxyl half of the Pro region might be more permissive to mutations and may bind more ligands than the amino half [Purdy et al., 2012].

Curiously, analysis of HEV Pro region sequences has suggested that HEV-3 and HEV-4 strains share a common ancestor and are twofold more heterogenous than HEV-1 strains [Purdy et al., 2012]. At the same time, the zoonotic strains share a certain similarity in their purine/pyrimidine content in the amino half of the Pro domain. The same study also showed that this region is the only one within ORF1 in HEV-1, HEV-3, and HEV-4 that contains sites that are under positive selection, with 4–10 codons with a dN/dS ratio greater than 1, and it possesses the highest density of sites with homoplasy values greater than 0.5. Particularly, HEV-3 and HEV-4 showed threefold higher homoplastic values, whereas no difference was observed in HEV-1. This presence of numerous highly homoplastic sites indicates the operation of recurrent selection pressure on Pro in the zoonotic genotypes [Purdy et al., 2012].

Due to the numerous insertions and deletions, this region is the main one responsible for size differences in HEV genomes among genotypes [Pudupakam et al., 2011]. Indeed, sequence analysis at the amino acid level has revealed that the HVR region represents up to 71% of the sequence divergence between genotypes, with an intra-genotype variability of 31–46%. [Pudupakam et al., 2011], which is possibly related to adaptation to a wide range of hosts [Purdy et al., 2012].

Although it was demonstrated, using deletion mutants of HEV-1 replicons in Huh7 cells, that the HVR is not required for viral infectivity *in vitro*, it was observed that it influenced the efficiency of RNA replication, whereas deletion of nearly all of this region from an avian HEV infectious clone resulted in viral attenuation in chickens [Pudupakam et al., 2011, 2009]. Furthermore, it has been reported that HVR is functionally exchangeable between genotypes, resulting in genotype-specific differences in replication efficiency [Pudupakam et al., 2009, 2011]. Therefore, it has been suggested that the HVR may tolerate small deletions that do not affect infectivity but might be needed for interaction with viral and host factors for virus entry and assembly [Parvez, 2017b].

Additionally, the SH3 PxxP binding domains, which would seem to be a consequence of the proline content [Smith et al., 2012], were found in HVR of HEV1-4, and hence, these interaction motifs were believed to be employed by HEV to enhance its replication and/or infectivity [Pudupakam et al., 2011].

Further, an HEV-3 Pro 3D model protein was predicted to contain a peptide cleavage site modified by enzymes and that bind to proteins, nucleotides, and metal ions located in the conserved regions flanking the HVR, which have been shown to regulate cellular signal transduction, protein phosphorylation, transcription, and translation [Purdy et al., 2012]. Particularly, within the intrinsically disordered region (IDR) in the HVR/Pro domain of HEV1-4, seven putative linear motifs were located, including two

protease-cleavage sites, three ligand binding sites, and two kinase phosphorylation sites [Purdy et al., 2012]. Structure-based analysis showed that these linear motifs are able to bind a wide range of ligands.

In fact, peptides that contain a large number of proline residues act as ligands, since the cyclized side chain restricts movement of the backbone [Kay et al., 2000; Williamson, 1994]. Furthermore, the aforementioned Pro 3D model showed that this protein is highly polarized, negatively charged, and largely solvent accessible and flexible, which is common in IDRs [Purdy et al., 2012].

Interestingly, a 171-nt insertion of the human ribosomal protein S17 was detected in the HVR region of an isolate from a patient chronically infected with HEV and coinfected with HIV-1 (Kernow C1-p6 strain). This insertion has been suggested to confer a cell culture adaptation and growth advantage *in vitro* as well as expanding the host range, making it able to infect pig, deer, chicken, cat, dog, mouse, and hamster cells. Therefore, it has been proposed that the divergent HVR sequences might represent evolved host-derived sequences acquired during chronic infection [Nguyen et al., 2012; Shukla et al., 2012]. The authors suggest the possibility that this insertion might enhance the stability and/or translatability of the RNA or assist in the folding, processing, or stability of the ORF protein [Shukla et al., 2012]. Moreover, other HEV-3 strains have been reported to possess duplications or insertions in the HVR [Debing et al., 2016a; Legrand-Abravanel et al., 2009], suggesting that HEV recombination might not be such a rare event as previously thought [Parvez, 2017b]. This S17 gene insertion was demonstrated to confer nuclear/nucleolar trafficking ability to the ORF1 protein, and its lysine residues were associated with enhanced replication of that HEV strain [Kenney and Meng, 2015].

A recent study demonstrated that an HEV3 47832c strain (originally isolated from a chronically infected transplant patient) carries a bipartite insertion in the HVR, resulting from duplications of an adjacent part of the HVR and a part of its RdRp region, which can also enhance HEV cell culture replication. This effect seemed to be dependent on the translated amino acid sequence of the insertion instead of the RNA sequence [Scholz et al., 2021].

Additional recombinant events in the HEV Pro region have been reported in 11% (3/27) of strains isolated from French chronically infected solid-organ transplant recipients, and these involved parts of the Pro and RdRp, a fragment of a human tyrosine aminotransferase gene and a fragment of the human inter-α-trypsin inhibitor (ITI) gene, suggesting that the ITI gene insertion might confer increased HEV growth capacity *in vitro*. *In silico* analysis showed that these sequences, which are rich in aliphatic and basic amino acids, could provide acetylation, ubiquitination, and phosphorylation sites [Lhomme et al., 2014a]. However, in another study, three out of seven HEV-3 strains with genomic rearrangements were found in the acute phase of infection, six of which represented virus-host recombinants [Lhomme et al., 2020b]. Other human genes have been found to insert into this region as well, such as the eukaryotic translation elongation factor EEF1A1P13, the 18S ribosomal pseudogene RNA 18SP5, the kinesin family member KIF1B, and the zinc finger protein ZNF787 [Lhomme et al., 2020b].

A host-virus interaction analysis showed that HVR interacts directly with C3 (core component of the classical and alternative complement activation pathways), suggesting that this binding might alter or inhibit complement activation as a host immune evasion strategy [Subramani et al., 2018].

In summary, the Pro/HVR domain could be important for viral replication, with a structural rather than a regulatory or enzymatic function [Smith et al., 2012].

Due to the characteristics mentioned above, this region has been proposed as a target for development of novel antiviral drugs [Purdy et al., 2012].

X domain

The X domain is also known as the macrodomain, since it resembles the non-histone domain of the histone macro H2A and is recognized as a very conserved protein throughout evolution in all eukaryotic organisms, bacteria, and archaea, and is even present in members of three ss + RNA virus families: *Coronaviridae, Togaviridae*, and *Hepeviridae* [Li et al., 2016].

HEV domain X is classified as a member of the macrodomain protein family of ADP-ribose-1′′-monophosphatase (Appr-1″-pase), which catalyzes the reaction converting ADP-ribose-1″-monophosphate (a side product of cellular pre-tRNA splicing) to ADP-ribose [Parvez, 2015b]. Furthermore, the HEV macrodomain has been shown to have hydrolytic activity for mono-ADP-ribose (MAR) and poly-ADP-ribose (PAR) chain removal, known as de-MARylation and de-PARylation, respectively [Li et al., 2016]. Indeed, the HEV Hel domain, when located in *cis*, drastically increases the binding of the macrodomain to poly-ADP-ribose, promoting de-PARylation activity [Li et al., 2016].

When molecular modeling of the X domain was carried out in order to predict possible active ligand binding sites, 10 potential sites were identified, including sites for metallic ligands such as Mg^{2+} and Zn^{2+} [Vikram and Kumar, 2018].

In silico and *in vitro* analysis identified a putative Appr-1″-pase catalytic site "N806, N809, H812, G815, G816, and G817". The "G" triad forms a loop that connects "N" containing β-strand 3 and α-helix 1, homologous to RUBV

[Parvez, 2015b, 2013]. The mutations G816V and G817V have been shown to be lethal for replication of HEV strain Sar55 in S10-3 cells. Therefore, the regulatory or catalytic role of the X domain depends on this "N, N, H, G, G, G" sequence and/or secondary structure elements. It was then concluded that the HEV macrodomain is vital for genome replication at the post-translational stage [Parvez, 2015b], but not during the transcription process [Parvez, 2013].

Moreover, it was proposed that the C-terminal region of the X domain can interact directly with ORF3 and MT through "I66-I67" and "L101-L102", respectively, which are highly conserved residues among HEV genotypes [Anang et al., 2016]. The X domain binding region identified in this study was located almost inside the putative core MT domain (56–146 aa) [Anang et al., 2016].

Subsequently, HEV-human protein-protein interaction analysis showed that the PSMB1 protein (a component of the 20S proteasome) interacts with the X domain, apparently altering the processing of major histocompatibility complex (MHC) class I peptides [Subramani et al., 2018]. Additionally, the HEV X domain was found to interact with the RACK1 protein, which is believed to promote viral translation/replication [Subramani et al., 2018]. Interestingly, the HEV macrodomain has been shown to downregulate type I IFN synthesis *in vitro* by inhibiting poly(I:C)-induced phosphorylation of IRF-3, a key transcription factor for IFN induction [Nan et al., 2014b]. It has been suggested that this domain can bind directly to the light chain subunit of human ferritin, sequestering it in order to prevent its secretion and possibly suppressing the cellular innate immune response, since ferritin has been reported to be an acute-phase protein in viral hepatitis patients [Ojha and Lole, 2016].

On the other hand, it has been suggested that the great genetic heterogeneity within HEV quasispecies in the macrodomain for chronically HEV infected patients might favor the appearance of persistent variants [Lhomme et al., 2014b].

Hel domain

The helicases of RNA viruses can be classified into two superfamilies: SF1 and SF2 [Kadaré and Haenni, 1997]. The helicase of HEV, like those of other alphavirus-like superfamily members, belongs to the SF1 superfamily and contains a purine nucleoside triphosphate (NTP)-binding motif composed of the two conserved sites Walker A (aa 975–982) and Walker B (aa 1029–1032). The A site contains a stretch of hydrophobic residues followed by the conserved sequence GxxxxGKS/T (x being any amino acid), and it has been reported that it is directly involved in binding to the β and γ phosphates of the NTP. The B site is formed by a D residue and hydrophobic amino acids, and this site acts as a chelator of the Mg^{+2} of the Mg-NTP complex [Kadaré and Haenni, 1997].

Seven signature motifs, I (site A), Ia, II (site B), III, IV, V, and VI in colinear disposition, have been identified [Kadaré and Haenni, 1997; Koonin et al., 1992; Nan and Zhang, 2016]. Motifs Ia, III, and IV are the most variable, and their function is unknown [Kadaré and Haenni, 1997], while motif VI is believed to bind nucleic acids because it is rich in basic residues [Kadaré and Haenni, 1997].

The HEV Hel domain has been demonstrated to have NTPase activity and to be able to unwind duplex RNA with 5' overhangs with a 5′-3′ polarity [Karpe and Lole, 2010a]. Furthermore, HEV Hel can also hydrolyze rNTPs and dNTPs, but with lower efficiency [Karpe and Lole, 2010a]. This domain exhibits RNA 5′-triphosphatase activity (removal of γ-phosphate from the 5′ end of primary transcripts) and is suggested to participate in the first step of 5′ cap synthesis along with MT [Karpe and Lole, 2010b].

A mutagenesis study showed that motifs Ia and III are critical for Hel function, whereas I, IV, and VI are not essential [Mhaindarkar et al., 2014]. Moreover, in patients with fulminant hepatic failure, unique and highly conserved mutations in Hel domain have been reported. L1110F is specific to HEV1, and V1120I is frequent in HEV3 and rare in HEV4. These mutants expressed *in vitro* in *Escherichia coli* showed a slight decrease in ATPase activity; however, RNA unwinding activity was not affected. These mutations may be responsible for modifying virus-host protein-protein interaction, leading to an alteration in the host responses, which could therefore manifest as a more severe disease [Devhare et al., 2014]. On the other hand, expression in S10-3 cells resulted in a lower viral replication rate for the V1120I mutant. Altogether, the mutants′ replicons showed lower replication efficiency [Devhare et al., 2014].

Notably, mutations in the Walker A and Walker B motifs drastically reduced ATPase and RNA unwinding activity [Karpe and Lole, 2010a], while replacement of critical residues (GKS to GAS in site A and DE to AA in site B) completely eliminated viral RNA replication in a hepatoma cell line [Karpe and Lole, 2010a].

In another study, it was observed that the V1213A mutant had very low replication efficiency, and it was suggested that the amino acid V1213 favors the replication of HEV3 and HEV4, but not HEV1 [Cao et al., 2018a].

Interestingly, the substitution V239A found in Japanese patients infected with HEV3 of zoonotic origin was associated with increased virulence [Takahashi et al., 2009].

Recently, a 3D model of HEV Hel was constructed by homology modelling with tomato mosaic virus as a template (sharing 33% structural identity) for testing potential Hel compounds inhibitors *in silico*. According to the data, the most promising results were obtained with three molecules

(PubChem ID: JFD02650, RDR03130, and HTS11136), which interacted with residues in the Walker A site [Parvez and Subbarao, 2018].

Moreover, the interaction of the Hel domain with host factors C4a and C8 was identified by a protein-protein interaction analysis (components of the classical and alternative complement activation pathways), suggesting that this domain might also somehow alter or inhibit complement activation [Subramani et al., 2018].

RdRp domain

HEV has a type 3 RdRp, typical of the "alpha-like" supergroup III of RNA ss + viruses, where HEV RdRp, RubV RdRp, and BNYVV RdRp form a distinct close cluster. In this supergroup, eight conserved motifs (I-VIII) have been described [Koonin et al., 1992].

HEV RdRp contains the highly conserved motif GDD, which in general plays a crucial role in catalytic activity and metal ion coordination [Wang and Meng, 2021], which explains its conservation among a wide range of RdRps [Koonin et al., 1992]. In fact, *in vitro* substitutions in the GDD motif can abolish the RdRp activity of HEV [Emerson et al., 2004], HCV [Yamashita et al., 1998], RUBV [Wang and Gillam, 2001], calicivirus [Vázquez et al., 2000], and poliovirus [Jablonski and Morrow, 1995].

Localization studies revealed that HEV RdRp is present in the ER, suggesting the involvement of the ER membrane in HEV replication [Rehman et al., 2008].

Furthermore, it has been suggested that HEV RdRp can either initiate *de novo* synthesis from the RNA template or employ the template end to prime the synthesis from the 3′ OH end [Mahilkar et al., 2016]. Moreover, it has been demonstrated that the HEV RdRp binds specifically to the 3′ end of the HEV RNA, requiring two stem-loop structures known as SL1 (nt 7173–7194) and SL2 (nt 7089–7163) domains at the poly(A) stretch, which are separated by a single-stranded region. Therefore, the 3′ end of the viral genome acts as a CRE that is critical for the initiation of HEV genome replication [Agrawal et al., 2001].

The second CRE is located in the junction region (JR) (between ORF1 and the start site of the subgenomic region) of the HEV genome, which contains a highly conserved stem-loop structure that is essential for subgenomic RNA synthesis. This JR region exhibits sequence similarity to its homologue of RubV [Huang et al., 2004]. Recently, it was reported that the last 41 nt at the 3′ end of ORF1 (surrounding the JR) also fold into a stem-loop structure that might act as an enhancer for the subgenomic RNA promoter [Cao et al., 2018b]. In summary, it has been proposed that HEV RdRp binds to the SL in the JR and that the upstream nucleotides at the 3′ end of ORF1 stabilize the binding of RdRp to the minus-strand RNA to promote replication, suggesting that the 3′ end of ORF1 might be a component of the subgenomic RNA promoter [Cao et al., 2018b].

Protein-protein interaction analysis revealed that the RdRp interacts with cellular C3, C8, and C4a proteins, possibly altering or inhibiting complement activation [Subramani et al., 2018], as mentioned for the other domains (Hel and HVR) described in this review. Interestingly, HEV RdRp interacts directly with eIF4A2, recruiting the host factors eIF4E and eIF4G into the viral replication complex, forming the eIF4F complex (an element of the host translation machinery). HEV RdRp is also able to interact with the factor eIF3A, which has been shown to be involved in the viral replication process, and the modulation of its activity might favor the translation of viral RNA by shutting down host protein synthesis. Indeed, it was observed that the host factor eEF1A1 is key for RdRp activity and for the stabilization of the viral translation/replication complex [Subramani et al., 2018]. Recently, the interaction of the host proteins HNRNPK and HNRNPA2B1 (nuclear ribonucleoproteins) with HEV RdRp was reported, and these proteins are believed to play a crucial role in viral replication [Kanade et al., 2019].

Some attention has been given to the role of the tetratricopeptide repeat 1 protein (IFIT1), which is part of the interferon-stimulated gene cascade activated by the host´s innate antiviral response. IFIT1 recognizes cap0 RNA structures (m7G) and blocks the binding of the eukaryotic translation initiation factor eIF4E to the RNA, thus inhibiting translation [Andrejeva et al., 2013]. In this case, it was demonstrated that HEV RdRp interacts directly with IFIT1, thereby protecting HEV RNA by preventing its binding to IFIT1, leaving HEV RNA available for the translation process [Pingale et al., 2019].

On the other hand, an analysis of the intraviral interactome showed that HEV RdRp can self-interact, which is apparently important for its polymerase function, and at the same time, it can interact with the PCP domain [Osterman et al., 2015].

Ribavirin (RBV) (1-β-D-ribofuranosyl-1,2,4-triazole), a synthetic guanosine/adenosine analog with a broad antiviral spectrum, is the only drug approved for the treatment of chronic HEV infection. RBV can be incorporated by the RdRp into the nascent viral RNA, where it induces base transitions, causes early chain termination, and interferes with replication by competitively inhibiting the binding of nucleotides [Feld and Hoofnagle, 2005]. Recently, treatment failure in chronically infected patients has been reported to be due to HEV antiviral resistance, probably associated with G1634R, Y1320H, and K1383N substitutions in the RdRp [Debing et al., 2016b]. The K1383N substitution strongly decreases viral replication and increases RBV sensitivity *in*

vitro, opposite to the observed clinical phenotype [Debing et al., 2016b]. However, the Y1320H substitution increases HEV replication efficiency without altering RBV sensitivity, and this may be a compensatory change that helps to overcome the fitness loss resulting from the K1383N mutation. The G1634R substitution seemed to increase the replicative capacity of HEV and reduce the efficiency of RBV [Debing et al., 2014]. This substitution has also been demonstrated to increase viral titers in cell culture [Todt et al., 2020].

Other substitutions have also been reported in HEV-infected patients (D1384G, K1398R, V1479I, Y1587F) that possibly affect HEV replication by modulating RdRp activity [Debing et al., 2016a; Todt et al., 2016b, 2016a]. The substitutions mutants C1483W and N1530T isolated from acute liver failure patients with HEV have been strongly associated with high viral loads and mortality [Mishra et al., 2013], and the substitution F1439Y has been reported to be significantly associated with fulminant liver failure [Smith and Simmonds, 2015].

Recently, our group reported *in silico* 3D modelling studies of the HEV3 RdRp from a chronic patient in whom we identified a region of the HEV RdRp that hypothetically interacts with incoming nucleotides or RBV and performed molecular docking and molecular dynamics simulations between the enzyme and RBV triphosphate or GTP. The RBVT-HEV3 RdRp interaction was mediated by six hydrogen-bonds Q195-O14, S198-O11, E257-O13, S260-O2, O3, and S311-O11 [Cancela et al., 2021].

Moreover, with the aim of exploring novel antiviral therapy strategies for hepatitis E management, one research group reported the role of the microRNA miR-122 in HEV infection and replication. MicroRNA miR-122 is the most abundant liver-specific miRNA and is involved in numerous pathophysiological processes. *In silico* analysis of HEV1 to HEV4 sequences predicted most of them to have at least one miR-122 site. Notably, HEV1 genome sequences contained a highly conserved miR-122 target site in the RdRp region. *In vitro* studies employing HEV1 and HEV3 replicons in hepatoma cells showed that miR-122 promotes HEV replication, while inhibition of miR-122 decreased HEV replication dramatically. Thus, this role of miR-122 in HEV replication represents an opportunity for the development of new potential HEV antiviral drugs [Haldipur et al., 2018].

ORF2

ORF2 is 1983 nt in length, starting 37 nt downstream of the ORF1 stop codon and overlapping with ORF3 except for 14 nt, ending 65 nt upstream of the poly-A tail. The encoded viral structural protein has 660 aa residues and a predicted molecular mass of 72 kDa [Nan and Zhang, 2016].

It has been suggested recently that the ORF2 protein present in the serum of HEV-infected patients and the supernatant cultured cells exists mostly as a free form that is not associated with viral particles. Two forms have been described for the ORF2 protein, a secreted form ($ORF2^s$) and a capsid-associated form ($ORF2^c$). $ORF2^c$ is translated at a previously unknown internal AUG codon (15 aa downstream from the start of $ORF2^s$) and remains in the cytosol to be incorporated into infectious virus particles.

On the other hand, $ORF2^s$ is secreted in the extracellular space in the form of a glycosylated dimer, and it lacks the regions involved in cell binding. In cultured cells, studies have suggested that $ORF2^s$ is not essential in the HEV life cycle but is capable of reducing antibody-mediated neutralization [Montpellier et al., 2018; Yin et al., 2018].

A 3.5-Å crystal structure was obtained from an HEV virus-like particle (VLP), in which three linear domains were identified: S, the shell domain (aa 129–319); M, the middle domain (aa 320–455); and P, the protruding domain, also known as E2s (aa 456–606). The icosahedral S domain adopts a classical antiparallel jelly-roll β-barrel fold with eight β-strands (named B to I) and four short α-helices strengthened by 3-fold protrusions formed by M and 2-fold spikes of P. Its inner region is rich in basic amino acids (six arginine residues per subunit), which could participate in neutralizing the negative charges of the genomic RNA [Guu et al., 2009]. Four loops have been identified between the β-sheets in the S domain, named loops B–C (aa 139–152), D–E (aa 196–206), F–G (aa 236–241), and H–I (aa 281–296), around the center of the pentamer structure, in which α1 and α4 were found between strands C/D and D/F, respectively [Yamashita et al., 2009].

The M domain, which is closely associated with the S domain (through βB, βC, and loops CD, EF, GH) and positioned on the surface around the icosahedral 3-fold axis, forms a twisted antiparallel squashed β-barrel structure consisting of six β-strands and four short α-helices and is involved in the trimeric interaction [Yamashita et al., 2009]. This domain also contains a putative sialic acid binding site in a helix-turn-helix motif (aa 376–391) positioned at one end of the β-barrel [Guu et al., 2009].

The P domain in the HEV VLP forms a twisted antiparallel β-sheet structure and is connected to the M domain by a long proline-rich hinge "445-NQHEQDRPTPSPAP-SRPF-462" (making the capsid more resistant to proteases), contributing to dimer formation on the capsid surface [Yamashita et al., 2009]. The P domain contains a large insertion (aa 504–533), compared to the M region, between β20 and β22 of the central β-barrel. This 30-aa insertion (three β-strands and one α-helix) mediates the interaction between the surface spike and the 3-fold protrusion [Guu et al., 2009]. Three highly exposed loop insertions (aa

482–490, 550–566 and 583–593) can be found on the top of this surface spike, which is suggested to participate in antigenicity determination [Guu et al., 2009].

The region located at residues 118–131 of the HEV capsid protein form the N-terminal arm, which makes a sharp turn at the beginning of βB, initiating an extended loop interacting with a 2-fold-related and a 3-fold-related adjacent molecule [Guu et al., 2009].

The HEV capsid protein contains a signal sequence in the N-terminal region of 22 aa (consisting of arginine-rich residues, a 14-aa hydrophobic core and a turn-inducing stretch of proline residues) and N-linked glycosylation sites (N137, N310, and N562). N562 appears to be important for dimerization of the capsid protein [Xu et al., 2016]. It also contains a putative ER localization signal at its N-terminus [Surjit et al., 2007].

Interestingly, expression of the complete ORF2 in insect cells resulted in proteolytic cleavage of the first 111 and the last 52 residues (lacking the signal sequence) [Zhang et al., 1997], producing a 55-kDa protein that can self-assemble into VLPs [Xing et al., 1999]. However, its expression in mammalian cells yielded two protein forms, a 74-kDa form corresponding to the unglycosylated protein and an 88-kDa form corresponding to the glycosylated protein [Jameel et al., 1996].

Xing et al. reported that infection of insect cells with an ORF2-producing recombinant baculovirus (with a deletion of the N-terminal 13 aa) resulted in two types of particles, HEV-VLP/ T = 1 and HEV-VLP/ T = 3 [Xing et al., 2010].

HEV-VLP/T = 1 produced *in vitro* has icosahedral symmetry with an external diameter of 270 Å and is composed of 60 subunits of truncated capsid protein producing the icosahedral 2-, 3-, and 5-fold axes.

The capsid subunit interactions needed for HEV-VLP T = 1 packaging are dimeric, trimeric, and pentameric, occurring at the 2-, 3-, and 5-fold axes [Guu et al., 2009]. The particle also has 30 dimeric protrusions at the 2-fold axes of the surface with deep depressions at the 3- and 5-fold axes. Moreover, the P domain dimer produces the protruding spikes around the 2-fold axes of HEV-VLP T = 1, stabilizing capsid protein interactions [Guu et al., 2009]. Dimerization of the P domain is mediated by an extended loop (aa 550–566) and three β-strands from the central β-barrel (β18, β24, and β27).

Mutagenesis analysis revealed that residues A597, V598, A599, L601, and A602 are critical for the dimeric interaction [Li et al., 2005]. Additionally, it was shown that amino acid substitutions in β-strand 27 at the dimer interface formed by residues 585–610 could possibly lead to a folding alteration resulting in a disruption of the compact packing between the two β-sheets [Guu et al., 2009].

In contrast to the T = 1 particle, the T = 3 particle (180 capsid subunits), with an outer diameter of 370Å, has a total of 90 surface spikes (dimers C-C and A-B) and 60 trimeric protrusions (A-B-C) [Guu et al., 2009]. Structural modeling analysis showed that the assembly of the native T = 3 capsid, unlike HEV-VLP T = 1, requires flat capsid protein dimers [Yamashita et al., 2009]. The A-B subunits form a dimer with bent conformation around the 5-fold axis, whereas the C monomers have a flat conformation at the 2-fold icosahedral axis. The orientation of the P domain C-C dimer in the HEV-VLP T = 3 particle relative to the M and S domains is turned by 90° compared to the A-B dimer and the dimer in HEV-VLP T = 1, possibly facilitated by the proline-rich hinge between the P and M domains [Mori and Matsuura, 2011].

However, the HEV-VLP T = 1 particle seemed to exhibit properties similar to those of the native virion with respect to antigenicity and surface substructure [Li et al., 2004; Xing et al., 1999].

The capsid protein has been demonstrated to inhibit type I and type III IFNs by interacting with the MAVS-TBK1-IRF3 complex, thus blocking the phosphorylation of IRF3. The arginine-rich motif within the N-terminus of the ORF2 protein is critical for this inhibition [Lin et al., 2019].

The capsid protein has also been found to inhibit signaling by the RIG-1 and Toll-like receptor (TLR) adapters IPS-1, MyD88, and TRIF [Hingane et al., 2020].

It has also been demonstrated that cells expressing ORF2 can activate the pro-apoptotic gene CHOP, mediated by ATF4. ORF2 is also able to increase phosphorylation of eukaryotic initiation factor 2 alpha and promote ATF4 translation. However, no apoptosis has been reported in these cases. Contrarily, ORF2 can induce upregulation of chaperones (such as HS70B' and Hsp72) and co-chaperones (such as Hsp40), which could correspond to a survival mechanism instead [John et al., 2011].

Interestingly, the glycosylated form of ORF2 is associated with NF-κB inhibition activity by its direct association with the protein βTRCP and thus blocks the assembly of the IκBα ubiquitination complex [Surjit et al., 2012].

The HEV virion resembles plant RNA ss + viruses (tombusviruses and sobemoviruses) in its assembly pathway due to the employment of a long electropositive N-terminal domain to interact with genomic RNA. Molecular simulations have suggested that the ORF2 decamer is the assembly intermediate of the T = 3 HEV particle [Yamashita et al., 2009].

The E2s domain (P domain) has been identified as the minimum antigenic domain (aa 455–602) capable of inducing HEV-neutralizing antibodies [Zhao et al., 2015], as it contains the immunodominant epitopes [Guu et al., 2009; Li et al., 2009; Yamashita et al., 2009]. The crystal structure

of E2s has been reported previously [Li et al., 2009], and the dimerization of this domain has been demonstrated to be important for host interactions in all HEV genotypes [Li et al., 2009].

It has been observed that the packing of this domain results in a flat conformation of the dimer, which is thought to be stabilized by the hydrophobic residues 585–595 [Bai et al., 2020].

E2s forms a β-barrel in which the residues from β2, β3, β6, and β7 as well as the loops protrude at one side of the structure in order to produce a surface groove (15-Å width and 11-Å depth). This β-barrel possesses nine antiparallel β-strands, in which on one side there are three loops that connect adjacent β-strands, while on the other side, three loops and a double-stranded β-sheet link the adjacent β-strand. The inner pore consists of 28 hydrophobic residues blocked by loops at the top and bottom of the cavity connecting residues T586-A590 and A467-F462, which are possibly involved in recognizing hydrophobic ligands [Li et al., 2009].

In 2018, a liver-transplanted patient with hepatitis E caused by rat HEV-C (species C) was reported for the first-time [Sridhar et al., 2018]. Very recently, the crystal structure of the HEV-C E2s domain was determined at 1.8Å resolution. HEV-C E2s has 41% aa sequence identity to HEV E2s from species A (HEV-A E2s), but they nevertheless share a conserved overall structure. HEV-C E2s consists of a compact barrel with 12 β-strands linked by loops and a unique groove region. Inside the β-barrel, a highly hydrophobic cavity (30 Å deep) was identified, blocked by loops containing residues that are conserved (I583-P594 and T552-D567) among members of the family *Hepeviridae* [Bai et al., 2020]. The groove region (15 Å wide and 10.5 Å deep) formed by β2, β6, β7, β9, and β10 were connected by fusion loops at one side containing hydrophobic residues (A481, A486, M487, G488, P491, G433, and L534) [He et al., 2008] and was reported to be the likely antibody recognition site of HEV [Li et al., 2009].

Interestingly, structure-based mutagenesis done with VLPs revealed that E549A, K554A, G591A, and D430A substitutions in the E2s region completely abolished HEV host-cell penetration [Gu et al., 2015]. Furthermore, the amino acid mutations F51L, T59A, and S390L have been associated with attenuation of HEV in pig models [Córdoba et al., 2011].

A monoclonal antibody, 8C11, has been reported to recognize a neutralizing conformational epitope exclusively on HEV1 (preventing the VLP from binding and entering the host cell). The 8C11 epitopes on E2s, identified by X-ray crystallography, were D496-T499, V510-L514, and N573-R578, where R512 was recognized as the key residue for neutralization [Tang et al., 2011].

Moreover, using the monoclonal antibodies 3E8 and 1B5 against avian HEV capsid protein, it was shown that the motifs I/VPHD and VKLYM/TS are critical for the interaction, and both epitopes seemed to be present in avian, swine, and human HEV [Wang et al., 2015].

Although the cell receptor for HEV has not been identified, several host factors have been suggested to be involved in cell attachment and/or entry of HEV. In the case of the naked HEV particle, the following putative cell receptors have been described: heparan sulfate proteoglycans (HSPGs), glucose-regulated protein 78 (GRP78/Bip), asialoglycoprotein receptor (ASGPR), ATP synthase subunit 5β (ATP5B), and integrin alpha 3 (ITGA3) [Wißing et al., 2021; Yin and Feng, 2019].

VLPs from recombinant ORF2 have been reported to bind target cells via cell-surface HSPGs on syndecans in Huh7 cells [Kalia et al., 2009], whereas for the "quasi-enveloped" HEV, HSPGs were not essential for cell attachment and infection [Yin et al., 2016].

GRP78/Bip, a molecular chaperone located in the ER, was found by interaction studies to bind the recombinant ORF2 protein (aa 368–606), p239 [Zheng et al., 2010].

ASGPR is present in the basolateral membrane of hepatocytes, and its expression in HeLa cells resulted in an increase in HEV binding ability, while a depletion of ASGPR in PLC/PRF/5 cells decreased HEV binding, but not virion release [Zhang et al., 2016].

On the other hand, the "quasi-enveloped" HEV membrane contains phosphatidylserine, which might bind to the cell surface receptor T cell immunoglobulin mucin domain 1 (TIM-1) on target cells acting as an attachment factor [Wißing et al., 2021; Yin and Feng, 2019].

In the past few years, significant efforts have been made in the development of HEV vaccines based on the ORF2 protein as a subunit or as a VLP. So far, no success has been achieved in the production of VLPs in plants [Ma et al., 2003; Maloney et al., 2005; Mazalovska et al., 2017; Zhou et al., 2006]. Similarly, in baculovirus-insect cell system the expression of the whole ORF2 did not produce VLPs [Li et al., 1997]. However, in the Tn5 cell line, VLP formation was achieved once the N-terminal region was truncated [T.-C. Li et al., 2015; Zhou et al., 2015].

Expression of recombinant ORF2 in *E. coli* has produced highly immunogenic VLPs (HEV 239), which have been shown to be safe and effective for humans in phase II and phase III clinical trials [Zhang et al., 2009; Zhu et al., 2010]. This Hecolin® (HEV 239) vaccine has been licensed for use in China since 2012 [S.-W. Li et al., 2015; Park, 2012], providing long-term protection for 4.5 years with 86.6% efficacy [Zhang et al., 2015]. However, for global use, further assessment of safety and efficacy in risk groups must be still carried out. Indeed, two clinical trials are taking place:

phase I in the USA – NCT03827395 and phase IV in Bangladesh in pregnant women – NCT02759991 [Zaman et al., 2020]. A phase I clinical trial for a very recent VLP vaccine (p179) generated from HEV4 in China is ongoing [Cao et al., 2017].

ORF3

ORF3 is the smallest ORF in the HEV genome. It is translated from a subgenomic RNA and overlaps with ORF2 by 300 nt in a different frame, producing a 113- to 115-aa protein. This overlapping region (nt 5145–5475) has been identified as the most conserved region in various HEV strains [Nan and Zhang, 2016]. This phosphoprotein (also known as VP13) has a molecular weight of 13 kDa [Holla et al., 2013].

VP13 contains two major N-terminal hydrophobic domains D1 (aa 7–23) and D2 (aa 28–53) and two proline-rich regions in its C-terminus, P1 (aa 66–77) and P2 (aa 95–111) [Holla et al., 2013]. The D1 domain is rich in cysteine and is necessary for to association of VP13 with the cytoskeleton [Holla et al., 2013].

It has been demonstrated that VP13 interacts with microtubules through both hydrophobic N-terminal domains by electrostatic interactions (behaving like a microtubule-associated protein), and this interaction possibly inhibits the release of cytochrome c, thus protecting the cell from apoptosis and favouring successful HEV infection. Moreover, VP13 has been suggested to be transported to the microtubule organizing center by its association with dynein [Kannan et al., 2009].

The P1 domain contains a PMSP motif in which the residue S71 can be phosphorylated by extracellular signal-regulated kinase (ERK), a member of the mitogen-activated protein kinase (MAPK) family [Nan and Zhang, 2016]. It has been suggested that VP13 phosphorylation is not necessary for HEV replication and infection in cultured cells and rhesus monkeys [Graff et al., 2005].

Moreover, VP13 binds to the linker region of MAPK phosphatase 3 (MKP-3), and this interaction blocks the conformational change needed for its correct function, leading to activation of ERK by inhibiting this phosphatase [Kar-Roy et al., 2004]. Furthermore, the activation of ERK also reduces the levels of pSTAT3 [Chandra et al., 2008a], thus promoting cell proliferation.

The P2 domain has one PSAP motif (aa 95–98) that is conserved in all HEV strains, while HEV3 possess one additional PSAP motif located at aa 86–89. The PSAP motif at aa 95–98 has been shown to be a functional domain for virion release. The PXXP motifs in the P2 domain can bind many SRC homology 3 (SH3) domains from other proteins [Nagashima et al., 2011b], which suggests that the ORF3 protein can modulate the cellular environment for infection [Holla et al., 2013]. This P2 forms a type II polyproline helix with SH3, with three residues per turn [Cohen et al., 1995; Pawson, 1995], and this structure is stabilized by a salt bridge between the terminal arginine of P2 and a conserved acidic residue in SH3 [Korkaya et al., 2001].

VP13 interacts with CIN85 (a protein involved in the downregulation of receptor tyrosine kinases) and delays the internalization of activated growth factor receptors [Chandra et al., 2008a].

Another protein that has been shown to bind the D2 domain of VP13 is human hemopexin, which is an acute-phase protein involved in heme transport in plasma and protection of hemoglobin against oxidative damage [Ratra et al., 2008].

Cells expressing ORF3 also exhibit high levels of hexokinase and oligomeric forms of the voltage-dependent anion channel, resulting in downregulation of the signaling pathway for mitochondrial death [Moin et al., 2007]. All of this results in a reduced inflammatory response in the liver to facilitate HEV infection [Holla et al., 2013].

The ORF3 protein has also been reported to interact with α_1 microglobulin bikunin precursor protein (AMBP) and its corresponding product α_1m (an immunosuppressive molecule), promoting its secretion, mediated by tumor susceptibility gene 101 (Tsg101), which is a central component of the endosomal sorting pathway (ESCRT). VP13 binds to Tsg101 through the conserved PSAP motif in the P2 domain, and overexpression of this immunosuppressive molecule creates a protective state for the infected hepatocyte [Surjit et al., 2006]. ESCRT is involved in the budding of several enveloped viruses, and studies have shown that HEV forms membrane-associated particles in the cytoplasm, possibly mediated by the interaction with ESCRT machinery, induced by the enzyme class E vacuolar protein sorting (Vps4) [Nagashima et al., 2011a]. The multivesicular body pathway is afterwards required to release the "quasi-enveloped" viral particles [Nagashima et al., 2014]. It has been reported that VP13 binds to the surface of "quasi-enveloped" HEV virions in the patients' blood and in cell-culture, but not in feces [Takahashi et al., 2008]. Thus, the PSAP motif acts as a functional domain for HEV egress [Nagashima et al., 2011b]. Also, VP13 phosphorylated at S80 has been reported to interact with non-glycosylated ORF2. [Tyagi et al., 2002].

Interestingly, VP13 has been shown to be an ion channel viroporin (similar to class IA viroporins) that is required for the release of infectious viral particles [Ding et al., 2017].

VP13 stabilizes the highly unstable α subunit of hypoxia inducible factor (HIF-α) by activating the PI3K/Akt signaling pathway, which accumulates HIF-α and recruits phosphorylated p300/CBP, leading to transcriptional activation

of genes encoding glycolytic enzymes. This action may regulate energy homeostasis to create a favorable environment in HEV-infected cells [Moin et al., 2009].

Notably, it has been observed that VP13 is able to regulate several hepatotropic proteins through the induction of phosphorylation of hepatocyte nuclear factor 4 (HNF4), resulting in its reduced translocation to the nucleus and thus in diminished transcription factor activity, which could also contribute to the HEV infection state [Chandra et al., 2011].

In vitro studies have also demonstrated that VP13 enhances IFN expression in HeLa cells induced by the synthetic analog of double-stranded RNA (dsRNA), poly I:C, by increasing RIG-1 expression. VP13 interacts with N-terminal domain of RIG-1 and promotes its ubiquitination, which is necessary for RIG-1 activation. Of note, it has been observed that only HEV1 and HEV3 are able to enhance RIG-1 signaling, while HEV2 and HEV4 do not have this effect. Since VP13 is required for HEV infection *in vivo*, it has been suggested that this enhancement may be involved in HEV invasion [Nan et al., 2014a].

Moreover, the P2 domain of VP13 represses the NF-κB pathway via Toll-like receptor 3 signaling (TLR3 detects dsRNA) by degrading tumor necrosis factor receptor type 1 (TRADD) and decreasing receptor-interacting serine/threonine-protein kinase 1 (RIP1) K63 ubiquitination in A549 poly-I:C-induced cells. This effect reduces the inflammatory response and therefore likely promotes cell survival [He et al., 2016].

On the other hand, VP13 has been reported to block STAT1 phosphorylation by inhibiting IFN-α signaling, and also to downregulate some IFN-α-stimulated genes in A549 cells [Dong et al., 2012].

Additional *in vitro* interaction studies revealed that VP13 can associate with hepsin, which is a type II transmembrane serine protease related to the progression of cancer [Wang et al., 2014], and with the fibrinogen Bβ chain (FBG), which is involved in the inflammatory response [Ratra et al., 2009]. Furthermore, VP13 has been found to interact with 32 proteins, mostly ones related to blood coagulation and homeostasis, suggesting that this viral protein may alter the coagulation and fibrinolysis processes [Geng et al., 2013]. In fact, in patients with hepatitis E, elevated levels of transaminase enzymes have been associated with coagulopathies and severe disease [Ibrahim et al., 2009].

VP13 can also activate the MAPK-JNK1/2 pathway in infected hepatocytes *ex vivo*, which has been suggested to induce pro-survival cell signaling, thus allowing chronic HEV infection [Parvez and Al-Dosari, 2015].

In addition, VP13 has been found to be palmitoylated in a cysteine-rich part of the N-terminal region. This palmitoylation is critical for VP13 membrane association and subcellular localization, and it is possibly involved in stabilization of the viral protein. These cysteine residues have also been shown to be necessary for the secretion of infectious virions, indicating that posttranslational modifications mediated by the host cell play a key functional role for HEV [Gouttenoire et al., 2018].

ORF4

ORF4 (nt 2835–3308), which is present exclusively in HEV1, is synthesized only under ER stress conditions, in an alternative reading frame. It is a short-lived protein, and its amino acid sequence is generally conserved among HEV1 strains. ORF4 translation is dependent on an IRES-like element at nt 2701–2787. The ORF4 product is indispensable for HEV1 replication and interacts with multiple viral proteins to assemble a viral replication complex of RdRp, Hel, and X proteins, and the ORF4 protein promotes RdRp activity by interacting with host eEF1α1 and tubulin β [Nair et al., 2016].

Interestingly, ORF4 has been demonstrated to be degraded by the host proteasome, as it possesses a proteasomal degradation signal, which might be an antiviral strategy to restrict virus spread. This putative ubiquitination site is located in a region containing residue K51, which is flanked by two P residues. Sequence analysis of HEV from infected patients showed that most of the HEV1 isolates analyzed demonstrated conservation of K51, whereas the ubiquitination site was lost in some strains due to an amino acid change from P50 to L50, suggesting that HEV in those patients produced a proteasome-resistant ORF4.

Since ORF4 is produced under ER stress, HEV1 replication in cell culture is very inefficient, except in cell lines stably expressing ORF4 or with viral mutants with proteasome-resistant ORF4 [Nair et al., 2016].

In silico sequence and structure analysis has shown that ORF4 has an IDR that is enriched in typically disorder-promoting residues (R, P, and S) and neutral residues (A, G, and T). Moreover, a high abundance of structure-breaking residues (G and P) reinforces this hypothesis [Shafat et al., 2021].

Recently, ORF4 codon usage analysis patterns showed an overrepresentation of C, while A was the least represented nucleotide. It was also observed that the preferred codons mostly ended with C and G, which might be useful information for efficient expression of the ORF4 protein [Shafat et al., 2022].

Table 1 Important questions about different aspects of the HEV ORF1, ORF2, ORF3, and ORF4 proteins that remain to be elucidated

	Remaining questions
• What is the structure of the *cis*-acting elements? • Can this RNA structures be a target of novel drugs for antiviral purposes?	
ORF1	• Is the polyprotein processed into several domains? Can factor Xa and thrombin cleave it? Is it critical for HEV replication? • Which function does the MT domain have with or without the “iceberg region”? • What is the Y domain structure? • What is the exact role of the zinc finger in the PCP domain? Is it structural or catalytic? • Is it possible to develop antiviral drugs targeting the Pro and HVR domains? • How do the insertion of human genes and the insertion of duplications from the HEV genome itself in the HVR domain contribute to cell culture adaptation? • Does the genetic variability of the X domain contribute to chronic HEV infection? • How does the RdRp self-interact and interact with the PCP domain? • What is the function of the RBV-associated substitutions G1634R, Y1320H and K1383N?
ORF2	• What is the structure of ORF2^{s}? How does it differ from that of ORF2^{c}? • What are the cell receptors involved in the attachment of enveloped and non-enveloped particles?
ORF3	• How does VP13 interact with the microtubules? • How is VP13 palmitoylated? • Is VP13 phosphorylation critical for the HEV life cycle? • What is the VP13 viroporin structure? • How is VP13 involved in the acquisition of the "quasi-envelope" of the viral particle?
ORF4	• Why is ORF4 present exclusively in HEV1 strains? • What is the structure of ORF4? • What is the exact role of ORF4?

Conclusions and perspectives

Although important breakthroughs have been achieved in the last few years in terms of deciphering HEV protein structure and function, many crucial aspects involving functional domains, host-cell interactions, pathogenesis, and interactions with antiviral drugs remain to be elucidated, which therefore hinders our understanding of HEV biology. Some important and interesting issues regarding HEV proteins that need to be clarified are summarized in Table 1.

A particularly interesting question that remains to be addressed is the involvement of the ORF3 protein in the formation of "quasi-enveloped" particles and virion release. Determining the molecular mechanisms of this process might be helpful for understanding why the two HEV particles types (naked and "quasi-enveloped") seem to bind different cellular receptors, and, at the same time, it would be relevant to study if this difference in cellular receptor use might influence tissue tropism, as several extrahepatic manifestations have been reported.

Another relevant aspect that needs to be studied is the structure and function of ORF2^{s} which could help to explain its role in immune evasion and infection, mainly its possible immunomodulatory function in HEV persistence. In fact, during an HEV infection, ORF2^{s} has been suggested to act as a decoy against the humoral immunity, as the "quasi-enveloped" particles in the bloodstream are insensitive to neutralizing antibodies.

From the start, *in vitro* isolation of HEV has posed a challenge, and the lack of an efficient and standardized system has hampered the characterization of this virus. However, some *in vitro* and *in vivo* models, including novel human liver chimeric mice, have been reported to carry out HEV replication (especially in certain adapted strains) from HEV replicons, recombinant proteins, or fully infectious particles [Fu et al., 2019; Sayed et al., 2019]. Recently, a human-liver-derived 3D organoid system was reported to be highly permissive for HEV infection [Li et al., 2022], representing an interesting strategy for future research on cellular receptors for HEV and antiviral drug development.

To fill some knowledge gaps about HEV proteins, more-efficient cell-culture- or animal-model-based studies are still needed. For instance, recent methodologies such as CRISPR/Cas9 and approaches such as ribosome profiling (Ribo-Seq) could help to deepen our knowledge about HEV molecular biology. CRISPR/Cas9 is a powerful, valuable, and robust tool for gene editing that could allow the host factors acting as cellular receptors for the naked and "quasi-enveloped" particles to be identified. Ribo-Seq has not been employed in HEV research so far. This approach, developed by Ingolia et al. in 2009 [Ingolia et al., 2009], allows viral elements that are being actively translated in infected cells to be identified and characterized by high-throughput sequencing. Additionally, it is possible to calculate the translation efficiency of the expressed genes [Stern-Ginossar, 2015]. So far, the ribosome profile has been reported for only a few viruses, including SARS-CoV-2 [Finkel et al., 2020]. In the case of HEV, this method would allow mapping of the HEV translatome, quantification of the expression of the canonical ORFs, identification of possible unannotated ORFs, and investigation of virus-cell interactions.

Finally, structural data obtained by NMR or X-ray crystallography or *in silico* 3D modelling is still needed to determine the structural features of the remaining HEV proteins.

Author contributions Conceptualization was done by Santiago Mirazo and Florencia Cancela. Writing of the original draft was done by Florencia Cancela and Ofelia Noceti. Reviewing and editing of the manuscript were done by Santiago Mirazo and Juan Arbiza. All authors read and approved the final manuscript.

Funding F.C. PhD fellowship by Comisión Académica de Posgrado-

UdelaR.

Declarations

Conflict of interest The authors declare that there are no conflicts of interest.

Ethical approval This article does not contain any studies with human participants or animals performed by any of the authors.

References

Agrawal S, Gupta D, Panda SK (2001) The 3' end of hepatitis E virus (HEV) genome binds specifically to the viral RNA-dependent RNA polymerase (RdRp). Virology 282:87–101. https://doi.org/10.1006/viro.2000.0819

Ahola T, Karlin DG (2015) Sequence analysis reveals a conserved extension in the capping enzyme of the alphavirus supergroup, and a homologous domain in nodaviruses. Biol Direct 10:16. https://doi.org/10.1186/s13062-015-0050-0

Anang S, Subramani C, Nair VP, Kaul S, Kaushik N, Sharma C, Tiwari A, Ranjith-Kumar CT, Surjit M (2016) Identification of critical residues in Hepatitis E virus macro domain involved in its interaction with viral methyltransferase and ORF3 proteins. Sci Rep 6:25133. https://doi.org/10.1038/srep25133

Andrejeva J, Norsted H, Habjan M, Thiel V, Goodbourn S, Randall RE (2013) ISG56/IFIT1 is primarily responsible for interferon-induced changes to patterns of parainfluenza virus type 5 transcription and protein synthesis. J Gen Virol 94:59–68. https://doi.org/10.1099/vir.0.046797-0

Ansari IH, Nanda SK, Durgapal H, Agrawal S, Mohanty SK, Gupta D, Jameel S, Panda SK (2000) Cloning, sequencing, and expression of the hepatitis E virus (HEV) nonstructural open reading frame 1 (ORF1). J Med Virol 60:275–283

Bagdassarian E, Doceul V, Pellerin M, Demange A, Meyer L, Jouvenet N, Pavio N (2018) The Amino-Terminal Region of Hepatitis E Virus ORF1 Containing a Methyltransferase (Met) and a Papain-Like Cysteine Protease (PCP) Domain Counteracts Type I Interferon Response. https://doi.org/10.3390/v10120726. Viruses 10

Bai C, Cai J, Han P, Qi J, Yuen K-Y, Wang Q (2020) The crystal structure of the emerging human-infecting hepatitis E virus E2s protein. Biochem Biophys Res Commun 532:25–31. https://doi.org/10.1016/j.bbrc.2020.07.074

Batts W, Yun S, Hedrick R, Winton J (2011) A novel member of the family Hepeviridae from cutthroat trout (Oncorhynchus clarkii). Virus Res 158:116–123. https://doi.org/10.1016/j.virusres.2011.03.019

Borkakoti J, Ahmed G, Rai A, Kar P (2017) Report of novel H105R, D29N, V27A mutations in the methyltransferase region of the HEV genome in patients with acute liver failure. J Clin Virol Off Publ Pan Am Soc Clin Virol 91:1–4. https://doi.org/10.1016/j.jcv.2017.03.017

Campen A, Williams RM, Brown CJ, Meng J, Uversky VN, Dunker AK (2008) TOP-IDP-scale: a new amino acid scale measuring propensity for intrinsic disorder. Protein Pept Lett 15:956–963. https://doi.org/10.2174/092986608785849164

Cancela F, Rendon-Marin S, Quintero-Gil C, Houston DR, Gumbis G, Panzera Y, Pérez R, Arbiza J, Mirazo S (2021) Modelling of Hepatitis E virus RNA-dependent RNA polymerase genotype 3 from a chronic patient and in silico interaction analysis by molecular docking with Ribavirin. J Biomol Struct Dyn 1–17. https://doi.org/10.1080/07391102.2021.2011416

Cao D, Huang Y-W, Meng X-J (2010) The nucleotides on the stem-loop RNA structure in the junction region of the hepatitis E virus genome are critical for virus replication. J Virol 84:13040–13044. https://doi.org/10.1128/JVI.01475-10

Cao D, Ni Y-Y, Meng X-J (2018a) Substitution of amino acid residue V1213 in the helicase domain of the genotype 3 hepatitis E virus reduces virus replication. Virol J 15:32. https://doi.org/10.1186/s12985-018-0943-5

Cao D, Ni Y-Y, Walker M, Huang Y-W, Meng X-J (2018b) Roles of the genomic sequence surrounding the stem-loop structure in the junction region including the 3' terminus of open reading frame 1 in hepatitis E virus replication. J Med Virol 90:1524–1531. https://doi.org/10.1002/jmv.25215

Cao Y-F, Tao H, Hu Y-M, Shi C-B, Wu X, Liang Q, Chi C-P, Li L, Liang Z-L, Meng J-H, Zhu F-C, Liu Z-H, Wang X-P (2017) A phase 1 randomized open-label clinical study to evaluate the safety and tolerability of a novel recombinant hepatitis E vaccine. Vaccine 35:5073–5080. https://doi.org/10.1016/j.vaccine.2017.05.072

Chandra V, Holla P, Ghosh D, Chakrabarti D, Padigaru M, Jameel S (2011) The hepatitis E virus ORF3 protein regulates the expression of liver-specific genes by modulating localization of hepatocyte nuclear factor 4. PLoS ONE 6:e22412. https://doi.org/10.1371/journal.pone.0022412

Chandra V, Kar-Roy A, Kumari S, Mayor S, Jameel S (2008a) The hepatitis E virus ORF3 protein modulates epidermal growth factor receptor trafficking, STAT3 translocation, and the acute-phase response. J Virol 82:7100–7110. https://doi.org/10.1128/JVI.00403-08

Chandra V, Taneja S, Kalia M, Jameel S (2008b) Molecular biology and pathogenesis of hepatitis E virus. J Biosci 33:451–464. https://doi.org/10.1007/s12038-008-0064-1

Cohen GB, Ren R, Baltimore D (1995) Modular binding domains in signal transduction proteins. Cell 80:237–248. https://doi.org/10.1016/0092-8674(95)90406-9

Colson P, Decoster C (2019) Recent data on hepatitis E. Curr Opin Infect Dis 32:475–481. https://doi.org/10.1097/QCO.0000000000000590

Córdoba L, Huang Y-W, Opriessnig T, Harral KK, Beach NM, Finkielstein CV, Emerson SU, Meng X-J (2011) Three amino acid mutations (F51L, T59A, and S390L) in the capsid protein of the hepatitis E virus collectively contribute to virus attenuation. J Virol 85:5338–5349. https://doi.org/10.1128/JVI.02278-10

d'Azzo A, Bongiovanni A, Nastasi T (2005) E3 ubiquitin ligases as regulators of membrane protein trafficking and degradation. Traffic 6:429–441. https://doi.org/10.1111/j.1600-0854.2005.00294.x

Debing Y, Gisa A, Dallmeier K, Pischke S, Bremer B, Manns M, Wedemeyer H, Suneetha PV, Neyts J (2014) A mutation in the hepatitis e virus RNA polymerase promotes its replication and associates with ribavirin treatment failure in organ transplant recipients. Gastroenterology 147:1008–1011. https://doi.org/10.1053/j.gastro.2014.08.040

Debing Y, Moradpour D, Neyts J, Gouttenoire J (2016a) Update on hepatitis E virology: Implications for clinical practice. J Hepatol 65:200–212. https://doi.org/10.1016/j.jhep.2016.02.045

Debing Y, Ramiere C, Dallmeier K, Piorkowski G, Trabaud M-A, Lebosse F, Scholtes C, Roche M, Legras-Lachuer C, de Lamballerie X, Andre P, Neyts J (2016b) Hepatitis E virus mutations associated with ribavirin treatment failure result in altered viral fitness and ribavirin sensitivity. J Hepatol 65:499–508. https://doi.org/10.1016/j.jhep.2016.05.002

Decroly E, Ferron F, Lescar J, Canard B (2011) Conventional and unconventional mechanisms for capping viral mRNA. Nat Rev Microbiol 10:51–65. https://doi.org/10.1038/nrmicro2675

Devhare P, Sharma K, Mhaindarkar V, Arankalle V, Lole K (2014) Analysis of helicase domain mutations in the hepatitis E virus derived from patients with fulminant hepatic failure: effects on

enzymatic activities and virus replication. Virus Res 184:103–110. https://doi.org/10.1016/j.virusres.2014.02.018

Ding Q, Heller B, Capuccino JMV, Song B, Nimgaonkar I, Hrebikova G, Contreras JE, Ploss A (2017) Hepatitis E virus ORF3 is a functional ion channel required for release of infectious particles. Proc. Natl. Acad. Sci. U. S. A. 114, 1147–1152. https://doi.org/10.1073/pnas.1614955114

Dong C, Zafrullah M, Mixson-Hayden T, Dai X, Liang J, Meng J, Kamili S (2012) Suppression of interferon-α signaling by hepatitis E virus. Hepatology 55:1324–1332. https://doi.org/10.1002/hep.25530

Dunker AK, Oldfield CJ, Meng J, Romero P, Yang JY, Chen JW, Vacic V, Obradovic Z, Uversky VN (2008) The unfoldomics decade: an update on intrinsically disordered proteins. BMC Genomics 9(Suppl 2):S1. https://doi.org/10.1186/1471-2164-9-S2-S1

Emerson SU, Nguyen H, Graff J, Stephany DA, Brockington A, Purcell RH (2004) In vitro replication of hepatitis E virus (HEV) genomes and of an HEV replicon expressing green fluorescent protein. J Virol 78:4838–4846. https://doi.org/10.1128/jvi.78.9.4838-4846.2004

Fang SY, Han H (2017) Hepatitis E viral infection in solid organ transplant patients. Curr Opin Organ Transplant 22:351–355. https://doi.org/10.1097/MOT.0000000000000432

Feld JJ, Hoofnagle JH (2005) Mechanism of action of interferon and ribavirin in treatment of hepatitis C. Nature 436:967–972. https://doi.org/10.1038/nature04082

Finkel Y, Mizrahi O, Nachshon A, Weingarten-Gabbay S, Morgenstern D, Yahalom-Ronen Y, Tamir H, Achdout H, Stein D, Israeli O, Beth-Din A, Melamed S, Weiss S, Israely T, Paran N, Schwartz M, Stern-Ginossar N (2020) The coding capacity of SARS-CoV-2. Nature. https://doi.org/10.1038/s41586-020-2739-1

Fu RM, Decker CC, Thi D, V.L (2019) Cell Culture Models for Hepatitis E Virus. https://doi.org/10.3390/v11070608. Viruses 11

Geng Y, Yang J, Huang W, Harrison TJ, Zhou Y, Wen Z, Wang Y (2013) Virus host protein interaction network analysis reveals that the HEV ORF3 protein may interrupt the blood coagulation process. PLoS ONE 8:e56320. https://doi.org/10.1371/journal.pone.0056320

Gerolami R, Moal V, Colson P (2008) Chronic hepatitis E with cirrhosis in a kidney-transplant recipient. N Engl J Med. https://doi.org/10.1056/NEJMc0708687

Gouttenoire J, Pollán A, Abrami L, Oechslin N, Mauron J, Matter M, Oppliger J, Szkolnicka D, Thi D, van der Goot VL, Moradpour FG, D (2018) Palmitoylation mediates membrane association of hepatitis E virus ORF3 protein and is required for infectious particle secretion. PLoS Pathog 14:e1007471. https://doi.org/10.1371/journal.ppat.1007471

Gouvea V, Snellings N, Popek MJ, Longer CF, Innis BL (1998) Hepatitis E virus: complete genome sequence and phylogenetic analysis of a Nepali isolate. Virus Res 57:21–26. https://doi.org/10.1016/s0168-1702(98)00079-3

Graff J, Nguyen H, Yu C, Elkins WR, St Claire M, Purcell RH, Emerson SU (2005) The open reading frame 3 gene of hepatitis E virus contains a cis-reactive element and encodes a protein required for infection of macaques. J Virol 79:6680–6689. https://doi.org/10.1128/JVI.79.11.6680-6689.2005

Graff J, Torian U, Nguyen H, Emerson SU (2006) A bicistronic subgenomic mRNA encodes both the ORF2 and ORF3 proteins of hepatitis E virus. J Virol 80:5919–5926. https://doi.org/10.1128/JVI.00046-06

Gu Y, Tang X, Zhang X, Song C, Zheng M, Wang K, Zhang J, Ng M-H, Hew C-L, Li S, Xia N, Sivaraman J (2015) Structural basis for the neutralization of hepatitis E virus by a cross-genotype antibody. Cell Res 25:604–620. https://doi.org/10.1038/cr.2015.34

Guu TSY, Liu Z, Ye Q, Mata DA, Li K, Yin C, Zhang J, Tao YJ (2009) Structure of the hepatitis E virus-like particle suggests mechanisms for virus assembly and receptor binding. Proc. Natl. Acad. Sci. U. S. A. 106, 12992–12997. https://doi.org/10.1073/pnas.0904848106

Haglund K, Dikic I (2005) Ubiquitylation and cell signaling. EMBO J 24:3353–3359. https://doi.org/10.1038/sj.emboj.7600808

Haldipur B, Bhukya PL, Arankalle V, Lole K (2018) Positive Regulation of Hepatitis E Virus Replication by MicroRNA-122. J Virol 92. https://doi.org/10.1128/JVI.01999-17

He M, Wang M, Huang Y, Peng W, Zheng Z, Xia N, Xu J, Tian D (2016) The ORF3 Protein of Genotype 1 Hepatitis E Virus Suppresses TLR3-induced NF-κB Signaling via TRADD and RIP1. Sci Rep 6:27597. https://doi.org/10.1038/srep27597

He S, Miao J, Zheng Z, Wu T, Xie M, Tang M, Zhang J, Ng M-H, Xia N (2008) Putative receptor-binding sites of hepatitis E virus. J Gen Virol 89:245–249. https://doi.org/10.1099/vir.0.83308-0

Hingane S, Joshi N, Surjit M, Ranjith-Kumar CT (2020) Hepatitis E Virus ORF2 Inhibits RIG-I Mediated Interferon Response. Front Microbiol 11:656. https://doi.org/10.3389/fmicb.2020.00656

Holla RP, Ahmad I, Ahmad Z, Jameel S (2013) Molecular virology of hepatitis E virus. Semin. Liver Dis 33:3–14. https://doi.org/10.1055/s-0033-1338110

Horvatits T, Zur Wiesch JS, Lütgehetmann M, Lohse AW, Pischke S (2019) The clinical perspective on hepatitis E. Viruses 11:1–19. https://doi.org/10.3390/v11070617

Huang FF, Sun ZF, Emerson SU, Purcell RH, Shivaprasad HL, Pierson FW, Toth TE, Meng XJ (2004) Determination and analysis of the complete genomic sequence of avian hepatitis E virus (avian HEV) and attempts to infect rhesus monkeys with avian HEV. J Gen Virol 85:1609–1618. https://doi.org/10.1099/vir.0.79841-0

Ibrahim AS, Alkhal A, Jacob J, Ghadban W, Almarri A (2009) Hepatitis E in Qatar imported by expatriate workers from Nepal: epidemiological characteristics and clinical manifestations. J Med Virol 81:1047–1051. https://doi.org/10.1002/jmv.21474

Ingolia NT, Ghaemmaghami S, Newman JRS, Weissman JS (2009) Genome-Wide Analysis in Vivo of Resolution Using Ribosome Profiling. Science 324:218–223. https://doi.org/10.1126/science.1168978

Jablonski SA, Morrow CD (1995) Mutation of the aspartic acid residues of the GDD sequence motif of poliovirus RNA-dependent RNA polymerase results in enzymes with altered metal ion requirements for activity. J Virol 69:1532–1539. https://doi.org/10.1128/jvi.69.3.1532-1539.1995

Jameel S, Zafrullah M, Ozdener MH, Panda SK (1996) Expression in animal cells and characterization of the hepatitis E virus structural proteins. J Virol 70:207–216. https://doi.org/10.1128/JVI.70.1.207-216.1996

Ji H, Chen S, He Q, Wang W, Gong S, Qian Z, Zhang Y, Wei D, Yu W, Huang F (2021) The different replication between nonenveloped and quasi-enveloped hepatitis E virus. J Med Virol 93:6267–6277. https://doi.org/10.1002/jmv.27121

John L, Thomas S, Herchenröder O, Pützer BM, Schaefer S (2011) Hepatitis E virus ORF2 protein activates the pro-apoptotic gene CHOP and anti-apoptotic heat shock proteins. PLoS ONE 6:e25378. https://doi.org/10.1371/journal.pone.0025378

Ju X, Xiang G, Gong M, Yang R, Qin J, Li Y, Nan Y, Yang Y, Zhang QC, Ding Q (2020) Identification of functional cis-acting RNA elements in the hepatitis E virus genome required for viral replication. PLoS Pathog 16:e1008488. https://doi.org/10.1371/journal.ppat.1008488

Kadaré G, Haenni AL (1997) Virus-encoded RNA helicases. J Virol 71:2583–2590. https://doi.org/10.1128/JVI.71.4.2583-2590.1997

Kalia M, Chandra V, Rahman SA, Sehgal D, Jameel S (2009) Heparan sulfate proteoglycans are required for cellular binding of the hepatitis E virus ORF2 capsid protein and for viral infection. J Virol 83:12714–12724. https://doi.org/10.1128/JVI.00717-09

Kanade GD, Pingale KD, Karpe YA (2019) Protein Interactions Network of Hepatitis E Virus RNA and Polymerase With Host Proteins. Front Microbiol 10:2501. https://doi.org/10.3389/fmicb.2019.02501

Kanade GD, Pingale KD, Karpe YA (2018) Activities of Thrombin and Factor Xa Are Essential for Replication of Hepatitis E Virus and Are Possibly Implicated in ORF1 Polyprotein Processing. J Virol 92. https://doi.org/10.1128/JVI.01853-17

Kang S, Choi C, Choi I, Han K-N, Rho SW, Choi J, Kwon J, Park M-K, Kim S-J, Myoung J (2018) Hepatitis E Virus Methyltransferase Inhibits Type I Interferon Induction by Targeting RIG-I. J Microbiol Biotechnol 28:1554–1562. https://doi.org/10.4014/jmb.1808.08058

Kang S, Myoung J (2017a) Host Innate Immunity against Hepatitis E Virus and Viral Evasion Mechanisms. J Microbiol Biotechnol 27:1727–1735. https://doi.org/10.4014/jmb.1708.08045

Kang S, Myoung J (2017b) Primary lymphocyte infection models for KSHV and its putative tumorigenesis mechanisms in B cell lymphomas. J Microbiol 55:319–329. https://doi.org/10.1007/s12275-017-7075-2

Kannan H, Fan S, Patel D, Bossis I, Zhang Y-J (2009) The hepatitis E virus open reading frame 3 product interacts with microtubules and interferes with their dynamics. J Virol 83:6375–6382. https://doi.org/10.1128/JVI.02571-08

Kar-Roy A, Korkaya H, Oberoi R, Lal SK, Jameel S (2004) The hepatitis E virus open reading frame 3 protein activates ERK through binding and inhibition of the MAPK phosphatase. J Biol Chem 279:28345–28357. https://doi.org/10.1074/jbc.M400457200

Karpe YA, Lole KS (2011) Deubiquitination activity associated with hepatitis E virus putative papain-like cysteine protease. J Gen Virol 92:2088–2092. https://doi.org/10.1099/vir.0.033738-0

Karpe YA, Lole KS (2010a) NTPase and 5' to 3' RNA duplex-unwinding activities of the hepatitis E virus helicase domain. J Virol 84:3595–3602. https://doi.org/10.1128/JVI.02130-09

Karpe YA, Lole KS (2010b) RNA 5'-triphosphatase activity of the hepatitis E virus helicase domain. J Virol 84:9637–9641. https://doi.org/10.1128/JVI.00492-10

Kay BK, Williamson MP, Sudol M (2000) The importance of being proline: the interaction of proline-rich motifs in signaling proteins with their cognate domains. FASEB J Off Publ Fed Am Soc Exp Biol 14:231–241

Kenney SP, Meng X-J (2015) The lysine residues within the human ribosomal protein S17 sequence naturally inserted into the viral nonstructural protein of a unique strain of hepatitis E virus are important for enhanced virus replication. J Virol 89:3793–3803. https://doi.org/10.1128/JVI.03582-14

Kim E, Myoung J (2018) Hepatitis E Virus Papain-Like Cysteine Protease Inhibits Type I Interferon Induction by Down-Regulating Melanoma Differentiation-Associated Gene 5. J Microbiol Biotechnol 28:1908–1915. https://doi.org/10.4014/jmb.1809.09028

Koonin EV, Dolja VV (1993) Evolution and taxonomy of positive-strand RNA viruses: implications of comparative analysis of amino acid sequences. Crit Rev Biochem Mol Biol 28:375–430. https://doi.org/10.3109/10409239309078440

Koonin EV, Gorbalenya AE, Purdy MA, Rozanov MN, Reyes GR, Bradley DW (1992) Computer-assisted assignment of functional domains in the nonstructural polyprotein of hepatitis E virus: delineation of an additional group of positive-strand RNA plant and animal viruses. Proc. Natl. Acad. Sci. U. S. A. 89, 8259–8263. https://doi.org/10.1073/pnas.89.17.8259

Korkaya H, Jameel S, Gupta D, Tyagi S, Kumar R, Zafrullah M, Mazumdar M, Lal SK, Xiaofang L, Sehgal D, Das SR, Sahal D (2001) The ORF3 protein of hepatitis E virus binds to Src homology 3 domains and activates MAPK. J Biol Chem 276:42389–42400. https://doi.org/10.1074/jbc.M101546200

Kumar M, Hooda P, Khanna M, Patel U, Sehgal D (2020) Development of BacMam Induced Hepatitis E Virus Replication Model in Hepatoma Cells to Study the Polyprotein Processing. Front Microbiol 11:1347. https://doi.org/10.3389/fmicb.2020.01347

Kumar S, Subhadra S, Singh B, Panda BK (2013) Hepatitis E virus: the current scenario. Int J Infect Dis 17:e228–e233. https://doi.org/10.1016/j.ijid.2012.11.026

Legrand-Abravanel F, Mansuy JM, Dubois M, Kamar N, Peron JM, Rostaing L, Izopet J (2009) Hepatitis E virus genotype 3 diversity. France Emerg Infect Dis 15:110–114. https://doi.org/10.3201/eid1501.080296

Lhomme S, Abravanel F, Dubois M, Sandres-saune K, Mansuy J, Rostaing L, Kamar N, Izopet J (2014a) Characterization of the Polyproline Region of the Hepatitis E Virus in. J Virol 88:12017–12025. https://doi.org/10.1128/JVI.01625-14

Lhomme S, Garrouste C, Kamar N, Dubois M, Rostaing L, Izopet J (2014b) Influence of Polyproline Region and Macro Domain Genetic Heterogeneity on HEV Persistence in Immunocompromised Patients. J Infect Dis 209:300–303. https://doi.org/10.1093/infdis/jit438

Lhomme S, Migueres M, Abravanel F, Marion O, Kamar N, Izopet J (2020a) Hepatitis E Virus: How It Escapes Host Innate Immunity. Vaccines 8. https://doi.org/10.3390/vaccines8030422

Lhomme S, Nicot F, Jeanne N, Dimeglio C, Roulet A, Lefebvre C, Carcenac R, Manno M, Dubois M, Peron J-M, Alric L, Kamar N, Abravanel F, Izopet J (2020b) Insertions and Duplications in the Polyproline Region of the Hepatitis E Virus. Front Microbiol 11:1. https://doi.org/10.3389/fmicb.2020.00001

Li C, Debing Y, Jankevicius G, Neyts J, Ahel I, Coutard B, Canard B (2016) Viral Macro Domains Reverse Protein ADP-Ribosylation. J Virol 90:8478–8486. https://doi.org/10.1128/JVI.00705-16

Li H, Zheng Z, Zhou P, Zhang B, Shi Z, Hu Q, Wang H (2010) The cysteine protease domain of porcine reproductive and respiratory syndrome virus non-structural protein 2 antagonizes interferon regulatory factor 3 activation. J Gen Virol 91:2947–2958. https://doi.org/10.1099/vir.0.025205-0

Li P, Li Y, Wang, Yijin, Liu J, Lavrijsen M, Li, Yang, Zhang R, Verstegen MMA, Wang Y, Li T-C, Ma Z, Kainov DE, Bruno MJ, de Man RA, van der Laan LJW, Peppelenbosch MP, Pan Q (2022) Recapitulating hepatitis E virus-host interactions and facilitating antiviral drug discovery in human liver-derived organoids. Sci Adv 8:eabj5908. https://doi.org/10.1126/sciadv.abj5908

Li S-W, Zhao Q, Wu T, Chen S, Zhang J, Xia N-S (2015) The development of a recombinant hepatitis E vaccine HEV 239. Hum Vaccin Immunother 11:908–914. https://doi.org/10.1080/21645515.2015.1008870

Li S, Tang X, Seetharaman J, Yang C, Gu Y, Zhang J, Du H, Shih JWK, Hew C-L, Sivaraman J, Xia N (2009) Dimerization of hepatitis E virus capsid protein E2s domain is essential for virus-host interaction. PLoS Pathog 5:e1000537. https://doi.org/10.1371/journal.ppat.1000537

Li T-C, Kataoka M, Takahashi K, Yoshizaki S, Kato T, Ishii K, Takeda N, Mishiro S, Wakita T (2015) Generation of hepatitis E virus-like particles of two new genotypes G5 and G6 and comparison of antigenic properties with those of known genotypes. Vet Microbiol 178:150–157. https://doi.org/10.1016/j.vetmic.2015.04.020

Li T-C, Suzaki Y, Ami Y, Dhole TN, Miyamura T, Takeda N (2004) Protection of cynomolgus monkeys against HEV infection by oral administration of recombinant hepatitis E virus-like particles. Vaccine 22:370–377. https://doi.org/10.1016/j.vaccine.2003.08.004

Li T-C, Takeda N, Miyamura T, Matsuura Y, Wang JCY, Engvall H, Hammar L, Xing L, Cheng RH (2005) Essential elements of the capsid protein for self-assembly into empty virus-like particles of hepatitis E virus. J Virol 79:12999–13006. https://doi.org/10.1128/JVI.79.20.12999-13006.2005

Li TC, Yamakawa Y, Suzuki K, Tatsumi M, Razak MA, Uchida T, Takeda N, Miyamura T (1997) Expression and self-assembly of empty virus-like particles of hepatitis E virus. J Virol 71:7207–7213. https://doi.org/10.1128/JVI.71.10.7207-7213.1997

Li Y, Qu C, Yu P, Ou X, Pan Q, Wang W (2019) The Interplay between Host Innate Immunity and Hepatitis E Virus. https://doi.org/10.3390/v11060541. Viruses 11

Lin S, Yang Y, Nan Y, Ma Z, Yang L, Zhang Y-J (2019) The Capsid Protein of Hepatitis E Virus Inhibits Interferon Induction via Its N-terminal Arginine-Rich Motif. https://doi.org/10.3390/v11111050. Viruses 11

Liu H, Fu Y, Jiang D, Li G, Xie J, Peng Y, Yi X, Ghabrial SA (2009) A novel mycovirus that is related to the human pathogen hepatitis E virus and rubi-like viruses. J Virol 83:1981–1991. https://doi.org/10.1128/JVI.01897-08

Loo Y-M, Fornek J, Crochet N, Bajwa G, Perwitasari O, Martinez-Sobrido L, Akira S, Gill MA, García-Sastre A, Katze MG, Gale MJ (2008) Distinct RIG-I and MDA5 signaling by RNA viruses in innate immunity. J Virol 82:335–345. https://doi.org/10.1128/JVI.01080-07

Ma Y, Lin S-Q, Gao Y, Li M, Luo W-X, Zhang J, Xia N-S (2003) Expression of ORF2 partial gene of hepatitis E virus in tomatoes and immunoactivity of expression products. World J Gastroenterol 9:2211–2215. https://doi.org/10.3748/wjg.v9.i10.2211

Magden J, Takeda N, Li T, Auvinen P, Ahola T, Miyamura T, Merits A, Kääriäinen L (2001) Virus-specific mRNA capping enzyme encoded by hepatitis E virus. J Virol 75:6249–6255. https://doi.org/10.1128/JVI.75.14.6249-6255.2001

Mahilkar S, Paingankar MS, Lole KS (2016) Hepatitis E virus RNA-dependent RNA polymerase: RNA template specificities, recruitment and synthesis. J Gen Virol 97:2231–2242. https://doi.org/10.1099/jgv.0.000528

Maloney BJ, Takeda N, Suzaki Y, Ami Y, Li TC, Miyamura T, Arntzen CJ, Mason HS (2005) Challenges in creating a vaccine to prevent hepatitis E. Vaccine 23:1870–1874. https://doi.org/10.1016/j.vaccine.2004.11.020

Mazalovska M, Varadinov N, Koynarski T, Minkov I, Teoharov P, Lomonossoff GP, Zahmanova G (2017) Detection of Serum Antibodies to Hepatitis E Virus Based on HEV Genotype 3 ORF2 Capsid Protein Expressed in Nicotiana benthamiana. Ann Lab Med 37:313–319. https://doi.org/10.3343/alm.2017.37.4.313

Mendoza-Lopez C, Lopez-Lopez P, Atienza-Ayala S, Rivero-Juarez A, Benito R (2020) Parsonage-Turner syndrome associated with hepatitis E infection in immunocompetent patients. Virus Res 290:198165. https://doi.org/10.1016/j.virusres.2020.198165

Mhaindarkar V, Sharma K, Lole KS (2014) Mutagenesis of hepatitis E virus helicase motifs: effects on enzyme activity. Virus Res 179:26–33. https://doi.org/10.1016/j.virusres.2013.11.022

Mishra N, Walimbe AM, Arankalle VA (2013) Hepatitis E virus from India exhibits significant amino acid mutations in fulminant hepatic failure patients. Virus Genes 46:47–53. https://doi.org/10.1007/s11262-012-0833-7

Moin SM, Chandra V, Arya R, Jameel S (2009) The hepatitis E virus ORF3 protein stabilizes HIF-1alpha and enhances HIF-1-mediated transcriptional activity through p300/CBP. Cell Microbiol 11:1409–1421. https://doi.org/10.1111/j.1462-5822.2009.01340.x

Moin SM, Panteva M, Jameel S (2007) The hepatitis E virus Orf3 protein protects cells from mitochondrial depolarization and death. J Biol Chem 282:21124–21133. https://doi.org/10.1074/jbc.M701696200

Montpellier C, Wychowski C, Sayed IM, Meunier J-C, Saliou J-M, Ankavay M, Bull A, Pillez A, Abravanel F, Helle F, Brochot E, Drobecq H, Farhat R, Aliouat-Denis C-M, Haddad JG, Izopet J, Meuleman P, Goffard A, Dubuisson J, Cocquerel L (2018) Hepatitis E Virus Lifecycle and Identification of 3 Forms of the ORF2 Capsid Protein. Gastroenterology 154:211–223e8. https://doi.org/10.1053/j.gastro.2017.09.020

Mori Y, Matsuura Y (2011) Structure of hepatitis E viral particle. Virus Res 161:59–64. https://doi.org/10.1016/j.virusres.2011.03.015

Muñoz-Chimeno M, Cenalmor A, Garcia-Lugo MA, Hernandez M, Rodriguez-Lazaro D, Avellon A (2020) Proline-Rich Hypervariable Region of Hepatitis E Virus: Arranging the Disorder. Microorganisms 8. https://doi.org/10.3390/microorganisms8091417

Myoung J, Lee JY, Min KS (2019) Methyltransferase of a cell culture-adapted hepatitis E inhibits the MDA5 receptor signaling pathway. J Microbiol 57:1126–1131. https://doi.org/10.1007/s12275-019-9478-8

Nagashima S, Takahashi M, Jirintai S, Tanaka T, Nishizawa T, Yasuda J, Okamoto H (2011a) Tumour susceptibility gene 101 and the vacuolar protein sorting pathway are required for the release of hepatitis E virions. J Gen Virol 92:2838–2848. https://doi.org/10.1099/vir.0.035378-0

Nagashima S, Takahashi M, Jirintai S, Tanggis, Kobayashi T, Nishizawa T, Okamoto H (2014) The membrane on the surface of hepatitis E virus particles is derived from the intracellular membrane and contains trans-Golgi network protein 2. Arch Virol 159:979–991. https://doi.org/10.1007/s00705-013-1912-3

Nagashima S, Takahashi M, Jirintai, Tanaka T, Yamada K, Nishizawa T, Okamoto H (2011b) A PSAP motif in the ORF3 protein of hepatitis E virus is necessary for virion release from infected cells. J Gen Virol 92:269–278. https://doi.org/10.1099/vir.0.025791-0

Nair VP, Anang S, Subramani C, Madhvi A, Bakshi K, Srivastava A, Shalimar, Nayak B, Kumar R, Surjit CT, M (2016) Endoplasmic Reticulum Stress Induced Synthesis of a Novel Viral Factor Mediates Efficient Replication of Genotype-1 Hepatitis E Virus. PLoS Pathog 12:e1005521. https://doi.org/10.1371/journal.ppat.1005521

Nan Y, Ma Z, Wang R, Yu Y, Kannan H, Fredericksen B, Zhang Y-J (2014a) Enhancement of interferon induction by ORF3 product of hepatitis E virus. J Virol 88:8696–8705. https://doi.org/10.1128/JVI.01228-14

Nan Y, Yu Y, Ma Z, Khattar SK, Fredericksen B, Zhang Y-J (2014b) Hepatitis E virus inhibits type I interferon induction by ORF1 products. J Virol 88:11924–11932. https://doi.org/10.1128/JVI.01935-14

Nan Y, Zhang Y-J (2016) Molecular Biology and Infection of Hepatitis E Virus. Front Microbiol 7:1419. https://doi.org/10.3389/fmicb.2016.01419

Narayanan S, Abutaleb A, Sherman KE, Kottilil S (2019) Clinical features and determinants of chronicity in hepatitis E virus infection. J Viral Hepat 26:414–421. https://doi.org/10.1111/jvh.13059

Nguyen HT, Torian U, Faulk K, Mather K, Engle RE, Thompson E, Bonkovsky HL, Emerson SU (2012) A naturally occurring human/hepatitis e recombinant virus predominates in serum but not in faeces of a chronic hepatitis E patient and has a growth advantage in cell culture. J Gen Virol 93:526–530. https://doi.org/10.1099/vir.0.037259-0

Ojha NK, Lole KS (2016) Hepatitis E virus ORF1 encoded macro domain protein interacts with light chain subunit of human ferritin and inhibits its secretion. Mol Cell Biochem 417:75–85. https://doi.org/10.1007/s11010-016-2715-0

Osterman A, Stellberger T, Gebhardt A, Kurz M, Friedel CC, Uetz P, Nitschko H, Baiker A, Vizoso-Pinto MG (2015) The Hepatitis E virus intraviral interactome. Sci Rep 5:13872. https://doi.org/10.1038/srep13872

Paliwal D, Panda SK, Kapur N, Varma SPK, Durgapal H (2014) Hepatitis E virus (HEV) protease: a chymotrypsin-like enzyme that processes both non-structural (pORF1) and capsid (pORF2) protein. J Gen Virol 95:1689–1700. https://doi.org/10.1099/vir.0.066142-0

Palta S, Saroa R, Palta A (2014) Overview of the coagulation system. Indian J Anaesth 58:515–523. https://doi.org/10.4103/0019-5049.144643

Park S, Bin (2012) Hepatitis E vaccine debuts. Nature. https://doi.org/10.1038/491021a

Parvez MK (2017a) Mutational analysis of hepatitis E virus ORF1 "Y-domain": Effects on RNA replication and virion infectivity. World J Gastroenterol 23:590–602. https://doi.org/10.3748/wjg.v23.i4.590

Parvez MK (2017b) The hepatitis E virus nonstructural polyprotein. Future Microbiol 12:915–924. https://doi.org/10.2217/fmb-2017-0016

Parvez MK (2015a) The intergenic-junction variant (genotype 2 isolate) of hepatitis E virus restores the CREX "stem-loop" structural integrity, essential for viral life cycle. Gene 559:149–154. https://doi.org/10.1016/j.gene.2015.01.033

Parvez MK (2015b) The hepatitis E virus ORF1 "X-domain" residues form a putative macrodomain protein/Appr-1″-pase catalytic-site, critical for viral RNA replication. Gene 566:47–53. https://doi.org/10.1016/j.gene.2015.04.026

Parvez MK (2013) Molecular characterization of hepatitis E virus ORF1 gene supports a papain-like cysteine protease (PCP)-domain activity. Virus Res 178:553–556. https://doi.org/10.1016/j.virusres.2013.07.020

Parvez MK, Al-Dosari MS (2015) Evidence of MAPK-JNK1/2 activation by hepatitis E virus ORF3 protein in cultured hepatoma cells. Cytotechnology 67:545–550. https://doi.org/10.1007/s10616-014-9785-1

Parvez MK, Khan AA (2014) Molecular modeling and analysis of hepatitis E virus (HEV) papain-like cysteine protease. Virus Res 179:220–224. https://doi.org/10.1016/j.virusres.2013.11.016

Parvez MK, Subbarao N (2018) Molecular Analysis and Modeling of Hepatitis E Virus Helicase and Identification of Novel Inhibitors by Virtual Screening. Biomed Res. Int. 2018, 5753804. https://doi.org/10.1155/2018/5753804

Pawson T (1995) Protein modules and signalling networks. Nature 373:573–580. https://doi.org/10.1038/373573a0

Perttilä J, Spuul P, Ahola T (2013) Early secretory pathway localization and lack of processing for hepatitis E virus replication protein pORF1. J Gen Virol 94:807–816. https://doi.org/10.1099/vir.0.049577-0

Pingale KD, Kanade GD, Karpe YA (2019) Hepatitis E virus polymerase binds to IFIT1 to protect the viral RNA from IFIT1-mediated translation inhibition. J Gen Virol 100:471–483. https://doi.org/10.1099/jgv.0.001229

Pischke S, Suneetha PV, Baechlein C, Barg-Hock H, Heim A, Kamar N, Schlue J, Strassburg CP, Lehner F, Raupach R, Bremer B, Magerstedt P, Cornberg M, Seehusen F, Baumgaertner W, Klempnauer J, Izopet J, Manns MP, Grummer B, Wedemeyer H (2010) Hepatitis E virus infection as a cause of graft hepatitis in liver transplant recipients. Liver Transpl Off Publ Am Assoc Study Liver Dis Int Liver Transpl Soc 16:74–82. https://doi.org/10.1002/lt.21958

Proudfoot A, Hyrina A, Holdorf M, Frank AO, Bussiere D (2019) First Crystal Structure of a Nonstructural Hepatitis E Viral Protein Identifies a Putative Novel Zinc-Binding Protein. J Virol 93. https://doi.org/10.1128/JVI.00170-19

Pudupakam RS, Huang YW, Opriessnig T, Halbur PG, Pierson FW, Meng XJ (2009) Deletions of the hypervariable region (HVR) in open reading frame 1 of hepatitis E virus do not abolish virus infectivity: evidence for attenuation of HVR deletion mutants in vivo. J Virol 83:384–395. https://doi.org/10.1128/JVI.01854-08

Pudupakam RS, Kenney SP, Córdoba L, Huang Y-W, Dryman BA, Leroith T, Pierson FW, Meng X-J (2011) Mutational analysis of the hypervariable region of hepatitis e virus reveals its involvement in the efficiency of viral RNA replication. J Virol 85:10031–10040. https://doi.org/10.1128/JVI.00763-11

Purdy MA (2012) Evolution of the hepatitis E virus polyproline region: order from disorder. J Virol 86:10186–10193. https://doi.org/10.1128/JVI.01374-12

Purdy MA, Lara J, Khudyakov YE (2012) The hepatitis E virus polyproline region is involved in viral adaptation. PLoS ONE 7:e35974. https://doi.org/10.1371/journal.pone.0035974

Radivojac P, Iakoucheva LM, Oldfield CJ, Obradovic Z, Uversky VN, Dunker AK (2007) Intrinsic disorder and functional proteomics. Biophys J 92:1439–1456. https://doi.org/10.1529/biophysj.106.094045

Ratra R, Kar-Roy A, Lal SK (2009) ORF3 protein of hepatitis E virus interacts with the Bbeta chain of fibrinogen resulting in decreased fibrinogen secretion from HuH-7 cells. J Gen Virol 90:1359–1370. https://doi.org/10.1099/vir.0.009274-0

Ratra R, Kar-Roy A, Lal SK (2008) The ORF3 protein of hepatitis E virus interacts with hemopexin by means of its 26 amino acid N-terminal hydrophobic domain II. Biochemistry 47:1957–1969. https://doi.org/10.1021/bi7016552

Rehman S, Kapur N, Durgapal H, Panda SK (2008) Subcellular localization of hepatitis E virus (HEV) replicase. Virology 370:77–92. https://doi.org/10.1016/j.virol.2007.07.036

Reyes-Turcu FE, Ventii KH, Wilkinson KD (2009) Regulation and cellular roles of ubiquitin-specific deubiquitinating enzymes. Annu Rev Biochem 78:363–397. https://doi.org/10.1146/annurev.biochem.78.082307.091526

Rozanov MN, Koonin EV, Gorbalenya AE (1992) Conservation of the putative methyltransferase domain: a hallmark of the "Sindbis-like" supergroup of positive-strand RNA viruses. J Gen Virol 73(Pt 8):2129–2134. https://doi.org/10.1099/0022-1317-73-8-2129

Saraswat S, Chaudhary M, Sehgal D (2019) Hepatitis E Virus Cysteine Protease Has Papain Like Properties Validated by in silico Modeling and Cell-Free Inhibition Assays. Front Cell Infect Microbiol 9:478. https://doi.org/10.3389/fcimb.2019.00478

Sayed IM, Elkhawaga AA, El-Mokhtar MA (2019) In vivo models for studying Hepatitis E virus infection; Updates and applications. Virus Res 274:197765. https://doi.org/10.1016/j.virusres.2019.197765

Sayed IM, Meuleman P (2019) Updates in Hepatitis E virus (HEV) field; lessons learned from human liver chimeric mice. Rev. Med. Virol. e2086. https://doi.org/10.1002/rmv.2086

Scholz J, Falkenhagen A, Johne R (2021) The Translated Amino Acid Sequence of an Insertion in the Hepatitis E Virus Strain 47832c Genome, But Not the RNA Sequence, Is Essential for Efficient Cell Culture Replication. Viruses 13. https://doi.org/10.3390/v13050762

Sehgal D, Thomas S, Chakraborty M, Jameel S (2006) Expression and processing of the Hepatitis E virus ORF1 nonstructural polyprotein. Virol J 3:38. https://doi.org/10.1186/1743-422X-3-38

Shafat Z, Ahmed A, Parvez MK, Parveen S (2022) Analysis of codon usage patterns in open reading frame 4 of hepatitis E viruses. Beni-Suef Univ J basic Appl Sci 11:65. https://doi.org/10.1186/s43088-022-00244-w

Shafat Z, Ahmed A, Parvez MK, Parveen S (2021) Sequence to structure analysis of the ORF4 protein from Hepatitis E virus. Bioinformation 17:818–828. https://doi.org/10.6026/97320630017818

Shukla P, Nguyen HT, Faulk K, Mather K, Torian U, Engle RE, Emerson SU (2012) Adaptation of a genotype 3 hepatitis E virus to efficient growth in cell culture depends on an inserted human gene segment acquired by recombination. J Virol 86:5697–5707. https://doi.org/10.1128/JVI.00146-12

Smith DB, Simmonds P (2015) Hepatitis E virus and fulminant hepatitis–a virus or host-specific pathology? Liver Int. Off J Int Assoc Study Liver 35:1334–1340. https://doi.org/10.1111/liv.12629

Smith DB, Simmonds P, Jameel S, Emerson SU, Harrison TJ, Meng X-J, Okamoto H, Van der Poel WHM, Purdy MA (2014) Consensus

proposals for classification of the family Hepeviridae. J Gen Virol 95:2223–2232. https://doi.org/10.1099/vir.0.068429-0

Smith DB, Vanek J, Ramalingam S, Johannessen I, Templeton K, Simmonds P (2012) Evolution of the hepatitis E virus hypervariable region. J Gen Virol 93:2408–2418. https://doi.org/10.1099/vir.0.045351-0

Sridhar S, Yip CCY, Wu S, Cai J, Zhang AJ-X, Leung K-H, Chung TWH, Chan JFW, Chan W-M, Teng JLL, Au-Yeung RKH, Cheng VCC, Chen H, Lau SKP, Woo PCY, Xia N-S, Lo C-M, Yuen K-Y (2018) Rat Hepatitis E Virus as Cause of Persistent Hepatitis after Liver Transplant. Emerg Infect Dis 24:2241–2250. https://doi.org/10.3201/eid2412.180937

Stern-Ginossar N (2015) Decoding Viral Infection by Ribosome Profiling. J Virol 89:6164–6166. https://doi.org/10.1128/jvi.02528-14

Strauss JH, Strauss EG (1994) The alphaviruses: gene expression, replication, and evolution. Microbiol Rev 58:491–562. https://doi.org/10.1128/mr.58.3.491-562.1994

Subramani C, Nair VP, Anang S, Mandal S, Das, Pareek M, Kaushik N, Srivastava A, Saha S, Shalimar, Nayak B, Ranjith-Kumar CT, Surjit M (2018) Host-Virus Protein Interaction Network Reveals the Involvement of Multiple Host Processes in the Life Cycle of Hepatitis E Virus. mSystems 3 https://doi.org/10.1128/mSystems.00135-17

Sun Z, Chen Z, Lawson SR, Fang Y (2010) The cysteine protease domain of porcine reproductive and respiratory syndrome virus nonstructural protein 2 possesses deubiquitinating and interferon antagonism functions. J Virol 84:7832–7846. https://doi.org/10.1128/JVI.00217-10

Suppiah S, Zhou Y, Frey TK (2011) Lack of processing of the expressed ORF1 gene product of hepatitis E virus. Virol J 8:245. https://doi.org/10.1186/1743-422X-8-245

Surjit M, Jameel S, Lal SK (2007) Cytoplasmic localization of the ORF2 protein of hepatitis E virus is dependent on its ability to undergo retrotranslocation from the endoplasmic reticulum. J Virol 81:3339–3345. https://doi.org/10.1128/JVI.02039-06

Surjit M, Oberoi R, Kumar R, Lal SK (2006) Enhanced alpha1 microglobulin secretion from Hepatitis E virus ORF3-expressing human hepatoma cells is mediated by the tumor susceptibility gene 101. J Biol Chem 281:8135–8142. https://doi.org/10.1074/jbc.M509568200

Surjit M, Varshney B, Lal SK (2012) The ORF2 glycoprotein of hepatitis E virus inhibits cellular NF-κB activity by blocking ubiquitination mediated proteasomal degradation of IκBα in human hepatoma cells. BMC Biochem 13:7. https://doi.org/10.1186/1471-2091-13-7

Takahashi K, Okamoto H, Abe N, Kawakami M, Matsuda H, Mochida S, Sakugawa H, Suginoshita Y, Watanabe S, Yamamoto K, Miyakawa Y, Mishiro S (2009) Virulent strain of hepatitis E virus genotype 3, Japan. Emerg Infect Dis 15:704–709. https://doi.org/10.3201/eid1505.081100

Takahashi M, Yamada K, Hoshino Y, Takahashi H, Ichiyama K, Tanaka T, Okamoto H (2008) Monoclonal antibodies raised against the ORF3 protein of hepatitis E virus (HEV) can capture HEV particles in culture supernatant and serum but not those in feces. Arch Virol 153:1703–1713. https://doi.org/10.1007/s00705-008-0179-6

Takeuchi O, Akira S (2010) Pattern recognition receptors and inflammation. Cell 140:805–820. https://doi.org/10.1016/j.cell.2010.01.022

Tang X, Yang C, Gu Y, Song C, Zhang X, Wang Y, Zhang J, Hew CL, Li S, Xia N, Sivaraman J (2011) Structural basis for the neutralization and genotype specificity of hepatitis E virus. Proc. Natl. Acad. Sci. U. S. A. 108, 10266–10271. https://doi.org/10.1073/pnas.1101309108

Todt D, Friesland M, Moeller N, Praditya D, Kinast V, Brüggemann Y, Knegendorf L, Burkard T, Steinmann J, Burm R, Verhoye L, Wahid A, Meister TL, Engelmann M, Pfankuche VM, Puff C, Vondran FWR, Baumgärtner W, Meuleman P, Behrendt P, Steinmann E (2020) Robust hepatitis E virus infection and transcriptional response in human hepatocytes. Proc. Natl. Acad. Sci. U. S. A. 117, 1731–1741. https://doi.org/10.1073/pnas.1912307117

Todt D, Gisa A, Radonic A, Nitsche A, Behrendt P, Suneetha PV, Pischke S, Bremer B, Brown RJP, Manns MP, Cornberg M, Bock CT, Steinmann E, Wedemeyer H (2016a) In vivo evidence for ribavirin-induced mutagenesis of the hepatitis E virus genome. Gut 65:1733–1743. https://doi.org/10.1136/gutjnl-2015-311000

Todt D, Walter S, Brown RJP, Steinmann E (2016b) Mutagenic Effects of Ribavirin on Hepatitis E Virus-Viral Extinction versus Selection of Fitness-Enhancing Mutations. Viruses 8. https://doi.org/10.3390/v8100283

Tsai CJ, Ma B, Sham YY, Kumar S, Nussinov R (2001) Structured disorder and conformational selection. Proteins 44:418–427. https://doi.org/10.1002/prot.1107

Tyagi S, Korkaya H, Zafrullah M, Jameel S, Lal SK (2002) The phosphorylated form of the ORF3 protein of hepatitis E virus interacts with its non-glycosylated form of the major capsid protein, ORF2. J Biol Chem 277:22759–22767. https://doi.org/10.1074/jbc.M200185200

van der Heijden MW, Bol JF (2002) Composition of alphavirus-like replication complexes: involvement of virus and host encoded proteins. Arch Virol 147:875–898. https://doi.org/10.1007/s00705-001-0773-3

van der Poel WH, Verschoor F, van der Heide R, Herrera MI, Vivo A, Kooreman M, de Roda Husman AM (2001) Hepatitis E virus sequences in swine related to sequences in humans, The Netherlands. Emerg Infect Dis 7:970–976. https://doi.org/10.3201/eid0706.010608

Vázquez AL, Alonso JM, Parra F (2000) Mutation analysis of the GDD sequence motif of a calicivirus RNA-dependent RNA polymerase. J Virol 74:3888–3891. https://doi.org/10.1128/jvi.74.8.3888-3891.2000

Vikram T, Kumar P (2018) Analysis of Hepatitis E virus (HEV) X-domain structural model. Bioinformation 14:398–403. https://doi.org/10.6026/97320630014398

Villarroya-Beltri C, Guerra S, Sánchez-Madrid F (2017) ISGylation - a key to lock the cell gates for preventing the spread of threats. J Cell Sci 130:2961–2969. https://doi.org/10.1242/jcs.205468

Wang B, Meng X-J (2021) Structural and molecular biology of hepatitis E virus. Comput Struct Biotechnol J 19:1907–1916. https://doi.org/10.1016/j.csbj.2021.03.038

Wang C, Guo L, Yu D, Hua X, Yang Z, Yuan C, Cui L (2014) HEV-ORF3 Encoding Phosphoprotein Interacts With Hepsin. Hepat Mon 14:e13902. https://doi.org/10.5812/hepatmon.13902

Wang X, Gillam S (2001) Mutations in the GDD motif of rubella virus putative RNA-dependent RNA polymerase affect virus replication. Virology 285:322–331. https://doi.org/10.1006/viro.2001.0939

Wang X, Zhao Q, Dang L, Sun Y, Gao J, Liu B, Syed SF, Tao H, Zhang G, Luo J, Zhou E-M (2015) Characterization of Two Novel Linear B-Cell Epitopes in the Capsid Protein of Avian Hepatitis E Virus (HEV) That Are Common to Avian, Swine, and Human HEVs. J Virol 89:5491–5501. https://doi.org/10.1128/JVI.00107-15

Webb GW, Dalton HR (2019) Hepatitis E: an underestimated emerging threat. Ther Adv Infect Dis 6:2049936119837162. https://doi.org/10.1177/2049936119837162

Welchman RL, Gordon C, Mayer RJ (2005) Ubiquitin and ubiquitin-like proteins as multifunctional signals. Nat Rev Mol Cell Biol 6:599–609. https://doi.org/10.1038/nrm1700

Williams RM, Obradovi Z, Mathura V, Braun W, Garner EC, Young J, Takayama S, Brown CJ, Dunker AK (2001) The protein nonfolding problem: amino acid determinants of intrinsic order

and disorder. Pac. Symp. Biocomput. 89–100. https://doi.org/10.1142/9789814447362_0010
Williamson MP (1994) The structure and function of proline-rich regions in proteins. Biochem J 297:249–260. https://doi.org/10.1042/bj2970249
Wißing MH, Brüggemann Y, Steinmann E, Todt D (2021) Virus-Host Cell Interplay during Hepatitis E Virus Infection. Trends Microbiol 29:309–319. https://doi.org/10.1016/j.tim.2020.07.002
Wood JP, Silveira JR, Maille NM, Haynes LM, Tracy PB (2011) Prothrombin activation on the activated platelet surface optimizes expression of procoagulant activity. Blood 117:1710–1718. https://doi.org/10.1182/blood-2010-09-311035
Wu J, Xiang Z, Zhu C, Yao Y, Bortolanza M, Cao H, Li L (2021) Extrahepatic manifestations related to hepatitis E virus infection and their triggering mechanisms. J Infect 83:298–305. https://doi.org/10.1016/j.jinf.2021.07.021
Xing L, Kato K, Li T, Takeda N, Miyamura T, Hammar L, Cheng RH (1999) Recombinant hepatitis E capsid protein self-assembles into a dual-domain T = 1 particle presenting native virus epitopes. Virology 265:35–45. https://doi.org/10.1006/viro.1999.0005
Xing L, Li T-C, Mayazaki N, Simon MN, Wall JS, Moore M, Wang C-Y, Takeda N, Wakita T, Miyamura T, Cheng RH (2010) Structure of hepatitis E virion-sized particle reveals an RNA-dependent viral assembly pathway. J Biol Chem 285:33175–33183. https://doi.org/10.1074/jbc.M110.106336
Xu M, Behloul N, Wen J, Zhang J, Meng J (2016) Role of asparagine at position 562 in dimerization and immunogenicity of the hepatitis E virus capsid protein. Infect Genet Evol 37:99–107. https://doi.org/10.1016/j.meegid.2015.11.006
Yadav KK, Kenney SP (2021) Hepatitis E Virus Immunopathogenesis. Pathog. (Basel, Switzerland) 10. https://doi.org/10.3390/pathogens10091180
Yamashita T, Kaneko S, Shirota Y, Qin W, Nomura T, Kobayashi K, Murakami S (1998) RNA-dependent RNA polymerase activity of the soluble recombinant hepatitis C virus NS5B protein truncated at the C-terminal region. J Biol Chem 273:15479–15486. https://doi.org/10.1074/jbc.273.25.15479
Yamashita T, Mori Y, Miyazaki N, Cheng RH, Yoshimura M, Unno H, Shima R, Moriishi K, Tsukihara T, Li TC, Takeda N, Miyamura T, Matsuura Y (2009) Biological and immunological characteristics of hepatitis E virus-like particles based on the crystal structure. Proc. Natl. Acad. Sci. U. S. A. 106, 12986–12991. https://doi.org/10.1073/pnas.0903699106
Yin X, Ambardekar C, Lu Y, Feng Z (2016) Distinct Entry Mechanisms for Nonenveloped and Quasi-Enveloped Hepatitis E Viruses. J Virol 90:4232–4242. https://doi.org/10.1128/jvi.02804-15
Yin X, Feng Z (2019) Hepatitis E Virus Entry. https://doi.org/10.3390/v11100883. Viruses 11
Yin X, Ying D, Lhomme S, Tang Z, Walker CM, Xia N, Zheng Z, Feng Z (2018) Origin, antigenicity, and function of a secreted form of ORF2 in hepatitis E virus infection. Proc. Natl. Acad. Sci. U. S. A. 115, 4773–4778. https://doi.org/10.1073/pnas.1721345115
Zaman K, Dudman S, Stene-Johansen K, Qadri F, Yunus M, Sandbu S, Gurley ES, Overbo J, Julin CH, Dembinski JL, Nahar Q, Rahman A, Bhuiyan TR, Rahman M, Haque W, Khan J, Aziz A, Khanam M, Streatfield PK, Clemens JD (2020) HEV study protocol: design of a cluster-randomised, blinded trial to assess the safety, immunogenicity and effectiveness of the hepatitis E vaccine HEV 239 (Hecolin) in women of childbearing age in rural Bangladesh. BMJ Open 10:e033702. https://doi.org/10.1136/bmjopen-2019-033702
Zhang J, Liu C-B, Li R-C, Li Y-M, Zheng Y-J, Li Y-P, Luo D, Pan B-B, Nong Y, Ge S-X, Xiong J-H, Shih JW-K, Ng M-H, Xia N-S (2009) Randomized-controlled phase II clinical trial of a bacterially expressed recombinant hepatitis E vaccine. Vaccine 27:1869–1874. https://doi.org/10.1016/j.vaccine.2008.12.061
Zhang J, Zhang X-F, Huang S-J, Wu T, Hu Y-M, Wang Z-Z, Wang H, Jiang H-M, Wang Y-J, Yan Q, Guo M, Liu X-H, Li J-X, Yang C-L, Tang Q, Jiang R-J, Pan H-R, Li Y-M, Shih JW-K, Ng M-H, Zhu F-C, Xia N-S (2015) Long-term efficacy of a hepatitis E vaccine. N Engl J Med 372:914–922. https://doi.org/10.1056/NEJMoa1406011
Zhang L, Tian Y, Wen Z, Zhang F, Qi Y, Huang W, Zhang H, Wang Y (2016) Asialoglycoprotein receptor facilitates infection of PLC/PRF/5 cells by HEV through interaction with ORF2. J Med Virol 88:2186–2195. https://doi.org/10.1002/jmv.24570
Zhang Y, McAtee P, Yarbough PO, Tam AW, Fuerst T (1997) Expression, characterization, and immunoreactivities of a soluble hepatitis E virus putative capsid protein species expressed in insect cells. Clin Diagn Lab Immunol 4:423–428. https://doi.org/10.1128/cdli.4.4.423-428.1997
Zhao M, Li X-J, Tang Z-M, Yang F, Wang S-L, Cai W, Zhang K, Xia N-S, Zheng Z-Z (2015) A Comprehensive Study of Neutralizing Antigenic Sites on the Hepatitis E Virus (HEV) Capsid by Constructing, Clustering, and Characterizing a Tool Box. J Biol Chem 290:19910–19922. https://doi.org/10.1074/jbc.M115.649764
Zheng Z-Z, Miao J, Zhao M, Tang M, Yeo AET, Yu H, Zhang J, Xia N-S (2010) Role of heat-shock protein 90 in hepatitis E virus capsid trafficking. J Gen Virol 91:1728–1736. https://doi.org/10.1099/vir.0.019323-0
Zhou X, Kataoka M, Liu Z, Takeda N, Wakita T, Li T-C (2015) Characterization of self-assembled virus-like particles of dromedary camel hepatitis e virus generated by recombinant baculoviruses. Virus Res 210:8–17. https://doi.org/10.1016/j.virusres.2015.06.022
Zhou Y-X, Lee MY-T, Ng JM-H, Chye M-L, Yip W-K, Zee S-Y, Lam E (2006) A truncated hepatitis E virus ORF2 protein expressed in tobacco plastids is immunogenic in mice. World J Gastroenterol 12:306–312. https://doi.org/10.3748/wjg.v12.i2.306
Zhou Y, Tzeng W-P, Ye Y, Huang Y, Li S, Chen Y, Frey TK, Yang JJ (2009) A cysteine-rich metal-binding domain from rubella virus non-structural protein is essential for viral protease activity and virus replication. Biochem J 417:477–483. https://doi.org/10.1042/BJ20081468
Zhou Y, Tzeng W-P, Yang W, Zhou, Yumei, Ye Y, Lee H, Frey TK, Yang J (2007) Identification of a Ca2+-binding domain in the rubella virus nonstructural protease. J Virol 81:7517–7528. https://doi.org/10.1128/JVI.00605-07
Zhu F-C, Zhang J, Zhang X-F, Zhou C, Wang Z-Z, Huang S-J, Wang H, Yang C-L, Jiang H-M, Cai J-P, Wang Y-J, Ai X, Hu Y-M, Tang Q, Yao X, Yan Q, Xian Y-L, Wu T, Li Y-M, Miao J, Ng M-H, Shih JW-K, Xia N-S (2010) Efficacy and safety of a recombinant hepatitis E vaccine in healthy adults: a large-scale, randomised, double-blind placebo-controlled, phase 3 trial. Lancet (London England) 376:895–902. https://doi.org/10.1016/S0140-6736(10)61030-6

2. OBJETIVOS

2.1. Objetivo general

En esta Tesis de Doctorado se persiguieron cuatro objetivos centrales.

En primer lugar, implementar un amplio relevamiento serológico y molecular de HEV en diversas especies y matrices biológicas.

En segundo lugar, obtener genomas completos de HEV para una completa clasificación y asignación de subtipo de las cepas circulantes en el país.

En tercer lugar, caracterizar la interacción molecular entre la RdRp de HEVc y RBV.

En cuarto lugar, optimizar un método de aislamiento *in vitro* de HEVc y HEVa, determinar el perfil diferencial de proteoma y realizar análisis de resistencia a RBV.

2.2. Objetivos específicos

- Caracterización de variantes de HEV circulantes y actualización de la epidemiologia en el país en animales silvestres y de cautiverio.
- Obtención y clasificación de genomas completos de HEV3 por NGS.
- Modelado de la RdRp de HEVc y análisis *in silico* de la interacción con RBV.
- Aislamiento de HEVc y HEVa *in vitro* en las líneas celulares continuas A549, A549/D3, análisis de resistencia de RBV y estudio del perfil de expresión diferencial de citoquinas, proteínas de apoptosis y sus vías de señalización.

Esta Tesis se estructura en 4 capítulos, correspondientes a cada uno de los objetivos específicos.

3. CAPÍTULO 1

Caracterización de variantes de HEV circulantes y actualización de la epidemiologia en el país en animales silvestres y de cautiverio.

3.1. Fundamento teórico y antecedentes

Se estima que aproximadamente el 75% de las enfermedades infecciosas emergentes (EID) son zoonosis, representando una causa significativa de mortalidad y morbilidad, siendo los principales factores que promueven su emergencia biológicos, medioambientales, socioeconómicos y políticos [77].

Entre ellos, el contacto cercano entre humanos y especies animales puede favorecer un proceso conocido como *spill-over* o salto interespecie infectando la población humana susceptible a partir de los virus que circulan en reservorios salvajes. Sin embargo, también puede ocurrir el proceso opuesto, definido como zoonosis-reversa o zooantroponosis.

Los eventos de *spill-over* pueden dar lugar a hospederos terminales o a brotes epidémicos, que incluso podrían llegar a ser endémicos. Para ello, resulta crucial identificar los reservorios naturales y hospederos intermedios en estos eventos de *spill-over* [78].

Actualmente, HEV es considerado una preocupación creciente para la seguridad de la industria agro-alimentaria y salud pública ya que su variabilidad genética, constante evolución viral y la existencia de un gran número de cepas en hospederos humanos y animales podrían contribuir a la diseminación viral y a su potencial expansión de rango de hospedero [31].

En Uruguay, así como en toda América del Sur, la situación epidemiológica sobre reservorios potenciales de HEV (no cerdos ni jabalíes) tanto silvestres como de cautiverio, se encuentra mayormente inexplorada.

Debido a lo expuesto anteriormente, la vigilancia de patógenos zoonóticos en animales silvestres y de cautiverio con un enfoque holístico de Una Salud, resulta crucial para comprender la epidemiología, dinámica y potencial riesgo que puedan tener las EID en la salud humana y animal, donde infecciones emergentes endémicas y zoonóticas como HEV son importantes para controlar su impacto [31].

3.2. Hipótesis

HEV posee una activa circulación en población humana de Uruguay y un amplio rango de hospedero que se encuentra en constante expansión. Es posible identificar evidencias de eventos de *spill-over* en potenciales hospederos animales alternativos.

3.3. Objetivo específico

Caracterización de variantes de HEV circulantes y actualización de la epidemiologia en el país. Explorar la circulación de HEV en potenciales hospederos animales e investigar el eventual impacto zoonótico de transmisión que pueden tener dichos reservorios mediante la implementación de un amplio relevamiento serológico y molecular de HEV a través del desarrollo de metodologías optimizadas específicamente para esta Tesis.

3.4. Cancela et al., 2023. Co-circulation of Hepatitis E virus (HEV) genotype 3 and HEV variants in free-ranging spotted deer (*Axis axis*).

En el presente trabajo se exploró la circulación de HEV en ciervos *Axis axis* de vida silvestre y en cautiverio de Uruguay mediante métodos moleculares y serológicos. Además, mediante el uso de la metodología de fototrampeo buscamos profundizar y aportar información sobre la ecología de HEV en la naturaleza (Punto *1.4* de la Sección *Introducción*). Se detectó una seropositividad de 11,1% (6/54) en ciervos de vida silvestre y un 68,4% (13/19) presentaban ARN de HEV. Mediante estudios filogenéticos y de p-distancia se reportó la co-circulación de cepas HEV3 y de variantes HEV-*like* sin clasificar.

Por lo tanto, los resultados obtenidos presentan evidencia de que los ciervos *Axis axis* deberían ser considerados como un nuevo reservorio zoonótico para HEV.

Los resultados derivados de este Capítulo fueron publicados en un artículo científico que se adjunta a continuación:

Cancela F, Cravino A, Icasuriaga R, González P, Bentancor F, Leizagoyen C, Echaides C, Ferreiro I, Cabrera A, Arbiza J, Mirazo S. Co-circulation of Hepatitis E Virus (HEV) Genotype 3 and Moose-HEV-Like Strains in Free-Ranging-Spotted Deer (Axis axis) in Uruguay. Food Environ Virol. 2023 Aug 29. doi: 10.1007/s12560-023-09563-2.

Food and Environmental Virology
https://doi.org/10.1007/s12560-023-09563-2

RESEARCH

Co-circulation of Hepatitis E Virus (HEV) Genotype 3 and Moose-HEV-Like Strains in Free-Ranging-Spotted Deer (*Axis axis*) in Uruguay

Florencia Cancela[1,2] · Alexandra Cravino[3] · Romina Icasuriaga[1] · Pablo González[4] · Federico Bentancor[4] · Carmen Leizagoyen[5] · César Echaides[5] · Irene Ferreiro[2] · Andrés Cabrera[6] · Juan Arbiza[2] · Santiago Mirazo[1]

Received: 30 May 2023 / Accepted: 14 August 2023

Abstract

Hepatitis E caused by hepatitis E virus (HEV) is considered an emerging foodborne zoonosis in industrialized, non-endemic countries. Domestic pigs and wild boars are considered the main reservoir of HEV. However, HEV can also infect an ever-expanding host range of animals, but they exact role in transmitting the virus to other species or humans is mostly unknown. In this work, we investigated the spread of HEV in free-living and captive spotted deer (*Axis axis*) from Uruguay in a 2-year period (2020–2022) and examined the role of this invasive species as a new potential reservoir of the virus. In addition, with the aim to gain new insights into viral ecology in the context of One Health, by using camera trapping, we identified and quantified temporal and spatial coexistence of spotted deer, wild boars, and cattle. In free-living animals, we detected an anti-HEV seropositivity of 11.1% (6/54). HEV infection and viral excretion in feces were assessed by RT-PCR. Thirteen of 19 samples (68.4%) had HEV RNA. Six samples were amplified using a broadly reactive RT-PCR and sequenced. No captive animal showed evidence of HEV infection. Additionally, HEV RNA was detected in a freshwater pond shared by these species. Phylogenetic and *p*-distance analysis revealed that zoonotic HEV genotype 3 strains circulate together with unclassified variants related to moose HEV whose potential risk of transmission to humans and other domestic and wild animals is unknown. The data presented here suggest that spotted deer (*A. axis*) may be a novel host for zoonotic HEV strains.

Keywords Hepatitis E virus · *Axis axis* · Ecologic reservoirs · HEV-like variants · Genotype 3

Introduction

Hepatitis E virus (HEV) causes 20 million HEV infections and 70,000 deaths annually and is now recognized as an important causative agent of acute hepatitis in developed countries (World Health Organization, 2017).

HEV (family *Hepeviridae*) is currently divided into two subfamilies: *Orthohepevirinae* and *Parahepevirinae*. *Orthohepevirinae* is divided into four genera: *Avihepevirus, Chirohepevirus, Paslahepevirus,* and *Rocahepevirus*, as well as several unclassified isolates. *Paslahepevirus balayani* species include HEV genotypes 1–8 (HEV1–HEV8), which are further subdivided into subtypes based on *p*-distance values (Smith et al., 2020). HEV3 and HEV4 infections have been associated with direct contact with infected animals or consumption of contaminated raw or undercooked meat (Colson & Decoster, 2019). In non-endemic countries, acute HEV infection is usually self-limiting in the general population. However,

✉ Santiago Mirazo
smirazo@higiene.edu.uy

1 Departamento de Bacteriología y Virología, Instituto de Higiene, Facultad de Medicina, Universidad de la República, Av. Alfredo Navarro 3051, 11600 Montevideo, Uruguay

2 Sección Virología, Facultad de Ciencias, Universidad de la República, Montevideo, Uruguay

3 Grupo Biodiversidad y Ecología de la Conservación, Instituto de Ecología y Ciencias Ambientales, Facultad de Ciencias, Universidad de la República, Montevideo, Uruguay

4 Dosel S.A, Montevideo, Uruguay

5 Parque Lecocq, Intendencia Municipal de Montevideo, Montevideo, Uruguay

6 Departamento de Parasitología, Instituto de Higiene, Facultad de Medicina, Universidad de la República, Montevideo, Uruguay

Published online: 29 August 2023

chronic hepatitis E, mainly due to HEV3, has been recognized as a clinical manifestation of major concern in organ transplant recipients and immunocompromised individuals (Fang & Han, 2017).

Domestic pigs and wild boars are the main reservoirs of these zoonotic genotypes, but the virus has an ever-expanding host range that includes camels and rabbits (Kenney, 2019; Wang and Meng, 2021; Ahmed & Nasheri, 2023).

Paslahepevirus alci species consists of moose HEV strains that has been detected mainly from Swedish moose (*Alces alces*) in the region of Scandinavia where these animals are commonly hunted for consumption. These moose HEV genomes showed a nucleotide identity of 37–63% and an aminoacid identity of 45–70% in relation to the HEV strains from *Orthohepevirinae* and *Parahepevirinae* subfamilies (Lin et al., 2014, 2015).

In addition, a recent report based on detailed phylodynamic studies suggests that several cervid species may be reservoirs of HEV, with stable transmission of the virus between cervid populations (Karlsen et al., 2023). However, whether these species are true reservoirs of HEV or if they can be infected by spill-over events is currently under debate (Anheyer-Behmenburg et al., 2017; Schotte et al., 2022).

The spotted deer or chital (*Axis axis*) is the third largest deer in the Indian subcontinent and has been introduced to several countries worldwide, including Australia, USA, Croatia, Brazil, and Argentina (Duckworth et al., 2015). This invasive and exotic deer species was also introduced to Uruguay in the early 1900s for hunting and esthetic purposes. Since 2000, a significant overpopulation of spotted deer has been observed, resulting in harvest losses and habitat degradation. Therefore, the introduction of population control measures for this species has recently been prioritized (Informe Comité de Especies Exóticas Invasoras, 2021). For this reason, hunting of *A. axis* is allowed throughout the year under strict specific licenses.

Due to its abundance, spotted deer usually coexists with livestock and large populations of wild boar (*Sus scrofa*), an important exotic species widely distributed in Uruguay (Informe Comité de Especies Exóticas Invasoras, 2021). In this context, we have previously reported a high prevalence of HEV in free-ranging wild pig populations and captive white-collared peccaries (New World pigs), suggesting that wild reservoirs may play a role in amplifying viral infection cycles in the wild (Ferreiro et al., 2020; Mirazo et al., 2018).

Therefore, surveillance of zoonotic and enzootic pathogens in wildlife is critical to understand the epidemiology and dynamics of infectious diseases that can significantly impact human and animal health from a One Health perspective. However, wildlife species are generally elusive and mostly nocturnal, making them difficult to monitor through direct observation. For this reason, camera traps (i.e., remotely operated infrared cameras) are the preferred tool for monitoring mammals (Burton et al., 2015; Wearn & Glover-Kapfer, 2019).

In this article, we examined the occurrence of HEV in spotted deer (*A. axis*) in areas coexisting with both native and wild susceptible species to gain additional insight into the viral and host ecology and dynamics of this infectious zoonotic disease.

Materials and Methods

Study Areas

Uruguay is located in southeastern South America (30° 05′ 08″–34° 58′ 27″ S, 53° 10′ 58″–58° 26′ 01″ W) and has a continental area of 176,215 km^2. The climate is classified as humid subtropical or temperate (Beck et al., 2018; Instituto Uruguayo de Meteorología, 2020). According to the 2015 official land cover map, natural grasslands are the predominant ecosystem (~60%) in the Uruguayan landscape, with native forests accounting for 4.8% and other native ecosystems (e.g., wetlands, scrublands) accounting for less than 1% (Ministerio de Vivienda, Ordenamiento Territorial y Medio Ambiente, 2015). The most widespread productive activity is livestock production for meat and milk, mainly on grasslands (natural and semi-natural), but also in forests, savannas, and some wetlands (Ministerio de Ganadería Agricultura y Pesca, 2019). Among anthropogenic cover, cropland (including artificial grassland) accounts for 27.5% of the territory, afforestation for 7.9%, and urban and other artificial areas for about 0.8% (Ministerio de Vivienda, Ordenamiento Territorial y Medio Ambiente, 2012).

This study was conducted in 12 study areas scattered throughout the country (Fig. 1).

Camera Trapping

In order to collect data on the coexistence of medium-sized and large mammals, especially wild boar, spotted deer, and cattle, in the study areas, a camera trap design was developed using Stealth Cam G42NG cameras. To this end, surveys were conducted at 47 sites for at least 100 days between March 2020 and March 2023, representing a total effort of 16,544 camera nights (Table 1). Freshwater ponds were targeted directly because they better describe species coexistence and their influence on infectious disease ecology (Johnson and Paull, 2010; Narkkul et al., 2021).

Sampling stations were spaced 0.8 km to 1 km apart (mean spacing = 0.93 km, min = 0.82 km, max = 1.1 km) within each survey area to reduce the likelihood of detecting the same individuals in different cameras (i.e., independence between stations) while optimizing the area to be surveyed. The absence of autocorrelation between

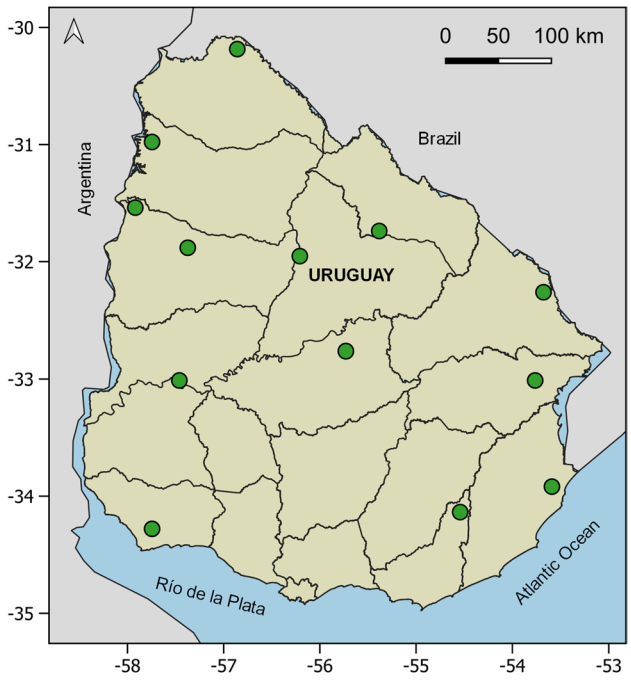

Fig. 1 Surveyed areas, Uruguay

stations was further confirmed using Moran's Index (p-value > 0.05) in the ape R package (Paradis & Schliep, 2019).

Exifpro image management software (Kowalski, 2013) was used for image processing, species labeling, and extraction of image metadata. Analysis continued using the camtrapR package (Niedballa et al., 2016) in the R program (R Core Team, 2022).

To avoid multiple counts of the same individual at a sampling station, all images of the same species taken within an hour were considered as a single independent event (Cravino & Brazeiro, 2021; Cravino et al., 2023).

Using the complete set of captures of spotted deer, wild boar, and cattle—independent of photographs—we determined their respective capture rates (CR) along sampling stations and habitat types. Species CR was calculated as the number of independent events (records) relative to sampling effort (camera nights) (CR units hereafter: records/camera nights). Special attention was paid to freshwater ponds because water samples were collected from ponds where CRs of the three species mentioned were highest.

Sample Collection

A total of 67 blood samples were collected between the years 2020 and 2022 from spotted deer: 54 were free-ranging adults hunted in crop farms and cattle ranches in western and eastern Uruguay, where coexistence with livestock and wild boar was documented using camera traps, as explained in the previous section. Thirteen samples corresponded to captive animals from the Parque Lecocq Wildlife Reserve (34° 47′ 30″ S 56° 20′ 03″ E), located in southern Uruguay. Samples were obtained by intracardiac bleeding from hunted animals and kept at 4 °C. For captive animals, individuals were chemically immobilized with 2.4–3 mg/kg tiletamine-zolazepam and 4–6 mg/kg xylazine administered with an anesthetic gun. Blood was collected aseptically by venipuncture by trained personnel. After clotting, serum samples were stored at − 70 °C until use.

Feces were collected during the same time period in sterile bags from the rectum of 19 of the 54 hunted animals, and nine samples (naturally pooled) were collected from the deer enclosure. Samples were stored on ice until processing.

In addition, two (#3 and #5) samples (50 ml) were collected from freshwater ponds in the hunting areas. These two ponds were selected based on the presence of fresh new tracks, feces, and information from camera traps on the frequency of spotted deer, wild boar, and cattle coexistence (see Sect.

Table 1 Species confirmed coexistence among sampling stations and habitats surveyed

Species coexistence	Habitat				
	Native forest	Native grassland	Freshwater pond	Crop	Tree plantation
	83% (10)	25% (3)	100% (8)	33% (2)	56% (5)
	58% (7)	42% (5)	100% (8)	–	44% (4)
	67% (8)	33% (4)	100% (8)	–	67% (6)
	75% (9)	17% (2)	100% (8)	–	22% (2)
References:		Spotted deer		Wild boar	Cattle

Values are expressed in percentages and the corresponding number of stations between brackets

"Camera Trapping"). Virus particles in the water samples were concentrated by precipitation/centrifugation as described (Wu et al., 2020).

ELISA Testing

Total anti-HEV Ig antibodies in serum samples from the 67 spotted deer were tested using ELISA HEV Ab (Dia. Pro Diagnostic Bioprobs, Italy). The kit can be used for total anti-HEV antibodies testing in zoonotic studies from a wide variety of animal species, according to the manufacturer´s specifications. The OD (optical density)/cut-off ratio was calculated for each sample tested. The reported sensitivity of this ELISA kit is 100% and the specificity is over 99.5%.

RNA Extraction, Real-Time RT-PCR, and RT-PCR Amplification

According to the manufacturer's instructions, RNA was extracted from stool and pond samples using the Quick-RNA Miniprep Kit (Zymo Research, USA).

HEV was detected in stool and water samples by broadly reactive one-step real-time RT-PCR (RT-qPCR_1) (Jothikumar et al., 2006) and one-step real-time RT-PCR (RT-qPCR_2) (Lin et al., 2015) designed to detect Moose-HEV sequences using Taqman® probes with the SensiFAST™ Probe Lo- ROX One-Step Kit (Bioline, UK).

Amplification of a conserved region of viral RNA-dependent RNA polymerase (RdRp) within ORF1 was also attempted from each stool and water sample using a broad-spectrum RT-PCR (bsRT-PCR) designed for the detection of *Hepeviridae* (Drexler et al., 2012). Amplicons of the expected size (338 bp) were sequenced by Macrogen automatic sequencing service (South Korea) to perform phylogenetic analysis and generate nucleotide *p*-distance matrices.

Phylogenetic Analysis and Identity Matrices

The phylogenetic tree was reconstructed using the neighbor-joining method with Kimura-2 parameters as the most appropriate substitution method using Molecular Evolutionary Genetics Analysis (MEGA) v10.0 software. The reference sequences of each genotype were retrieved from GenBank and included in the analysis (Smith et al., 2020). Bootstrap values for significant evidence of phylogenetic grouping were determined using 1000 replicate samples of the datasets. Nucleotide *p*-distance matrices were generated using MEGA v10.0 (Tamura et al., 2021).

Results

Camera Trapping

During the systematic surveys, we obtained 12,446 independent records for the three target species: spotted deer, wild boar, and cattle in 47 camera stations with a total sampling effort of 16,544 camera nights. Of the total records, cattle accounted for 10,230 independent records and the exotic species accounted for 2216 (1765 for spotted deer and 451 for wild boar). Species coexistence was analyzed for each habitat studied, and the records obtained are shown in Table 1. The temporal and spatial coexistence of cattle, spotted deer, and/or wild boar was confirmed in all habitat types (Table 1; Fig. 2).

For freshwater ponds, coexistence of the three species was confirmed in all sampling stations (Table 1). Two ponds (#3 and #5) with the highest frequency of species detections were selected for sampling (Fig. 3).

ELISA Testing and HEV Detection

ELISA testing for HEV revealed an overall positivity rate of 11.1% (6/54) in free-living spotted deer (Table 2), whereas none of the captive deer had anti-HEV antibodies.

In addition, HEV RNA was detected by RT-qPCR_1 in 68.4% (13/19) stool samples from free-ranging deer with C_t values ranging from 31.35 to 36.9, whereas it was detected in 21.0% (4/19) samples with C_t values ranging from 28.90 to 35.73 when RT-qPCR_2 was used (Table 3). The RT-qPCR_2 only detected the moose HEV variants and was not able to amplify the HEV3 strains.

In addition, traces of HEV RNA were detected in the #3 pond sample by RT-qPCR_1 with a C_t value of 37.45. For this RT-qPCR_1 assay, an *in-house* standard curve from an in vitro transcribed fragment was used (linear range of 4×10^8 RNA copies/µl to 4×10^3 RNA copies/µl). However, the samples had a C_t value outside the linear range and, therefore, could not be quantified.

HEV RNA was amplified and sequenced in 31.6% (6/19) stool samples by bsRT-PCR, including one (sample 66) that was negative by both RT-qPCR (Table 3). Five (66, 67, 71, 9, and 10) of these six samples were collected from the same cattle farm.

No co-infection with the two virus species was observed in the infected animals.

In contrast, no viral RNA was amplified from the captive deer samples by any method. All sequences were deposited in the GenBank database (accession numbers OP536849–OP536850 and OP536852–OP536855).

Fig. 2 Images of free-range spotted deer (*Axis axis*) obtained by camera trapping. **A** *Axis axis* and *Sus scrofa* co-occurrence in a freshwater pond. **B** *Axis axis* and *Sus scrofa* temporal co-occurrence in a native forest. **C** *Axis axis* temporal co-occurrence with livestock (*Bos taurus*) in a native forest

In addition, RNA was also extracted from all serum samples and analyzed by RT-qPCR with negative results.

On the other hand, additional RT-PCR primer sets were used to further characterize the HEV3 and HEV-like strains, but no amplification was obtained (Lin et al., 2015; Mirazo et al., 2013).

Precautions were taken to avoid contamination of the quantitative and qualitative RT-PCR assays with separate spatial areas, and a no-template control was added. In addition, the results were confirmed by multiple independent experiments and subsequent sequencing.

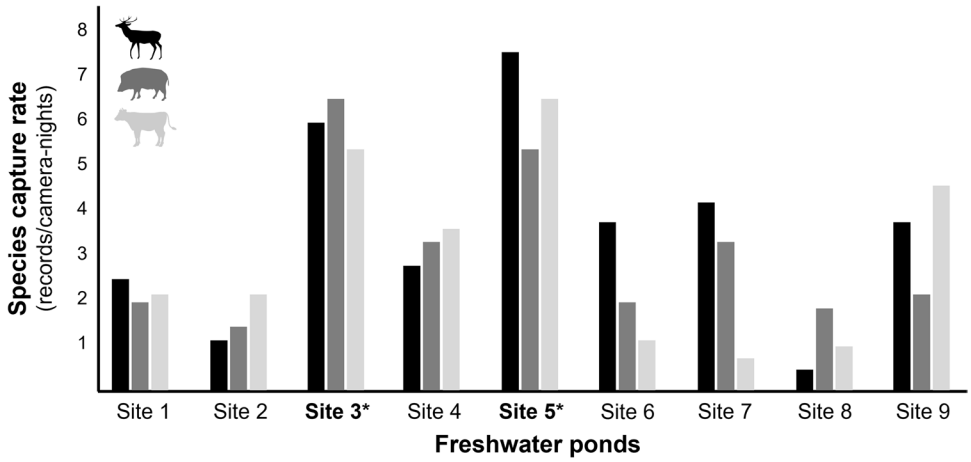

Fig. 3 Species capture rate in each freshwater pond. Species references are found in Table 1. Ponds with higher capture rates are shown in bold and with an *

Table 2 Summary of the anti-HEV antibodies, RNA detection by broad-spectrum PCR (bsRT-PCR) and RT-qPCR results

Anti-HEV % ($N+/N_{total}$)	RT-qPCR_1% ($N+/N_{total}$)	RT-qPCR_2% ($N+/N_{total}$)	bsRT-PCR % ($N+/N_{total}$)
11.1 (6/54)	68.4 (13/19)	21.0 (4/19)	31.6 (6/19)

Phylogenetic Studies

Phylogenetic analysis showed that strains 66 and 67 within *P. balayani* HEV3 were grouped in a monophyletic cluster. These sequences had the lowest nucleotide *p*-distance values (0–0.0057) and the highest nucleotide identity (88.5–98.4%) with a set of Uruguayan human and swine strains previously reported (MW596896, MZ969073, and OP536851), which in turn could not be assigned to any known HEV3 subtype according to Smith et al. (2020) (Fig. 4; Table 4). Conversely, strains 10, 71, 6, and 9 were more closely related (*p*-distance values 0.103–0.126 and nucleotide identity of 42.1–79.6%) to *P. alci* species (KF951328 and KP640885) detected in a Swedish moose (*A. alces*) (Lin et al., 2015) (Fig. 4; Table 4).

Strains 6, 9, 10, 71 (OP536852-55) and 67, 66 (OP536849-50) detected in this study as well as Uruguayan HEV3 strains from human and swine are highlighted in bold.

Table 3 Anti-HEV antibodies, C_t value, bsRT-PCR, and HEV species identified for free-ranging *Axis axis* deer

Sample ID	Anti-HEV	C_t value RT-qPCR_1	C_t value RT-qPCR_2	bsRT-PCR	*Orthohepevirinae* subfamilies
10	+	31.35	35.48	+	HEV-like unassigned species
80	+	32.83	–	–	
63	–	33.89	–	–	
65	–	33.93	–	–	
904	+	33.94	–	–	
71	+	34.12	28.90	+	HEV-like unassigned species
64	–	34.62	–	–	
19	–	34.71	–	–	
6	–	34.95	35.73	+	HEV-like unassigned species
9	–	35.37	30.64	+	HEV-like unassigned species
20	–	35.75	–	–	
67	+	36.47	–	+	*Paslahepevirus balayani* HEV3
70	+	36.91	–	–	
66	–	–	–	+	*Paslahepevirus balayani* HEV3
#3[a]		37.45	–	–	

[a]Water pond sample

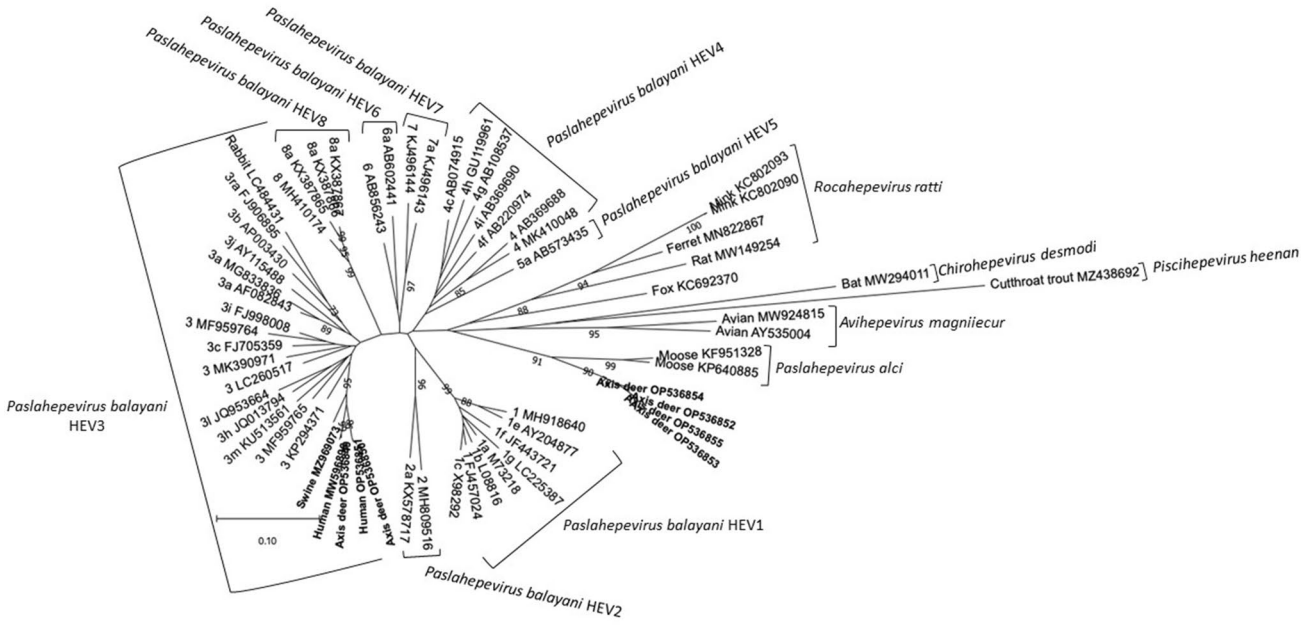

Fig. 4 Phylogenetic reconstruction based on a 338 bp fragment within the ORF1 (RdRp). Only values ≥ 60% are shown. Reference sequences from *Orthohepevirinae* subfamilies included: HEV1-8 strains and their subtypes (*Paslahepevirus balayani*), avian (*Avihepevirus magniiecur*), rat, ferret, mink (*Rocahepevirus ratti*), bat (*Chirohepevirus eptesici*), fox (unassigned species), and moose (*Paslahepevirus alci*) and from *Parahepevirinae* subfamily: cutthroat trout isolate (*Piscihepevirus heenan*)

Table 4 Summary of nucleotide p-distances for the RdRp ORF1 region between spotted deer HEV3 sequences and HEV-like sequences vs. HEV reference strains from different genus, genotypes, subtypes and species (Smith et al., 2020)

Species	Genotype/subtype/host	HEV3 sequences[a]	HEV-like sequences[b]
Paslahepevirus balayani	1a-g (Human)	0.172–0.230 (71.8–79.6%)	0.195–0.253 (35.4–74.4%)
Paslahepevirus balayani	2-2a (Human)	0.195–0.230 (73.4–78.1%)	0.230–0.253 (35.9–69.7%)
Paslahepevirus balayani	3a-n (Human/swine/wild boar)	0.080–0.172 (75.5–87.5%)	0.207–0.299 (34.8–74.4%)
Paslahepevirus balayani	3 (Unclassified subtype) (swine/wild boar)	0.034–0.138 (76.5–88.5%)	0.207–0.253 (33.3–71.3%)
Paslahepevirus balayani	3 (Uruguayan strains)	0.000–0.057 (88.5–98.4%)	0.230–0.276 (35.4–69.7%)
Paslahepevirus balayani	3ra (Rabbit)	0.080–0.103 (79.1–82.2%)	0.264–0.276 (34.8–65.1%)
Paslahepevirus balayani	4-4i (Human/swine)	0.138–0.195 (72.3–79.6%)	0.207–0.264 (35.4–70.8%)
Paslahepevirus balayani	5a (Wild boar)	0.138–0.161 (75.1–79.1%)	0.195–0.218 (36.4–70.3%)
Paslahepevirus balayani	6-6a (Wild boar)	0.161–0.195 (72.3–80.7%)	0.230–0.241 (35.4–68.7%)
Paslahepevirus balayani	7-7a (Camel)	0.184–0.218 (72.9–80.2%)	0.207–0.241 (36.4–70.3%)
Paslahepevirus balayani	8-8a (Camel)	0.172–0.207 (75.0–81.2%)	0.218–0.241 (36.4–69.2%)
Avihepevirus magniiecur	Avian	0.264–0.287 (63.5–68.7%)	0.310–0.333 (31.7–64.0%)
Rocahepevirus ratti	Rat	0.276–0.287 (64.5–67.7%)	0.276–0.299 (34.3–65.6%)
Rocahepevirus ratti	Ferret	0.276–0.310 (64.0–67.7%)	0.241–0.253 (36.4–66.6%)
Rocahepevirus ratti	Mink	0.264–0.287 (51.0–57.0%)	0.310–0.333 (41.4–57.2%)
Chirohepevirus desmodi	Bat	0.310–0.322 (57.8–62.5%)	0.345–0.368 (30.2–60.9%)
NA	Fox	0.264–0.264 (57.2–60.8%)	0.264–0.276 (41.6–55.9%)
Paslahepevirus alci	Moose	0.218–0.253 (64.0–72.9%)	0.103–0.126 (42.1–79.6%)
Piscihepevirus heenan	Cutthroat trout	0.310–0.333 (50.0–55.2%)	0.345–0.356 (30.7–52.0%)

The nucleotide identity percentages are indicated between brackets

NA not assigned

[a]66 and 67

[b]10, 71, 6 and 9

Discussion

HEV is a major cause of acute viral hepatitis worldwide and the only one that has an animal reservoir (Sayed, 2023). HEV has an ever-expanding host range (Ahmed & Nasheri, 2023) and although zoonotic hepatitis E is primarily associated with HEV3 and HEV4, with pigs, wild boar, and to a lesser extent cervids being the main source of infection, the recent report of zoonotic transmission of HEVC-1 (*Rocahepevirus ratti*) by infected rats has raised concerns about the frequency of these events involving other species (Sridhar et al., 2022). With this in mind, it remains entirely unclear whether other novel HEV strains present in unreported reservoirs can infect humans or other hosts, including livestock. Therefore, a One Health approach (World Health Organization, 2021) that provides new insights into HEV ecology and transmission networks in the wild and human–animal–environment interphases is urgently needed.

In this work, we performed a serological and molecular study of HEV in free-ranging and captive Axis deer, an exotic and highly invasive deer from Uruguay.

Interestingly, the rate of HEV antibodies detected in this study (11.1%) is consistent with previous reports in other species of the family Cervidae in Europe and North America, with rates ranging from 1.4 to 19% (Lin et al., 2015; Loikkanen et al., 2020; Sacristán et al., 2021; Weger et al., 2017).

Of note, of the 19 samples of free-living spotted deer analyzed by nucleic acid amplification techniques (NAAT), 8 were positive with RT-qPCR_1 but could not be further amplified with bsRT-PCR. Because the nucleic acids were isolated from stool samples, low-quality or partially degraded RNA might be the more plausible explanation. In fact, all positive samples amplified with RT-qPCR_1 had a low viral load, and they could not be quantified because the C_t values were outside the linear range of the standard curve. On the other hand, sample 66 could only be amplified by bsRT-PCR.

In addition, the samples that could not be amplified by RT-qPCR_2 but were positive by RT -qPCR_1 could correspond to HEV3 or other undescribed HEV-like species.

All these data suggest that detection of HEV, at least in some animal hosts, must be evaluated with multiple NAATs. In addition, the negative results of serum samples suggest that feces may be the more ideal sample in these cases, as it has been reported that the detection time of HEV RNA in feces is longer than viremia (Velavan et al., 2021).

Possibly, the HEV-like sequences reported in moose and detected in spotted deer in this study may correspond to virus strains restricted to *Cervidae*, as they have not been reported in other species. Of note, although the sequences of the two *Cervidae* species showed some similarity, the data nevertheless showed considerable divergence between them (nucleotide *p*-distance 0.103–0.126 and nucleotide identity of 42.1–79.6%), at least when comparing the nucleotide sequence of RNA-dependent RNA polymerase. For instance, a distance-based criterion cut-off of 0.093 has been recently proposed to construct a consistent HEV3 subtyping classification using complete genome nucleotide sequences, simplifying molecular epidemiology analysis (Nicot et al., 2021).

Full-length genome studies of Axis deer HEV strains are being performed at the time of writing this manuscript but have not yet been completed, and this is a clear limitation of our study. However, the molecular, serologic, and epidemiologic data presented here suggest spotted deer as a novel host for HEV and should be further investigated to determine if they can serve as an HEV reservoir in nature. According to our data, in the case of the moose HEV strains, infection of these animals does not seem to occur as a spill-over event from pigs or wild boars, as this virus species have been reported only for cervids so far. Nevertheless, this would be probably the case for the infection with HEV3 strains.

In fact, we have shown that spotted deer, like other deer species (Anheyer-Behmenburg et al., 2017; Moraes et al., 2022), can become infected with HEV3 and likely transmit it to their congeners and other potentially susceptible species through direct contact or the fecal–oral route, as well as to hunters through consumption of contaminated food (Tei et al., 2003; Sooryanarain and Meng 2019). The trading of game meat is prohibited in Uruguay since it is not subjected to any bromatological analysis; therefore, deer meat-based preparations were not available for analysis.

Furthermore, co-circulation and co-infection of genetically distant HEV variants in animals can promote the emergence of viral strains that can become critical threats to human and animal health. Surprisingly, both HEV3 sequences detected in spotted deer share a high percentage of nucleotide identity (a low *p*-distance value) with a cluster of sequences that group samples from humans, swine, wild boars, and *Pecari tajacu* (New World pigs) from Uruguay (Mirazo et al., 2018; Ferreiro et al., 2020; Cancela et al., 2021). While wild boars are widespread at high densities in Uruguay, HEV is prevalent in these animals, with a seroprevalence of 22% and infection rates of 22% and 10%, respectively (Mirazo et al., 2018). Thus, the tight and frequent interaction of these animals with spotted deer populations, e.g., sharing niches and feeding sites, might promote spill-over events involving HEV3 viruses (Anheyer-Behmenburg et al., 2017), exploiting local non-species-specific circuits of viral dissemination in the wild (Schotte et al., 2022). Furthermore, evidence of a likely presence of HEV in freshwater ponds shared by several species, including deer and

wild boars, argues in favor of this notion, given that these water sources may act as a potential additional hub for the infection of HEV, as reported for other pathogens (Ahrens et al., 2022; Tagliapietra et al., 2021). Unfortunately, the infectiousness of these water ponds could not be assessed.

The negative results obtained by ELISA testing and RT-PCR for the captive spotted deer could be mainly attributed to the wildlife reserve conditions as this is a closed population with no contact with other animal species, as it has been previously reported (Kubankova et al., 2015; Trojnar et al., 2020; Xia et al., 2015).

Camera trapping has been demonstrated to be an excellent tool for assessing the dynamics of zoonotic and epizootic infectious diseases and pathogens surveillance in nature (Acevedo et al., 2007; Bollen et al., 2021; Cadenas-Fernández et al., 2019). Results obtained from camera trapping analysis, together with molecular and phylogenetic data, strongly suggest active circuits of transmission of HEV through direct contact or shared water sources, which involves Axis deer individuals and wild boars.

This issue is particularly interesting since spotted deer, like other cervids, might serve as source of infection to susceptible domestic ruminants by harboring *Orthohepevirinae* strains, some of them with unknown consequences that may enter in the food chain. In fact, a growing body of evidence has revealed that domestic ruminants are susceptible to HEV, raising concerns about the possible implications for public health (Di Profio et al., 2022).

In summary, our work provides novel insights into HEV's complex epidemiological features and transmission cycles in nature. *Axis axis* should be considered as a potential novel host for HEV. The co-circulation of *P. balayani* HEV3 and moose HEV-like unclassified variants raises concerns about an increased potential risk for zoonotic and/or epizootic transmission, which may impact human and animal health.

Author contributions S.M, J.A. and F.C. conceived the manuscript, discuss data and wrote the draft. A. Cravino set camera trapping, analyzed data and prepared table 1and figures 1, 2 and 3. F.C, R.I., I.F. and A.Cabrera. performed the experiments and prepared figure 3 and tables 2, 3 and 4. C.L., P.G., F.B., and C.E.performed field work and collected the samples. All authors reviewed the manuscript.

Funding F.C. PhD Fellowship by Comisión Académica de Posgrado-UdelaR. This work was funded by the Comisión Sectorial de Investigación Científica-UdelaR under Grant CSIC I+D 2018 Number 245.

Declarations

Conflict of interest The authors declare that there are no conflicts of interest.

Ethical Approval This work was approved by the Animal Experimentation National Committee, Resolutions 951/2019 and 933/2020, and performed under the Scientific Collection Permit 11293/2020 issued by Ministerio de Ambiente, Uruguay.

References

Acevedo, P., Vicente, J., Höfle, U., Cassinello, J., Ruiz-Fons, F., & Gortazar, C. (2007). Estimation of European wild boar relative abundance and aggregation: A novel method in epidemiological risk assessment. *Epidemiology and Infection, 135*(3), 519–527. https://doi.org/10.1017/S0950268806007059

Ahmed, R., & Nasheri, N. (2023). Animal reservoirs for hepatitis E virus within the *Paslahepevirus* genus. *Veterinary Microbiology, 278*, 109618. https://doi.org/10.1016/j.vetmic.2022.109618

Ahrens, A. K., Selinka, H.-C., Mettenleiter, T. C., Beer, M., & Harder, T. C. (2022). Exploring surface water as a transmission medium of avian influenza viruses—Systematic infection studies in mallards. *Emerging Microbes and Infections, 11*, 1250–1261. https://doi.org/10.1080/22221751.2022.2065937

Anheyer-Behmenburg, H. E., Szabo, K., Schotte, U., Binder, A., Klein, G., & Johne, R. (2017). Hepatitis E virus in wild boars and spillover infection in red and roe deer, Germany, 2013–2015. *Emerging Infectious Diseases, 23*, 130–133. https://doi.org/10.3201/eid2301.161169

Beck, H. E., Zimmermann, N. E., McVicar, T. R., Vergopolan, N., Berg, A., & Wood, E. F. (2018). Present and future Köppen–Geiger climate classification maps at 1-km resolution. *Scientific Data, 5*, 180214. https://doi.org/10.1038/sdata.2018.214. Erratum in: Sci Data 2020 Aug 17;7(1):274.

Bollen, M., Neyens, T., Fajgenblat, M., De Waele, V., Licoppe, A., Manet, B., Casaer, J., & Beenaerts, N. (2021). Managing African swine fever: Assessing the potential of camera traps in monitoring wild boar occupancy trends in infected and non-infected zones, using spatio-temporal statistical models. *Frontiers in Veterinary Science, 8*, 726117. https://doi.org/10.3389/fvets.2021.726117

Burton, A. C., Neilson, E., Moreira, D., Ladle, A., Steenweg, R., Fisher, J. T., Bayne, E., & Boutin, S. (2015). REVIEW: Wildlife camera trapping: A review and recommendations for linking surveys to ecological processes. *Journal of Applied Ecology, 52*, 675–685.

Cancela, F., Panzera, Y., Mainardi, V., Gerona, S., Ramos, N., Pérez, R., Arbiza, J., & Mirazo, S. (2021). Complete genome sequence of hepatitis E Virus genotype 3 obtained from a chronically infected individual in uruguay. *Microbiology Resource Announcements, 10*(22):e0036721. https://doi.org/10.1128/MRA.00367-21.

Cadenas-Fernández, E., Sánchez-Vizcaíno, J. M., Pintore, A., Denurra, D., Cherchi, M., Jurado, C., Vicente, J., & Barasona, J. A. (2019). Free-ranging pig and wild boar interactions in an endemic area of African swine fever. *Frontiers in Veterinary Science, 6*, 376. https://doi.org/10.3389/fvets.2019.00376

Colson, P., & Decoster, C. (2019). Recent data on hepatitis E. *Current Opinion in Infectious Diseases, 32*, 475–481. https://doi.org/10.1097/QCO.0000000000000590

Cravino, A., & Brazeiro, A. (2021). Grassland afforestation in South America: Local scale impacts of Eucalyptus plantations on Uruguayan mammals. *Forest Ecology and Management, 484*, 118937. https://doi.org/10.1016/j.foreco.2021.118937

Cravino, A., Martínez-Lanfranco, J. A., & Brazeiro, A. (2023). Community structure of medium-large mammals across a tree plantation cycle in natural grasslands of Uruguay. *Forest Ecology and Management, 529*, 120713. https://doi.org/10.1016/j.foreco.2022.120713

Di Profio, F., Sarchese, V., Palombieri, A., Fruci, P., Lanave, G., Robetto, S., Martella, V., & Di Martino, B. (2022). Current knowledge of hepatitis E virus (HEV) epidemiology in ruminants. *Pathogens (Basel, Switzerland)*. https://doi.org/10.3390/pathogens11101124

Drexler, J. F., Seelen, A., Corman, V. M., Fumie Tateno, A., Cottontail, V., Melim Zerbinati, R., Gloza-Rausch, F., Klose, S. M., Adu-Sarkodie, Y., Oppong, S. K., Kalko, E. K. V., Osterman,

A., Rasche, A., Adam, A., Müller, M. A., Ulrich, R. G., Leroy, E. M., Lukashev, A. N., & Drosten, C. (2012). Bats worldwide carry hepatitis E virus-related viruses that form a putative novel genus within the family Hepeviridae. *Journal of Virology, 86*, 9134–9147. https://doi.org/10.1128/jvi.00800-12

Duckworth, J. W., Kumar, N. S., Anwarul, I. M., Sagar, B. H., & Timmins, R. (2015). Axis axis. The IUCN Red List of Threatened Species 2015. Retrieved May 10, 2023, from https://doi.org/10.2305/IUCN.UK.2015-4.RLTS.T41783A22158006.en

Fang, S. Y., & Han, H. (2017). Hepatitis E viral infection in solid organ transplant patients. *Current Opinion in Organ Transplantation, 22*, 351–355. https://doi.org/10.1097/MOT.0000000000000432

Ferreiro, I., Herrera, M. L., González, I., Cancela, F., Leizagoyen, C., Loureiro, M., Arellano, H., Echaides, C., Bon, B., Castro, G., Arbiza, J., & Mirazo, S. (2020). Hepatitis E Virus (HEV) infection in captive white-collared peccaries (*Pecari tajacu*) from Uruguay. *Transboundary and Emerging Diseases*. https://doi.org/10.1111/tbed.13790

Informe Comité de Especies Exóticas Invasoras (CEEI) (2021). *Especies exóticas invasoras de Uruguay: distribución, impactos socioambientales y estrategias de gestión*, C. XII. Informe Comité de Especies Exóticas Invasoras (CEEI).

Instituto Uruguayo de Meteorología. (2020). *Climatic characteristics*. Instituto Uruguayo de Meteorología. https://www.inumet.gub.uy

Jothikumar, N., Cromeans, T. L., Robertson, B. H., Meng, X. J., & Hill, V. R. (2006). A broadly reactive one-step real-time RT-PCR assay for rapid and sensitive detection of hepatitis E virus. *Journal of Virological Methods, 131*, 65–71. https://doi.org/10.1016/j.jviromet.2005.07.004

Karlsen, A. A., Kichatova, V. S., Kyuregyan, K. K., & Mikhailov, M. I. (2023). Phylodynamic analysis suggests that deer species may be a true reservoir for hepatitis E virus genotypes 3 and 4. *Microorganisms*. https://doi.org/10.3390/microorganisms11020375

Kenney, S. P. (2019). The current host range of hepatitis E viruses. *Viruses*. https://doi.org/10.3390/v11050452

Kowalski, M. (2013). *Exifpro 2.1*. California, US.

Kubankova, M., Kralik, P., Lamka, J., Zakovcik, V., Dolanský, M., & Vasickova, P. (2015). Prevalence of hepatitis E virus in populations of wild animals in comparison with animals bred in game enclosures. *Food and Environmental Virology, 7*, 159–163. https://doi.org/10.1007/s12560-015-9189-1

Lin, J., Karlsson, M., Olofson, A. S., Belák, S., Malmsten, J., Dalin, A. M., Widén, F., & Norder, H. (2015). High prevalence of hepatitis E virus in Swedish moose—A phylogenetic characterization and comparison of the virus from different regions. *PLoS ONE, 10*, 1–14. https://doi.org/10.1371/journal.pone.0122102

Lin, J., Norder, H., Uhlhorn, H., Belák, S., & Widén, F. (2014). Novel hepatitis E like virus found in Swedish moose. *Journal of General Virology, 95*, 557–570. https://doi.org/10.1099/vir.0.059238-0

Loikkanen, E., Oristo, S., Hämäläinen, N., Jokelainen, P., Kantala, T., Sukura, A., & Maunula, L. (2020). Antibodies against hepatitis E virus (HEV) in European moose and white-tailed deer in Finland. *Food Environment and Virology, 12*, 333–341. https://doi.org/10.1007/s12560-020-09442-0

Ministerio de Ganadería Agriculatura y Pesca. (2019). *Anuario Estadístico Agropecuario 2019*. Ministerio de Ganadería Agriculatura y Pesca.

Ministerio de Vivienda y Ordenamiento Territorial. (2015). *Atlas de Cobertura del Suelo de Uruguay. Cobertura de Suelo y Cambios* 2000–2011. Ministerio de Vivienda y Ordenamiento Territorial.

Ministerio de Vivienda, Ordenamiento Territorial y Medio Ambiente. (2012). *Mapa de coberturas del suelo de Uruguay*. MVOTMA/MGAP/OPP.

Mirazo, S., Gardinali, N. R., Cecilia, D., Verger, L., Ottonelli, F., Ramos, N., Castro, G., Pinto, M. A., Ré, V., Pisano, B., Lozano, A., de Oliveira, J. M., & Arbiza, J. (2018). Serological and virological survey of hepatitis E virus (HEV) in animal reservoirs from Uruguay reveals elevated prevalences and a very close phylogenetic relationship between swine and human strains. *Veterinary Microbiology., 213*, 21–27. https://doi.org/10.1016/j.vetmic.2017.11.013

Mirazo, S., Ramos, N., Russi, J. C., & Arbiza, J. (2013). Genetic heterogeneity and subtyping of human Hepatitis E virus isolates from Uruguay. *Virus Research, 173*, 364–370. https://doi.org/10.1016/j.virusres.2013.01.005

Moraes, Df., Lopez-Lopez, P., Palmeira, J. D., Torres, R. T., Rivero-Juarez, A., Dutra, V., Nascimento, M., & Mesquita, J. R. (2022). Screening for hepatitis E virus genotype 3 in red deer (*Cervus elaphus*) and fallow deer (*Dama dama*), Portugal, 2018–2020. *Transboundary and Emerging Diseases, 69*, 2764–2768. https://doi.org/10.1111/tbed.14427

Narkkul, U., Thaipadungpanit, J., Srisawat, N., Rudge, J. W., Thongdee, M., Pawarana, R., & Pan-Ngum, W. (2021). Human, animal, water source interactions and leptospirosis in Thailand. *Scientific Reports, 11*(1), 3215. https://doi.org/10.1038/s41598-021-82290-5

Nicot, F., Dimeglio, C., Migueres, M., Jeanne, N., Latour, J., Abravanel, F., et al. (2021). Classification of the zoonotic hepatitis E virus genotype 3 into distinct subgenotypes. *Frontiers in Microbiology, 11*, 634430. https://doi.org/10.3389/fmicb.2020.634430

Niedballa, J., Sollmann, R., & Courtiol, A. (2016). camtrapR: An R package for efficient camera trap data management. *Methods in Ecology and Evolution, 7*, 1457–1462. https://doi.org/10.1111/2041-210X.12600

Paradis, E., & Schliep, K. (2019). ape 5.0: An environment for modern phylogenetics and evolutionary analyses in R. *Bioinformatics, 35*, 526–528. https://doi.org/10.1093/bioinformatics/bty633

R Core Team. (2022). *R: A language and environment for statistical computing*. R Foundation for Statistical Computing. https://doi.org/10.4135/9781473920446.n12

Sacristán, C., Madslien, K., Sacristán, I., Klevar, S., & das Neves, C. G. (2021). Seroprevalence of hepatitis E virus in moose (*Alces alces*), reindeer (*Rangifer tarandus*), red deer (*Cervus elaphus*), roe deer (*Capreolus capreolus*), and muskoxen (*Ovibos moschatus*) from Norway. *Viruses*. https://doi.org/10.3390/v13020224

Sayed, I. M. (2023). Dual infection of hepatitis A virus and hepatitis E virus-What is known? *Viruses*, *15*(2):298. https://doi.org/10.3390/v15020298

Schotte, U., Martin, A., Brogden, S., Schilling-Loeffler, K., Schemmerer, M., Anheyer-Behmenburg, H. E., Szabo, K., Müller-Graf, C., Wenzel, J. J., Kehrenberg, C., Binder, A., Klein, G., & Johne, R. (2022). Phylogeny and spatiotemporal dynamics of hepatitis E virus infections in wild boar and deer from six areas of Germany during 2013–2017. *Transboundary and Emerging Diseases, 69*, e1992–e2005. https://doi.org/10.1111/tbed.14533

Smith, D. B., Izopet, J., Nicot, F., Simmonds, P., Jameel, S., Meng, X.-J., Norder, H., Okamoto, H., Poel, W. H. M., Van Der, Reuter, G., & Purdy, M. A. (2020). Update: Proposed reference sequences for subtypes of hepatitis E virus (species Orthohepevirus A) 1–7. https://doi.org/10.1099/jgv.0.001435

Sridhar, S., Yip, C. C. Y., Lo, K. H. Y., Wu, S., Situ, J., Chew, N. F. S., Leung, K. H., Chan, H. S. Y., Wong, S. C. Y., Leung, A. W. S., Tse, C. W. S., Fung, K. S. C., Tsang, O. T. Y., Hon, K. L., Cheng, V. C. C., Ng, K. H. L., & Yuen, K. Y. (2022). Hepatitis E virus species C infection in humans, Hong Kong. *Clinical Infectious Diseases: an Official Publication of Infectious Diseases Society of America, 75*, 288–296. https://doi.org/10.1093/cid/ciab919

Tagliapietra, V., Boniotti, M. B., Mangeli, A., Karaman, I., Alborali, G., Chiari, M., D'Incau, M., Zanoni, M., Rizzoli, A., & Pacciarini, M. L. (2021). *Mycobacterium microti* at the environment and

wildlife interface. *Microorganisms*. https://doi.org/10.3390/microorganisms9102084

Tamura, K., Stecher, G., & Kumar, S. (2021). MEGA11: Molecular Evolutionary Genetics Analysis version 11. *Molecular Biology and Evolution, 38*, 3022–3027.

Tei, S., Kitajima, N., Takahashi, K., & Mishiro, S. (2003). Zoonotic transmission of hepatitis E virus from deer to human beings. *Lancet (london, England), 362*, 371–373. https://doi.org/10.1016/S0140-6736(03)14025-1

Trojnar, E., Kästner, B., & Johne, R. (2020). No evidence of hepatitis E virus infection in farmed deer in Germany. *Food Environment and Virology, 12*, 81–83. https://doi.org/10.1007/s12560-019-09407-y

Velavan, T. P., Pallerla, S. R., Johne, R., Todt, D., Steinmann, E., Schemmerer, M., Wenzel, J. J., Hofmann, J., Shih, J. W. K., Wedemeyer, H., & Bock, C.-T. (2021). Hepatitis E: An update on One Health and clinical medicine. *Liver International: Official Journal of International Association for the Study of Liver, 41*, 1462–1473. https://doi.org/10.1111/liv.14912

Wearn, O. R., & Glover-Kapfer, P. (2019). Snap happy: Camera traps are an effective sampling tool when compared with alternative methods. *Royal Society Open Science, 6*(3), 181748. https://doi.org/10.1098/rsos.181748

Weger, S., Elkin, B., Lindsay, R., Bollinger, T., Crichton, V., & Andonov, A. (2017). Hepatitis E virus seroprevalence in free-ranging deer in Canada. *Transboundary and Emerging Diseases, 64*, 1008–1011. https://doi.org/10.1111/tbed.12462

World Health Organization. (WHO). (2017). *Hepatitis E*. WHO https://www.who.int/news-room/fact-sheets/detail/hepatitis-e

Wu, F., Zhang, J., Xiao, A., Gu, X., Lee, W. L., Armas, F., Kauffman, K., Hanage, W., Matus, M., Ghaeli, N., Endo, N., Duvallet, C., Poyet, M., Moniz, K., Washburne, A. D., Erickson, T. B., Chai, P. R., Thompson, J., & Alm, E. J. (2020). SARS-CoV-2 titers in wastewater are higher than expected from clinically confirmed cases. *mSystems*. https://doi.org/10.1128/mSystems.00614-20

Xia, J., Zeng, H., Liu, L., Zhang, Y., Liu, P., Geng, J., Wang, L., Wang, L., & Zhuang, H. (2015). Swine and rabbits are the main reservoirs of hepatitis E virus in China: Detection of HEV RNA in feces of farmed and wild animals. *Archives of Virology., 160*, 2791–2798. https://doi.org/10.1007/s00705-015-2574-0

3.5. Experimentos complementarios no incluidos en el artículo.

3.5.1. Relevamiento serológico y molecular de HEV en animales de cautiverio

A fin de explorar la eventual circulación de HEV en diversos potenciales reservorios animales silvestres en cautiverio, se colectaron sueros de 137 ovinos (de diferentes rebaños del país) y 17 antílopes adax (*Addax nasomaculatus*), 19 venados de campo (*Ozotoceros bezoarticus*) y 10 pecaríes (*Pecari tajacu*), todos de la reserva del Parque Lecocq (34°47'30"S 56°20'03"O), situado al oeste de Uruguay.

Las investigaciones con animales estuvieron amparadas bajo protocolos aprobados por el Comité Nacional de Experimentación Animal, resoluciones número 951/2019 y 933/2020 y realizadas bajo el permiso de colecta científico número 11293/2020 emitido por el Ministerio de Ambiente. Las muestras de antílopes y venados fueron de archivo, provistas por la Facultad de Veterinaria, UdelaR

Los sueros fueron analizados por medio del kit HEV Ab IgG, IgM, IgA versión ULTRA multiespecie (Dia.Pro Diagnostic Bioprobs, Italia).

Se obtuvo una seroprevalencia de 0,73% (1/137) para ovinos, 20% (2/10) para pecaríes, 10,5% (2/19) para venados y no se detectaron anticuerpos anti-HEV en antílopes (Tabla 4).

Tabla 4. Resumen de resultados de seroprevalencia y detección molecular obtenidos en el Capítulo 1 para las especies animales y ambientales analizadas. Se indica procedencia de las muestras, anticuerpos anti-HEV, detección de ARN por RT-qPCR_1 (*screening*), RT-qPCR_2 (cérvidos), PCR amplio espectro para *Hepeviridae* (bsRT-PCR) y genotipo de HEV identificado.

Sitio de colecta	**Especies/muestras**	**Anti-HEV % (N+/N total)**	**RT-qPCR_1 % (N+/N total)**	**RT-qPCR_2 % (N+/N total)**	**bsRT-PCR % (N+/N total)**	***Orthohepevirinae*** especie/genotipos identificados
Silvestres de vida libre	Ciervos *(Axis axis)*	11,1% (6/54)	68,4% (13/19)	21,0% (4/19)	31,6% (6/19)	4 de HEV-*like* especie sin asignar 2 de *Paslahepevirus balayani* HEV3
Silvestres en cautiverio (Parque Lecocq)	Venados de campo *(Ozotoceros bezoarticus)*	10,5% (2/19)	-	-	-	-
	Antílopes adax *(Addax nasomaculatus)*	0% (0/17)	-	-	-	-
	Pecaríes (*Pecari tajacu*)	20% (2/10)	-	-	-	-
Ganado	Ovinos (*Ovis orientalis aries*)	0,73% (1/137)	0% (0/1)	-	0% (0/1)	-
Hábitat de ciervos silvestres de vida libre	Cañadas	-	50% (1/2)	0% (0/2)	0% (0/2)	-

3.5.2. RT-PCR para obtención de genomas de HEV de cérvido

Se implementaron RT-PCR solapantes para amplificar y secuenciar 5-6 Kb del total de 7,2 Kb de HEV a partir de la muestra 71 de Axis según lo reportado previamente en Lin et al. 2014, utilizando los sets de *primers* que se detallan en la Tabla 5.

Sin embargo, no fue posible obtener productos de amplificación para ninguna de las 3 PCR.

Tabla 5. *Primers* utilizados para amplificar el genoma de HEV de ciervo.

Nombre del Primer	Posición nucleotídica*	Secuencia	Tamaño de fragmento (Kb)
ESP	4248-6410	CATGGTAAAGTGGGTCAGGGTAT	2,16
HE041R		GCCAATGGCGAGCCGACAGTGAA	
HEV5979F	5979-7258	CGAGGAGGAGGCTACGTCTGGTCTGGTA	1,3
HEVAXR		CGCTACGTAACGGCATGACAGTG	
HEV108F	108/2176-4585	GCCTTGGCGAATGCTGTGGT	2,5-4,4
HEV4585R		GGACTCCTTCGGAGCCTGCAGCGTCCAA	

*Las posiciones son según la secuencia SWX07-E1 (EU360977).

4. CAPÍTULO 2

Obtención de genomas completos de HEV3 por NGS.

4.1. Fundamento teórico y antecedentes

HEV3 es considerado el genotipo con mayor diversidad genética, con una variabilidad intra-genotipo de hasta el 19,3% [27], conteniendo múltiples linajes dentro de los hospedadores [79]. Por lo tanto, las cepas de HEV3 son a su vez subdivididas en 13 subtipos (3a-3n) basados en los valores de p-distancia nucleotídica a partir de genomas completos, definiéndose secuencias de referencia [28]. Recientemente, se propuso un criterio basado en un valor *cut-off* de p-distancia de 0,093 con el objetivo de realizar sub-tipificaciones de HEV3 de forma más consistente [80].

Los análisis filogenéticos realizados previamente con secuencias parciales provenientes de reservorios animales y casos clínicos [34, 71] indicaron que todas las cepas uruguayas forman un *cluster* monofilético y no pertenecen a ningún subtipo conocido. Por ello, para llevar a cabo una clasificación robusta que permita la asignación de las cepas de nuestro país a un nuevo subtipo, así como para realizar análisis genéticos más minuciosos, es necesario obtener genomas completos de HEV.

Obtener genomas completos, particularmente de HEV, supone un gran desafío ya que este virus presenta gran variabilidad genética. Cabe destacar que la secuenciación masiva (NGS) basada en PCR no es de los métodos más adecuados para llevar a cabo dicho objetivo ya que puede reducir la posibilidad de detectar variantes nuevas por el sesgo introducido por los *primers* [81]. Además, si bien recientemente se describió un panel de sondas de captura de HEV1-4 para el enriquecimiento específico de las librerías [82], este se diseñó tomando en cuenta los subtipos de referencia de la Organización Mundial de la Salud (OMS) [83, 84], no permitiendo la identificación de nuevos subtipos.

En este sentido, la secuenciación metagenómica o virómica por *shotgun* (Fig. 8) es una de las aproximaciones más utilizadas para la secuenciación de genomas virales [85] y particularmente para la secuenciación de genomas de HEV, ya que no implica un conocimiento previo de la secuencia nucleotídica.

Sin embargo, es importante tener en cuenta que uno de los principales obstáculos para obtener genomas virales por estas estrategias radica en la posibilidad de implementar de forma exitosa el enriquecimiento de partículas virales en la muestra, que usualmente se encuentran en baja proporción con respecto al genoma bacteriano y del hospedero [85, 86]. Para ello, se han desarrollado una serie de métodos para mejorar el enriquecimiento viral como tratamiento con DNAsa I, filtración y ultracentrifugación [87–89].

De hecho, evidenciando la dificultad en la obtención de genomas de HEV, hasta el momento se encuentran reportados solo 642 genomas completos para todos los genotipos en la base de datos de GenBank [82].

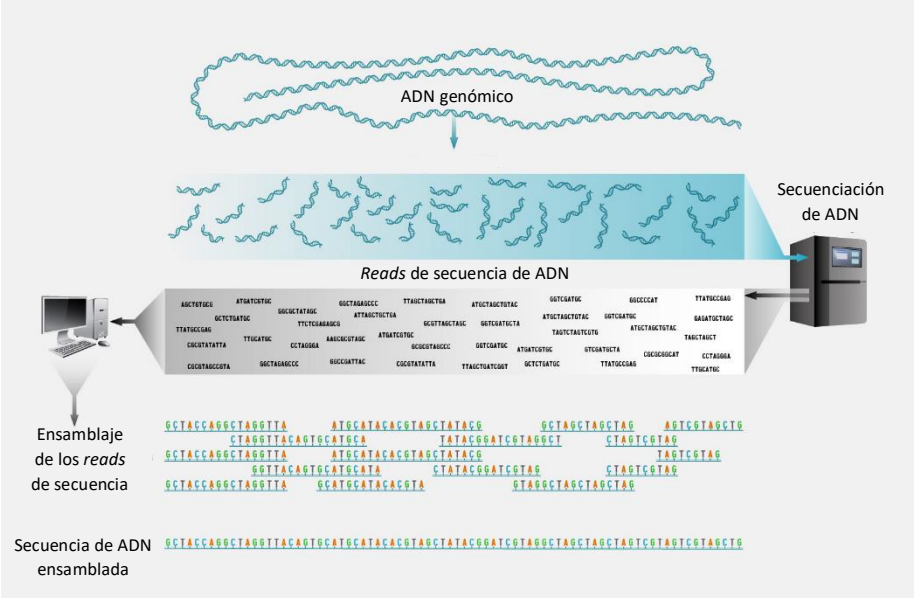

Fig. 8. Representación esquemática de la secuenciación masiva tipo *shotgun*. Este método consiste en fragmentar al azar el ADN en pequeños fragmentos que serán secuenciados individualmente. Posteriormente, por medio de programas bioinformáticos se ensamblan estos fragmentos en base a regiones solapantes para reconstruir el genoma. Extraído y adaptado de [90]. https://www.genome.gov/genetics-glossary/Shotgun-Sequencing

4.2. Hipótesis

Las cepas de HEV3 de Uruguay no agrupan en ningún subtipo conocido. Por lo tanto, es posible obtener los primeros genomas completos de HEV para Sudamérica y clasificarlos de forma robusta en un nuevo subtipo.

4.3. Objetivo específico

Obtención y clasificación de genomas completos de HEV3 por NGS. Contribuir a profundizar la información sobre la epidemiología de HEV en Sudamérica por medio de la obtención de genomas completos de HEV3 de diversas especies mediante secuenciación masiva con el fin de clasificar adecuadamente las cepas circulantes en el país y asignarle un subtipo y, más importante, entender desde la filogenética las rutas de trasmisión viral asociadas a los casos clínicos detectados.

4.4. Cancela et al., 2021. Complete Genome Sequence of Hepatitis E Virus Genotype 3 Obtained from a Chronically Infected Individual in Uruguay.

En este trabajo se reportó el primer genoma completo de HEV de Sudamérica proveniente de un paciente uruguayo trasplantado y con infección crónica por HEV. El genoma se obtuvo mediante secuenciación masiva por tecnología Illumina y presentó 7229 nt de longitud con un contenido GC de 54,8%. A través de análisis filogenéticos y de p-distancia se clasificó a esta secuencia en el genotipo 3, la cual exhibió un 86% de identidad nucleotídica con la secuencia de referencia más cercanamente relacionada, pero no fue posible clasificarla en ningún subtipo conocido, para lo que se requiere la obtención de genomas completos adicionales.

Los resultados derivados de este trabajo fueron publicados en un artículo científico que se adjunta a continuación:

Cancela F, Panzera Y, Mainardi V, Gerona S, Ramos N, Pérez R, Arbiza J, Mirazo S. Complete Genome Sequence of Hepatitis E Virus Genotype 3 Obtained from a Chronically Infected Individual in Uruguay. Microbiol Resour Announc. 2021 Jun 3;10(22):e0036721. doi: 10.1128/MRA.00367-21. Epub 2021 Jun 3.

AMERICAN SOCIETY FOR MICROBIOLOGY | Microbiology Resource Announcements

GENOME SEQUENCES

Complete Genome Sequence of Hepatitis E Virus Genotype 3 Obtained from a Chronically Infected Individual in Uruguay

Florencia Cancela,[a] Yanina Panzera,[b] Victoria Mainardi,[c] Solange Gerona,[c] Natalia Ramos,[a] Ruben Pérez,[b] Juan Arbiza,[a] Santiago Mirazo[a]

[a]Sección Virología, Facultad de Ciencias, Universidad de la República, Montevideo, Uruguay
[b]Sección Genética Evolutiva, Facultad de Ciencias, Universidad de la República, Montevideo, Uruguay
[c]Programa de Trasplante Hepático, Hospital Central de las Fuerzas Armadas, Montevideo, Uruguay

ABSTRACT Hepatitis E virus (HEV) is a leading cause of acute viral hepatitis worldwide. We report the full-length genome sequence of an HEV-3 strain obtained from a chronically infected patient from Uruguay. This strain shared only 86% nucleotide sequence identity with the most closely related reference strain belonging to subtype 3m.

Hepatitis E is a zoonotic infection of increasing concern and a leading cause of acute hepatitis of viral origin in developed regions and regions of nonendemicity (1). The etiological agent, hepatitis E virus (HEV), belongs to the *Orthohepevirus A* species, *Hepeviridae* family, and is classified into 8 genotypes (HEV-1 to HEV-8), of which HEV-1 to HEV-4 and HEV-7 are recognized as human pathogens (2). Due to the extensive genetic diversity, HEV genotypes are further divided into subtypes (2, 3). HEV usually causes an acute and self-limiting disease in immunocompetent individuals. However, novel aspects regarding HEV infection have been recently uncovered, including the possibility of the disease becoming chronic in immunocompromised individuals or solid organ transplant (SOT) recipients (4).

We recently reported a case study of an autochthonous chronic HEV infection in a SOT recipient who was further diagnosed with a posttransplant lymphoproliferative disorder (5). That HEV strain, named C1, was identified as belonging to HEV-3, and in this study, we report the full-length genome sequence.

RNA was extracted from a stool sample with a Quick-RNA miniprep kit (Zymo Research Corp., USA). Double-stranded cDNA (ds-cDNA) was generated using a Maxima H Minus ds-cDNA synthesis kit (Thermo Fisher Scientific, USA) with random primers. The ds-cDNA was further amplified by multiple displacement amplification (MDA) technology using a REPLI-g minikit (Qiagen, Germany), followed by purification and quantification using an AMPure XP device (Beckman Coulter, USA) and a Qubit fluorometer (Qubit DNA high-sensitivity [HS] assay kit), respectively.

A Nextera DNA flex library preparation kit (Illumina, USA) with dual indexing was used with 50 ng of ds-cDNA. Quality control was performed on a Fragment Analyzer 5200 system (Agilent Technologies, USA) by using the standard-sensitivity next-generation sequencing (NGS) analysis kit (Agilent Technologies, USA). The library was sequenced on an Illumina MiniSeq genomic platform at Facultad de Ciencias (Universidad de la República [UdelaR], Uruguay) using a midoutput reagent cartridge (300 cycles, 150-bp paired-end reads) following the standard Illumina protocols.

A total of 286,928 sequencing raw reads were demultiplexed automatically on the MiniSeq platform with the default settings. Adapter/quality trimming and filtering were performed with the BBDuk plugin (default settings), and the reads were then mapped to the HEV genome (GenBank accession number FJ998008) using the

Citation Cancela F, Panzera Y, Mainardi V, Gerona S, Ramos N, Pérez R, Arbiza J, Mirazo S. 2021. Complete genome sequence of hepatitis E virus genotype 3 obtained from a chronically infected individual in Uruguay. Microbiol Resour Announc 10:e00367-21. https://doi.org/10.1128/MRA.00367-21.

Editor Kenneth M. Stedman, Portland State University

Address correspondence to Santiago Mirazo, smirazo@fcien.edu.uy.

Received 9 April 2021
Accepted 13 May 2021
Published 3 June 2021

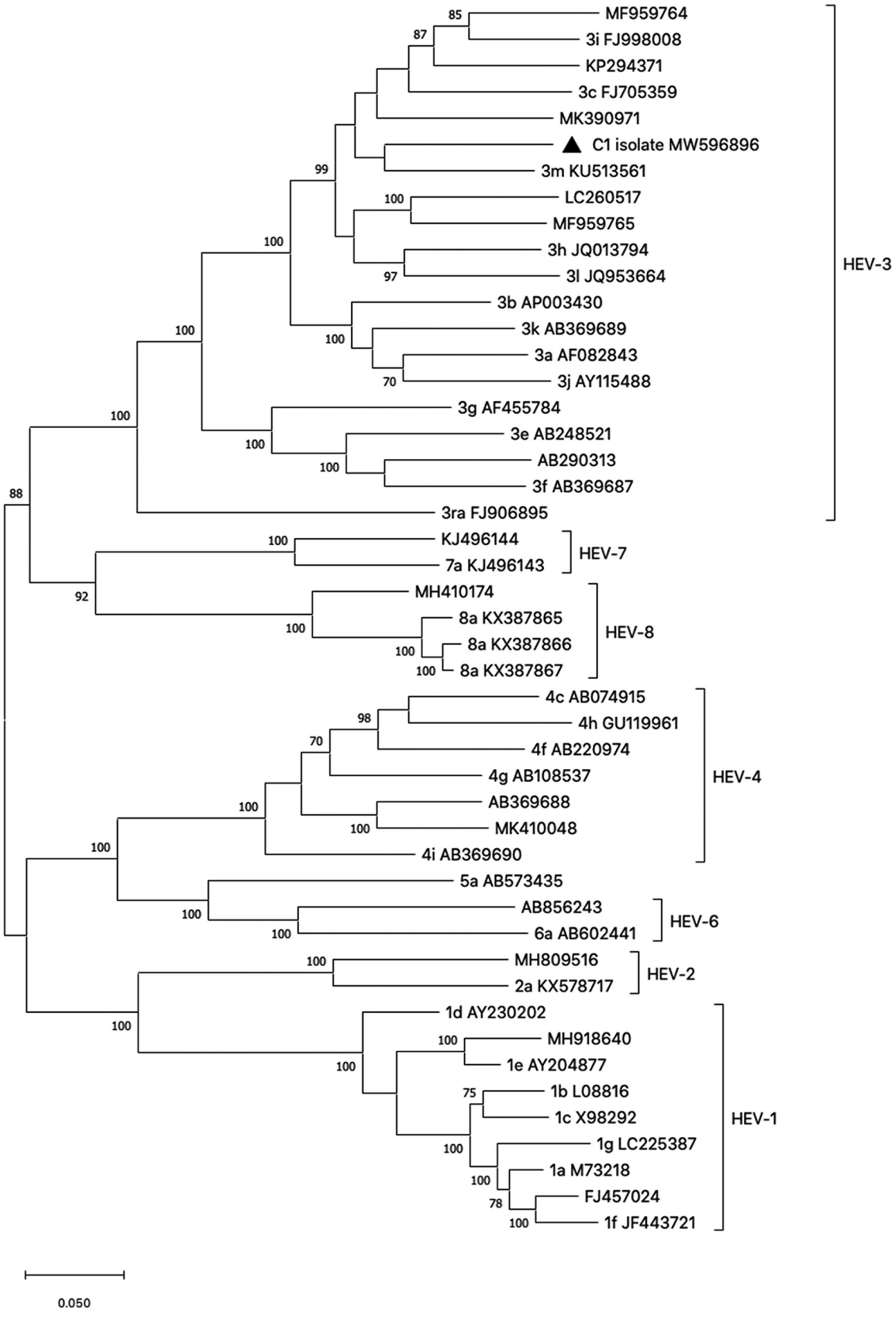

FIG 1 Phylogenetic tree based on the full-length genome sequences of proposed representative HEV genotype reference strains, according to Smith et al. (7). Subtype reference strains are also indicated. Tree reconstruction was performed using the maximum-likelihood method with Tamura-Nei as the best substitution model. The robustness of the tree was determined by bootstrap analysis (1,000 replicates), and only values of ≥60% are shown. The GenBank accession numbers are shown for each sequence. Letters indicate the subtype classification. The C1 strain from this study is marked with a solid triangle.

Geneious mapper (medium-low sensitivity) available in the Geneious Prime 2020.2.1 software. Annotation was done with SeqMan NGen 12.0 (DNASTAR, Madison, WI). Complete sequence alignment, with ClustalW, and phylogenetic tree reconstruction were performed with MEGA X software (6).

The complete sequence of the C1 strain was 7,229 nucleotides long with a 54.8% GC content, 7,507 mapped reads, and 114× coverage. The genome comprises three open reading frames (ORFs) that encode the viral proteins as follows: ORF1, positions 13 to 5124; ORF2, 5159 to 7141; and ORF3, 5121 to 5489. C1 clustered within HEV-3 sequences, and it shared 86% nucleotide sequence identity (complete sequence comparison in BLAST [https://blast.ncbi.nlm.nih.gov/Blast.cgi]) with the isolate KU513561, identified as the reference strain of the 3m subtype (7), the most closely related sequence according to the phylogenetic reconstruction (Fig. 1).

The use of the patient sample was approved by the Ethics Committee from the Hospital Central de las Fuerzas Armadas from Uruguay. The patient gave his written consent prior to the inclusion in this study.

To conclude, we present a complete HEV genome sequence obtained from a chronically infected patient. Further research is needed in order to attain deeper knowledge of the molecular epidemiology of HEV in Latin America.

Data availability. The complete genome sequence of C1 has been deposited in the GenBank database under the accession number MW596896 and in the SRA under BioSample accession number SAMN19016784 and study number PRJNA727355.

ACKNOWLEDGMENTS

We thank Programa de Desarrollo de las Ciencias Básicas for the excellent administrative support.

This work was funded by the Comisión Sectorial de Investigación Científica-UdelaR, under grant CSIC I+D 2018 number 245. F.C. was funded by a Ph.D. fellowship from Comisión Académica de Posgrado-UdelaR. The funder had no role in the design of the study, in the collection, analyses, or interpretation of data, in the writing of the manuscript, or in the decision to publish the results.

REFERENCES

1. World Health Organization. 2017. Global hepatitis report. https://www.who.int/hepatitis/publications/global-hepatitis-report2017/en/.
2. Primadharsini PP, Nagashima S, Okamoto H. 2019. Genetic variability and evolution of hepatitis E virus. Viruses 11:456. https://doi.org/10.3390/v11050456.
3. Nicot F, Dimeglio C, Migueres M, Jeanne N, Latour J, Abravanel F, Ranger N, Harter A, Dubois M, Lameiras S, Baulande S, Chapuy-Regaud S, Kamar N, Lhomme S, Izopet J. 2020. Classification of the zoonotic hepatitis E virus genotype 3 into distinct subgenotypes. Front Microbiol 11:634430. https://doi.org/10.3389/fmicb.2020.634430.
4. Lhomme S, Marion O, Abravanel F, Izopet J, Kamar N. 2020. Clinical manifestations, pathogenesis and treatment of hepatitis E virus infections. J Clin Med 9:331. https://doi.org/10.3390/jcm9020331.
5. Mainardi V, Gerona S, Ardao G, Ferreira N, Ramírez G, Arbiza J, Mirazo S. 2019. Locally acquired chronic hepatitis E followed by Epstein-Barr virus reactivation and Burkitt lymphoma as a suspected extrahepatic manifestation in a liver transplant recipient. Am J Case Rep 20:1016–1021. https://doi.org/10.12659/AJCR.916253.
6. Stecher G, Tamura K, Kumar S. 2020. Molecular Evolutionary Genetics Analysis (MEGA) for macOS. Mol Biol Evol 37:1237–1239. https://doi.org/10.1093/molbev/msz312.
7. Smith DB, Izopet J, Nicot F, Simmonds P, Jameel S, Meng XJ, Norder H, Okamoto H, van der Poel WHM, Reuter G, Purdy MA. 2020. Update: proposed reference sequences for subtypes of hepatitis E virus (species *Orthohepevirus A*). J Gen Virol 101:692–698. https://doi.org/10.1099/jgv.0.001435.

4.5. Cancela et al., 2023. Epidemiology Update of Hepatitis E Virus (HEV) in Uruguay: Subtyping, Environmental Surveillance and Zoonotic Transmission.

En este trabajo se reportó un genoma completo de HEV3 proveniente de un cerdo de granja de Uruguay mediante secuenciación masiva por método de Illumina. Los estudios filogenéticos realizados con las secuencias completas y parciales de HEV reportadas en Uruguay, evidenciaron que las cepas uruguayas agrupan en un *cluster* monofilético con una alta identidad nucleotídica y presentaron valores de p-distancia por encima del *cut-off* establecido de 0,093 comparándolo con las secuencias de referencia de subtipos.

Por lo tanto, estos resultados sugieren que las secuencias uruguayas de HEV pueden pertenecer a un nuevo subtipo putativo, HEV-3o.

Los resultados derivados de este trabajo fueron publicados en un artículo científico que se adjunta a continuación:

Cancela, F.; Icasuriaga, R.; Cuevas, S.; Hergatacorzián, V.; Olivera, M.; Panzera, Y.; Pérez, R.; López, J.; Borzacconi, L.; González, E.; et al. Epidemiology Update of Hepatitis E Virus (HEV) in Uruguay: Subtyping, Environmental Surveillance and Zoonotic Transmission. Viruses 2023, 15, 2006. doi: 10.3390/v15102006.

---

viruses

MDPI

Article

Epidemiology Update of Hepatitis E Virus (HEV) in Uruguay: Subtyping, Environmental Surveillance and Zoonotic Transmission

Florencia Cancela [1,2], Romina Icasuriaga [1], Santiago Cuevas [2], Valentina Hergatacorzián [2], Mauricio Olivera [2], Yanina Panzera [3], Ruben Pérez [3], Julieta López [4], Liliana Borzacconi [5], Elizabeth González [4], Natalia Montaldo [2], Melissa Gaitán [6], Sandra López-Verges [6,7], Viviana Bortagaray [8], Matías Victoria [8], Rodney Colina [8], Juan Arbiza [2], Mabel Berois [2] and Santiago Mirazo [1,*]

1 Departamento de Bacteriología y Virología, Instituto de Higiene, Facultad de Medicina, Universidad de la República, Montevideo 11600, Uruguay; fcancela@higiene.edu.uy (F.C.)
2 Sección Virología, Instituto de Química Biológica, Facultad de Ciencias, Universidad de la República, Montevideo 11600, Uruguay; nmontaldo@fcien.edu.uy (N.M.)
3 Sección Genética Evolutiva, Instituto de Biología, Facultad de Ciencias, Universidad de la República, Montevideo 11600, Uruguay; rperez@fcien.edu.uy (R.P.)
4 Departamento de Ingeniería Ambiental, Facultad de Ingeniería, Universidad de la República, Montevideo 11600, Uruguay
5 Instituto de Ingeniería Química, Facultad de Ingeniería, Universidad de la República, Montevideo 11600, Uruguay
6 Departamento de Virología y Biotecnología, Instituto Conmemorativo Gorgas de Estudios de la Salud, Panamá 0801, Panama
7 Sistema Nacional de Investigación, Senacyt, Panamá 0801, Panama
8 Laboratorio de Virología molecular, Departamento de Ciencias Biológicas, CENUR Litoral Norte, Sede Salto, Universidad de la República, Salto 50000, Uruguay; matvicmon@gmail.com (M.V.)
* Correspondence: smirazo@higiene.edu.uy; Tel.: +598-2-4871288

Abstract: Hepatitis E Virus (HEV) infection is an emergent zoonotic disease of increasing concern in developed regions. HEV genotype 3 (HEV-3) is mainly transmitted through consumption of contaminated food in high-income countries and is classified into at least 13 subtypes (3a–3n), based on *p*-distance values from complete genomes. In Latin America, HEV epidemiology studies are very scant. Our group has previously detected HEV3 in clinical cases, swine, wild boars, captive white-collared peccaries, and spotted deer from Uruguay. Herein, we aimed to provide novel insights and an updated overview of the molecular epidemiology of zoonotic HEV in Uruguay, including data from wastewater-based surveillance studies. A thorough analysis of HEV whole genomes and partial ORF2 sequences from Uruguayan human and domestic pig strains showed that they formed a separate monophyletic cluster with high nucleotide identity and exhibited p-distance values over the established cut-off (0.093) compared with reference subtypes' sequences. Furthermore, we found an overall prevalence of 10.87% (10/92) in wastewater, where two samples revealed a close relationship with humans, and animal reservoirs/hosts isolates from Uruguay. In conclusion, a single, new HEV-3 subtype currently circulates in different epidemiological settings in Uruguay, and we propose its designation as 3o along with its reference sequence.

Keywords: Hepatitis E virus; subtype 3o; wastewater; Uruguay; molecular epidemiology

Citation: Cancela, F.; Icasuriaga, R.; Cuevas, S.; Hergatacorzián, V.; Olivera, M.; Panzera, Y.; Pérez, R.; López, J.; Borzacconi, L.; González, E.; et al. Epidemiology Update of Hepatitis E Virus (HEV) in Uruguay: Subtyping, Environmental Surveillance and Zoonotic Transmission. *Viruses* **2023**, *15*, 2006. https://doi.org/10.3390/v15102006

Academic Editor: Siddharth Sridhar

Received: 3 September 2023
Revised: 19 September 2023
Accepted: 21 September 2023
Published: 27 September 2023

1. Introduction

Hepatitis E virus (HEV) infection causes 20 million HEV infections and 70,000 deaths annually.

Particularly in industrialized non-endemic countries, it has been recently acknowledged as an important zoonotic agent of acute hepatitis [1].

The HEV virion consists of an icosahedral non-enveloped particle of 32–34 nm in feces and a "quasi-enveloped" particle of ~40 nm in circulating blood and culture supernatants [2]. The viral genome is a single-stranded positive-sense RNA molecule of approximately 7.2 Kb with a methyl guanosine cap at the 5′ end and a polyA tail at the 3′ end and contains three overlapping open reading frames (ORF1-3) [3]. ORF1 encodes a non-structural polyprotein, ORF2 encodes a capsid protein, and ORF3 is a multifunctional protein [4].

HEV belongs to the Hepeviridae family; the Orthohepevirinae subfamily and is divided into four genera: Avihepevirus, Chirohepevirus, Paslahepevirus, and Rocahepevirus. Paslahepevirus genus includes Paslahepevirus balayani and Paslahepevirus alci species, where the Paslahepevirus balayani species consists of HEV genotypes 1-8 (HEV1-HEV8) [5], which can be further divided into subtypes [6]. In developed countries, foodborne or direct contact with animal reservoirs, mostly domestic pigs and wild boars, are considered the main routes of HEV-3 and HEV-4 transmission. In this context, HEV causes generally self-limiting acute hepatitis, however, it can become chronic in immunocompromised and solid organ transplant patients, mainly related to HEV-3 infections [7].

HEV genotypes can be subdivided into subtypes and HEV-3 is considered the genotype with the highest genetic diversity, comprising 13 recognized subtypes and multiple lineages [6,8–10]. Recently, a distance-based criterion cut-off of 0.093 has been proposed to carry out consistent HEV-3 subtyping classification, simplifying the molecular epidemiology analysis [11].

HEV is an enteric virus that can be excreted as a non-enveloped particle in the feces of humans (wastewater) and animals (runoff from slaughterhouses, pig farms, or free-ranging animals). Waterborne HEV transmission can be direct, through contact with contaminated water, or indirect, by consumption of shellfish or crops irrigated with contaminated water [12].

In countries with poor sanitation conditions and inadequate treatment of sewage, waterborne fecal–oral route transmission of HEV-1 and HEV-2 can lead to epidemic outbreaks [12]. However, the transmission risk of zoonotic HEV-3 through water in developed or non-endemic countries is still under debate [12,13]. The HEV prevalence in water matrices worldwide is estimated to be about 15.14% in untreated wastewater, 3.81% in treated wastewater, and 7.46% in surface waters [12]. It has been suggested that HEV does not present high resistance to physical or chemical inactivators (UV, heat, chlorine, etc.) in contrast to other enteric pathogens such as the hepatitis A virus. Nevertheless, no other factors such as genotypes and quasi- or non-enveloped forms were considered in these studies [13].

Hepatitis E outbreaks or sporadic cases are reportedly annually in countries with limited access to clean water, in refugee camps, and in regions with humanitarian emergencies, and the World Health Organization (WHO) has released a technical report with several recommendations to plan and execute responses to contain these HEV waterborne outbreaks [14]. The main control strategies for these cases are divided into four categories of action: (1) prevention of exposure; (2) prevention of infection; (3) prevention of disease; and (4) prevention of death. Particularly, this manual strongly advises implementing diagnostics tests for HEV by trained personnel, since this disease is frequently mistaken for other forms of acute viral hepatitis because of specific tests being unavailable, which can result in an inadequate diagnosis and management of the patients [14].

In Uruguay, HEV-3 infections have been previously identified among human [15] and animal hosts (swine, wild boars, and white-collared peccaries) [16,17]. Extensive molecular and serological data have been obtained and recently we described a HEV-3 complete genome obtained from a solid organ transplant patient with chronic hepatitis E [18]. However, several knowledge gaps in the molecular epidemiology and modes of transmission of HEV remain. Though in the country HEV infection is notifiable within one week of the diagnosis, in the last decade as few as 25 cases have been officially recorded [19]. However, recent findings among blood donors evidenced a seroprevalence of 10% which

suggests that the virus is being intensively and cryptically transmitted [20]. That might be explained, among other reasons, by the fact that hepatitis E is usually asymptomatic or subclinical, and is frequently indistinguishable from liver disease of a different viral etiology [21].

It is generally assumed that zoonotic events are the main source of HEV infection in developed regions and compiling molecular and epidemiological evidence supports this notion [22]. However, in less developed non-endemic areas this is more poorly understood and normally a source for human infection cannot be identified.

Wastewater surveillance is a useful epidemiological tool that can provide data on the circulation of pathogens and has been used to evaluate infection trends in the community, monitor public health interventions, and make timely, evidence-based decisions to mitigate the impact of epidemic waves or outbreaks [23]. In Latin America, only a few HEV prevalence reports involving environmental and wastewater samples have been published [24–27]. Given the increasing trends of HEV seroprevalence in the region [28], developing efficient and standardized methodologies for the detection and characterization of HEV in the environment has been a real challenge. However, since the SARS-CoV-2 pandemic, WWS has undergone considerable improvement mainly due to an optimization of the concentrating and detecting protocols [29–31]. We have recently reported results from a country-wide-scaled WWS program for the early identification of SARS-CoV-2 VOCs [32].

The aim of this work was to reexamine the molecular epidemiology of zoonotic HEV in Uruguay by providing whole-genome data, updated sequence information with novel insights into the occurrence and the genetic features of HEV circulating in water matrices (wastewater and surface water), and more robust and detailed HEV-3 phylogenetic analyses.

2. Materials and Methods

2.1. RNA Extraction and Reverse-Transcription Nested PCR (RT-nPCR) from Domestic Pigs Samples

Eighteen stool samples (10–15 gr) were collected in 2020 in sterile bags from a small-sized farm situated in Salto City, where the highest seroprevalence of HEV had been reported in a previous study [16]. Samples were kept on dry ice and sent to the laboratory where they were processed.

Pig fecal samples were resuspended at 10% *w/v* in sterile phosphate buffer saline (PBS) and vigorously vortexed. After centrifugation for 30 min, 8000× *g* at 4 °C, the supernatant was filtered to 0.22 µM. Total RNA was extracted with a Quick-RNA™ Miniprep Kit and treated with DNase I (Zymo Research Corp., Tustin, CA, USA) according to the manufacturer's instructions.

For the detection of HEV, RNA was subjected to RT-nPCR targeting a 330-bp region within ORF2 as previously reported [17]. PCR products were gel-visualized under UV light and amplicons of the expected size were sequenced in both directions by Macrogen Inc. (Seoul, Republic of Korea).

The HEV-positive samples were filtered (0.45 µM) and viral particles were concentrated in a 30% sucrose gradient and ultra-centrifuged for 2:30 h at 100,000× *g*, 4 °C in a Sorvall™ WX+ Ultracentrifuge (Thermo Scientific, Waltham, MA, USA). The pellet was resuspended in 200 µL of PBS 1× and RNA was then extracted as mentioned above.

2.2. Wastewater and Surface Water Concentration, RNA Extraction and HEV Detection

Three sampling strategies were employed (Figure 1). Firstly, 4 h composite untreated samples were obtained from a timeline sampling carried out once a month from December 2020 to July 2021 (33 samples in total) at a wastewater treatment plant in Melo City. Secondly, a total of 5 samples (24 h composite) from four other cities (July 2021) across the country were included: Montevideo, Salto, Rivera, and Castillos. All these samples were part of the WWS program performed for SARS-CoV-2 [32].

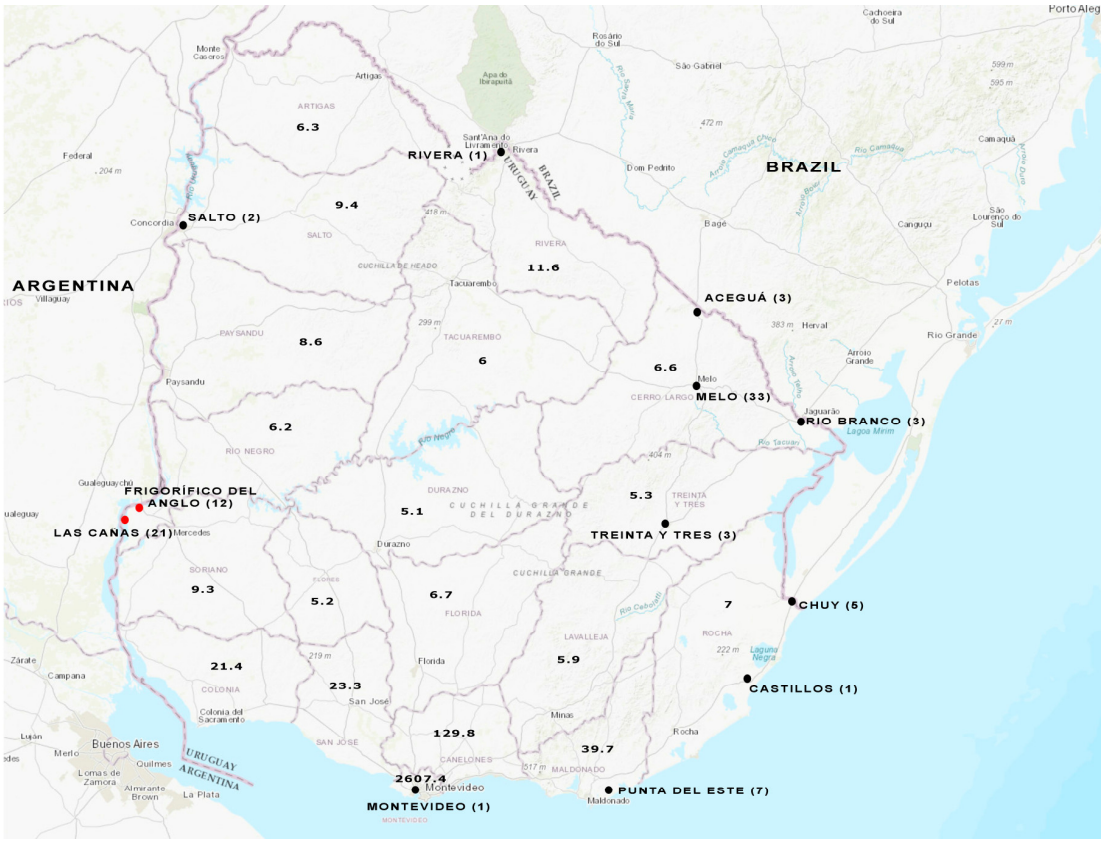

Figure 1. Water sampling from different cities throughout Uruguay. Wastewater samples were analyzed from the cities indicated with a black full circle. Surface water samples were analyzed from the places indicated with a red full circle. The number of samples studied is shown in brackets for each location. Population density (People/Sq Km) per department is indicated in the map, based on the values extracted from Anuario Estadistico Nacional 2019, 96ª version, Instituto Nacional de Estadística (INE), www.ine.gub.uy (accessed on 12 June 2023). The map of Uruguay was obtained from the USGS National Map Viewer (http://viewer.nationalmap.gov/viewer/, accessed on 12 June 2023).

Thirdly, 21 additional wastewater samples (4 h composite, 24 h composite, and/or simple) collected weekly during the period May–July 2023 were included. Sampling sites corresponded to the treatment plants of five other cities: Treinta y Tres, Rio Branco, Aceguá, Chuy, and Punta del Este.

Additionally, a total of 33 surface water samples from Las Cañas Beach and Frigorífico del Anglo area were included in the analysis [33]. As previously reported, these samples were collected monthly from May 2018 to April 2019.

Wastewater concentration was performed as described [32]. Total RNA was extracted from the wastewater concentrates with the Quick-RNA™ Miniprep Kit (Zymo Research Corp., Tustin, CA, USA) according to the manufacturer's instructions.

The RNA from surface water concentrates of Las Cañas and FA was already available [33].

HEV detection was performed with a broadly reactive one-step real-time RT-PCR [34] employing a specific Taqman® probe with the SensiFAST™ Probe Lo-ROX One-Step kit (Bioline, London, UK).

A region within the ORF2 was amplified from the HEV-positive samples using a RT-nested PCR as previously described [15]. Amplicons of the expected size (958 bp) were sequenced by the Macrogen Inc. automatic sequencing service (Seoul, Korea) to perform phylogenetic analyses and construct nucleotide p-distance matrices.

2.3. Full-Length Genome Sequencing by Next Generation Sequencing (NGS), Sequence Analysis and Phylogenetic Reconstruction

RNA obtained from concentrated viral particles present in swine stool samples was subjected to NGS. For this, double-stranded cDNA (dscDNA) was generated with random primers using Maxima H Minus Double-Stranded cDNA Synthesis Kit (ThermoFisher Scientific, Waltham, MA, USA). dscDNA was amplified via Multiple Displacement Amplification (MDA) technology using a REPLI-g Mini Kit (Qiagen, Hilden, Germany) followed by purification and quantification using AMPure XP (Beckman Coulter, Brea, CA, USA) and a Qubit fluorometer (Qubit™ DNA-HS Assay kit, Thermo Scientific, Waltham, MA, USA), respectively.

Libraries were constructed from 50 ng of dscDNA using the Nextera DNA Flex Library Preparation kit (Illumina, San Diego, CA, USA) with dual indexing. Control quality libraries were performed on a Fragment Analyzer 5200 system (Agilent Technologies, Santa Clara, CA, USA) using the Standard Sensitivity NGS Analysis Kit (Agilent Technologies, Santa Clara, CA, USA). The library was sequenced on an Illumina MiniSeq Genomic Platform at Facultad de Ciencias (Universidad de la República, Montevideo, Uruguay) using a Mid Output Reagent Cartridge (300-cycles, 150 base-pair paired-end reads) and following standard Illumina protocols.

Raw reads were demultiplexed automatically on the MiniSeq platform. Adapter/quality trimming and filtering were performed with the BBDuk plugin and clean reads were mapped to a previous Uruguayan hepatitis E genome (MW596896) using Geneious mapper (medium-low sensitivity) available in the Geneious Prime 2020.2.1 software (https://www.geneious.com accessed on 3 February 2022).

Sequences were assembled and annotated with SeqMan NGen® Version 12.0 (DNASTAR. Madison, WI, USA).

Nested-PCR and subsequent sequencing of partial ORF1 and ORF2 [15] were performed to corroborate the NGS data.

The phylogenetic tree was reconstructed based on HEV3 full-length genomes using the neighbor-joining method with Tamura Nei as the substitution method, using Molecular Evolutionary Genetics Analysis (MEGA) v7 software [35]. Reference sequences of subtypes 3a to 3n according to Smith et al. [6] were retrieved from GenBank and included in the analysis. The substitution model that best fitted the data was obtained with MEGA v7 [35]. The robustness of the tree was determined via bootstrap v10 analysis (1000 replicates).

To further characterize the sequences obtained from water sources (wastewater and/or surface water), an additional analysis of HEV-3 subtypes was performed with a 768 bp region within the ORF2. A subset of previously reported human HEV partial-genome sequences from Uruguay were included [15]. The phylogenetic tree for the partial ORF2 region was reconstructed as described for the whole genome dataset.

Nucleotide p-distance matrices between Uruguayan strains and reference sequences of each HEV-3 subtype were constructed with MEGA v7 software for both the partial ORF2 region and full-length genomes.

3. Results

3.1. HEV Detection in Domestic Pig Stool Samples via RT-nPCR

Investigation of HEV was performed in swine fecal samples from a farm with elevated seroprevalence [16]. Three out of the 18 stool samples from the pigs were positive for HEV-RNA. Further sequence analysis of the partial ORF2 region grouped them within the HEV-3 genotype.

3.2. Whole-Genome Analysis of a Swine HEV Strain

NGS of the HEV-positive RNAs was successful in only one sample, HEV-8_uy. The whole genome sequence had 7082 nt and a 55.4% GC content. The analysis performed revealed a high percentage of identity (91.83%) with a human full-length HEV-3 strain recently described by our group (C1UY18, GenBank accession MW596896) [18]. Phyloge-

netic reconstruction grouped these strains together but according to bootstrapping analysis, they did not cluster in any of the known or assigned subtypes (Figure 2). For practical purposes, this cluster which also includes recently reported strains from Brazil [36] was named the putative 3o subtype in this study. Furthermore, the percentage of nucleotide identity between genomes from Uruguay (C1UY18, HEV-8_uy) and Brazil (PRsw1, RJ-sw1) within this cluster showed a range of 84.7% to 88.1%.

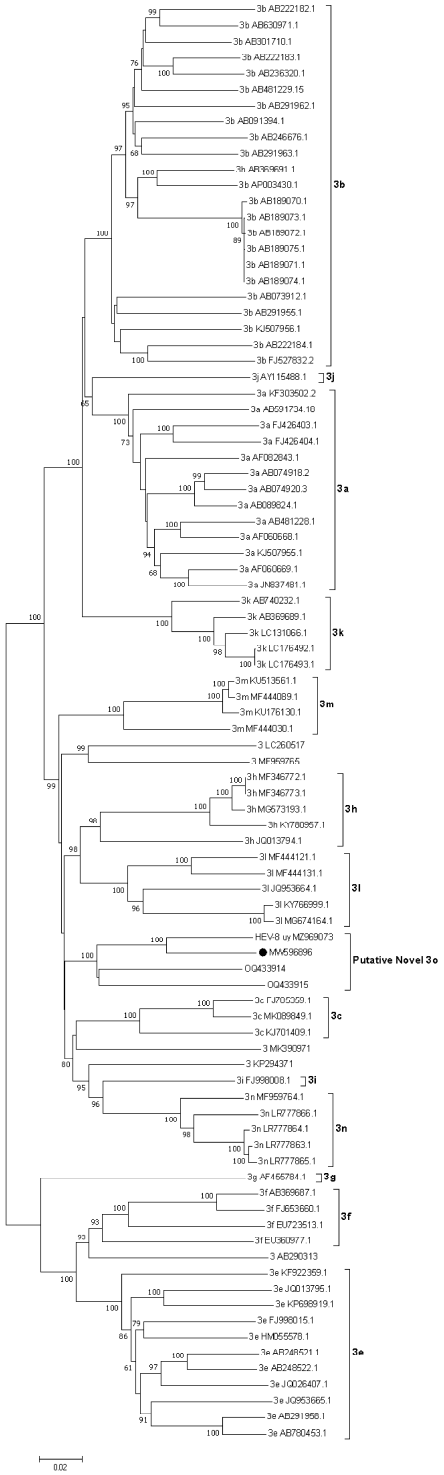

Figure 2. Phylogenetic reconstruction of HEV complete genomes for genotype 3. The tree was generated with the Neighbor-Joining algorithm using the Tamura-Nei parameters method employing

Molecular Evolutionary Genetics Analysis (MEGA) v7 software. The robustness of the tree was determined via bootstrap analysis for 1000 replicates. Only values ≥60% are shown. Reference sequences for the subtypes 3a–3n and unclassified isolates are included. The putative new 3o subtype proposed for Uruguayan (MW598896 and MZ969073) and Brazilian sequences (OQ433914 and OQ433915) is shown and the proposed reference strain for this subtype (MW596896) is indicated with a black full circle.

Given its extreme variability at the nucleotide level and the considerable amount of insertions and deletions observed among sequences, the hypervariable region was excluded from the analysis, as previously proposed [6].

The HEV-8_uy sequence was deposited in the GenBank database with the accession number MZ969073.

3.3. Analysis of Wastewater and Surface Water Samples

HEV RNA was detected via RT-qPCR in 10.87% of untreated wastewater samples (10/92), with Ct values ranging from 32.42 to 35.81 (Table S1). All the HEV-positive samples belonged from the 4 h composite sampling from Melo City. The partial ORF2 region was successfully amplified in two of these samples (named HE-67-WW and HE-112-WW).

The phylogenetic analysis showed that the HE-67-WW and HE-112-WW strains were grouped in a separate cluster (putative 3o HEV-3 subtype) with previously reported partial and complete HEV-3 sequences detected in swine and human cases from Uruguay (Figure 3).

HE-67-WW and HE-112-WW sequences were deposited in the GenBank database with the accession numbers OR267146 and OR267147.

On the other hand, HEV RNA was not detected in any of the surface water samples analyzed.

3.4. HEV Subtyping

To go further into the characterization of the HEV whole genomes and the wastewater sequences at the subtype level, p-distance matrices were constructed for the 768-nt ORF2 region and full-length genomes using reference strains (Table 1). We performed this analysis because it has been proposed and extensively used as the reference method for HEV-3 subtyping classification [6,11].

The analysis also included a set of reported human HEV ORF2 partial sequences from Uruguay for which no complete genome was available (Table 1) [15]. Comparison at the ORF2 region between the HEV-8_uy swine strain with human and wastewater isolates (all belonging to the putative 3o subtype) showed a percentage of nucleotide identity ranging from 94.7% to 95.4%.

Using whole-genome analysis, Uruguayan samples were compared to the two recently reported HEV-3 swine sequences from Brazil (PRsw1-OQ433914 and RJsw1-OQ433915) [36] and subtype reference strains (3a–3n). Nucleotide sequence distance values of 0.118–0.125 and 0.132 to 0.177 were observed, respectively.

Furthermore, a p-distance matrix constructed with the Uruguayan strains showed that the two complete genomes exhibited a p-distance value of 0.075. On the other hand, the p-distance values calculated for the partial ORF2 region from all 14 Uruguayan strains ranged from 0.000 to 0.096 (Table 2).

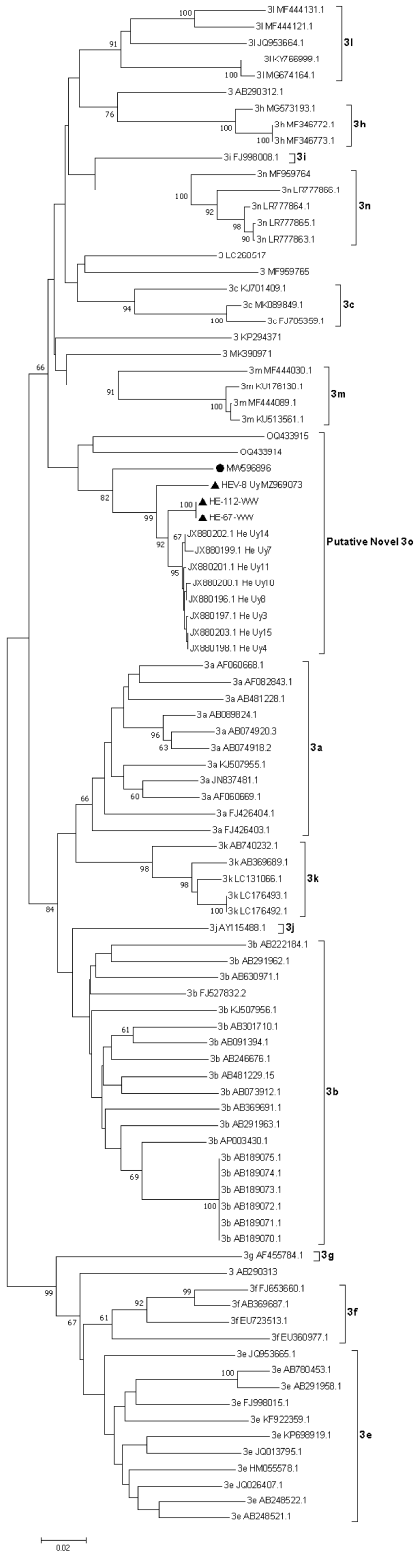

Figure 3. Phylogenetic tree based on a 719 bp fragment within ORF2. Tree reconstruction was performed using the Neighbor-Joining method with the Tamura-Nei model using Molecular Evolutionary Genetics Analysis (MEGA) v7 software. The robustness of the tree was determined via bootstrap analysis for 1000 replicates. Only values of ≥60% are shown. Reference sequences for the subtypes 3a–3n and unclassified strains are included. The HEV-3 wastewater sequences (HE-67-WW and HE-112-WW) and the swine complete genome HEV-8_uy (MZ969073) reported in this study are indicated with a black triangle. Proposed reference sequence for the novel 3o subtype is indicated with a black circle.

Table 1. Summary of *p*-distances between Uruguayan strains, proposed here as a new subtype 3o vs. reference subtypes (3a–3n), and unassigned strains comparing complete genomes and partial ORF2 region. Brazilian sequences (putative 3o subtype) are indicated (*).

Accession Number	Subtype	Complete Genome [a]	Partial ORF2 [a]
AF082843	3a	0.147–0.150	0.131–0.141
AP003430	3b	0.144–0.145	0.133–0.146
FJ705359	3c	0.136–0.140	0.134–0.147
AF296165-7	3d [b]	-	0.132–0.149
AB248521	3e	0.171–0.177	0.137–0.163
AB369687	3f	0.174–0.176	0.143–0.158
AF455784	3g	0.169–0.174	0.160–0.170
JQ013794	3h	0.132–0.137	0.114–0.128
FJ998008	3i	0.132	0.120–0.136
AY115488	3j	0.151–0.155	0.133–0.143
AB369689	3k	0.146–0.148	0.130–0.136
JQ953664	3l	0.136–0.139	0.124–0.143
KU513561	3m	0.134–0.135	0.120–0.143
MF959764	3n	0.133–0.137	0.120–0.146
PRsw1 OQ433914 *	Putative 3o	0.118–0.119	0.110–0.126
RJ-sw1 OQ433915 *	Putative 3o	0.121–0.125	0.115–0.122
KP294371	Unassigned	0.136	0.126–0.136
LC260517	Unassigned	0.142–0.146	0.117–0.148
MF959765	Unassigned	0.134–0.141	0.143–0.153
MK390971	Unassigned	0.142–0.145	0.116–0.136
AB290313	Unassigned	0.175–0.180	0.150–0.168

[a] minimum and maximum values are shown. [b] Only 304 bp fragment within ORF2 is available for this subtype.

Table 2. Summary of *p*-distances between Uruguayan strains comparing complete genomes and the partial ORF2 region.

Strains	Subtype	Complete Genome	Partial ORF2 *
Uruguayan isolates	Putative 3o	0.075	0.000–0.096

* Minimum and maximum values are shown.

4. Discussion

HEV is a major cause of acute viral hepatitis worldwide and the only one that has an animal reservoir [37]. In developed areas, zoonotic seems to be the main route of infection of HEV-3 with infected pigs and/or wild boars as the main sources. The importance of the viral epidemiology of other routes and the role of potential animal hosts or reservoirs that could transmit the virus, including deer, rat, and livestock is still a matter of current debate [38]. There is a consensus that a better understanding of the transmission paths is needed especially for zoonotic HEV, in areas where a waterborne transmission is questioned. On the contrary, in less developed areas with heterogeneous socio-economic levels and non-optimal hygiene/sanitary conditions, the waterborne transmission of HEV-3 is likely to occur, as it is frequently detected in water matrices and aquatic environments [13].

Previously reported data by our group has shown that HEV infection occurs frequently in Uruguay, with a seroprevalence rate of 10% among blood donors, including three viremic individuals [20]. The fact that only a handful of cases have been reported in the last decade likely suggests a high rate of asymptomatic infection [39]. HEV infection has also been identified and characterized in domestic pigs, with an antibody and RNA prevalence of 46.8% and 16.6%, respectively, and in wild boars, indicating a widespread circulation of the virus in their natural reservoirs [16]. Additionally, we showed that HEV-3 could also infect and be transmitted among white-collared peccaries (New World pigs) and spotted deer (*Axis axis*) [17,40]. In this work, to provide novel insights into the molecular epidemiology and transmission patterns of HEV in Uruguay we reexamined the phylogenetic relationships with updated data and additional analyses.

First, the whole-genome comparison of the HEV strain identified in swine in this study (named HEV-8_uy) exhibited a high nucleotide sequence percentage of identity with a previously reported strain detected in 2019 in a chronically infected patient [18]. Even though the source of infection could not be identified in any of the human cases in our country, this finding confirms previous data [16] and raises concern about the zoonotic role that domestic pigs are playing in the dynamics of hepatitis E. In addition, these sequences were grouped in a monophyletic cluster within HEV-3 with two recently published Brazilian swine HEV-3 genomes from the Paraná and Rio de Janeiro states (OQ433914-OQ433915) [36]. Surprisingly, this cluster could not be assigned to any known (or currently unassigned) HEV subtype according to bootstrap analysis. To confirm this finding, p-distance matrices were constructed covering all assigned (3a–3n) subtypes' reference strains and those sequences not assigned to any subtype of HEV-3. According to the proposed criteria, a cut-off value of 0.093 is usually applied to define subtypes [11] and the sequence distance values obtained here (0.132 to 0.180) suggest that the Uruguayan HEV-8_uy and MW596896 strains indeed comprise a novel HEV-3 subtype. Thus, we propose the sequence C1UY18 (GenBank accession number MW596896) to be the reference sequence for this new 3o subtype, as it was the first one reported for this cluster. On the other hand, though p-distance values (0.118–0.125) between OQ433914 and OQ433915 and the Uruguayan sequences exceed the cut-off value, and strictly they could belong to two different new subtypes, this is not always an absolute criterion, and considering that the four strains come from neighboring countries in South America, we suggest that they can be initially classified into the same subtype.

As a second goal, in this study, we investigated the presence of HEV in wastewater and surface water to provide additional data on the epidemiology of the infection and the viral transmission patterns in the country. Wastewater-based epidemiology and surveillance of aquatic environment matrices have been employed as cost-effective tools for monitoring the circulation of pathogens to make public health decisions [23] but they can also be useful for assessing transmission chains and investigating epidemiologic links during outbreaks or clusters of cases [24].

HEV RNA was detected in 10.87% (10/92) of the wastewater samples collected. In a regional context, this frequency of detection is markedly higher than the 1.6% reported in environmental samples from northeast Argentina (Salta City) [26] but lower than the detected in sewage samples from western Argentina (Mendoza City) (22.5%) [26] and in wastewater from Colombia (16.7%). Of note, all HEV-positive samples belonged to Melo City. The wastewater treatment in Melo City consists of a separate system in which domestic sewage and rainwater runoff do not mix, nevertheless, this is a leaky system where rainwater enters the sewage collector and the effluent is consequently diluted when precipitation occurs [41]. Considering that the wastewater treatment system in this city is similar to others (Rivera, Salto, and Castillos) and that there are no significant social or environmental differences between the places studied, it is striking that HEV was only detected in Melo City. However, as previously reported, SARS-CoV-2 had been detected in all these cities throughout the WWS program [32]. The analysis of the partial ORF2 sequence of the HE-67-WW and HE-112-WW strains identified in wastewater demonstrated that they share a high nucleotide identity between them and are clustered within the novel proposed 3o subtype of HEV-3. In addition, as expected, they exhibited a marked nucleotide divergence with other described HEV-3 subtypes. Altogether, all these findings support previous data that suggested that HEV had a recent introduction in Uruguay and likely from a single geographic origin [42], which is in sharp contrast to other South American countries [43,44] Significant research efforts have been made to obtain additional complete genomes from Uruguay through different enrichment methods, but the low HEV titers in the sample and the lack of an efficient cell culture system have severely hampered the results.

Even though analysis of partial sequences is in general not suitable for HEV-3 subtyping, it has been proposed and accepted that the ORF2 region could eventually be used for

this purpose, since it largely reflects the data obtained with whole-genome analysis [45]. The 3d subtype was designated based exclusively on three partial 304 bp regions within ORF2 from swine samples [6,45,46]. Furthermore, the phylogenetic and nucleotide analysis performed in this work involving partial HEV ORF2 from Uruguayan strains, including several previously identified in human cases [15], showed similar p-distance values and phylogenetic tree topology to the analysis performed with full-length genomes. Unfortunately, ORF2 sequences from white-collared peccaries and spotted deer were not available for this study and this is a limitation in terms of exploring potential transmission paths involving other ecological reservoirs/hosts. However, previous analyses carried out with ORF1 partial sequences had shown close phylogenetic relationships with sequences of human origin [17,40].

In summary, we provide updated data on the molecular epidemiology of zoonotic HEV-3 in Uruguay and propose the designation of a new subtype 3o with its reference sequence. The data presented here suggest that our country is unique in terms of the molecular epidemiology and transmission paths of HEV, in that a single circulating subtype has been identified in humans, animal reservoirs and hosts, and environmental samples. Furthermore, despite the environmental and domestic pig samples being collected about 10 years after the first human cases were described [47], low genetic heterogeneity is still observed between strains within this new subtype, suggesting little diversification over time. On the other hand, waterborne transmission of HEV remains to be confirmed and further investigated by assessing virus particle stability and infectiousness using standardized cell culture systems [48].

Supplementary Materials: The following supporting information can be downloaded at: https://www.mdpi.com/article/10.3390/v15102006/s1, Table S1: Real-time PCR Ct value, date, and sampling site from Uruguayan HEV-positive wastewater samples. The two samples that were amplified by RT-nested PCR are indicated.

Author Contributions: Conceptualization, S.M., M.B. and F.C.; methodology, F.C., R.I., S.C., V.H., M.O., Y.P., M.G., V.B., M.V. and N.M.; software, F.C., Y.P. and R.P.; validation, F.C., Y.P. and R.I. formal analysis, F.C.; investigation, F.C., R.I., S.C., V.H., M.O., Y.P., R.P., L.B., E.G., N.M., M.G., V.B., M.V. and R.C.; resources, S.M., J.A., J.L., E.G. and L.B.; data curation, S.M. and F.C.; writing—original draft preparation, F.C. and S.M.; writing—review and editing, F.C.; S.M., R.C. and S.L.-V.; supervision, S.M.; project administration, S.M., M.B. and J.L.; funding acquisition, S.M., M.B. and J.L. All authors have read and agreed to the published version of the manuscript.

Funding: F.C.'s PhD fellowship is from the Comisión Académica de Posgrado-UdelaR. This work was funded by the Comisión Sectorial de Investigación Científica-UdelaR, under grant CSIC I+D 2018 number 245 and grant PAIE 2020 number 102.

Institutional Review Board Statement: Not applicable.

Data Availability Statement: The sequence data presented in this study are openly available in Genbank (https://www.ncbi.nlm.nih.gov/genbank accessed on 18 September 2023).

Acknowledgments: The authors would like to particularly thank Donald Smith (International Committee on Taxonomy of Viruses) for his invaluable assistance and technical opinion on the HEV-3 subtyping analyses; OSE and Dirección Nacional de Aguas (Ministerio de Ambiente) for their excellent support; and Karina Cabrera and Gustavo Castro for their assistance in the sampling of domestic pig specimens.

Conflicts of Interest: The authors declare no conflict of interest. The sponsors had no role in the design, execution, interpretation, or writing of the study.

References

1. World Health Organization. *Global Hepatitis Report*. 2017. Available online: https://www.who.int/publications/i/item/9789241565455 (accessed on 10 January 2022).
2. Ji, H.; Chen, S.; He, Q.; Wang, W.; Gong, S.; Qian, Z.; Zhang, Y.; Wei, D.; Yu, W.; Huang, F. The different replication between nonenveloped and quasi-enveloped hepatitis E virus. *J. Med. Virol.* **2021**, *93*, 6267–6277. [CrossRef] [PubMed]

3. Kumar, S.; Subhadra, S.; Singh, B.; Panda, B.K. Hepatitis E virus: The current scenario. *Int. J. Infect. Dis.* **2013**, *17*, e228–e233. [CrossRef] [PubMed]
4. Nan, Y.; Zhang, Y.-J. Molecular Biology and Infection of Hepatitis E Virus. *Front. Microbiol.* **2016**, *7*, 1419. [CrossRef] [PubMed]
5. Purdy, M.A.; Drexler, J.F.; Meng, X.J.; Norder, H.; Okamoto, H.; Van der Poel, W.H.M.; Reuter, G.; de Souza, W.M.; Ulrich, R.G.; Smith, D.B. ICTV Virus Taxonomy Profile: Hepeviridae 2022. *J. Gen. Virol.* **2022**, *103*, 1778. [CrossRef] [PubMed]
6. Smith, D.B.; Izopet, J.; Nicot, F.; Simmonds, P.; Jameel, S.; Meng, X.-J.; Norder, H.; Okamoto, H.; van Der Poel, W.H.M.; Reuter, G.; et al. Update: Proposed reference sequences for subtypes of hepatitis E virus (species *Orthohepevirus A*). *J. Gen. Virol.* **2020**, *101*, 692–698. [CrossRef] [PubMed]
7. Fang, S.Y.; Han, H. Hepatitis E viral infection in solid organ transplant patients. *Curr. Opin. Organ Transplant.* **2017**, *22*, 351–355. [CrossRef] [PubMed]
8. Abravanel, F.; Lhomme, S.; El Costa, H.; Schvartz, B.; Peron, J.-M.; Kamar, N.; Izopet, J. Rabbit Hepatitis E Virus Infections in Humans, France. *Emerg. Infect. Dis.* **2017**, *23*, 1191–1193. [CrossRef]
9. Oliveira-Filho, E.F.; König, M.; Thiel, H.-J. Genetic variability of HEV isolates: Inconsistencies of current classification. *Vet. Microbiol.* **2013**, *165*, 148–154. [CrossRef]
10. Smith, D.B.; Simmonds, P.; Izopet, J.; Oliveira-Filho, E.F.; Ulrich, R.G.; Johne, R.; Koenig, M.; Jameel, S.; Harrison, T.J.; Meng, X.-J.; et al. Proposed reference sequences for hepatitis E virus subtypes. *J. Gen. Virol.* **2016**, *97*, 537–542. [CrossRef]
11. Nicot, F.; Dimeglio, C.; Migueres, M.; Jeanne, N.; Latour, J.; Abravanel, F.; Ranger, N.; Harter, A.; Dubois, M.; Lameiras, S.; et al. Classification of the Zoonotic Hepatitis E Virus Genotype 3 Into Distinct Subgenotypes. *Front. Microbiol.* **2021**, *11*, 634430. [CrossRef]
12. Takuissu, G.R.; Kenmoe, S.; Ndip, L.; Ebogo-Belobo, J.T.; Kengne-Ndé, C.; Mbaga, D.S.; Bowo-Ngandji, A.; Oyono, M.G.; Kenfack-Momo, R.; Tchatchouang, S.; et al. Hepatitis E Virus in Water Environments: A Systematic Review and Meta-analysis. *Food Environ. Virol.* **2022**, *14*, 223–235. [CrossRef] [PubMed]
13. Fenaux, H.; Chassaing, M.; Berger, S.; Gantzer, C.; Bertrand, I.; Schvoerer, E. Transmission of hepatitis E virus by water: An issue still pending in industrialized countries. *Water Res.* **2019**, *151*, 144–157. [CrossRef] [PubMed]
14. World Health Organization. *Waterborne Outbreaks of Hepatitis E: Recognition, Investigation and Control*; World Health Organization: Geneva, Switzerland, 2014.
15. Mirazo, S.; Ramos, N.; Russi, J.C.; Arbiza, J. Genetic heterogeneity and subtyping of human Hepatitis E virus isolates from Uruguay. *Virus Res.* **2013**, *173*, 364–370. [CrossRef] [PubMed]
16. Mirazo, S.; Gardinali, N.R.; Cecilia, D.A.; Verger, L.; Ottonelli, F.; Ramos, N.; Castro, G.; Pinto, M.A.; Ré, V.; Pisano, B.; et al. Serological and virological survey of hepatitis E virus (HEV) in animal reservoirs from Uruguay reveals elevated prevalences and a very close phylogenetic relationship between swine and human strains. *Vet. Microbiol.* **2018**, *213*, 21–27. [CrossRef] [PubMed]
17. Ferreiro, I.; Herrera, M.L.; González, I.; Cancela, F.; Leizagoyen, C.; Loureiro, M.; Arellano, H.; Echaides, C.; Bon, B.; Castro, G.; et al. Hepatitis E Virus (HEV) infection in captive white-collared peccaries (*Pecari tajacu*) from Uruguay. *Transbound. Emerg. Dis.* **2020**, *68*, 1040–1045. [CrossRef] [PubMed]
18. Cancela, F.; Panzera, Y.; Mainardi, V.; Gerona, S.; Ramos, N.; Pérez, R.; Arbiza, J.; Mirazo, S. Complete Genome Sequence of Hepatitis E Virus Genotype 3 Obtained from a Chronically Infected Individual in Uruguay. *Microbiol. Resour. Announc.* **2021**, *10*, e0036721. [CrossRef] [PubMed]
19. MSP. Dirección General de la Salud División Epidemiología Departamento de Vigilancia en Salud. Montevideo, Uruguay. Report Provided upon Request for Information Made by the Author (received on 10 December 2022). Available online: https://www.gub.uy/ministerio-salud-publica/tramites-y-servicios/formularios/formularios-division-epidemiologia-departamento-vigilancia-salud (accessed on 18 September 2023).
20. Bangueses, F.; Abin-Carriquiry, J.A.; Cancela, F.; Curbelo, J.; Mirazo, S. Serological and molecular prevalence of hepatitis E virus among blood donors from Uruguay. *J. Med. Virol.* **2020**, *93*, 4010–4014. [CrossRef]
21. Songtanin, B.; Molehin, A.J.; Brittan, K.; Manatsathit, W.; Nugent, K. Hepatitis E Virus Infections: Epidemiology, Genetic Diversity, and Clinical Considerations. *Viruses* **2023**, *15*, 1389. [CrossRef]
22. Velavan, T.P.; Pallerla, S.R.; Johne, R.; Todt, D.; Steinmann, E.; Schemmerer, M.; Wenzel, J.J.; Hofmann, J.; Shih, J.W.K.; Wedemeyer, H.; et al. Hepatitis E: An update on One Health and clinical medicine. *Liver Int.* **2021**, *41*, 1462–1473. [CrossRef]
23. Kumar, M.; Jiang, G.; Thakur, A.K.; Chatterjee, S.; Bhattacharya, T.; Mohapatra, S.; Chaminda, T.; Tyagi, V.K.; Vithanage, M.; Bhattacharya, P.; et al. Lead time of early warning by wastewater surveillance for COVID-19: Geographical variations and impacting factors. *Chem. Eng. J.* **2022**, *441*, 135936. [CrossRef]
24. Lo Castro, I.; Espul, C.; de Paula, V.S.; Altabert, N.R.; Gonzalez, J.E.; Lago, B.V.; Villar, L.M. High prevalence of hepatitis A and E viruses in environmental and clinical samples from West Argentina. *Braz. J. Infect. Dis.* **2023**, *27*, 102738. [CrossRef] [PubMed]
25. Baez, P.A.; Lopez, M.C.; Duque-Jaramillo, A.; Pelaez, D.; Molina, F.; Navas, M.C. First evidence of the Hepatitis E virus in environmental waters in Colombia. *PLoS ONE* **2017**, *12*, e0177525. [CrossRef] [PubMed]
26. Pisano, M.B.; Lugo, B.C.; Poma, R.; Cristobal, H.A.; Raskovsky, V.; Martinez Wassaf, M.G.; Rajal, V.B.; Re, V.E. Environmental hepatitis E virus detection supported by serological evidence in the northwest of Argentina. *Trans. R. Soc. Trop. Med. Hyg.* **2018**, *112*, 181–187. [CrossRef] [PubMed]
27. Heldt, F.H.; Staggmeier, R.; Gularte, J.S.; Demoliner, M.; Henzel, A.; Spilki, F.R. Hepatitis E Virus in Surface Water, Sediments, and Pork Products Marketed in Southern Brazil. *Food Environ. Virol.* **2016**, *8*, 200–205. [CrossRef] [PubMed]

28. Pisano, M.B.; Mirazo, S.; Re, V.E. Hepatitis E Virus Infection: Is It Really a Problem in Latin America? *Clin. Liver Dis.* **2020**, *16*, 108. [CrossRef] [PubMed]
29. Ahmed, W.; Simpson, S.L.; Bertsch, P.M.; Bibby, K.; Bivins, A.; Blackall, L.L.; Bofill-Mas, S.; Bosh, A.; Brandao, J.; Choi, P.M.; et al. Minimizing errors in RT-PCR detection and quantification of SARS-CoV-2 RNA for wastewater surveillance. *Sci. Total Environ.* **2022**, *805*, 149877. [CrossRef] [PubMed]
30. Pérez-Cataluña, A.; Cuevas-Ferrando, E.; Randazzo, W.; Falcó, I.; Allende, A.; Sánchez, G. Comparing analytical methods to detect SARS-CoV-2 in wastewater. *Sci. Total Environ.* **2021**, *758*, 143870. [CrossRef]
31. Crits-Christoph, A.; Kantor, R.S.; Olm, M.R.; Whitney, O.N.; Al-Shayeb, B.; Lou, Y.C.; Flamholz, A.; Kennedy, L.C.; Greenwald, H.; Hinkle, A.; et al. Genome Sequencing of Sewage Detects Regionally Prevalent SARS-CoV-2 Variants. *mBio* **2021**, *12*, 10-1128. [CrossRef]
32. Cancela, F.; Ramos, N.; Smyth, D.S.; Etchebehere, C.; Berois, M.; Rodríguez, J.; Rufo, C.; Alemán, A.; Borzacconi, L.; López, J.; et al. Wastewater surveillance of SARS-CoV-2 genomic populations on a country-wide scale through targeted sequencing. *PLoS ONE* **2023**, *18*, e0284483. [CrossRef]
33. Bortagaray, V.; Gamazo, P.; Castro, S.; Grilli, M.; Colina, R.; Victoria, M. Comparison of the risk of infection of human rotavirus and astrovirus according to fishing and swimming activities at Las Cañas beach, Uruguay. *J. Appl. Microbiol.* **2022**, *133*, 3523–3533. [CrossRef]
34. Jothikumar, N.; Cromeans, T.L.; Robertson, B.H.; Meng, X.J.; Hill, V.R. A broadly reactive one-step real-time RT-PCR assay for rapid and sensitive detection of hepatitis E virus. *J. Virol. Methods* **2006**, *131*, 65–71. [CrossRef] [PubMed]
35. Kumar, S.; Stecher, G.; Tamura, K. MEGA7: Molecular Evolutionary Genetics Analysis Version 7.0 for Bigger Datasets. *Mol. Biol. Evol.* **2016**, *33*, 1870–1874. [CrossRef] [PubMed]
36. Dos Santos, D.R.L.; Durães-Carvalho, R.; Gardinali, N.R.; Machado, L.C.; de Paula, V.S.; da Luz Wallau, G.; de Oliveira, J.M.; Pena, L.J.; Pinto, M.A.; Gil, L.H.V.G.; et al. Uncovering neglected subtypes and zoonotic transmission of Hepatitis E virus (HEV) in Brazil. *Virol. J.* **2023**, *20*, 83. [CrossRef] [PubMed]
37. Sayed, I.M. Dual Infection of Hepatitis A Virus and Hepatitis E Virus- What Is Known? *Viruses* **2023**, *15*, 298. [CrossRef] [PubMed]
38. Ahmed, R.; Nasheri, N. Animal reservoirs for hepatitis E virus within the Paslahepevirus genus. *Vet. Microbiol.* **2023**, *278*, 109618. [CrossRef] [PubMed]
39. Mirazo, S.; Ramos, N.; Mainardi, V.; Gerona, S.; Arbiza, J. Transmission, diagnosis, and management of hepatitis E: An update. *Hepatic Med.* **2014**, *6*, 45–59. [CrossRef] [PubMed]
40. Cancela, F.; Cravino, A.; Icasuriaga, R.; González, P.; Bentancor, F.; Leizagoyen, C.; Echaides, C.; Ferreiro, I.; Cabrera, A.; Arbiza, J.; et al. Co-circulation of Hepatitis E Virus (HEV) Genotype 3 and Moose-HEV-Like Strains in Free-Ranging-Spotted Deer (Axis axis) in Uruguay. *Food Environ. Virol.* **2023**, 1–11. [CrossRef] [PubMed]
41. Uruguay Wastewater Treatment. Available online: http://www.ose.com.uy/saneamiento/tratamientos (accessed on 18 June 2023).
42. Mirazo, S.; Mir, D.; Bello, G.; Ramos, N.; Musto, H.; Arbiza, J. New insights into the hepatitis E virus genotype 3 phylodynamics and evolutionary history. *Infect. Genet. Evol.* **2016**, *43*, 267–273. [CrossRef]
43. Dell'Amico, M.C.; Cavallo, A.; Gonzales, J.L.; Bonelli, S.I.; Valda, Y.; Pieri, A.; Segund, H.; Ibañez, R.; Mantella, A.; Bartalesi, F.; et al. Hepatitis E virus genotype 3 in humans and Swine, Bolivia. *Emerg. Infect. Dis.* **2011**, *17*, 1488–1490. [CrossRef]
44. Pisano, M.B.; Culasso, A.C.A.; Altabert, N.; Wassaf, M.G.M.; Nates, S.V.; González, J.; Contigiani, M.S.; Campos, R.; Ré, V.E. Phylogeography and evolutionary history of hepatitis E virus genotype 3 in Argentina. *Trans. R. Soc. Trop. Med. Hyg.* **2022**, *116*, 34–42. [CrossRef]
45. Lu, L.; Li, C.; Hagedorn, C.H. Phylogenetic analysis of global hepatitis E virus sequences: Genetic diversity, subtypes and zoonosis. *Rev. Med. Virol.* **2006**, *16*, 5–36. [CrossRef]
46. Wu, J.-C.; Chen, C.-M.; Chiang, T.-Y.; Tsai, W.-H.; Jeng, W.-J.; Sheen, I.-J.; Lin, C.-C.; Meng, X.-J. Spread of hepatitis E virus among different-aged pigs: Two-year survey in Taiwan. *J. Med. Virol.* **2002**, *66*, 488–492. [CrossRef]
47. Mirazo, S.; Ramos, N.; Russi, J.C.; Gagliano, G.; Arbiza, J. Detection and molecular characterization of sporadic cases of acute human hepatitis E virus infection in Uruguay. *Arch. Virol.* **2011**, *156*, 1451–1454. [CrossRef]
48. Salvador, D.; Neto, C.; Benoliel, M.J.; Caeiro, M.F. Assessment of the Presence of Hepatitis E virus in Surface Water and Drinking Water in Portugal. *Microorganisms* **2020**, *8*, 761. [CrossRef]

4.6. Experimentos complementarios no incluidos en el artículo

4.6.1 Confirmación de las secuencias de genomas completos

En esta Tesis se pusieron a punto e implementaron cuatro RT-PCR (FL1, FL2, FL4 y FL6) para la amplificación de distintas regiones en la ORF1, ORF2 y ORF3 del genoma de HEV (Fig. 9A), con el objetivo de confirmar las secuencias de los genomas completos obtenidos por NGS.

Para ello, se realizó la retrotranscripción del ARN viral con *random hexamer primer* (Invitrogen™) y la enzima SuperScript™ II Reverse Transcriptase (Invitrogen™) seguido de la amplificación por PCR empleando la enzima Platinum™ Taq DNA Polymerase (Invitrogen™) como se describe previamente en Legran-Abravanel et al. [91]. Los *primers* utilizados fueron modificados de la publicación original y se detallan en la Tabla 6.

Las PCR se llevaron a cabo con el siguiente ciclado: 94°C por 2 minutos, 50 ciclos de 94°C durante 30 seg, 60°C por 1 min y 72°C por 3 min; con una extensión final a 72°C por 10 min.

Además, se amplificaron otras cuatro regiones por RT-nested PCR dentro de ORF1 y ORF2 de acuerdo a [34, 92].

Los productos obtenidos del tamaño deseado fueron purificados por gel con el PureLink™ Quick Gel Extraction Kit (Invitrogen™) y secuenciados por el servicio de secuenciación automática de Macrogen (Corea del Sur).

Tabla 6. Detalles de los *primers* utilizados para amplificar el genoma de HEV.

Nombre del Primer	Posición nucleotídica*	Secuencia	Tamaño de fragmento (pb)	N° de región en Fig 8
FL1F	1-990	TAGGCAGACCACGTATGTGGTCGATG	990	2
FL1R		GCCGGTCCCAGATRTGSACCGGRA		
FL2F	878-2172	ACAGAGGTGTATGTTAGATCCATATTT	1294	3
FL2R		GGGGAGAAGTCGCTAGAGAAACCTG		
FL4F	4542-5278	AGTGYGGCATGCCCCAGTGGCTTATC	736	5
FL4R		GCCGGTGGCGCGGGCAGCATAGGC		
FL6F	6363-7327	GACAGAATTRATTTCGTCGGC	964	8
FL6R		TTTCCMGGGRGCGCGGAACCCCGAA		

*Las posiciones nucleotídicas son respecto a la secuencia de referencia Burma, M73218.

Se obtuvo amplificación para las ocho regiones del genoma de la cepa HEV_C1_uy (Fig. 9B), mientras que para la muestra suina HEV-8_uy solo fue posible obtener amplificación para cuatro regiones correspondiéndose a las indicadas con los números 1, 3, 6 y 7 en la Fig. 8. En ambos casos, se observó 100% de identidad entre las secuencias de amplicones obtenidas por secuenciación Sanger y los genomas completos recuperados por NGS.

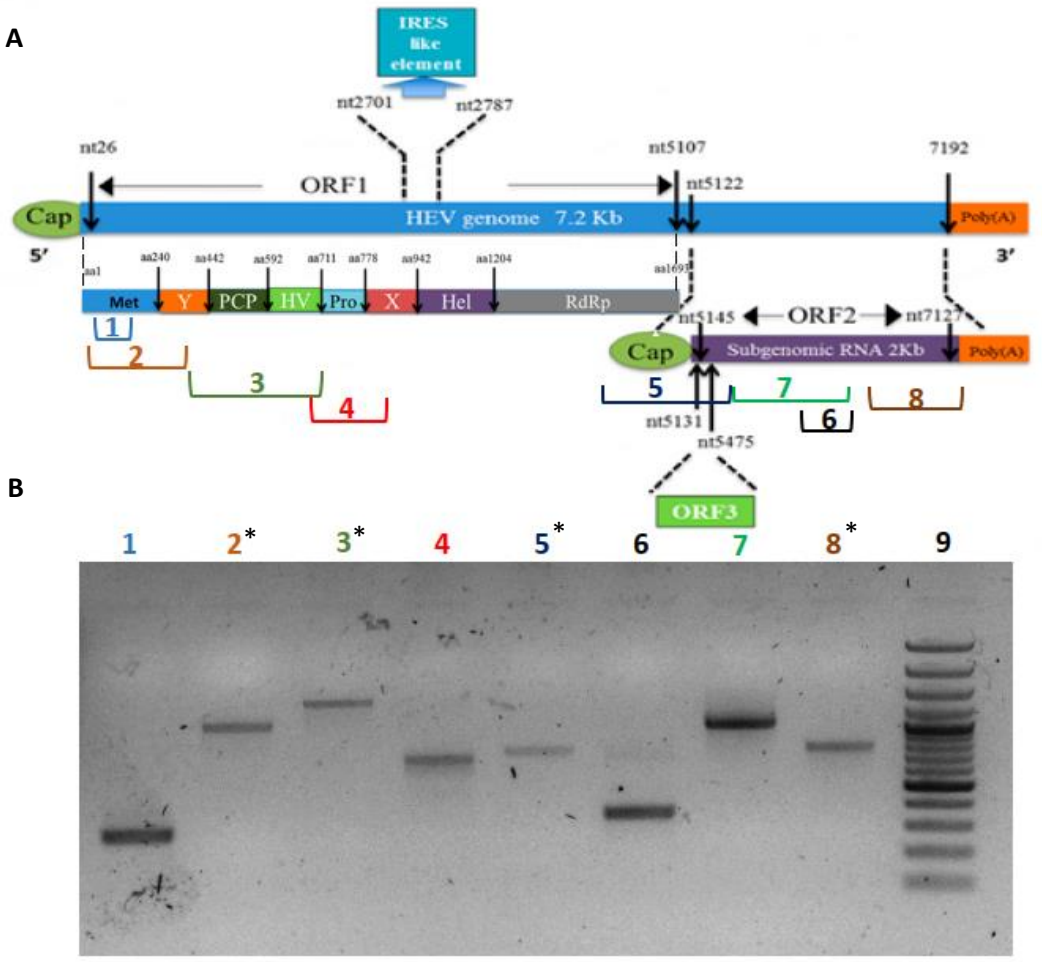

Figura 9. Diagrama de las distintas regiones del genoma de HEV amplificadas por RT-PCR.

A. Representación esquemática del genoma de HEV, del ARN subgenómico y de los ORFs. Se muestra el ORF1 (26-5107 nt) y sus dominios. El ORF2 (5145-7127 nt) y el ORF3 (5131-5475 nt) son codificados por el mismo ARN subgenómico. Extraído de [10].

B. Electroforesis en gel de agarosa de los productos obtenidos por RT-PCR para la muestra HEV_C1_Uy. Se muestran con números las regiones en el genoma correspondientes a los fragmentos obtenidos. El marcador de peso molecular de 100 pb GeneRuler™ Plus DNA Ladder (Thermo Scientific®) se observa en el carril 9. Las RT-PCR optimizadas en esta Tesis se indican con un *.

4.6.2 Obtención de genomas completos adicionales

Con el propósito de profundizar los resultados filogenéticos obtenidos basados en secuencias parciales de HEV-*like* en Axis (Capítulo 1), se llevaron a cabo numerosos intentos para la obtención del genoma completo de HEV para la muestra 71_Axis_Uy, evaluándose distintas condiciones de enriquecimiento para las muestras mediante las estrategias metagenómica y virómica como se describió en las publicaciones adjuntas.

Los archivos de secuenciación obtenidos fueron analizados con el Geneious Prime 2020.2.1 software y además por medio de otro método bioinformático, utilizando softwares libres en el sistema operativo Linux-Ubuntu. La limpieza de calidad se llevó a cabo con Trim Galore considerando una calidad de base >25 y se empleó el programa BWA-MEM para el alineamiento de referencia, utilizando las secuencias de referencia de HEV (N° accesos GenBank FJ998008, MW596896 y KF951328 para el caso de 71_Axis_Uy).

Sin embargo, en ningún caso fue posible recuperar el genoma completo de HEV-*like*.

Estos experimentos se realizaron en el marco de una pasantía financiada por PEDECIBA en la Plataforma Genómica de la Facultad de Ciencias-UdelaR bajo la supervisión de la Dr. Yanina Panzera, donde se realizó una capacitación en el flujo de trabajo completo que implica la preparación, obtención y análisis de las librerías de secuenciación masiva con tecnología Illumina.

4.6.3. Microscopía electrónica de transmisión

Para evaluar en un futuro la morfología de la partícula viral de las variantes de HEV-*like* dentro de *P. balayani,* así como las diferencias entre eHEV y HEV, se puso a punto y se implementó un protocolo de visualización de partículas virales en materia fecal mediante microscopía electrónica de transmisión para la cepa HEV_C1_Uy.

Para ello, se filtró el sobrenadante por un filtro de 0.22µm (Millipore), luego, se fijó la muestra con glutaraldehído y se realizaron dos ultracentrifugaciones a 100.000xg 4°C durante 1 hr, lavando el *pellet* viral. Se aplicó una tinción negativa por ácido fosfotúngstico y se visualizaron las partículas de un tamaño entre 33-37 nm con el microscopio de alta resolución del

Departamento de Desarrollo Tecnológico del Centro Universitario Regional del Este (CURE), UdelaR, sede Rocha (Figura 10).

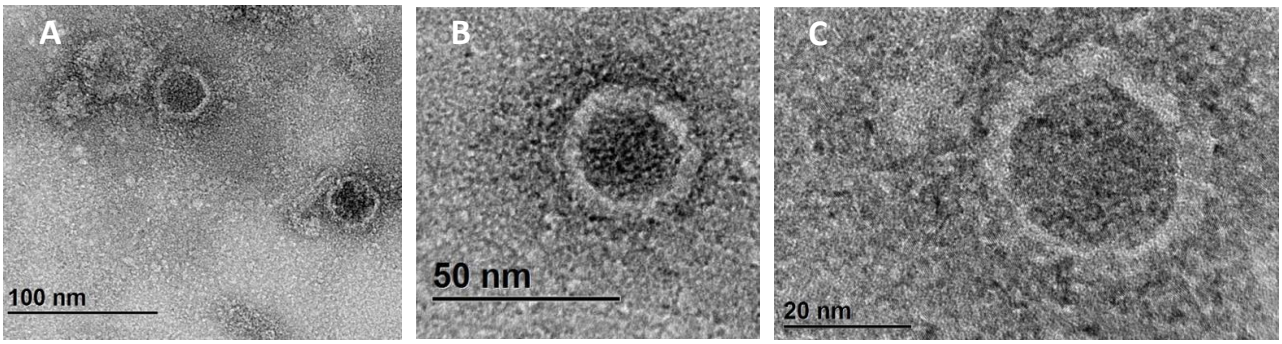

Figura 10. **Microscopía electrónica de transmisión de la cepa HEV_C1_Uy.** Las imágenes se obtuvieron con el microscopio de alta resolución del Departamento de Desarrollo Tecnológico del CURE Sede Rocha, a partir de la suspensión de materia fecal. **A-C**. Se muestran las partículas virales observadas de entre 33-37 nm a distintos aumentos.

5. CAPÍTULO 3

Modelado de la RdRp de HEVc y análisis *in silico* de la interacción con RBV

5.1. Fundamento teórico y antecedentes

El genoma completo de HEV obtenido en el *Punto 4.4*. del *Capítulo 2* (HEV_C1_Uy) proviene de un paciente de 62 años con trasplante de hígado (TH) presentando una infección autóctona crónica de HEV3 con un enzimograma hepático alterado y evidencia histológica de infección por HEV (1 año y 6 meses luego de TH), que fue luego tratado con RBV por 9 semanas (1200 mg/día) y mostró una respuesta virológica sostenida en el seguimiento de 24 meses [74].

Por lo tanto, resulta interesante estudiar desde un enfoque *in silico* la afinidad de unión y determinar los dominios de interacción entre la proteína RdRp y la molécula de RBV para una cepa autóctona derivada de una infección crónica (HEV_C1_Uy) que fue tratada con esta droga.

Es muy escaso el conocimiento sobre la RdRp de HEV, se ha sugerido que puede comenzar la síntesis *de novo* desde el molde de ARN o utilizar el final del molde para iniciar la síntesis desde el extremo 3´ OH [46]. Sin embargo, a pesar de tratarse de una proteína clave para la replicación de HEV, hasta el momento no hay información sobre sus dominios funcionales, selección de nucleótidos, estructura, rol y por lo tanto, sobre su interacción con la droga antiviral RBV, así como tampoco se encuentran disponibles estructuras cristalográficas o modelos.

La RBV (1-beta-D-ribofuranosil-1,2,4-triazol-3-carboxamida) es un análogo sintético de guanosina/adenosina con amplio espectro antiviral [93] y es fosforilada intracelularmente a las formas monofosfato (RBVM), difosfato (RBVD) y trifosfato (RBVT) por una quinasa de adenosina celular [94]. RBVM es un inhibidor competitivo de la inosina monofosfato deshidrogenasa que lleva a la depleción de los *pools* de GTP necesarios para la síntesis del ARN viral. Adicionalmente, RBVT puede ser erróneamente incorporado por la RdRp en el ARN viral naciente e inducir transición de bases, terminación temprana de la cadena e inhibir la replicación por medio de la inhibición competitiva de la unión a nucleótidos [94].

Las RdRp virales utilizan rNTPs para la síntesis del ARN, lo cual sumado a la alta tasa de mutación de los virus ARN, ha impulsado el interés en el estudio de análogos de nucleósidos

(como RBV) para inducir al virus a catástrofe de error. Para ello, los estudios estructurales de las RdRp virales en complejo con antivirales análogos de nucleósidos son importantes para comprender la actividad mutagénica sobre la replicación viral [95].

Actualmente, los avances en estudios genómicos y computacionales brindan una importante oportunidad para el desarrollo de posibles nuevas drogas, así como también para profundizar aspectos de las ya existentes, conocido como farmacología computacional. Uno de los objetivos principales de esta rama de la bioinformática consiste en la predicción de la interacción de la droga y su proteína blanco, siendo un método costo-efectivo para el estudio y diseño de drogas [96].

Los métodos de diseño de drogas basado en estructura (SBDD) son un factor destacado en la medicina química moderna [97], donde la comprensión de los principios de reconocimiento e interacción de pequeños ligandos con macromoléculas es de vital importancia en el área de investigación y desarrollo farmacéutico. Entre las estrategias más frecuentes de SBDD se encuentran los métodos de *docking o* acoplamiento molecular y simulaciones de dinámica molecular (MDS), ya que presentan un amplio rango de aplicaciones para el análisis de reconocimiento molecular incluyendo energías de unión, interacciones moleculares y cambios conformacionales [98].

El método de *docking* molecular, una herramienta esencial en *drug discovery*, es muy utilizado debido a su habilidad para predecir la conformación de pequeños ligandos dentro del sitio blanco más apropiado basado en la afinidad de unión. Complementariamente, la técnica de MDS considera en el análisis que las proteínas y sus ligandos pueden ser flexibles y sufrir cambios conformacionales durante el proceso de reconocimiento, los cuales pueden llegar a involucrar elementos de estructura secundaria o terciaria. Además, el MDS es utilizado para estimar la estabilidad del complejo proteína-ligando propuesto por el método de *docking* molecular [99].

La estrategia de SBDD ha sido ampliamente aplicada en el campo de la virología y recientemente, para el estudio de posibles agentes antivirales para SARS-CoV2 [100, 101].

5.2. Hipótesis

Es posible obtener el primer modelo 3D de la proteína RdRp de HEV3 por análisis bioinformáticos e identificar el sitio de interacción de esta proteína con la droga RBVT para comprender mejor su mecanismo de acción.

5.3. Objetivo específico

Modelado de la RdRp de HEVc y análisis *in silico* de la interacción con RBV. Obtener un modelo *in silico* 3D de la RdRp de HEV3 proveniente de un paciente con HEV-SOT crónica (HEVc). Además, se propuso implementar estrategias de SBDD, mediante *docking* molecular y simulaciones de dinámica molecular con la droga RBVT para brindar información sobre la interacción molecular del complejo enzima-droga antiviral.

5.4. Cancela et al., 2021. Modelling of Hepatitis E virus RNA-dependent RNA polymerase genotype 3 from a chronic patient and in silico interaction analysis by molecular docking with Ribavirin.

En este trabajo se reportó un modelo *in silico* 3D de la proteína RdRp de HEV3 perteneciente a la cepa HEV_C1_Uy, en el cual se realizaron análisis de *docking* molecular y simulaciones de dinámica molecular entre esta proteína de RdRp y la molécula RBVT.

Se obtuvo un modelo adecuado para la RdRp de HEV_C1_Uy con un C-Score= -1.33 y RMSD= 10.4 ± 4.6 Å. RBVT mostró una afinidad de -7.6 ± 0.2 Kcal/mol por *docking* molecular mediado por 6 enlaces de hidrógeno (Q195-O14, S198-O11, E257-O13, S260-O2, O3, S311-O11) entre los dominio de dedos-palma y una energía de unión libre de 31.26 ± 16.81 kcal/mol por simulaciones de dinámica molecular.

Por lo tanto, estos resultados obtenidos permitieron identificar el posible sitio de interacción de la RdRp de HEV con los nucleótidos o análogos entrantes, brindando información novedosa que pueda contribuir a mejorar el entendimiento de las interacciones moleculares de RBV con la enzima y el mecanismo de acción de esta droga antiviral.

Los resultados derivados de este Capítulo se publicaron en un artículo científico que se adjunta a continuación:

Cancela F, Rendon-Marin S, Quintero-Gil C, Houston DR, Gumbis G, Panzera Y, Pérez R, Arbiza J, Mirazo S. Modelling of Hepatitis E virus RNA-dependent RNA polymerase genotype 3 from a chronic patient and in silico interaction analysis by molecular docking with Ribavirin. J Biomol Struct Dyn. 2023 Feb;41(2):705-721. doi: 10.1080/07391102.2021.2011416. Epub 2021 Dec 3.

Taylor & Francis
Taylor & Francis Group

Journal of Biomolecular Structure and Dynamics

ISSN: (Print) (Online) Journal homepage: https://www.tandfonline.com/loi/tbsd20

Modelling of Hepatitis E virus RNA-dependent RNA polymerase genotype 3 from a chronic patient and *in silico* interaction analysis by molecular docking with Ribavirin

Florencia Cancela, Santiago Rendon-Marin, Carolina Quintero-Gil, Douglas R. Houston, Gediminas Gumbis, Yanina Panzera, Ruben Pérez, Juan Arbiza & Santiago Mirazo

To cite this article: Florencia Cancela, Santiago Rendon-Marin, Carolina Quintero-Gil, Douglas R. Houston, Gediminas Gumbis, Yanina Panzera, Ruben Pérez, Juan Arbiza & Santiago Mirazo (2021): Modelling of Hepatitis E virus RNA-dependent RNA polymerase genotype 3 from a chronic patient and *in silico* interaction analysis by molecular docking with Ribavirin, Journal of Biomolecular Structure and Dynamics, DOI: 10.1080/07391102.2021.2011416

To link to this article: https://doi.org/10.1080/07391102.2021.2011416

JOURNAL OF BIOMOLECULAR STRUCTURE AND DYNAMICS
https://doi.org/10.1080/07391102.2021.2011416

Modelling of Hepatitis E virus RNA-dependent RNA polymerase genotype 3 from a chronic patient and *in silico* interaction analysis by molecular docking with Ribavirin

Florencia Cancela[a#], Santiago Rendon-Marin[b#], Carolina Quintero-Gil[b], Douglas R. Houston[c], Gediminas Gumbis[c], Yanina Panzera[d], Ruben Pérez[d], Juan Arbiza[a] and Santiago Mirazo[a,e]

[a]Sección Virología, Facultad de Ciencias, Universidad de la República, Montevideo, Uruguay; [b]Grupo de Investigación en Ciencias Animales - GRICA, Facultad de Medicina Veterinaria y Zootecnia, Universidad Cooperativa de Colombia, sede Bucaramanga, Bucaramanga, Colombia; [c]Institute of Quantitative Biology, Biochemistry and Biotechnology, The University of Edinburgh, Edinburgh, UK; [d]Sección Genética Evolutiva, Instituto de Biología, Facultad de Ciencias, Universidad de la República, Montevideo, Uruguay[e]Departamento de Bacteriología y Virología, Instituto de Higiene, Facultad de Medicina, Universidad de la República, Montevideo, Uruguay

Communicated by Ramaswamy H. Sarma.

ABSTRACT

Hepatitis E Virus (HEV) infection is an emergent zoonotic disease, where chronic hepatitis E associated to solid organ transplant (SOT) recipients, related to genotype 3, is the clinical manifestation of major concern. In this setting, ribavirin (RBV) treatment is the only available therapy, though drug-resistant variants could emerge leading to a therapeutic failure. Crystallographic structures have not been reported for most of the HEV proteins, including the RNA-polymerase (RdRp). Therefore, the mechanism of action of RBV against HEV and the molecular interactions between this drug and RdRp are largely unknown. In this work, we aimed to model *in silico* the 3 D structure of a novel HEV3 RdRp (HEV_C1_Uy) from a chronically HEV infected-SOT recipient treated with RBV and to perform a molecular docking simulation between RBV triphosphate (RBVT), 7-methyl-guanosine-5′-triphosphate and the modelled protein. The models were generated using I-TASSER server and validated with multiple bioinformatics tools. The docking analysis were carried out with AutoDock Vina and LeDock software. We obtained a suitable model for HEV_C1_Uy (C-Score=-1.33, RMSD = 10.4 ± 4.6 Å). RBVT displayed a binding affinity of −7.6 ± 0.2 Kcal/mol by molecular docking, mediated by 6 hydrogen-bonds (Q195-O14, S198-O11, E257-O13, S260-O2, O3, S311-O11) between the finger's-palm-domains and a free binding energy of 31.26 ± 16.81 kcal/mol by molecular dynamics simulations. We identified the possible HEV RdRp interacting region for incoming nucleotides or analogs and provide novel insights that will contribute to better understand the molecular interactions of RBV and the enzyme and the mechanism of action of this antiviral drug.

ARTICLE HISTORY
Received 5 November 2020
Accepted 22 November 2021

KEYWORDS
Hepatitis E virus; RNA polymerase; ribavirin; molecular docking; interaction; structure

1. Introduction

Hepatitis E virus (HEV) is a leading cause of acute hepatitis, a worldwide enterically-transmitted zoonotic disease (Emerson & Purcell, 2003; Khuroo & Khuroo, 2008) that cause large waterborne epidemic outbreaks in developing countries (Panda et al., 1995; Tan et al., 1995; Wang et al., 2001; Yan et al., 2008). Nonetheless, in industrialized countries, HEV has become an increasing public-health concern as autochthonous cases have raised drastically in the last few years (Perez-Gracia et al., 2013). HEV is a small, 32-34 nm, non or quasi-enveloped particle with a single-stranded positive-sense RNA genome of 7.2 Kb approximately (Reyes et al., 1990). The viral genome is capped at the 5′-end and polyadenylated at the 3′-end, containing three partially overlapping open reading frames (ORFs) (Tam et al., 1991). ORF1 encodes a non-structural polyprotein of ∼1693 amino acids (aa) with eight putative functional domains including methyltransferase, protease, RNA-helicase and RNA-dependent RNA polymerase (RdRp) (Koonin et al., 1992). ORF2 encodes for the capsid protein (Guu et al., 2009; Li et al., 2005) and ORF3 produces a multifunctional phosphoprotein essential for virion release (Ding et al., 2017; Yamada et al., 2009).

HEV is classified into the *Orthohepevirus A* genus of the *Hepeviridae* family and comprises eight distinct genotypes (HEV1 to HEV8) (Smith et al., 2014). HEV3 genotype is globally distributed (Lu et al., 2006) and is more prevalent in high-income countries (Purcell & Emerson, 2008). Outbreaks of this genotype are associated to the consumption of contaminated raw or undercooked meat and liver sausages derived from pigs, the main reservoir of the disease (Mansuy et al., 2011; Servant-Delmas et al., 2016). HEV3 infection may evolve to a chronic hepatitis, particularly, in solid organ transplant (SOT) recipients and

CONTACT Santiago Mirazo smirazo@fcien.edu.uy Sección Virología, Facultad de Ciencias, Universidad de la República, Iguá 4225, Montevideo, PC11400, Uruguay

Supplemental data for this article can be accessed online at http://dx.doi.org/10.1080/07391102.2021.2011416

#Both authors equally contributed to this work

immunocompromised individuals with lymphoma, leukemia and HIV infection (Fang & Han, 2017; Gerolami et al., 2008; Le Coutre et al., 2009; Pischke et al., 2010), which could result in liver fibrosis, cirrhosis or liver failure (Arends et al., 2014; Gerolami et al., 2011; Jagjit Singh et al., 2013; Kamar et al., 2011).

HEV belongs to the "alpha-like" supergroup III of positive-strand viruses, where HEV RdRp along with Rubella virus RdRp (RUBV) and Beet necrotic yellow vein virus RdRp (BNYVV) conform a distinct close cluster (Koonin et al., 1992). In this supergroup, eight conserved motifs (I-VIII) have been described (Koonin et al., 1992). It has been suggested that HEV RdRp can either initiate *de novo* synthesis from the RNA template or employ the template end to prime the synthesis from the 3'OH end (Mahilkar et al., 2016). Localization studies revealed that HEV RdRp is present in the endoplasmic reticulum (ER), suggesting the involvement of ER membrane in HEV replication (Rehman et al., 2008).

Even though HEV RdRp is a crucial viral protein, information about its functional domains, template specificities, nucleotide selection, structure and functional role have not been described yet.

Ribavirin (RBV) (1-b-D-ribofuranosyl-1,2,4-triazole) is a guanosine/adenosine synthetic analog with broad-antiviral spectrum (Cameron & Castro, 2001) and is phosphorylated intracellularly by a cellular adenosine kinase to monophosphate (RBVM), diphosphate (RBVD) and triphosphate (RBVT) forms (Feld & Hoofnagle, 2005). RBVM is a competitive inhibitor of inosine monophosphate dehydrogenase that leads to a depletion in the GTP pools needed for RNA viral synthesis (Feld & Hoofnagle, 2005). Moreover, RBVT can be misincorporated by the RdRp in the nascent viral RNA inducing base transitions, producing an early chain termination and inhibition of replication by competitively inhibiting the binding of nucleotides (Feld & Hoofnagle, 2005). Modeling studies revealed that the base moiety of ribavirin, 1,2,4-triazole-3-carboxamide, forms base pairs with both cytosine and uracil by a rotation of the carboxamide group (Crotty et al., 2000). Furthermore, it was observed that once RBV is in the RNA, it could be trapped in the "anti" conformation of the "pseudo-base" and is then able to bind base pairs with incoming pyrimidines (Crotty et al., 2000). For these reasons, RBV has been also considered a viral mutagen that could exceed the "error-catastrophe" threshold in RNA viruses, causing mainly A to G and U to A substitutions (Young et al., 2011) that leads to lethal mutagenesis (Crotty et al., 2000; 2001; Contreras et al. 2002; Day et al., 2005; Feld & Hoofnagle, 2005; Severson et al. 2003).

Until several years ago, RBV was employed to treat Lassa fever virus infection (Andrei & De Clercq, 1993; Crotty & Andino, 2002; De Clercq, 2004) and in combination with interferon-α to treat hepatitis C virus (HCV) infection (Cummings et al., 2001; Di Bisceglie et al., 2001; Maag et al., 2001), vesicular stomatitis virus (Fernandez-Larsson et al., 1989; Toltzis et al., 1988), La Crosse encephalitis virus (Cassidy & Patterson, 1989), reovirus (Rankin et al., 1989), influenza (Eriksson et al., 1977; Wray et al., 1985) and human immunodeficiency virus (Fernandez-Larsson & Patterson, 1990).

Currently, RBV is used as a monotherapy only to treat respiratory syncytial virus infection under certain clinical circumstances (Krilov, 2001; Wyde, 1998; Xu et al., 2004).

In the case of chronic HEV infection, in which viral RNA remains detectable for at least 3-6 months, there is no specific antiviral treatment for the patients. The first therapeutic line consists in decreasing the immunosuppression therapy, which exhibits good outcome in only 30% of the patients (Kamar et al., 2011). In a high proportion of cases where HEV clearance could not be achieved, RBV is administered for another 3 months (Mirazo et al., 2014), with good results (Gerolami et al., 2011; Kamar et al., 2010; 2014; Mallet et al. 2010). However, RBV treatment failure has been reported frequently due to HEV antiviral resistance likely associated to G1634R, Y1320H and K1383N substitutions in the RdRp (Debing et al., 2016). The K1383N substitution is located in the F1-motif (177-180 aa in HEV RdRp) which is believed to bind the incoming nucleotide-triphosphate and select the correct one (Bruenn, 2003). Hence, RBV has been proposed to be mutagenic to HEV during a prolonged treatment. Interestingly, the K1383N substitution could strongly decrease viral replication and increase RBV sensitivity *in vitro*, opposite to the observed clinical phenotype (Debing et al., 2016). On the other hand, the Y1320H substitution increases HEV replication without altering RBV sensitivity, which may then be a compensatory change for the fitness loss resulting from K1383N. The G1634R substitution seemed to increase the replicative capacity of HEV and then reduce the efficiency of RBV (Debing et al., 2014).

In this work we pursued two goals. First, to obtain an HEV3 RdRp 3 D *in silico* model of a strain coming from a chronic HEV-SOT patient treated with RBV (Mainardi et al., 2019), as there is no crystallographic structures available in databases, in order to thoroughly analyze HEV RdRp structural characteristics. Second, to perform a comprehensive molecular docking simulation between RBVT and the modelled HEV protein, aimed to provide novel insights on the enzyme-antiviral drug molecular interaction.

2. Materials and methods

2.1. HEV strain and RNA extraction

The HEV strain employed in this study came from a chronic hepatitis E case belonging to genotype 3 recently reported in Uruguay by our group (HEV_C1_Uy) (Mainardi et al., 2019). The patient was a liver-transplanted (LT) 62-year-old man presenting an autochthonous chronic HEV3 infection with an altered liver enzymogram and histologic evidence of HEV infection (1 year and 6 months after LT), who was then treated with a 9-weeks course of RBV (1200 mg/day). After the RBV course he had a sustained virological response (SVR) in the 24 months follow-up.

Total RNA was extracted from a 10% fecal PBS suspension with *Quick*-RNA™ Miniprep Kit (Zymo Research Corp, USA) following manufacturer's instructions.

The consensus nucleotide sequence of the HEV RNA polymerase here described was submitted to GenBank under the accession number MT774175.

Table 1. Positive-strand viral RNA RdRp conserved motifs I-VIII between HEV_C1_Uy and RUBV.

	Conserved Motif	HEV_C1_Uy RdRp	RUBV RdRp
Position	I	177-185	489-496
	II	197-215	518-536
	III	228-238	549-559
	IV	253-264	574-586
	V	310-323	631-644
	VI	339-350	660-671
	VII	380-389	706-714
	VIII	391-404	716-729
Sequence	I	KDCNKFTTG	KATLKCVD
	II	ISAWSKTFCALFGPWFRAI	IRAWAKEWVQVMSPHFRAI
	III	FYGDAYEESVF	LVAAGHTEPEV
	IV	NDFSEFDSTQNN	VDFTEFDMNQTLA
	V	HSGEPGTLLWNTVW	TSGEPATLLHNTTV
	VI	VAAFKGDDSVVL	AGIFQGDDMVIF
	VII	LYAGVVVAPG	SFCGHVGTA
	VIII	GVLPDVVRFAGRLS	GLFHDVMHQAIKVL

2.2. Next generation sequencing (NGS) and data analysis

Double stranded cDNA (dscDNA) was generated using Maxima H Minus Double-Stranded cDNA Synthesis Kit (ThermoFisher Scientific, USA) with random primers and 12 µL of extracted RNA. The dscDNA was amplified by Multiple Displacement Amplification (MDA) technology using REPLI-g Mini Kit (Qiagen, Germany) followed by purification and quantification using AMPure XP (Beckman Coulter, USA) and a Qubit fluorometer (Qubit™ DNA-HS Assay kit), respectively.

Nextera DNA Flex Library Preparation kit (Illumina, USA) with dual indexing was used from 50 ng of dscDNA. Control quality libraries were performed on a Fragment Analyzer 5200 system (Agilent Technologies, USA) using the Standard Sensitivity NGS Analysis Kit (Agilent Technologies, USA). Library was sequenced on an Illumina MiniSeq Genomic Platform at the Faculty of Sciences (UdelaR, Uruguay) using Mid Output Reagent Cartridge (300-cycles, 150 base-pair paired-end reads) by following standard Illumina protocols.

Sequencing raw reads were demultiplexed automatically on the MiniSeq platform with the default settings. Adapter/quality trimming and filtering were performed with BBDuk plugin and clean reads were mapped to a hepatitis E genome (FJ998008) using Geneious mapper (medium-low sensitivity) available in the Geneious Prime 2020.2.1 software (https://www.geneious.com).

Reference assembly and annotation was done with SeqMan NGen® Version 12.0 (DNASTAR. Madison, WI) using the reference genome retrieved from the GenBank database FJ998008.

2.3. Rdrp sequence alignments

The RdRp domain was identified from the HEV_C1_Uy complete genome according to other HEV polymerase annotations in Uniprot database (UniProt, 2020).

Multiple RdRp nucleotide and amino acids (aa) sequence alignments of complete RdRp from HEV strains and of the catalytic site from HEV and other viruses were carried out with ClustalW in MEGA v.7 (Kumar et al., 2016). HEV_C1_Uy complete RdRp and HEV3 selected subtype reference strains 1a-8a (Smith et al., 2020) were included for the alignment (Table S1).

An alignment including only the catalytic site of different viral RdRp was also carried out for HEV_C1_Uy and HEV reference strains (Table S1).

Additionally, diverse RdRp sequences were selected from several viruses for further analysis: Hepatitis C virus 1a-*Flaviviridae*, Hepatitis A virus IB- *Picornaviridae*, Coxsackievirus B1-*Picornaviridae*, Norwalk virus of the *Caliciviridae* family (former HEV classification), RUBV-*Matonaviridae* (reported to exhibit conserved motifs with HEV RdRp (Koonin et al., 1992)) and BNYVV-*Benyviridae* a plant furovirus belonging to the "alpha-like" supergroup. Top first threading templates and structural analogs from I-TASSER modelling were also added to the alignment from RCSB:PDB database (RCSB: PDB, 2020) (Table S1). Viral RdRp catalytic site annotated sequences were obtained from Uniprot database. P-distance pairwise matrices for RdRp catalytic site between HEV strains and the other viral sequences were performed in MEGA v. 7. A phylogenetic tree for the RdRp catalytic sites was constructed in MEGA v.7 by the Neighbor-Joining method with the Poisson model as the best substitution model. Bootstrap values were determined with 1000 replicates of the dataset.

2.4. HEV RdRp 3 D modelling, structural analysis and validation

The amino acid sequences from the HEV_C1_Uy RdRp and a HEV3 RdRp from the swine Arkell strain (reference of subtype 3j) were employed to determine the 3 D-structure. The secondary structure was predicted using PSIPRED 4.0 tool (Jones, 1999) (UCL-CS Bioinformatics). Annotation information was retrieved from ExPASy-PROSITE (Sigrist et al., 2013) and Pfam database (El-Gebali et al., 2019). Chemical and physical parameters for this protein were obtained from ExPASy-ProtParam tool (ExPASy-ProtParam tool 2020).

Thorough sequence alignments analyses were performed in order to evaluate HEV RdRp homology modelling possibility, which was then discarded (data not shown). Therefore, the I-TASSER prediction server (Yang et al., 2015) was employed to obtain the 3 D structure models and the best

ranked structure in the hierarchical analysis in terms of the best C-Score and Root Mean Square Deviation (RMSD) were selected (Yang et al., 2015).

The models were assessed and validated using bioinformatics tools. ProSA-Web (Wiederstein & Sippl, 2007) was used to calculate the Z-score for the overall model quality which enables to establish whether the Z-score value of the model structure is located in the range of Z-scores exhibited by native proteins of similar size, with PDB as reference database. The Ramachandran plots (RAMPAGE) (RAMPAGE, 2020), were also constructed to establish amino acids in energetically favorable regions. Additionally, ERRAT (Colovos & Yeates, 1993), Verify 3 D (Eisenberg et al., 1997) and PROCHECK (Laskowski et al., 1993) software were employed. All these computational tools enable us to determine whether 3 D models of HEV RdRp are reliable models to employ in molecular docking analysis.

The generated models were structurally aligned to the best ranked structures to establish the RMSD differences between the model and best template structures utilizing TM-Align based on TM-score (Zhang & Skolnick, 2005). The crystallized structures (6R1I, 1SH0, 3N6L, 3CDU) were downloaded from the PDB database.

Molecular graphics were performed with UCSF Chimera v. 1.8 (Pettersen et al., 2004)..

2.5. Molecular docking

The 3 D structure of RBV and RBVT were downloaded in PDB format from PubChem-NIH (PubChem, 2020) (CID 37542 and 122108, respectively). 7-methyl-guanosine-5′-triphosphate (GTP) and Cinnamaldehyde (CIN) 3 D structures were downloaded in PDB format from the Drugbank database (Drugbank, 2020) (Accession Numbers DB02716 and DB14184, respectively). The GTP physiological nucleotide was employed as an internal control for the molecular interaction analyses. The CIN organic compound, which is the main component of the cinnamon, was included as a negative control since no affinity towards RdRp has been reported for this compound (Elfiky, 2020).

Interaction analysis of HEV_C1_Uy RdRp and HEV Arkell RdRp with RBV, RBVT, GTP and CIN were carried out with AutoDock Vina v. 1.1.2 (Trott & Olson, 2010). The grid box was defined with the online tool PeptiMap (Lavi et al., 2013), which predicts the best ligand-binding site on the protein surface. The models were minimized adding charges with the default parameters in PMV v.1.5.6 (MGLTools-The Scripps Research Institute) (Sanner, 1999) and saved in PDBQT file formats for the docking. Five runs of each docking assay were performed in a grid box with a spacing of 1 Å, presenting the dimensions $x = 24$, $y = 28$, $z = 22$ and its center located in $x = 74.853$, $y = 63.244$, $z = 55.892$ for HEV_C1_Uy RdRp. Concerning the HEV Arkell RdRp, conditions were the same as aforementioned but with dimensions $x = 24$, $y = 24$, $z = 28$ and the following coordinates $x = 65.309$, $y = 56.220$, $z = 61.801$.

Additional docking assay was carried out involving the analog sites between HCV-ribonucleoside triphosphates (rNTPS) interaction and HEV_C1_Uy RdRp and HEV Arkell RdRp. The grid box for HEV_C1_Uy RdRp had the following characteristics, size: $x = 20$, $y = 24$, $z = 28$, center: $x = 80.208$ $y = 63.928$, $z = 60.218$, whereas for HEV Arkell RdRp presented size: $x = 30$, $y = 24$, $z = 20$; center: $x = 64.757$, $y = 52.581$, $z = 68.09$. All the docking studies were also run five times in LeDock (Liu & Xu, 2019), employing the same grid box coordinates as in AutoDock Vina, with the ligand file format in SYBYL Mol2. In all cases, binding energies were reported as the mean Kcal/mol ± SD.

The 2 D protein-ligand interaction diagrams were built employing the software LigPlot + v. 4.5.3 (Wallace et al., 1995) and PoseView-Proteins*Plus* (Stierand et al., 2006). Analysis of the generated 3 D docking interactions were performed in UCSF Chimera v. 1.8.

2.6. Molecular dynamics simulation and binding free energy calculations

mol2 files for Cinnamaldehyde (ZINC1532777), RBVT (ZINC12402860), and 7-methyl-GTP (ZINC15601432) were downloaded from ZINC Database (Sterling & Irwin, 2015). These files were used for parametrization of the ligands with the help of SwissParam (Zoete et al., 2011). Using VMD, HEV_C1_Uy RdRp-ligand complexes were made, solvated, and, subsequently, the solvation box was ionized with 0.15 M of Na^+ and Cl^- (Humphrey et al., 1996). Molecular Dynamics (MD) simulations followed; for this, we utilized NAMD 2.14 (Phillips et al., 2020). Minimization was carried out for 10,000 steps while a step itself was 2 fs long. Following minimization, the three systems were equilibrated for 2 ns, and, finally, longer MD simulations were carried out so that the total length of the simulations were at least 100 ns. CaFE (Liu & Hou, 2016) was used to perform molecular mechanics Poisson-Boltzmann surface area (MM/PBSA) calculations. CaFE utilized NAMD for the MM component, APBS for PB calculations (Baker et al., 2001), and VMD for SA calculations. Trajectories derived from the MD simulations were analyzed using CaFE. Default parameters of CaFE were used for the calculations.

3. Results

3.1. Hev_C1 _UY RdRp showed non-reported amino acidic substitutions

The HEV3 C1 Uy complete genome from the HEV-SOT chronic patient was successfully obtained by Illumina sequencing with a mean average coverage of sequencing depth of 71.7.

The RdRp domain was identified at the 1217-1703 position of the nonstructural protein. This protein contained 487 residues, a molecular weight of 53526.49 Da and an isoelectric point of 5.94.

Due to the high sequence divergence of the complete RdRp sequence among viral families, the alignments and identity matrices analyses were conducted separately for the catalytic site. Sequence analysis of the catalytic site revealed

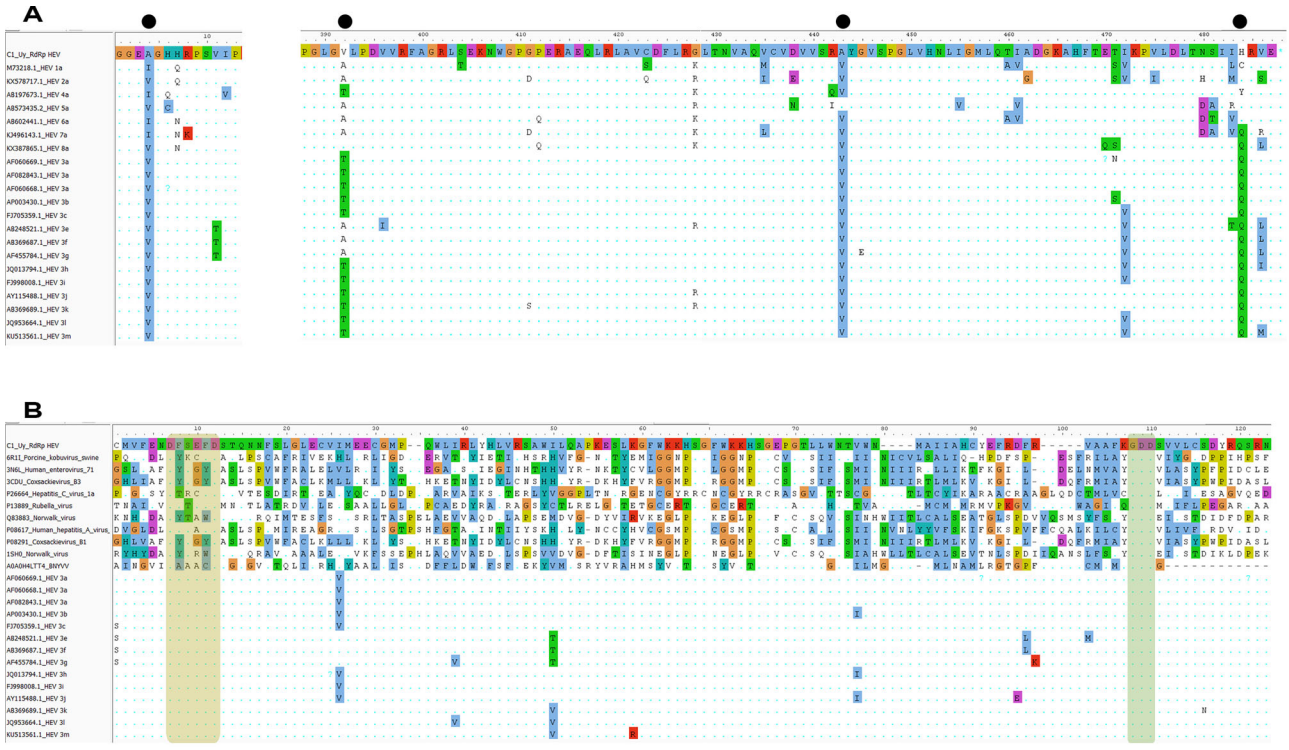

Figure 1. Multiple sequence alignment of viral RNA-dependent RNA polymerase (RdRp). A. Complete RdRp sequence alignment for Hepatitis E virus (HEV) reference genotypes (HEV1-HEV8), subtypes (HEV 3a-3m) and HEV_C1_Uy. The black dot indicates the non-reported substitution V/I4A and the infrequent ones T/A392V, V443A and Q484H. B. Sequence alignment for the RdRp catalytic site for Porcine Aichi virus (Kobuvirus), Enterovirus A71, Coxsackie B3, B1, Rubella virus, Norwalk virus, Hepatitis A, Beet necrotic yellow vein virus (BNYVV) and HEV_C1_Uy. The conserved motifs (D-x(4,5)-D) and GDD are highlighted in yellow and green, respectively.

an identity for HEV_C1_Uy RdRp ranging from 17% for Coxsackievirus B1 and B3 to 29.8%-26.6% for BNYVV and RUBV, respectively. The percentage of identity of HEV_C1_Uy with HEV3 reference strains ranges from 95.7% (3e) to 98.9% (3a, 3i and 3k). HEV_C1_Uy RdRp showed 86.89% of sequence identity with the closest related isolate (FJ705359).

HEV_C1_Uy presented several non-reported and infrequent substitutions, which were located outside the catalytic site. At the amino acidic level, a unique non-reported substitution V/I4A (V/I1220A referred to ORF1 position) was found in HEV_C1_Uy strain. The changes T/A392V (T/A1608V) and V443A (V1659A) in HEV_C1_Uy were exclusively found in HEV8a and 5a genotypes, respectively, which are very distantly related to HEV3, whereas the HEV_C1_Uy Q484H (Q1700H) change was previously reported in few strains from 2a, 5a and 6a genotypes (Figure 1).

The eight reported conserved motifs (I-VIII) of the positive-strand viral RNA RdRp (Koonin et al., 1992) were identified among the sequence alignments (Table 1). Motifs IV (D-x(4,5)-D) and VI (GDD) in the catalytic site were conserved among HEV strains and other viral families (Figure 1).

HEV proteins have not clustered with any other RdRp viral sequence but were closely related and shared the highest homology with the RUBV and BNYVV proteins (Figure 2). Analysis at the nucleotide level, exhibited that HEV_C1_Uy formed a separate cluster from other HEV3 subtypes strains (data not shown).

3.2. An acceptable HEV_C1_Uy RdRp 3 D structure was obtained

HEV_C1_Uy RdRp and HEV Arkell RdRp models obtained had a C-Score of −1.33, RMSD score of 10.4 ± 4.6 Å and a C-Score of −1.10, respectively. C-score values determines the model quality and ranges from [-2, 5], where a higher value means a higher confidence. Additionally, a C-Score > −1.5 supports a model with correct global topology. The RMSD values determines the divergence in angstroms between the modelled protein and its template. Therefore, the obtained HEV RdRp models exhibited a suitable global topology.

The top first templates used by I-TASSER to model the proteins corresponded to the Porcine Aichi virus (Kobuvirus) from the *Picornaviridae* family (6R1I), Norwalk virus (1SH0) and Enterovirus A71 (EV71)-*Picornaviridae* (3N6L).The top first structural analog obtained with I-TASSER for HEV_C1_Uy RdRp corresponded to Coxsackievirus B3 (3CDU).

These models were further validated employing different bioinformatics tools. PROCHECK server, which verified the stereochemical quality of a protein structure, analyzing each residue geometry and the general geometry, showed the best results. Similarly, acceptable Ramachandran plots were observed between the models (86.60%-HEV_C1_Uy and 84.10%-Arkell corresponding to aa in favorable region for torsions and rotations). Moreover, the crystallographic

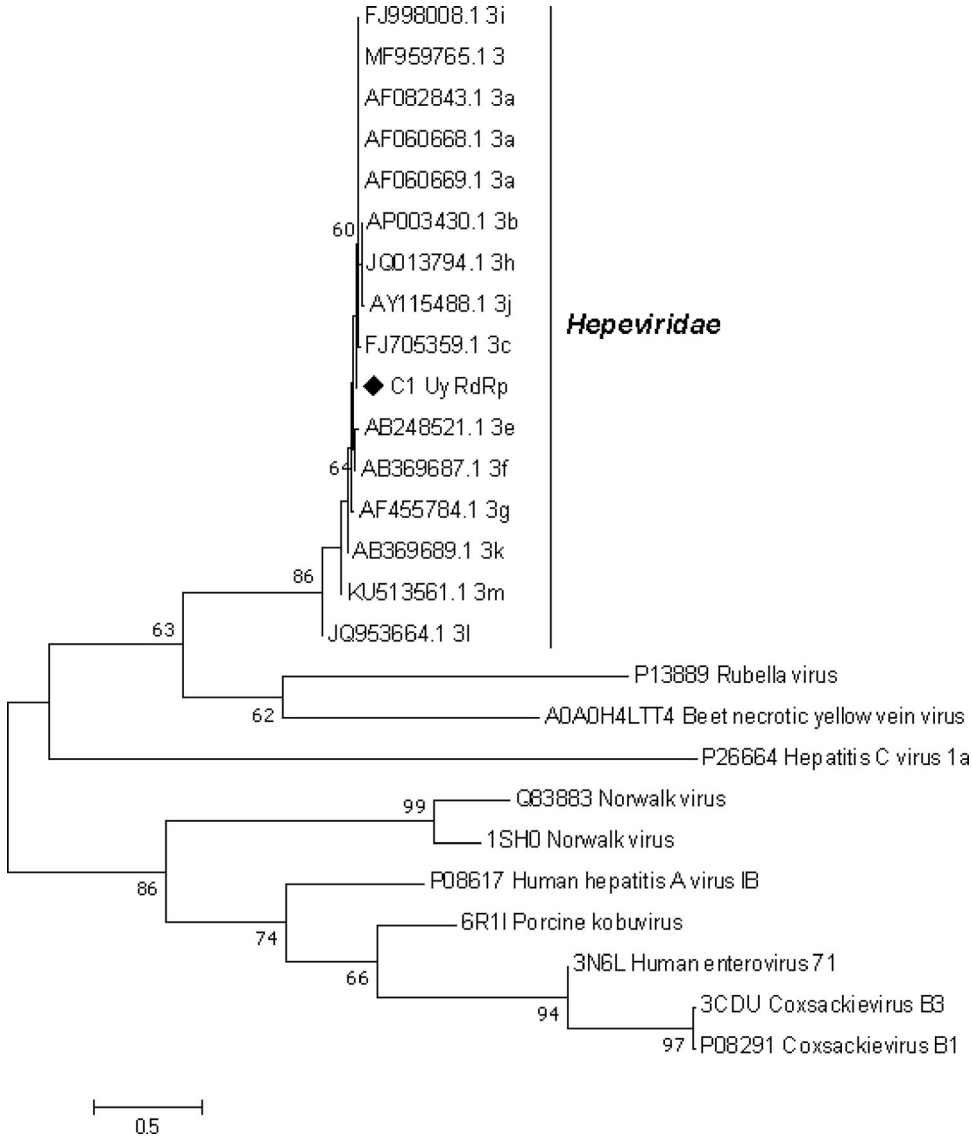

Figure 2. Phylogenetic tree based on the RdRp catalytic site constructed by the Neighbour-Joning method with Poisson model as the substitution model. HEV strain coming from the HEV-SOT recipient (◆) was compared to other viral RdRp. Only bootstrap values >60% are shown.

Table 2. RdRp multiple tests validation scores and structural alignment scores for the different models and templates.

	BIOINFORMATIC TOOL									
MODEL	PROSA (Z SCORE)	RAM PLOT (%)	ERRAT (%)	VERIFY 3D (%)	PROCHECK (%)	TM-ALIGN T1	TM-ALIGN T2	TM-ALIGN T3	TM-ALIGN T4	TM-ALIGN T5
HEV_C1_Uy	−4.22	86.60	79.33	71.87	90.70	0.84	0.76	0.87	0.86	0.88
6RLI (T1)	−9.81	100.00	96.07	96.15	99.80	–	–	–	–	–
1SH0 (T2)	−11.07	99.20	97.13	98.61	99.50	–	–	–	–	–
3CDU (T3)	−9.77	100.00	96.74	95.51	99.80	–	–	–	–	–
HEV Arkell (T4)	−3.19	84.10	62.00	77.41	87.40	0.91	0.77	0.86	–	0.87
3N6L (T5)	−10.06	99.2	93.61	99.78	98.80	–	–	–	–	–

structures used as templates were also validated for comparison. Overall, the two models exhibited acceptable validation values (Table 2).

Additionally, structural alignments between the two models, and between the two models and the templates were carried out. TM-Score for HEV_C1_Uy and HEV Arkell was 0.86, similar values were observed for the PDB templates. The highest TM-Scores registered were 0.88 for HEV_C1_Uy and the Enterovirus A71 and of 0.91 for HEV Arkell and Porcine Aichi virus. TM-Score are in the range of (0, 1], where 1 corresponds to a perfect match between two structures and values greater than 0.5 indicates the same fold. Therefore, all the TM-Scores obtained suggested that the structure of the models and the templates had the same fold. These results reinforce the confidence in the obtained structural models.

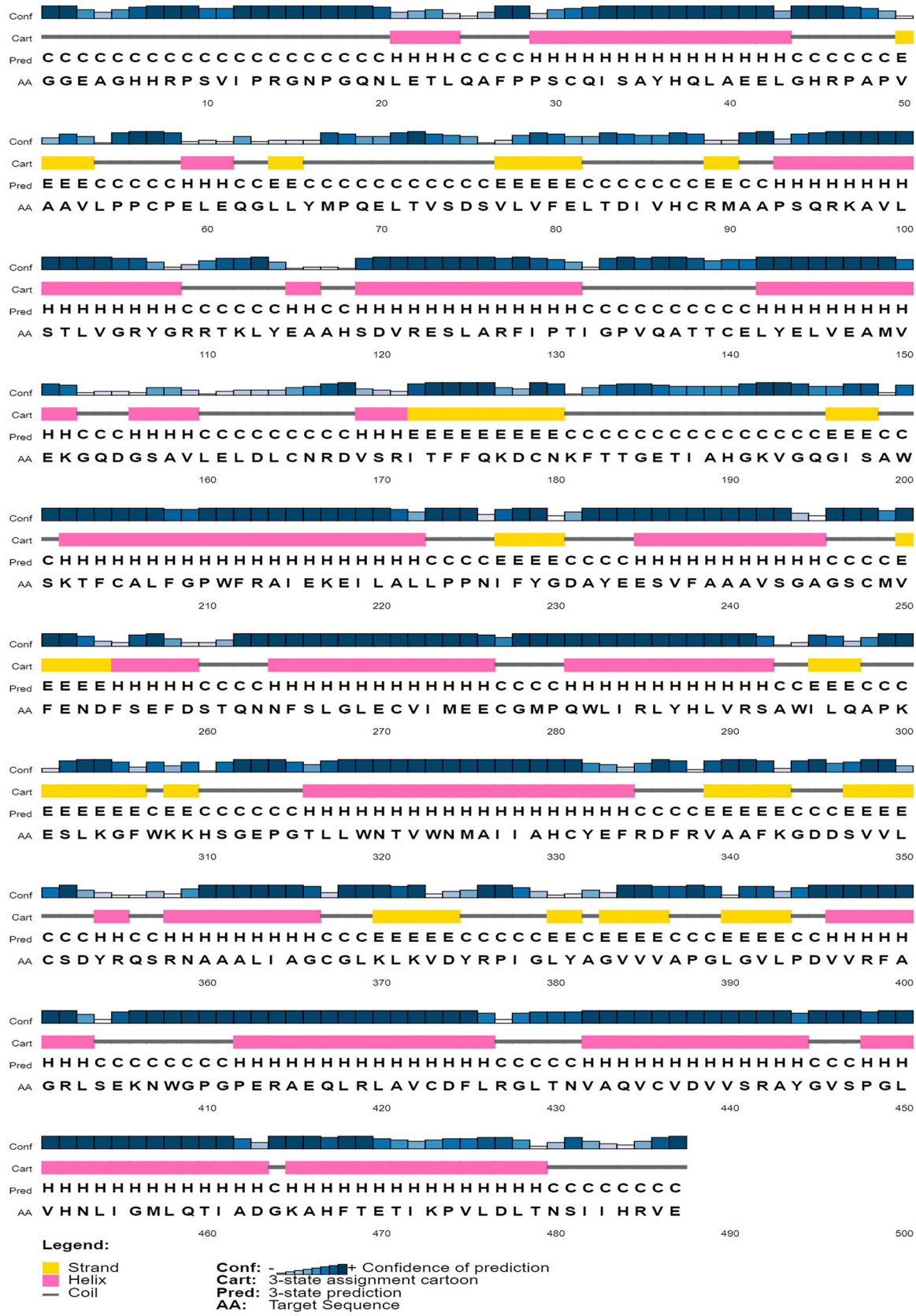

Figure 3. Secondary structure prediction for HEV_C1_Uy RdRp model employing PSIPRED. The Strand, Helix, Coil distribution and its confidence of prediction is shown for each residue throughout the sequence.

The secondary structure prediction chart for the HEV_C1_Uy model exhibited the distribution of the helix, strand and coil throughout the protein sequence and the confidence of prediction for each section (Figure 3).

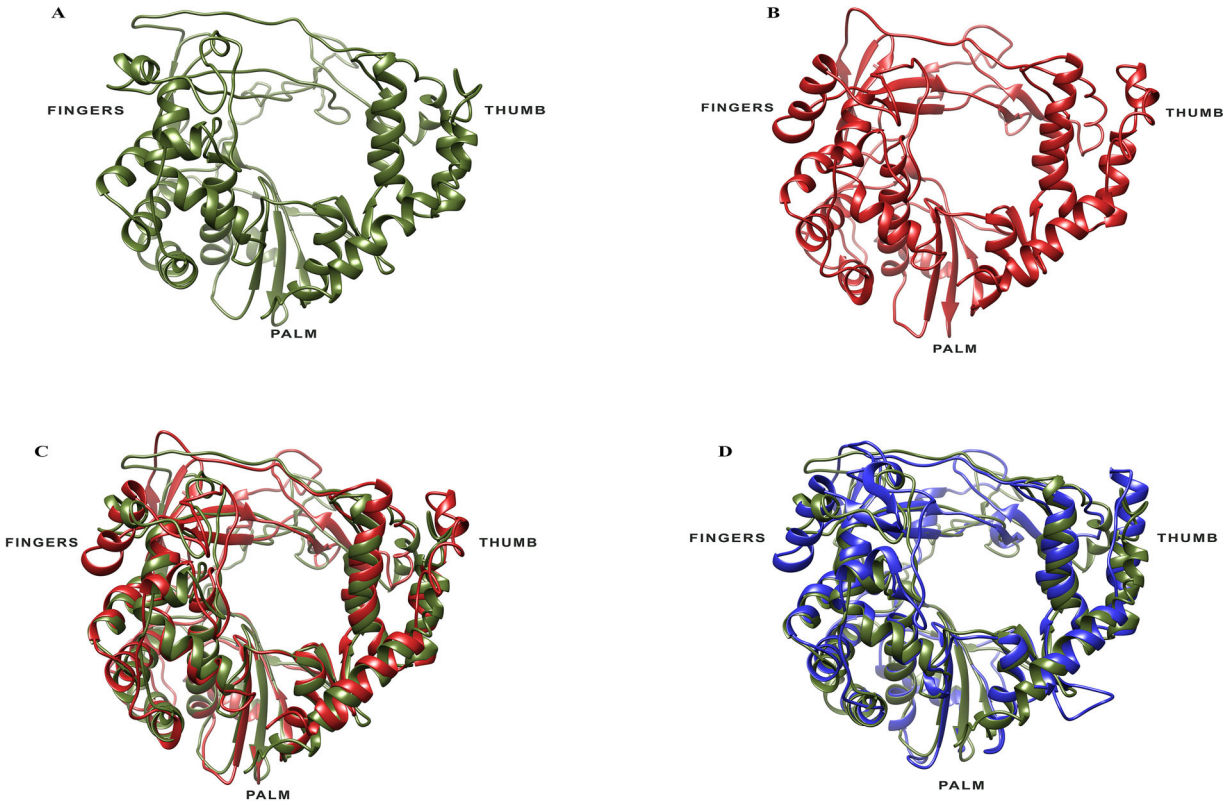

Figure 4. 3D Structural models of HEV RdRp obtained by I-TASSER. A. HEV_C1_Uy RdRp model. B. HEV Arkell RdRp model. C. Structural alignment between HEV_C1_Uy (green) and HEV Arkell (red). D. Structural alignment between HEV_C1_Uy (green) and the top threading template Porcine Aichi virus (Kobivirus) (blue) (PDB: 6R1I). The finger's, thumb and palm domains are indicated in all the models. Graphs were obtained with UCSF Chimera v. 1.8.

The finger's, thumb and palm domains were identified in the 3 D models (Figure 4). Also, the 3 D structural alignment revealed that HEV_C1_Uy and HEV Arkell, as well as HEV_C1_Uy and EV71 had similar structural folding as observed by the TM-align Scores (Figure 4).

3.3. Hev_C1_Uy exhibited very favorable binding affinity with RBVT

Molecular docking studies between RBVT and the modelled RdRp were executed in order to evaluate their interaction interface. HEV_C1_Uy RdRp and the control protein HEV Arkell showed very favorable binding energies with RBVT in AutoDock Vina (-7.6 ± 0.2 Kcal/mol and −8.0 ± 0.1 Kcal/mol, respectively) and LeDock (-8.01 ± 0.18 Kcal/mol and −8.16 ± 0.14 Kcal/mol, respectively) (Table 3). In fact, these values were under the −7.0 Kcal/mol threshold (Chang et al., 2007), and are indicative of a strongly binding ligand; this threshold was defined for a set of diverse antivirals ligands in Auto Dock against Human Immunodeficiency Virus (HIV). The interactions were mediated by 6 hydrogen bonds (H-bond) in the case of HEV_C1_Uy involving residues Q195-O14, S198-O11, E257-O13, S260-O2, O3, S311-O11 and 9 H-bonds for HEV Arkell. The closest distance between atoms of RBVT and HEV_C1_Uy was of 2.88 Å and the more distant one was of 3.07 Å (Figure 5).

The GTP interaction used as control showed the best binding affinity for HEV_C1_Uy. On the other hand, in HEV Arkell the most favorable interaction for AutoDock Vina corresponded to RBVT. However, according to LeDock the best score obtained was for GTP. Furthermore, the negative control (CIN) exhibited a weak binding energy (-5.0 ± 0 Kcal/mol and −2.99 ± 0.03 Kcal/mol with AutoDock Vina and LeDock, respectively), indicating a non-specific interaction. Unphosphorylated RBV was also evaluated by molecular docking as control, (data not shown), though further 3 D interaction analyses were carried out with RBVT, since it is the active form for RdRp interaction.

Additionally, since the residues for HCV and rNTP H-bond interaction have been previously identified (Bressanelli et al., 2002), through sequence alignment we extrapolated them to HEV_C1_Uy RdRp to carry out RBVT docking studies in those sites for comparison purposes. The analog sites HEV-HCV were: S367-Q262, R386-R291, R394-G305 and T390-E301. Highly similar favorable binding affinity was observed (-7.7 ± 0.2 Kcal/mol for RBVT with AutoDock Vina) compared to the previously mentioned molecular docking with the Peptimap prediction sites (-7.6 ± 0.2 Kcal/mol). The interaction of RBVT-HEV_C1_Uy in this case was mediated by 7 H-bonds, I197-N4, S198-O14, N4, S260-O4, K309-O12, O13, S311-O13, with 2.82 Å and 3.08 Å as the closest and furthest distance between atoms, respectively. Several interacting amino acids are the same that those observed with Peptimap sites.

3.4. Molecular dynamics simulation analysis

To a large degree, MM/PBSA results are in agreement with the docking results. For CIN, the estimated free binding

Table 3. Molecular mechanics Poisson-Boltzmann surface area (MM/PBSA) values and docking scores obtained with Auto Dock Vina and LeDock for Ribavirin triphosphate (RBVT), 7-methyl-guanosine-5′-triphosphate (GTP) and Cinnamaldehyde (CIN) with HEV_C1_Uy RdRp and HEV Arkell RdRp.

HEV_C1_Uy RdRp					LigPlot+ (Panda et al., 1995)			Poseview (Panda et al., 1995)
	Ligand	AutoDock Vina binding energy (kcal/mol) (Emerson & Purcell, 2003)	LeDock binding energy (kcal/mol) (Emerson & Purcell, 2003)	MM/PBSA (Khuroo & Khuroo, 2008) (Kcal/mol)	Number of H-bonds	H-bonds	H-bonds distance (Å)	H-bonds
	RBVT	−7.6 ± 0.2	−8.01 ± 0.18	31.26 ± 16.81	6		3.03	
						Q195-O14	2.97	E257
						S198-O11	2.97	S260
						E257-O13	2.82, 3.07	S311
						S260-O2, O3	2.88	
						S311-O11		
	GTP	−8.3 ± 0.3	−8.13 ± 0.20	5.38 ± 12.69	2		2.90	E257
						S198-O6	3.11	S260
						S311-O6		S198
								S311
	CIN	−5.0 ± 0	−2.83 ± 0	−7.65 ± 4.16	–	–	–	–
HEV Arkell RdRp	RBVT	−8.0 ± 0.1	−8.16 ± 0.14	–	9	H6-O7	3.05	H6
						M67-O12	2.96	K177
						Q69-O12	3.26	Q195
						E70-O12	3.13	S198
						K177-O3	3.06	
						Q195-O3	3.05	
						G196-O10	3.24	
						S198-O7	2.95	
						K309-O9	3.01	
	GTP	−7.9 ± 0.2	−8.41 ± 0.18	–	3	H6-013	2.87	H6
						S311-O6, O9	3.14, 3.31	Q195
								S198
								K309
								S311
	CIN	−5.0 ± 0	−2.99 ± 0.03	–	–	–	–	–

[1] Docking binding energy scores were calculated over 5 runs. Errors represent the standard deviation of the mean.
[2] Errors represent the standard deviation.
[3] LigPlot + results were selected for the 3 D analysis.

energy to HEV_C1_Uy RdRp is in the expected range (-7.65 ± 4.16 kcal/mol) when standard deviation (SD) values are taken into account. For GTP, when taken together with a considerable SD value, the free binding energy estimate confirms expectations (5.38 ± 12.69 kcal/mol). As for RBVT, the MM/PBSA results predict a binding affinity of 31.26 ± 16.81 kcal/mol to HEV_C1_Uy RdRp.

All simulations reached equilibrium states (Figure 6 A-C). Little fluctuation was seen in the residues, except for the range 50-200 (which contains the residues that form the binding pocket and some flexible loops) and, as would be expected, the termini (Figure 6 D-F).

4. Discussion

Chronic hepatitis E in SOT recipients and immunocompromised individuals, frequently associated to severe extrahepatic manifestations, is a disease of major concern in high-income and non-endemic countries where HEV3 is prevalent. In the last few years, product of a sharp increment of HEV cases and an improvement of the diagnosis, many aspects of chronic HEV infection have been uncovered and much more information is now available (Sayed et al., 2015). In this clinical setting, antiviral treatment with RBV, the only approved drug to treat HEV infection, is the main option since the risk of acute rejection prevents the use of pegylated interferon alpha as a therapeutic option (Kamar et al., 2010; 2014; Pischke et al., 2013). In fact, RBV administered for at least 3 months has shown favorable outcomes with confirmed efficacy in acute and chronic HEV cases (Gerolami et al., 2011; Kamar et al., 2010; 2014; Mallet et al. 2010).

Unfortunately, though significant advances have been achieved in terms of cell-culture isolation of HEV (Shukla et al., 2011; Tanaka et al., 2007) the lack of an efficient and standardized model has hampered the study of HEV viral cycle and therefore prevented the comprehension of the antiviral mechanisms of action, of RBV. Viral RdRp is believed to interact with RBV, though the molecular details of HEV-RBV interaction have not been identified yet. Remarkably, no HEV RdRp enzyme have been crystallized and the likely ligand-binding pocket for nucleotides or any other molecule is not known. This contrast with other viral RdRp which have been co-crystallized with nucleoside triphosphates or oligonucleotides to map the substrate-binding sites, as reported for HCV-rNTPs complex (Bressanelli et al., 2002). Hence, *in silico* computational approaches, which are widely employed to predict and evaluate molecule-target interactions for drug discovery (Lavecchia & Cerchia, 2016; Hodos et al., 2016),

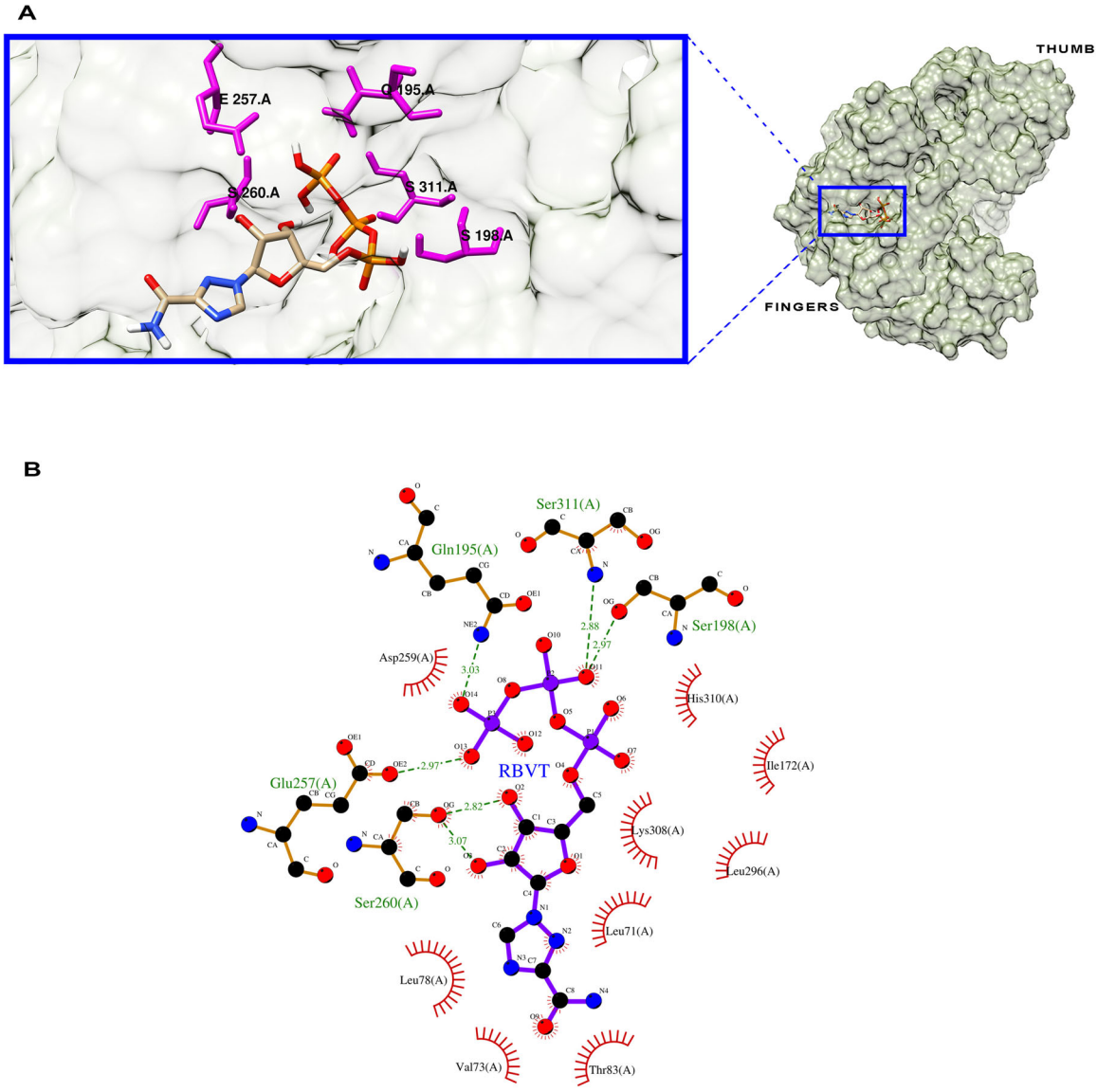

Figure 5. Molecular docking analysis between HEV_C1_Uy RdRp and RBVT. A. 3D interaction of the HEV RdRp with ligand RBVT in the defined finger's-palm domains binding pocket. Hydrogen-bonds interacting residues are indicated in purple with single-letter amino acid code. Graphs were obtained with UCSF Chimera v. 1.8. B. 2 D diagram of the HEV RdRp-RBVT showing the residues forming hydrogen-bonds and the distance between atoms, employing LigPlot + v. 4.5.3.

might be an useful tool for afford this knowledge gap. Structural studies on replicative complexes of RdRp and NTPs or analogs are currently needed to better understand the enzymes low copying fidelity and the mutagenic activity of the analogs on the viral replication (Ferrer-Orta et al., 2007).

In this work, we pursued two goals. First, to model *in silico* the HEV3 RdRp protein of a HEV chronic strain and second, to perform a detailed molecular docking study and molecular dynamics simulations, with the aim to identify the interacting domain of the viral enzyme and its binding affinity with the drug RBV.

Herein, we report a complete HEV RdRp sequence (HEV_C1_Uy), corresponding to a LT patient chronically infected with HEV3. The patient had been successfully treated with RBV in a 9-weeks course, and had an SVR during the 24 months follow-up. Sequence analysis identified the HEV_C1_Uy catalytic site corresponding to the region spanning residues 248 to 359. This catalytic site showed elevated sequence divergence among virus families, being the highest aa percentage identity observed with BNYVV and RUBV (29.8%-26.6%, respectively). These results support the notion that these viruses constitute a distinct monophyletic group in the "alpha-like" supergroup of positive-strand RNA viruses (Koonin et al., 1992). However, HEV3 strains formed a separate independent cluster from the RUBV and BNYVV group in the phylogenetic group reconstruction.

RNA and DNA polymerases share a basic structure, where RdRp are more similar to each other than to other different polymerases. There is almost no detectable sequence similarity between viral RdRps with the exception of some conserved motifs (Bruenn, 1993; Butcher et al., 2001). Indeed, this was the case with HEV and other virus, since sequence alignments needed to be performed including only the catalytic site due to the extreme divergence observed. Interestingly, all these diverse viruses have two conserved motifs, D-x(4,5)-D and GDD. It has been shown, that *in vitro*

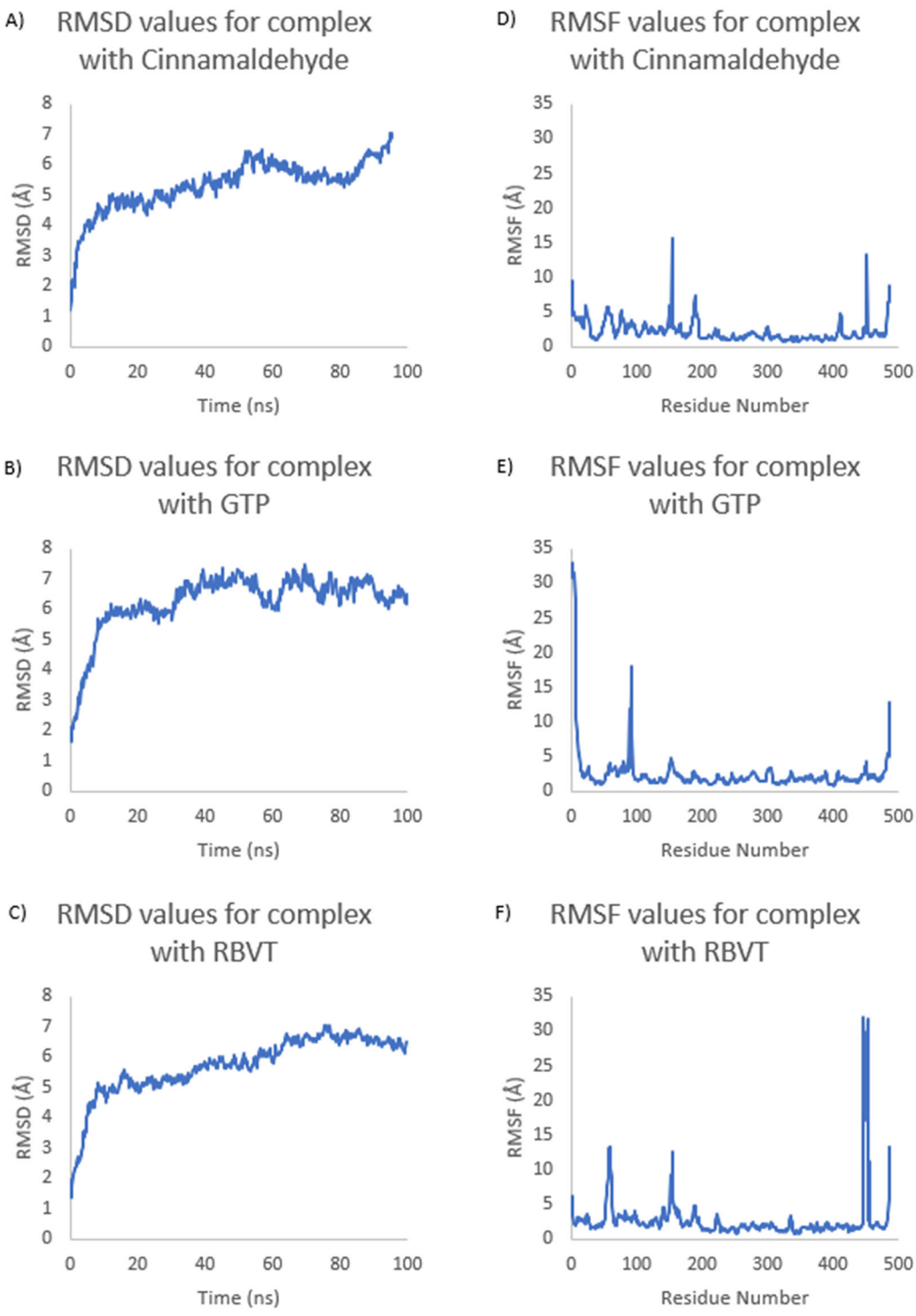

Figure 6. The RMSD and RMSF analysis of the MD trajectories. A – C. RMSD values expressed in Angstroms for the whole duration of the MD simulation for the complexes containing Cinnamaldehyde, GTP, and RBVT respectively. D – F. RMSF values expressed in Angstroms for the whole duration of the MD simulation and all the protein residues of complexes containing Cinnamaldehyde, GTP, and RBVT respectively. RMSD values were calculated for the protein backbone while RMSF values were calculated for Cα atoms of each residue.

substitutions in the GDD motif abolished the RdRp activity of HEV (Emerson et al., 2004), HCV (Yamashita et al., 1998), RUBV (Wang & Gillam, 2001), calicivirus (Vázquez et al., 2000) and poliovirus (Jablonski & Morrow, 1995). Thus, the GDD motif plays a crucial role in the catalytic activity and metal ion coordination (Oh et al., 1999; Qin et al., 2001), which could therefore explain its conservation among a wide range of RdRps.

On the other hand, there is enough sequence conservation in order to perform alignments and identify motifs within some viral families (Bruenn, 1993). Certainly, this was observed for HEV and RUBV alignment, where eight

conserved motifs (I-VIII) associated to positive-strand viral RNA RdRps were successfully identified. Furthermore, sequence comparison between HEV_C1_Uy with HEV genotypes and HEV3 subtypes revealed several differences, where few unique (V/I1220A) and infrequent substitutions (T/A1608V, V1659A and Q1700H) were observed. Single nucleotide variants at protein level have been reported to be less abundant at ligand binding sites and less rare variants were found to be located apart from enzyme active sites, resulting in moderate changes of the physic-chemical properties of the aa (Yamada et al., 2016). Moreover, it has been reported that mutations in the functional sites would alter the enzyme's catalytic activity, even mutations with no significant effects can modify the affinity of protein-drug interactions (Ma & Lu, 2011). Current *in vitro* research is being conducted to address if these HEV_C1_Uy substitutions, which were distantly located from the catalytic site, are involved in RBV sensitivity or in the enzymatic activity. Debing et al. (Debing et al., 2016) reported three substitutions likely associated to RBV resistance (Y1320H, K1383N and G1634R) located outside the catalytic site. Additionally, other substitutions have been reported in HEV infected patients (D1384G, K1398R, V1479I, Y1587F), which were suggested to be replication competent and to possibly affect the HEV replication by modulating the RdRp activity (Debing et al., 2014; 2016; Todt et al., 2016). Recently, substitutions mutants C1483W and N1530T isolated from HEV acute liver failure patients have been strongly associated to high viral load and mortality (Mishra et al., 2013).

Notably, a RdRp substitution was reported (F1439Y) to be significantly associated to HEV fulminant liver failure patients (Smith & Simmonds, 2015). Among the reported substitutions, HEV_C1_Uy RdRp presented F1439Y (F233Y in HEV_C1_Uy RdRp) and V1479I (V273I). The V1479I substitution has been previously reported in chronic HEV-SOT patients exhibiting RBV resistance, suggesting that this substitution could modulate the RdRp activity (Todt et al., 2016).

Interestingly, the HEV3 Arkell swine strain selected for modelling and docking comparison, presented the G1634R and the F1439Y substitutions.

Moreover, RBV has been suggested to act as a mutagen in patients chronically infected with HCV (Asahina et al., 2005). Several studies showed that *in vitro* growing of poliovirus (*Picornaviridae*) in the presence of RBVT promotes the selection of the mutant G64S, that showed a lower affinity to RBVT, thus increasing template copying fidelity (Arnold et al., 2005; Castro et al., 2005; Pfeiffer & Kirkegaard, 2003; Vignuzzi et al., 2005). Furthermore, it has been demonstrated that the G64R, G64T and S264L substitutions confer RBV resistance in EV71 by increasing the RdRp replication fidelity (Sadeghipour et al., 2013). Therefore, RBV may indeed exert its antiviral activity through a mutagenic effect also for HEV (Graci & Cameron, 2002; 2006; Parker, 2005), as it has been reported that RBV increases HEV quasispecies heterogeneity (Debing et al., 2014; 2016; Lhomme et al., 2015; Todt et al., 2016).

Validated HEV3 C1 Uy RdRp and HEV Arkell models were obtained through bioinformatics *de novo* strategies. These models exhibited a correct global topology and share the same folding with a high structural alignment score (0.91).

Previous reports have demonstrated that it is possible to acquire a reliable 3 D RdRp model *in silico*, even when there is low sequence identity with modelling templates (Vlachakis et al., 2013). The widely employed I-TASSER server is a powerful platform based on sequence-to-structure-to-function prediction paradigm, where the software first generates three-dimensional atomic models from multiple threading alignments and iterative structural assembly simulation. The threading methodology is used for identifying template proteins from solved structure databases that have a similar structure or similar structural motifs (Roy et al., 2010).

RdRps share a similar overall structure with the finger's, thumb and palm domain arranged in a cupped right-hand configuration, with an N-terminal domain bridging the finger's and thumb region (Ng et al., 2008), which were successfully identified in the HEV models.

Molecular docking analysis for RBVT with HEV_C1_Uy and HEV Arkell revealed a favorable binding affinity under the established threshold (-7.0 Kcal/mol) (Chang et al., 2007), with similar good values observed for the GTP control. The RBVT interactions were mediated by 6 H-bond for HEV_C1_Uy (Q195-O14, S198-O11, E257-O13, S260-O2, O3, S311-O11) and 9 H-bonds for HEV Arkell (H6-O7, M67-O12, Q69-O12, E70-O12, K177-O3, Q195-O3, G196-O10, S198-O7, K309-O9). These interaction sites were very similar between both models since similar regions were identified as best candidates for docking by Peptimap and were found to be buried between the finger's-palm domains of the HEV RdRp. Notably, the GTP binding region was located within the same interacting site for RBVT in the HEV models, suggesting that this is the region that could directly interact with incoming nucleotides or analogs.

The RdRp structure of poliovirus (*Picornaviridae*) has a N-terminal glycine residue buried in a pocket at the base of the finger's domain, forming 4 H-bonds that reposition the catalytic residue Asp238 into the active site (palm domain). The Asp238 residue was then able to establish a long H-bond interaction (2.8 Å) with the 2'OH of the incoming rNTP, as part of a flexible interdomain linker, a common molecular mechanism to most picornaviruses (Campagnola et al., 2008; Thompson & Peersen, 2004). A similar atom distance was obtained for RBVT-HEV_C1_Uy (2.82-3.07 Å). Indeed, HEV_C1_Uy and EV71 (*Picornaviridae*) exhibited the best structural alignment score, as well as HEV Arkell and Porcine Aichi virus, another *Picornaviridae* family member.

Substitutions V/I1220A, T/A1608V, V1659A and Q1700H identified in HEV_C1_Uy, occur in the finger's, thumb, thumb and in the protruding coil-thumb domain, respectively, while the substitutions F233Y and V273I were located in the bridge thumb-palm domain and in the finger's domain, respectively. These positions and particularly the domains where they are located were described in several viral families. To gain insight into the mutational effect of RBV, the X-ray structure of the foot-and-mouth disease virus (FMVD) (*Picornaviridae*) with natural substrates (ATP, UTP) and RBV had been obtained and reported (Ferrer-Orta et al., 2007). It was shown

that the loop β9-α11 of the finger's domain, can be flexible and necessary to adapt its conformation and interactions to the size and shape of the incoming nucleotides and, additionally, it contains the M296I substitution found in RBV resistant FMDV strains (Ferrer-Orta et al., 2007). Conversely, the HCV 3 D RdRp modelling revealed that the F415Y RBV resistant variant is located at the P helix region of the thumb domain, which is suggested to interact with the minor groove of the template-primer duplex in the putative-RNA binding site (Young et al., 2011). Furthermore, HCV-rNTPs reported binding sites (Bressanelli et al., 2002) were close to the RBV interaction region in our HEV models, with favorable docking simulation scores.

To explore into the stability of the HEV_C1_Uy-ligand complexes, further analysis was performed by a 100 ns MD simulation. The binding free energy calculations by MM/PBSA confirmed the previous docking results obtained for GTP and CIN taking the SD values into consideration. However, the MM/PBSA results for RBVT did not correspond to the favorable binding affinity observed by molecular docking. This observation is very interesting and raises additional questions concerning the role of selected mutations in the RBV antiviral activity. One explanation of this result might be that the HEV_C1_Uy strain presents several unique and infrequent substitutions in the RdRp protein (V/I1220A, T/A1608V, V1659A and Q1700H), as well as one associated with fulminant liver failure (F1439Y) and one identified in RBV resistant patients (V1479I), suggested to be involved in RdRp activity modulation. Therefore, this rare combination of substitutions might affect the binding stability of RBVT-HEV_C1_Uy complex. Particularly, the presence of the substitution V/I1220A, not previously reported in an HEV-RdRp, was located within the RBVT binding-pocket analyzed, which could then alter this complex binding affinity. Further reverse genetics-based *in vitro* research will be needed to shed light on this issue.

On the other hand, the MD force field may not represent the highly polar phosphate groups well, as for instance, it takes no account of the possibility of different ionization states or dynamic polarization effects induced by the interacting protein groups. MD simulations are also heavily dependent on the initial ligand conformation, so even a slight difference in ligand conformation would affect the binding affinity values (Durrant & McCammon, 2011; Perez-Aguilar et al., 2014).

In summary, by using a bioinformatics approach, we obtained the first acceptable models of HEV RdRp belonging to a viral strain isolated from a chronically infected patient and the reference HEV3 Arkell swine strain, in order to perform molecular docking studies and MD simulations with RBVT.

Results described here showed that RBVT could bind to the HEV3 RdRp finger's-palm domains, and the possible interaction site and H-bonds involved are described in detail. We also showed that RBVT and GTP might share the same binding site in the RdRp, suggesting that this could be the interacting region for incoming nucleotides or analogs. However, MM/PBSA results differed from the binding affinities obtained by molecular docking for the reasons previously mentioned.

Even tough additional research efforts should be performed *in vitro* aimed to corroborate all these data, our findings will contribute to better understand the mechanism of action of RBV in HEV RdRp, and therefore, this validated model could be an useful tool for the development of new potential HEV antiviral drugs on a rational basis by inferring the possible ligand-target interaction.

Disclosure statement

The authors declare that there are no conflicts of interest.

Funding

This work was supported by the Comisión Sectorial de Investigación Científica-UdelaR, under grant [CSIC I + D 2018 #245]. F.C. PhD fellowship by Comisión Académica de Posgrado-UdelaR. The funders had no role in the design of the study; in the collection, analyses, or interpretation of data; in the writing of the manuscript, or in the decision to publish the results.

Author contributions

Conceptualization, C.Q-G and F.C.; methodology, F.C., S.R-M., Y.P., R.P., D.R.H; software, F.C., S.R-M. D.R.H., G.G.; validation, F.C. and S.R-M.; formal analysis, F.C., S.R-M., C.Q-G. D.R.H., G.G and S.M.,; investigation, F.C.; S.M.; resources, S.M.; data curation, Y.P., R.P.; writing—original draft preparation, F.C.; writing—review and editing, C.Q-G., S.R-M., Y.P., R.P., D.R.H., G.G. and S.M.; visualization, F.C., S.M.; supervision, C.Q-G. and S.M.; project administration, S.M, J.A.; funding acquisition, S.M. and J.A. All authors have read and agreed to the published version of the manuscript.

Ethical approval

The study was approved by the Ethics Committee from the Hospital Central de las Fuerzas Armadas.

Ethical approval number 07/CE/19.

Informed consent

The patient gave written informed consent

References

Andrei, G., & De Clercq, E. (1993). Molecular approaches for the treatment of hemorrhagic fever virus infections. *Antiviral Research*, *22*(1), 45–75. https://doi.org/10.1016/0166-3542(93)90085-w

Arends, J. E., Ghisetti, V., Irving, W., Dalton, H. R., Izopet, J., Hoepelman, A. I. M., & Salmon, D. (2014). Hepatitis E: An emerging infection in high income countries. *Journal of Clinical Virology : The Official Publication of the Pan American Society for Clinical Virology*, *59*(2), 81–88. https://doi.org/10.1016/j.jcv.2013.11.013

Arnold, J. J., Vignuzzi, M., Stone, J. K., Andino, R., & Cameron, C. E. (2005). Remote site control of an active site fidelity checkpoint in a viral RNA-dependent RNA polymerase. *The Journal of Biological Chemistry*, *280*(27), 25706–25716. https://doi.org/10.1074/jbc.M503444200

Asahina, Y., Izumi, N., Enomoto, N., Uchihara, M., Kurosaki, M., Onuki, Y., Nishimura, Y., Ueda, K., Tsuchiya, K., Nakanishi, H., Kitamura, T., & Miyake, S. (2005). Mutagenic effects of ribavirin and response to interferon/ribavirin combination therapy in chronic hepatitis C. *Journal of Hepatology* , *43*(4), 623–629. https://doi.org/10.1016/j.jhep.2005.05.032

Baker, N. A., Sept, D., Joseph, S., Holst, M. J., & McCammon, J. A. (2001). Electrostatics of nanosystems: application to microtubules and the ribosome. *Proceedings of the National Academy of Sciences of the United States of America*, *98*(18), 10037–10041. https://doi.org/10.1073/pnas.181342398

Bressanelli, S., Tomei, L., Rey, F. A., & De, F. R. (2002). Structural Analysis of the Hepatitis C Virus RNA Polymerase in Complex with Ribonucleotides. *Journal of Virology*, *76*(7), 3482–3492. https://doi.org/10.1128/jvi.76.7.3482-3492.2002

Bruenn, J. A. (1993). A closely related group of RNA-dependent RNA polymerases from double-stranded RNA viruses. *Nucleic Acids Research*, *21*(24), 5667–5669. https://doi.org/10.1093/nar/21.24.5667

Bruenn, J. A. (2003). A structural and primary sequence comparison of the viral RNA-dependent RNA polymerases. *Nucleic Acids Research*, *31*(7), 1821–1829. https://doi.org/10.1093/nar/gkg277

Butcher, S. J., Grimes, J. M., Makeyev, E. V., Bamford, D. H., & Stuart, D. I. (2001). A mechanism for initiating RNA-dependent RNA polymerization. *Nature*, *410*(6825), 235–240. https://doi.org/10.1038/35065653

Cameron, C. E., & Castro, C. (2001). The mechanism of action of ribavirin: Lethal mutagenesis of RNA virus genomes mediated by the viral RNA-dependent RNA polymerase. *Current Opinion in Infectious Diseases*, *14*(6), 757–764.

Campagnola, G., Weygandt, M., Scoggin, K., & Peersen, O. (2008). Crystal structure of coxsackievirus B3 3Dpol highlights the functional importance of residue 5 in picornavirus polymerases. *Journal of Virology*, *82*(19), 9458–9464. https://doi.org/10.1128/JVI.00647-08

Cassidy, L. F., & Patterson, J. L. (1989). Mechanism of La Crosse virus inhibition by ribavirin. *Antimicrobial Agents and Chemotherapy*, *33*(11), 2009–2011. https://doi.org/10.1128/AAC.33.11.2009

Castro, C., Arnold, J. J., & Cameron, C. E. (2005). Incorporation fidelity of the viral RNA-dependent RNA polymerase: a kinetic, thermodynamic and structural perspective. *Virus Research*, *107*(2), 141–149. https://doi.org/10.1016/j.virusres.2004.11.004

Chang, M. W., Lindstrom, W., Olson, A. J., & Belew, R. K. (2007). Analysis of HIV wild-type and mutant structures via in silico docking against diverse ligand libraries. *Journal of Chemical Information and Modeling*, *47*(3), 1258–1262. https://doi.org/10.1021/ci700044s

Colovos, C., & Yeates, T. O. (1993). Verification of protein structures: Patterns of nonbonded atomic interactions. *Protein Science : a Publication of the Protein Society*, *2*(9), 1511–1519. https://doi.org/10.1002/pro.5560020916

Contreras, A. M., Hiasa, Y., He, W., Terella, A., Schmidt, E. V., & Chung, R. T. (2002). Viral RNA mutations are region specific and increased by ribavirin in a full-length hepatitis C virus replication system. *Journal of Virology*, *76*(17), 8505–8517. https://doi.org/10.1128/jvi.76.17.8505-8517.2002

Crotty, S., & Andino, R. (2002). Implications of high RNA virus mutation rates: lethal mutagenesis and the antiviral drug ribavirin. *Microbes and Infection*, *4*(13), 1301–1307. https://doi.org/10.1016/S1286-4579(02)00008-4

Crotty, S., Cameron, C. E., & Andino, R. (2001). RNA virus error catastrophe: direct molecular test by using ribavirin. *Proceedings of the National Academy of Sciences of the United States of America*, *98*(12), 6895–6900. https://doi.org/10.1073/pnas.111085598

Crotty, S., Maag, D., Arnold, J. J., Zhong, W., Lau, J. Y., Hong, Z., Andino, R., & Cameron, C. E. (2000). The broad-spectrum antiviral ribonucleoside ribavirin is an RNA virus mutagen. *Nature Medicine*, *6*(12), 1375–1379. https://doi.org/10.1038/82191

Cummings, K. J., Lee, S. M., West, E. S., Cid-Ruzafa, J., Fein, S. G., Aoki, Y., Sulkowski, M. S., & Goodman, S. N. (2001). Interferon and ribavirin vs interferon alone in the re-treatment of chronic hepatitis C previously nonresponsive to interferon: A meta-analysis of randomized trials. *Jama*, *285*(2), 193–199. https://doi.org/10.1001/jama.285.2.193

Day, C. W., Smee, D. F., Julander, J. G., Yamshchikov, V. F., Sidwell, R. W., & Morrey, J. D. (2005). Error-prone replication of West Nile virus caused by ribavirin. *Antiviral Research*, *67*(1), 38–45. https://doi.org/10.1016/j.antiviral.2005.04.002

De Clercq, E. (2004). Antiviral drugs in current clinical use. *Journal of Clinical Virology : The Official Publication of the Pan American Society for Clinical Virology*, *30*(2), 115–133. https://doi.org/10.1016/j.jcv.2004.02.009

Debing, Y., Moradpour, D., Neyts, J., & Gouttenoire, J. (2016). Update on hepatitis E virology: Implications for clinical practice. *Journal of Hepatology*, *65*(1), 200–212. https://doi.org/10.1016/j.jhep.2016.02.045

Debing, Y., Gisa, A., Dallmeier, K., Pischke, S., Bremer, B., Manns, M., Wedemeyer, H., Suneetha, P. V., & Neyts, J. (2014). A mutation in the hepatitis E virus RNA polymerase promotes its replication and associates with ribavirin treatment failure in organ transplant recipients. *Gastroenterology*, *147*(5), 1008–1008. https://doi.org/10.1053/j.gastro.2014.08.040

Debing, Y., Ramière, C., Dallmeier, K., Piorkowski, G., Trabaud, M.-A., Lebossé, F., Scholtès, C., Roche, M., Legras-Lachuer, C., de Lamballerie, X., André, P., & Neyts, J. (2016). Hepatitis E virus mutations associated with ribavirin treatment failure result in altered viral fitness and ribavirin sensitivity. *Journal of Hepatology*, *65*(3), 499–508. https://doi.org/10.1016/j.jhep.2016.05.002

Di Bisceglie, A. M., Thompson, J., Smith-Wilkaitis, N., Brunt, E. M., & Bacon, B. R. (2001). Combination of interferon and ribavirin in chronic hepatitis C: re-treatment of nonresponders to interferon. *Hepatology (Baltimore, Md.)*, *33*(3), 704–707. https://doi.org/10.1053/jhep.2001.22346

Ding, Q., Heller, B., Capuccino, J. M. V., Song, B., Nimgaonkar, I., Hrebikova, G., Contreras, J. E., & Ploss, A. (2017). Hepatitis E virus ORF3 is a functional ion channel required for release of infectious particles. *Proceedings of the National Academy of Sciences of the United States of America*, *114*(5), 1147–1152. https://doi.org/10.1073/pnas.1614955114

Drugbank. (2020). https://www.drugbank.ca/.

Durrant, J. D., & McCammon, J. A. (2011). Molecular dynamics simulations and drug discovery. *BMC Biology*, *9*, 71. https://doi.org/10.1186/1741-7007-9-71

Eisenberg, D., Lüthy, R., & Bowie, J. U. (1997). VERIFY3D: assessment of protein models with three-dimensional profiles. *Methods in Enzymology*, *277*, 396–404.

Elfiky, A. A. (2020). Ribavirin, Remdesivir, Sofosbuvir, Galidesivir, and Tenofovir against SARS-CoV-2 RNA dependent RNA polymerase (RdRp): A molecular docking study. *Life Sciences, 253*, 117592. https://doi.org/10.1016/j.lfs.2020.117592

El-Gebali, S., Mistry, J., Bateman, A., Eddy, S. R., Luciani, A., Potter, S. C., Qureshi, M., Richardson, L. J., Salazar, G. A., Smart, A., Sonnhammer, E. L. L., Hirsh, L., Paladin, L., Piovesan, D., Tosatto, S. C. E., & Finn, R. D. (2019). The Pfam protein families database in 2019. *Nucleic Acids Research*, *47*(D1), D427–D432. https://doi.org/10.1093/nar/gky995

Emerson, S. U., & Purcell, R. H. (2003). Hepatitis E virus. *Reviews in Medical Virology*, *13*(3), 145–154. https://doi.org/10.1002/rmv.384

Emerson, S. U., Nguyen, H., Graff, J., Stephany, D. A., Brockington, A., & Purcell, R. H. (2004). In vitro replication of hepatitis E virus (HEV) genomes and of an HEV replicon expressing green fluorescent protein. *Journal of Virology*, *78*(9), 4838–4846. https://doi.org/10.1128/jvi.78.9.4838-4846.2004

Eriksson, B., Helgstrand, E., Johansson, N. G., Larsson, A., Misiorny, A., Norén, J. O., Philipson, L., Stenberg, K., Stening, G., Stridh, S., & Oberg, B. (1977). Inhibition of influenza virus ribonucleic acid polymerase by ribavirin triphosphate. *Antimicrobial Agents and Chemotherapy*, *11*(6), 946–951. https://doi.org/10.1128/AAC.11.6.946

ExPASy-ProtParam Tool. (2020). https://web.expasy.org/protparam/.

Fang, S. Y., & Han, H. (2017). Hepatitis E viral infection in solid organ transplant patients. *Current Opinion in Organ Transplantation*, *22*(4), 351–355. https://doi.org/10.1097/MOT.0000000000000432

Feld, J. J., & Hoofnagle, J. H. (2005). Mechanism of action of interferon and ribavirin in treatment of hepatitis C. *Nature*, *436*(7053), 967–972. https://doi.org/10.1038/nature04082

Fernandez-Larsson, R., & Patterson, J. L. (1990). Ribavirin is an inhibitor of human immunodeficiency virus reverse transcriptase. *Molecular Pharmacology*, *38*(6), 766–770.

Fernandez-Larsson, R., O'Connell, K., Koumans, E., & Patterson, J. L. (1989). Molecular analysis of the inhibitory effect of phosphorylated ribavirin on the vesicular stomatitis virus in vitro polymerase reaction.

Antimicrobial Agents and Chemotherapy, *33*(10), 1668–1673. https://doi.org/10.1128/AAC.33.10.1668

Ferrer-Orta, C., Arias, A., Pérez-Luque, R., Escarmís, C., Domingo, E., & Verdaguer, N. (2007). Sequential structures provide insights into the fidelity of RNA replication. *Proceedings of the National Academy of Sciences of the United States of America*, *104*(22), 9463–9468. https://doi.org/10.1073/pnas.0700518104

Gerolami, R., Moal, V., & Colson, P. (2008). Chronic hepatitis E with cirrhosis in a kidney-transplant recipient. *The New England Journal of Medicine*, *358*(8), 859–860. https://doi.org/10.1056/NEJMc0708687

Gerolami, R., Borentain, P., Raissouni, F., Motte, A., Solas, C., & Colson, P. (2011). Treatment of severe acute hepatitis E by ribavirin. *Journal of Clinical Virology : The Official Publication of the Pan American Society for Clinical Virology*, *52*(1), 60–62. https://doi.org/10.1016/j.jcv.2011.06.004

Graci, J. D., & Cameron, C. E. (2002). Quasispecies, error catastrophe, and the antiviral activity of ribavirin. *Virology*, *298*(2), 175–180. https://doi.org/10.1006/viro.2002.1487

Graci, J. D., & Cameron, C. E. (2006). Mechanisms of action of ribavirin against distinct viruses. *Reviews in Medical Virology*, *16*(1), 37–48. https://doi.org/10.1002/rmv.483

Guu, T. S. Y., Liu, Z., Ye, Q., Mata, D. A., Li, K., Yin, C., Zhang, J., & Tao, Y. J. (2009). Structure of the hepatitis E virus-like particle suggests mechanisms for virus assembly and receptor binding. *Proceedings of the National Academy of Sciences of the United States of America*, *106*(31), 12992–12997. https://doi.org/10.1073/pnas.0904848106

Hodos, R. A., Kidd, B. A., Shameer, K., Readhead, B. P., & Dudley, J. T. (2016). In silico methods for drug repurposing and pharmacology. *Wiley Interdisciplinary Reviews: Systems Biology and Medicine, 8*(3), 186–210. https://doi.org/10.1002/wsbm.1337

Humphrey, W., Dalke, A., & Schulten, K. (1996). VMD: visual molecular dynamics. *Journal of Molecular Graphics*, *14*(1), 33–38. 27-28,https://doi.org/10.1016/0263-7855(96)00018-5

Jablonski, S. A., & Morrow, C. D. (1995). Mutation of the aspartic acid residues of the GDD sequence motif of poliovirus RNA-dependent RNA polymerase results in enzymes with altered metal ion requirements for activity. *Journal of Virology*, *69*(3), 1532–1539. https://doi.org/10.1128/JVI.69.3.1532-1539.1995

Jagjit Singh, G. K., Ijaz, S., Rockwood, N., Farnworth, S. P., Devitt, E., Atkins, M., Tedder, R., & Nelson, M. (2013). Chronic Hepatitis E as a cause for cryptogenic cirrhosis in HIV. *The Journal of Infection*, *66*(1), 103–106. https://doi.org/10.1016/j.jinf.2011.11.027

Jones, D. T. (1999). Protein secondary structure prediction based on position-specific scoring matrices. *Journal of Molecular Biology*, *292*(2), 195–202. https://doi.org/10.1006/jmbi.1999.3091

Kamar, N., Garrouste, C., Haagsma, E. B., Garrigue, V., Pischke, S., Chauvet, C., Dumortier, J., Cannesson, A., Cassuto-Viguier, E., Thervet, E., Conti, F., Lebray, P., Dalton, H. R., Santella, R., Kanaan, N., Essig, M., Mousson, C., Radenne, S., Roque-Afonso, A. M., Izopet, J., & Rostaing, L. (2011). Factors associated with chronic hepatitis in patients with hepatitis E virus infection who have received solid organ transplants. *Gastroenterology*, *140*(5), 1481–1489. https://doi.org/10.1053/j.gastro.2011.02.050

Kamar, N., Izopet, J., Tripon, S., Bismuth, M., Hillaire, S., Dumortier, J., Radenne, S., Coilly, A., Garrigue, V., D'Alteroche, L., Buchler, M., Couzi, L., Lebray, P., Dharancy, S., Minello, A., Hourmant, M., Roque-Afonso, A.-M., Abravanel, F., Pol, S., Rostaing, L., & Mallet, V. (2014). Ribavirin for chronic hepatitis E virus infection in transplant recipients. *The New England Journal of Medicine*, *370*(12), 1111–1120. https://doi.org/10.1056/NEJMoa1215246

Kamar, N., Rostaing, L., Abravanel, F., Garrouste, C., Lhomme, S., Esposito, L., Basse, G., Cointault, O., Ribes, D., Nogier, M. B., Alric, L., Peron, J. M., & Izopet, J. (2010). Ribavirin therapy inhibits viral replication on patients with chronic hepatitis e virus infection. *Gastroenterology*, *139*(5), 1612–1618. https://doi.org/10.1053/j.gastro.2010.08.002

Khuroo, M. S., & Khuroo, M. S. (2008). Hepatitis E virus. *Current Opinion in Infectious Diseases*, *21*(5), 539–543.

Koonin, E. V., Gorbalenya, A. E., Purdy, M. A., Rozanov, M. N., Reyes, G. R., & Bradley, D. W. (1992). Computer-assisted assignment of functional domains in the nonstructural polyprotein of hepatitis E virus: delineation of an additional group of positive-strand RNA plant and animal viruses. *Proceedings of the National Academy of Sciences of the United States of America*, *89*(17), 8259–8263. https://doi.org/10.1073/pnas.89.17.8259

Krilov, L. R. (2001). Respiratory syncytial virus: Update on infection, treatment, and prevention. *Current Infectious Disease Reports*, *3*(3), 242–246. https://doi.org/10.1007/s11908-001-0026-3

Kumar, S., Stecher, G., & Tamura, K. (2016). MEGA7: Molecular evolutionary genetics analysis version 7.0 for bigger datasets. *Molecular Biology and Evolution*, *33*(7), 1870–1874. https://doi.org/10.1093/molbev/msw054

Laskowski, R. A., MacArthur, M. W., Moss, D. S., & Thornton, J. M. (1993). PROCHECK: a program to check the stereochemical quality of protein structures. *Journal of Applied Crystallography*, *26*(2), 283–291. https://doi.org/10.1107/S0021889892009944

Lavecchia, A., & Cerchia, C. (2016). In silico methods to address polypharmacology: Current status, applications and future perspectives. *Drug Discovery Today*, *21*(2), 288–298. https://doi.org/10.1016/j.drudis.2015.12.007

Lavi, A., Ngan, C. H., Movshovitz-Attias, D., Bohnuud, T., Yueh, C., Beglov, D., Schueler-Furman, O., & Kozakov, D. (2013). Detection of peptide-binding sites on protein surfaces: the first step toward the modeling and targeting of peptide-mediated interactions. *Proteins*, *81*(12), 2096–2105. https://doi.org/10.1002/prot.24422

Le Coutre, P., Meisel, H., Hofmann, J., Röcken, C., Vuong, G. L., Neuburger, S., Hemmati, P. G., Dörken, B., & Arnold, R. (2009). Reactivation of hepatitis E infection in a patient with acute lymphoblastic leukaemia after allogeneic stem cell transplantation. *Gut*, *58*(5), 699–702. https://doi.org/10.1136/gut.2008.165571

Lhomme, S., Kamar, N., Nicot, F., Ducos, J., Bismuth, M., Garrigue, V., Petitjean-Lecherbonnier, J., Ollivier, I., Alessandri-Gradt, E., Goria, O., Barth, H., Perrin, P., Saune, K., Dubois, M., Carcenac, R., Lefebvre, C., Jeanne, N., Abravanel, F., & Izopet, J. (2015). Mutation in the Hepatitis E Virus Polymerase and Outcome of Ribavirin Therapy. *Antimicrobial Agents and Chemotherapy*, *60*(3), 1608–1614. https://doi.org/10.1128/AAC.02496-15

Li, T.-C., Takeda, N., Miyamura, T., Matsuura, Y., Wang, J. C. Y., Engvall, H., Hammar, L., Xing, L., & Cheng, R. H. (2005). Essential elements of the capsid protein for self-assembly into empty virus-like particles of hepatitis E virus. *Journal of Virology*, *79*(20), 12999–13006. https://doi.org/10.1128/JVI.79.20.12999-13006.2005

Liu, H., & Hou, T. (2016). CaFE: a tool for binding affinity prediction using end-point free energy methods. *Bioinformatics (Oxford, England)*, *32*(14), 2216–2218. https://doi.org/10.1093/bioinformatics/btw215

Liu, N., & Xu, Z. (2019). Using LeDock as a docking tool for computational drug design. *IOP Conference Series: Earth and Environmental Science*, *218*, 012143. https://doi.org/10.1088/1755-1315/218/1/012143

Lu, L., Li, C., & Hagedorn, C. H. (2006). Phylogenetic analysis of global hepatitis E virus sequences: genetic diversity, subtypes and zoonosis. *Reviews in Medical Virology*, *16*(1), 5–36. https://doi.org/10.1002/rmv.482

Ma, Q., & Lu, A. Y. H. (2011). Pharmacogenetics, pharmacogenomics, and individualized medicine. *Pharmacological Reviews*, *63*(2), 437–459. https://doi.org/10.1124/pr.110.003533

Maag, D., Castro, C., Hong, Z., & Cameron, C. E. (2001). Hepatitis C virus RNA-dependent RNA polymerase (NS5B) as a mediator of the antiviral activity of ribavirin. *The Journal of Biological Chemistry*, *276*(49), 46094–46098. https://doi.org/10.1074/jbc.C100349200

Mahilkar, S., Paingankar, M. S., & Lole, K. S. (2016). Hepatitis E virus RNA-dependent RNA polymerase: RNA template specificities, recruitment and synthesis. *The Journal of General Virology*, *97*(9), 2231–2242. https://doi.org/10.1099/jgv.0.000528

Mainardi, V., Gerona, S., Ardao, G., Ferreira, N., Ramírez, G., Arbiza, J., & Mirazo, S. (2019). Locally Acquired chronic hepatitis E followed by Epstein-Barr virus reactivation and Burkitt lymphoma as a suspected extrahepatic manifestation in a liver transplant recipient. *The American Journal of Case Reports*, *20*, 1016–1021. https://doi.org/10.12659/AJCR.916253

Mallet, V., Nicand, E., Sultanik, P., Chakvetadze, C., Tessé, S., Thervet, E., Mouthon, L., Sogni, P., & Pol, S. (2010). Brief communication: case

reports of ribavirin treatment for chronic hepatitis E. *Annals of Internal Medicine*, *153*(2), 85–89. https://doi.org/10.7326/0003-4819-153-2-201007200-00257

Mansuy, J. M., Saune, K., Rech, H., Abravanel, F., & Mengelle, C. (2011). Seroprevalence in blood donors reveals widespread, multi-source exposure to hepatitis E virus, southern France. *Euro Surveill Bull Eur Sur Les Mal Transm = Eur Commun Dis Bull 2015*, *20*, 27–34.

Mirazo, S., Ramos, N., Mainardi, V., Arbiza, J., & Gerona, S. (2014). Transmission, diagnosis, and management of hepatitis E: an update. *Hepatic Medicine: Evidence and Research*, *6*, 45–59. https://doi.org/10.2147/HMER.S63417

Mishra, N., Walimbe, A. M., & Arankalle, V. A. (2013). Hepatitis E virus from India exhibits significant amino acid mutations in fulminant hepatic failure patients. *Virus Genes*, *46*(1), 47–53. https://doi.org/10.1007/s11262-012-0833-7

Ng, K. K. S., Arnold, J. J., & Cameron, C. E. (2008). Structure-function relationships among RNA-dependent RNA polymerases. *Current Topics in Microbiology and Immunology*, *320*, 137–156.

Oh, J. W., Ito, T., & Lai, M. M. (1999). A recombinant hepatitis C virus RNA-dependent RNA polymerase capable of copying the full-length viral RNA. *Journal of Virology*, *73*(9), 7694–7702. https://doi.org/10.1128/JVI.73.9.7694-7702.1999

Panda, S. K., Nanda, S. K., Zafrullah, M., Ansari, I. H., Ozdener, M. H., & Jameel, S. (1995). An Indian strain of hepatitis E virus (HEV): cloning, sequence, and expression of structural region and antibody responses in sera from individuals from an area of high-level HEV endemicity. *Journal of Clinical Microbiology*, *33*(10), 2653–2659. https://doi.org/10.1128/jcm.33.10.2653-2659.1995

Parker, W. B. (2005). Metabolism and antiviral activity of ribavirin. *Virus Research*, *107*(2), 165–171. https://doi.org/10.1016/j.virusres.2004.11.006

Perez-Aguilar, J. M., Shan, J., LeVine, M. V., Khelashvili, G., & Weinstein, H. (2014). A functional selectivity mechanism at the serotonin-2A GPCR involves ligand-dependent conformations of intracellular loop 2. *Journal of the American Chemical Society*, *136*(45), 16044–16054. https://doi.org/10.1021/ja508394x

Perez-Gracia, M. T., Mateos Lindemann, M. L., & Caridad Montalvo Villalba, M. (2013). Hepatitis E: current status. *Reviews in Medical Virology*, *23*(6), 384–398. https://doi.org/10.1002/rmv.1759

Pettersen, E. F., Goddard, T. D., Huang, C. C., Couch, G. S., Greenblatt, D. M., Meng, E. C., & Ferrin, T. E. (2004). UCSF Chimera-a visualization system for exploratory research and analysis. *Journal of Computational Chemistry*, *25*(13), 1605–1612. https://doi.org/10.1002/jcc.20084

Pfeiffer, J. K., & Kirkegaard, K. (2003). A single mutation in poliovirus RNA-dependent RNA polymerase confers resistance to mutagenic nucleotide analogs via increased fidelity. *Proceedings of the National Academy of Sciences of the United States of America*, *100*(12), 7289–7294. https://doi.org/10.1073/pnas.1232294100

Phillips, J. C., Hardy, D. J., Maia, J. D. C., Stone, J. E., & Ribeiro, J. V. (2020). Scalable molecular dynamics on CPU and GPU architectures with NAMD. *Journal of Chemical Physics. , 153*, 44130.

Pischke, S., Hardtke, S., Bode, U., Birkner, S., Chatzikyrkou, C., Kauffmann, W., Bara, C. L., Gottlieb, J., Wenzel, J., Manns, M. P., & Wedemeyer, H. (2013). Ribavirin treatment of acute and chronic hepatitis E: A single-centre experience. *Liver International : official Journal of the International Association for the Study of the Liver*, *33*(5), 722–726. https://doi.org/10.1111/liv.12114

Pischke, S., Suneetha, P. V., Baechlein, C., Barg-Hock, H., Heim, A., Kamar, N., Schlue, J., Strassburg, C. P., Lehner, F., Raupach, R., Bremer, B., Magerstedt, P., Cornberg, M., Seehusen, F., Baumgaertner, W., Klempnauer, J., Izopet, J., Manns, M. P., Grummer, B., & Wedemeyer, H. (2010). Hepatitis E virus infection as a cause of graft hepatitis in liver transplant recipients. *Liver Transplantation : official Publication of the American Association for the Study of Liver Diseases and the International Liver Transplantation Society*, *16*(1), 74–82. https://doi.org/10.1002/lt.21958

PubChem. (2020). https://pubchem.ncbi.nlm.nih.gov/.

Purcell, R. H., & Emerson, S. U. (2008). Hepatitis E: an emerging awareness of an old disease. *Journal of Hepatology*, *48*(3), 494–503. https://doi.org/10.1016/j.jhep.2007.12.008

Qin, W., Yamashita, T., Shirota, Y., Lin, Y., Wei, W., & Murakami, S. (2001). Mutational analysis of the structure and functions of hepatitis C virus RNA-dependent RNA polymerase. *Hepatology (Baltimore, Md.)*, *33*(3), 728–737. https://doi.org/10.1053/jhep.2001.22765

RAMPAGE. (2020). http://mordred.bioc.cam.ac.uk/~rapper/rampage.php.

Rankin, J. T. J., Eppes, S. B., Antczak, J. B., & Joklik, W. K. (1989). Studies on the mechanism of the antiviral activity of ribavirin against reovirus. *Virology*, *168*(1), 147–158. https://doi.org/10.1016/0042-6822(89)90413-3

RCSB: PDB. (2020). RCSB: PDB. https://www.rcsb.org/.

Rehman, S., Kapur, N., Durgapal, H., & Panda, S. K. (2008). Subcellular localization of hepatitis E virus (HEV) replicase. *Virology*, *370*(1), 77–92. https://doi.org/10.1016/j.virol.2007.07.036

Reyes, G. R., Purdy, M. A., Kim, J. P., Luk, K. C., Young, L. M., Fry, K. E., & Bradley, D. W. (1990). Isolation of a cDNA from the virus responsible for enterically transmitted non-A, non-B hepatitis. *Science (New York, N.Y.)*, *247*(4948), 1335–1339. https://doi.org/10.1126/science.2107574

Roy, A., Kucukural, A., & Zhang, Y. (2010). I-TASSER: a unified platform for automated protein structure and function prediction. *Nature Protocols*, *5*(4), 725–738. https://doi.org/10.1038/nprot.2010.5

Sadeghipour, S., Bek, E. J., & Mcminn, P. C. (2013). Ribavirin-Resistant mutants of human enterovirus 71 express a high replication fidelity phenotype during growth in cell culture. *Journal of Virology*, *87*(3), 1759–1769. https://doi.org/10.1128/JVI.02139-12

Sanner, M. F. (1999). Python: a programming language for software integration and development. *Journal of Molecular Graphics & Modelling*, *17*(1), 57–61.

Sayed, I. M., Vercouter, A. S., Abdelwahab, S. F., Vercauteren, K., & Meuleman, P. (2015). Is hepatitis E virus an emerging problem in industrialized countries? *Hepatology (Baltimore, Md.)*, *62*(6), 1883–1892. https://doi.org/10.1002/hep.27990

Servant-Delmas, A., Abravanel, F., Lefrère, J.-J., Lionnet, F., Hamon, C., Izopet, J., & Laperche, S. (2016). New insights into the natural history of hepatitis E virus infection through a longitudinal study of multi-transfused immunocompetent patients in France. *Journal of Viral Hepatitis*, *23*(7), 569–575. https://doi.org/10.1111/jvh.12531

Severson, W. E., Schmaljohn, C. S., Javadian, A., & Jonsson, C. B. (2003). Ribavirin causes error catastrophe during Hantaan virus replication. *Journal of Virology*, *77*(1), 481–488. https://doi.org/10.1128/jvi.77.1.481-488.2003

Shukla, P., Nguyen, H. T., Torian, U., Engle, R. E., & Faulk, K. (2011). Cross-species infections of cultured cells by hepatitis E virus and discovery of an infectious virus – host recombinant. *Proc Natl Acad Sci U S A*, *108*, 1–6.

Sigrist, C. J. A., De Castro, E., Cerutti, L., Cuche, B. A., & Hulo, N. (2013). New and continuing developments at PROSITE. *Nucleic Acids Research. , 41*, 344–347.

Smith, D. B., Izopet, J., Nicot, F., Simmonds, P., & Jameel, S. (2020). Update: Proposed reference sequences for subtypes of hepatitis E virus (species Orthohepevirus A), *101*(7), 1–7.

Smith, D. B., & Simmonds, P. (2015). Hepatitis E virus and fulminant hepatitis-a virus or host-specific pathology? *Liver International : official Journal of the International Association for the Study of the Liver*, *35*(4), 1334–1340. https://doi.org/10.1111/liv.12629

Smith, D. B., Simmonds, P., Jameel, S., Emerson, S. U., & Harrison, T. J. (2014). Consensus proposals for classification of the family Hepeviridae. *Journal of General Virology*, *95*, 2223–2232. https://doi.org/10.1099/vir.0.068429-0

Sterling, T., & Irwin, J. J. (2015). ZINC 15-ligand discovery for everyone. *Journal of Chemical Information and Modeling*, *55*(11), 2324–2337. https://doi.org/10.1021/acs.jcim.5b00559

Stierand, K., Maass, P. C., & Rarey, M. (2006). Molecular complexes at a glance: Automated generation of two-dimensional complex diagrams. *Bioinformatics (Oxford, England)*, *22*(14), 1710–1716. https://doi.org/10.1093/bioinformatics/btl150

Tam, A. W., Smith, M. M., Guerra, M. E., Huang, C. C., Bradley, D. W., Fry, K. E., & Reyes, G. R. (1991). Hepatitis E virus (HEV): molecular cloning and sequencing of the full-length viral genome. *Virology*, *185*(1), 120–131. https://doi.org/10.1016/0042-6822(91)90760-9

Tan, D., Im, S. W., Yao, J. L., & Ng, M. H. (1995). Acute sporadic hepatitis E virus infection in southern China. *Journal of Hepatology* , *23*(3), 239–245. https://doi.org/10.1016/S0168-8278(95)80001-8

Tanaka, T., Takahashi, M., Kusano, E., & Okamoto, H. (2007). Development and evaluation of an efficient cell-culture system for Hepatitis E virus. *The Journal of General Virology*, *88*(Pt 3), 903–911. https://doi.org/10.1099/vir.0.82535-0

Thompson, A. A., & Peersen, O. B. (2004). Structural basis for proteolysis-dependent activation of the poliovirus RNA-dependent RNA polymerase. *The EMBO Journal*, *23*(17), 3462–3471. https://doi.org/10.1038/sj.emboj.7600357

Todt, D., François, C., Anggakusuma, Behrendt, P., & Engelmann, M. (2016). Antiviral activities of different interferon types and subtypes against hepatitis E virus replication. *Antimicrob Agents Chemother*, *60*, 2132–2139. https://doi.org/10.1128/AAC.02427-15

Todt, D., Walter, S., Brown, R. J. P., & Steinmann, E. (2016). Mutagenic Effects of Ribavirin on Hepatitis E Virus-Viral Extinction versus Selection of Fitness-Enhancing Mutations. *Viruses*, *8*(10), 283. Epub ahead of print Octoberhttps://doi.org/10.3390/v8100

Todt, D., Gisa, A., Radonic, A., Nitsche, A., Behrendt, P., Suneetha, P. V., Pischke, S., Bremer, B., Brown, R. J. P., Manns, M. P., Cornberg, M., Bock, C. T., Steinmann, E., & Wedemeyer, H. (2016). In vivo evidence for ribavirin-induced mutagenesis of the hepatitis E virus genome. *Gut*, *65*(10), 1733–1743. https://doi.org/10.1136/gutjnl-2015-311000

Toltzis, P., O'Connell, K., & Patterson, J. L. (1988). Effect of phosphorylated ribavirin on vesicular stomatitis virus transcription. *Antimicrobial Agents and Chemotherapy*, *32*(4), 492–497. https://doi.org/10.1128/AAC.32.4.492

Trott, O., & Olson, A. J. (2010). AutoDock Vina: improving the speed and accuracy of docking with a new scoring function, efficient optimization, and multithreading. *Journal of Computational Chemistry*, *31*(2), 455–461.

UniProt. (2020). UniProt. https://www.uniprot.org/.

Vázquez, A. L., Alonso, J. M., & Parra, F. (2000). Mutation analysis of the GDD sequence motif of a calicivirus RNA-dependent RNA polymerase. *Journal of Virology*, *74*(8), 3888–3891. https://doi.org/10.1128/jvi.74.8.3888-3891.2000

Vignuzzi, M., Stone, J. K., & Andino, R. (2005). Ribavirin and lethal mutagenesis of poliovirus: molecular mechanisms, resistance and biological implications. *Virus Research*, *107*(2), 173–181. https://doi.org/10.1016/j.virusres.2004.11.007

Vlachakis, D., Kontopoulos, D. G., & Kossida, S. (2013). Space constrained homology modelling: The paradigm of the RNA-dependent RNA polymerase of dengue (Type II) virus. *Computational and Mathematical Methods in Medicine*, *2013*, 108910. Epub ahead of print 2013. https://doi.org/10.1155/2013/108910

Wallace, A. C., Laskowski, R. A., & Thornton, J. M. (1995). Ligplot: A program to generate schematic diagrams of protein-ligand interactions. *Protein Engineering*, *8*(2), 127–134. https://doi.org/10.1093/protein/8.2.127

Wang, X., & Gillam, S. (2001). Mutations in the GDD motif of rubella virus putative RNA-dependent RNA polymerase affect virus replication. *Virology*, *285*(2), 322–331. https://doi.org/10.1006/viro.2001.0939

Wang, Y., Zhang, H., Li, Z., Gu, W., Lan, H., Hao, W., Ling, R., Li, H., & Harrison, T. J. (2001). Detection of sporadic cases of hepatitis E virus (HEV) infection in China using immunoassays based on recombinant open reading frame 2 and 3 polypeptides from HEV genotype 4. *Journal of Clinical Microbiology*, *39*(12), 4370–4379. https://doi.org/10.1128/JCM.39.12.4370-4379.2001

Wiederstein, M., & Sippl, M. J. (2007). ProSA-web: Interactive web service for the recognition of errors in three-dimensional structures of proteins. *Nucleic Acids Research.* , *35*, 407–410.

Wray, S. K., Gilbert, B. E., & Knight, V. (1985). Effect of ribavirin triphosphate on primer generation and elongation during influenza virus transcription in vitro. *Antiviral Research*, *5*(1), 39–48. https://doi.org/10.1016/0166-3542(85)90013-0

Wyde, P. R. (1998). Respiratory syncytial virus (RSV) disease and prospects for its control. *Antiviral Research*, *39*(2), 63–79. https://doi.org/10.1016/s0166-3542(98)00029-1

Xu, Z., Kuang, M., Okicki, J. R., Cramer, H., & Chaudhary, N. (2004). Potent inhibition of respiratory syncytial virus by combination treatment with 2-5A antisense and ribavirin. *Antiviral Research*, *61*(3), 195–206. https://doi.org/10.1016/j.antiviral.2003.10.005

Yamada, K. D., Nishi, H., Nakata, J., & Kinoshita, K. (2016). Structural characterization of single nucleotide variants at ligand binding sites and enzyme active sites of human proteins. *Biophysics and Physicobiology*, *13*, 157–163. https://doi.org/10.2142/biophysico.13.0_157

Yamada, K., Takahashi, M., Hoshino, Y., Takahashi, H., Ichiyama, K., Nagashima, S., Tanaka, T., & Okamoto, H. (2009). ORF3 protein of hepatitis E virus is essential for virion release from infected cells. *The Journal of General Virology*, *90*(Pt 8), 1880–1891. https://doi.org/10.1099/vir.0.010561-0

Yamashita, T., Kaneko, S., Shirota, Y., Qin, W., Nomura, T., Kobayashi, K., & Murakami, S. (1998). RNA-dependent RNA polymerase activity of the soluble recombinant hepatitis C virus NS5B protein truncated at the C-terminal region. *The Journal of Biological Chemistry*, *273*(25), 15479–15486. https://doi.org/10.1074/jbc.273.25.15479

Yan, Y., Zhang, W., Shen, Q., Cui, L., & Hua, X. (2008). Prevalence of four different subgenotypes of genotype 4 hepatitis E virus among swine in the Shanghai area of China. *Acta Veterinaria Scandinavica*, *50*, 12. https://doi.org/10.1186/1751-0147-50-12

Yang, J., Yan, R., Roy, A., Xu, D., Poisson, J., & Zhang, Y. (2015). The I-TASSER Suite: protein structure and function prediction. *Nature Methods*, *12*(1), 7–8. https://doi.org/10.1038/nmeth.3213

Young, K., Lindsay, K. L., Lee, K., Liu, W., & He, J. (2011). Identification of a ribavirin-resistant ns5b mutation of hepatitis C virus during ribavirin monotherapy. https://doi.org/10.1053/jhep.2003.50445

Zhang, Y., & Skolnick, J. (2005). TM-align: a protein structure alignment algorithm based on the TM-score. *Nucleic Acids Research.* , *33*(7), 2302–2309. https://doi.org/10.1093/nar/gki524

Zoete, V., Cuendet, M. A., Grosdidier, A., & Michielin, O. (2011). SwissParam: a fast force field generation tool for small organic molecules. *Journal of Computational Chemistry*, *32*(11), 2359–2368. https://doi.org/10.1002/jcc.21816

6. CAPÍTULO 4

Aislamiento de HEVc in vitro en las líneas celulares continuas A549, A549/D3, análisis de resistencia de RBV y estudio del perfil de expresión diferencial de citoquinas, proteínas de apoptosis y sus vías de señalización.

6.1. Fundamento teórico y antecedentes

Como se mencionó en el *punto 1.10*. de la Sección *Introducción,* en mi Tesis de Maestría se realizó el aislamiento de HEV3 en células A549, a partir del cual se implementaron estudios transcriptómicos, no obstante, este sistema *in vitro* demostró requerir mucho tiempo para desarrollar la infección además de ser poco reproducible.

La carencia de un sistema estandarizado y eficiente de aislamiento de HEV en cultivos celulares es una de las principales limitantes para profundizar el estudio de su biología y patogénesis viral [50]. Por ello, en esta Tesis se pretendió poner a punto un sistema de aislamiento *in vitro* más eficiente para aportar conocimientos sobre la biología viral de cepas de HEV3, especialmente proviniendo de una infección crónica, y de esta forma permitir también llevar a cabo estudios *in vitro* a futuro a partir de las variantes de HEV-*like* detectadas en esta Tesis.

Hasta el momento, las líneas celulares en las cuales se han reportado aislamiento de HEV corresponden a A549 (adenocarcinoma pulmonar humano), PLC/PRF/5 (hepatocarcinoma humano), HepG2/C3A y Huh7 (hepatocarcinoma humano) [102–104]. Particularmente, en un estudio se analizaron 21 potenciales líneas continuas para propagar HEV, obteniéndose los mejores resultados para A549 [51]. Precisamente, diversos estudios han demostrado que HEV fue capaz de infectar y replicar en A549 [102, 105–107]. Asimismo, recientemente fue mejorado el sistema de aislamiento de HEV por medio de la generación de la línea clonal A549/D3, demostrando mayor eficiencia de crecimiento para HEV [108]. Esta línea subclonal presenta 10 genes diferencialmente expresados en comparación a la línea A549 original, principalmente asociados a proteoglicanos de heparán sulfato. Sin embargo, no se ha comprobado hasta el momento si estos genes están involucrados en la replicación más eficiente en estas células [108].

Por otro lado, se ha demostrado que algunas cepas provenientes de casos de hepatitis crónica presentan variantes recombinantes virus-hospedador con divergencia de secuencia en la región hipervariable (ORF1) [56, 109], lo cual se ha propuesto que le podría conceder una ventaja replicativa *in vitro* [54]. De hecho, en los cuadros de hepatitis crónica en que se requiere tratamiento antiviral, se ha reportado para algunos casos falla terapéutica por RBV debido al desarrollo de resistencia de HEV posiblemente asociada a las sustituciones G1634R, Y1320H y K1383N en la RdRp [66]. La sustitución K1383N está localizada en el motivo-F1 (177-180 aa de RdRp) y se ha sugerido que es el responsable de la unión y selección del nucleótido trifosfato entrante [110]. Asimismo, esta sustitución es capaz de disminuir fuertemente la replicación viral y aumentar la sensibilidad *in vitro* a RBV, opuesto al fenotipo clínico observado. En cambio, la sustitución Y1320H incrementa la replicación de HEV, lo cual podría ser un efecto compensatorio por la pérdida de *fitness* producida por K1383N. La sustitución G1634R parecería aumentar la capacidad replicativa de HEV, reduciendo la eficiencia de RBV [111].

Por lo tanto, el principal mecanismo de acción de RBV consiste en inducir a la "catástrofe de error" en los virus ARN, provocando principalmente sustituciones A/G y U/A [112], dando lugar a mutagénesis letal [46, 113].

Cómo se mencionó en el *Capítulo 3*, la secuencia HEV_C1_Uy presenta algunas sustituciones únicas no reportadas previamente (V/I1220A) e infrecuentes (T/A1608V, V1659A y Q1700H) en la RdRp y debido a que el paciente recibió tratamiento con la droga resulta interesante implementar estudios de sensibilidad a RBV.

Recientemente, se propuso un modelo de activación de vías de señalización de la respuesta inmune innata ante una infección por HEV (Figura 11) [114].

En el contexto de una infección viral, los receptores tipo-*Toll* (TLRs) y receptores de tipo gen inducible por ácido retinoico I (RLRs) son cruciales en el reconocimiento de patrones moleculares asociados a patógenos (PAMPs) virales y en la inducción de la respuesta inmune. Una vez reconocidos los PAMPs por los TLRs, estos pueden activar dos vías de señalización dependiendo del tipo de receptor activado, por un lado, los TLR3 y TLR4 inician la señalización por medio de la proteína TRIF y por otro lado, todos los TLRs (excepto TLR3) activan la proteína MYD88. Además, el ARN foráneo en el citoplasma es reconocido por los RLRs como RIG-1,

MDA5 y LGP2. RIG-1 y MDA5 contienen ambos un dominio de activación de caspasas (CARDs) y a su vez ambos receptores son capaces de activar la proteína de señalización antiviral mitocondrial (MAVS), llevando al reclutamiento de otras proteínas de señalización. Este complejo también es capaz de activar quinasas como el complejo de IKK, TBK1 e IKKε que fosforilan los factores de transcripción de NFκB, IRF3 e IRF7, sintetizando moléculas de interferón (IFNs). Las moléculas de IFN-1 activan la vía JAK/STAT dando lugar a la expresión de factores de genes IFN-estimulados (ISG) [114].

Se ha propuesto que la respuesta inmune innata podría estar involucrada en la eliminación de HEV [115]. Por otro lado, la inmunidad mediada por células es clave para la contención de las infecciones virales en general, siendo posible que esta respuesta contra HEV esté involucrada en la patogénesis de la enfermedad, relacionándose con el daño celular del hospedador [115]. Particularmente, la respuesta inmune del hospedero ante una infección viral involucra la secreción de citoquinas y quimioquinas para regular las funciones efectoras innatas o adaptativas [116]. Las citoquinas son proteínas secretadas que modulan la activación, proliferación y diferenciación de células blanco [117], mientras que las quimioquinas son citoquinas quimiotácticas que regulan el reclutamiento de leucocitos [118]. Interesantemente, se han reportado diferencias significativas en el perfil de expresión de citoquinas para monos Rhesus infectados con HEV3 o HEV1 [57]. A su vez, se ha sugerido que altos niveles de citoquinas estarían correlacionados con un daño hepático severo en mujeres embarazadas [119], proponiéndose además, que la estimulación de las células de respuesta inmune productoras de citoquinas T helper (Th1 y Th2) pueden estar involucradas en el daño hepático entre pacientes con hepatitis E sintomática [120]. Particularmente, un estudio reveló que la infección *in vitro* de HEV1 en células A549 produjo una robusta respuesta de citoquinas y quimoquinas inflamatorias como IL-6, IL-8, TNF-α y RANTES [121].

Asimismo, estudios *in vitro* han sugerido que en células infectadas con HEV, la proteína de ORF3 (VP13) podría alterar diversos procesos celulares, principalmente el de apoptosis, promoviendo la supervivencia celular y así contribuir a la patogénesis. [62, 122].

Por ello, resulta interesante estudiar la expresión de proteínas relacionadas a apoptosis y sus principales vías de señalización entre células infectadas y no infectadas.

No obstante, si bien ha habido avances importantes en el estudio de la respuesta inmune celular durante la infección con HEV, aún son necesarios más análisis que contribuyan a

elucidar los mecanismos patogénicos en la infección por distintos genotipos y subtipos de HEV.

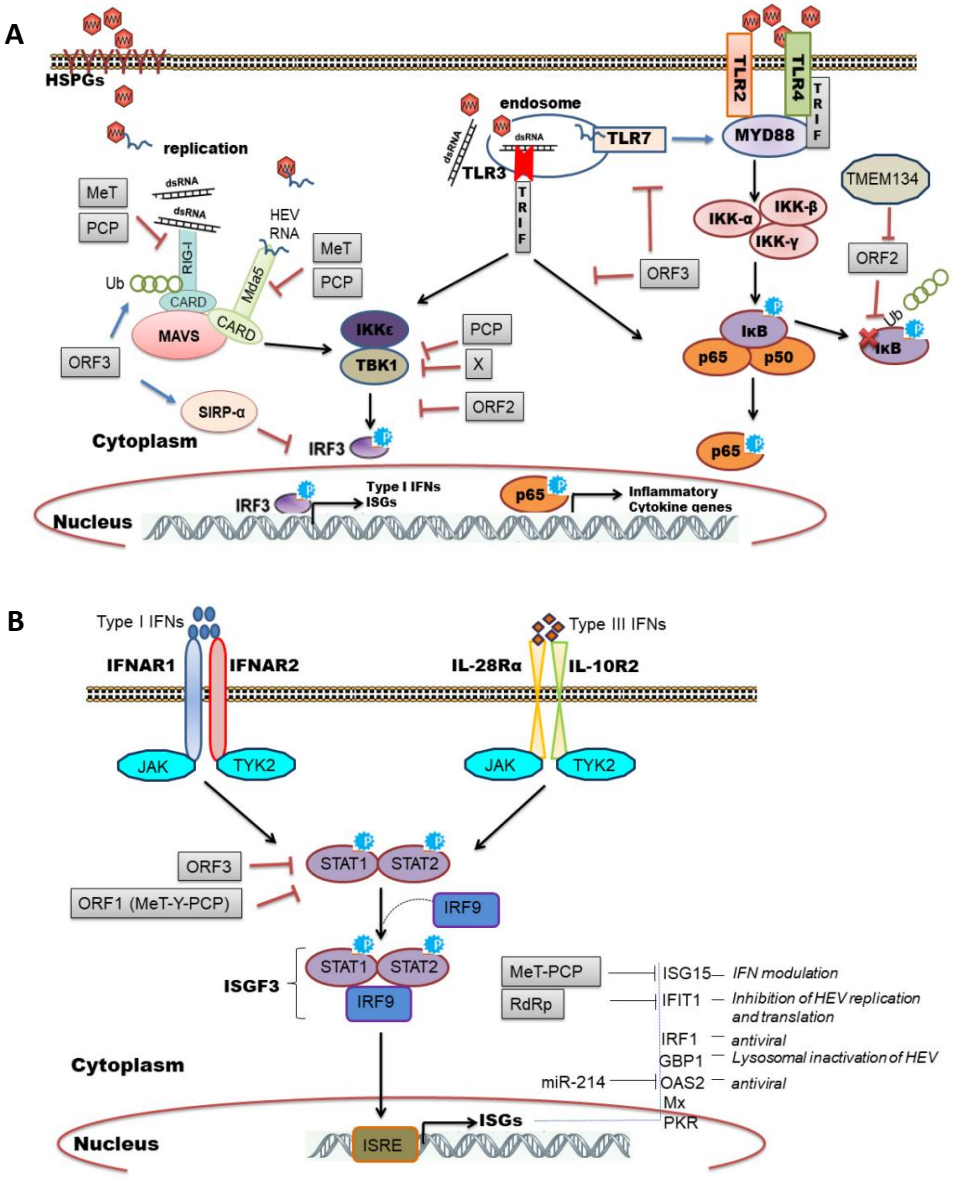

Figura 11. Modelos de activación de cascadas de señalización celular por HEV. A. HEV se une a los receptores proteoglicanos de heparán sulfato (HSPGs), entre otros, e ingresa por endocitosis mediadas por clatrina. El ARN viral liberado es reconocido por receptores de reconocimiento de patrones (PRRs) como RIG-1, MDA5 y TLR3, activando la cascada de señalización celular de IRF3 y NFκB, llevando a la producción de IFNs y citoquinas inflamatorias. Se muestran las interacciones entre los distintos dominios de HEV y las proteínas celulares que se sugieren alteran la activación de vías de señalización. **B.** Los IFNs tipo I y tipo III se unen a sus respectivos receptores, resultando en la fosforilación de STAT1 y STAT2, los cuales forman complejo con IRF9 (ISGF3), translocándose al núcleo para transcribir ISGs a partir del elemento promotor ISRE. Los ISGs presentan diferentes mecanismos antivirales, mientras que HEV emplea diversas estrategias para evadir la respuesta por IFN. Extraído de [114].

6.2. Hipótesis

Es posible desarrollar un método de aislamiento *in vitro* de HEV más eficiente. Existe un perfil de expresión diferencial de citoquinas, proteínas de apoptosis y sus vías de señalización (NFκB) entre distintas cepas de HEV3.

Es posible desarrollar una estrategia para estudiar la dinámica de resistencia a RBV *in vitro*.

6.3. Objetivo específico

Aislamiento de HEVc y HEVa *in vitro* en las líneas celulares continuas A549, A549/D3 y estudio del perfil de expresión diferencial de citoquinas, proteínas de apoptosis y de señalización. Explorar opciones metodológicas para optimizar el aislamiento viral y por lo tanto, poder aislar las cepas HEV_C1_Uy y HEV-7_uy en células A549 y A549/D3, para luego llevar a cabo un estudio de resistencia de RBV y un análisis comparativo del perfil de expresión *in vitro* de citoquinas solubles pro y anti inflamatorias, antivirales y anti-apoptóticas, así como de proteínas involucradas en la apoptosis celular y sus principales vías de señalización.

6.4. Metodología

6.4.1. Líneas celulares

Inicialmente, se utilizaron células A549 (ATCC CCL-185) (provenientes de epitelio alveolar humano con adenocarcinoma) que se crecieron en Dulbecco's modified Eagle's medium/Nutrient Mixture F-12 suplementado con 10% suero fetal bovino (SFB)(Gibco™, Thermo Scientific), 100U/ml penicilina G, 100µg/ml estreptomicina, 2.5µg/ml anfotericina B y 2mM glutamina (Thermo Scientific, USA) a 37°C en una atmósfera humedecida con 5% CO_2. Por otro lado, recientemente mediante un convenio con el Dr. Reimar Johne del German Federal Institute for Risk Assessment Berlín-Alemania, nos fue posible acceder a la línea subclonal A549/D3. Este sistema de A549/D3 demostró conferir mayor eficiencia de crecimiento y reproducibilidad para HEV [43]. Las células A549/D3 fueron crecidas como se describió anteriormente pero utilizando Minimum Essential Medium (MEM) (Thermo Scientific, USA) y aminoácidos no-esenciales (Capricorn, Scientific) que incluyen glicina, L-alanina, L-asparagina, L-ácido aspártico, L-ácido glutámico, L-prolina y L-serina.

6.4.2. Test de *Mycoplasma sp*. en las líneas celulares

Se estima que aproximadamente 20% de los cultivos celulares pueden llegar a estar infectados con bacterias del género *Mycoplasma* (carentes de pared celular), los cuales pueden pasar inadvertidos por el control de rutina, representando un grave problema para el trabajo *in vitro* ya que tienen efectos nocivos sobre las células eucariotas [123]. Por lo tanto, se realizó la detección específica de *Mycoplasma sp.* mediante PCR para ambas líneas celulares, según el protocolo descrito [124].

6.4.3. Aislamiento y detección de HEV *in vitro*

En el día 0, se sembraron 5 x 10^4 células A549 y A549/D3 en placas de 24 *wells* y en el día 1 fueron inoculadas con las cepas HEV_C1_Uy (*Capítulo 2*) y HEV-7_uy (perteneciente al mismo criadero de cerdos que la cepa HEV-8_uy mencionada en la *Sección 4.5 Capítulo 4*) en un volumen final de 300 µl, a partir de materia fecal resuspendida en 10% PBS y filtrada por 0,22 µm (millipore, Merck). Se evaluaron distintas concentraciones de inóculo viral y tiempos de infección.

Brevemente, las monocapas celulares fueron lavadas con medio sin SFB, para luego inocular 6.7x10^6 (dilución 1/8), 9.0x10^6 (dilución 1/6), 1.3x10^7 (dilución 1/4) y 2.7x10^7 (dilución 1/2) copias de ARN totales de la cepa HEV_C1_Uy (provenientes del inóculo original de 7,7x10^4 copias ARN/µl), incubándose por 1 hr o 3 hs a 37°C.

Para la cepa HEV-7_uy, se evaluaron las diluciones de inóculo viral 1/2 y 1/4, los cuáles se incubaron hasta por 3 hs a 37°C.

Posteriormente, el inóculo fue removido y se añadió medio completo con 10% SFB. Los cultivos infectados fueron subcultivados cada 72hs, colectándose *pellets* celulares periódicamente. Además, se incluyeron controles sin infectar.

En todos los casos, se extrajo el ARN total de los cultivos infectados y no-infectados con el Quick-RNA Miniprep Kit (Zymo Research, USA) de acuerdo a las especificaciones del proveedor.

A continuación, se realizó la confirmación de la infección viral por RT-qPCR con sonda Taqman® la cual amplifica una región conservada de solapamiento de ORF2-3 [125] y fue

optimizada utilizando el SensiFAST™ Probe Lo-ROX One-Step kit (Bioline, Meridian Bioscience), como se mencionó en el manuscrito del *Capítulo 1*.

Además, se diseñó una curva de ARN *in-house* para realizar cuantificación absoluta de HEV por RT-qPCR mediante síntesis comercial de un fragmento en la región 5263 al 5352 nt en la ORF2/ORF3 de HEV_C1_Uy y posterior transcripción *in vitro* (Synbio Technologies, USA). A partir del fragmento de ARN obtenido se realizaron diluciones seriadas en base 10 en el rango de $4X10^8$ - $4X10^1$ copias ARN/µl.

Por otro lado, a través del convenio establecido con el Dr. Reimar Johne, obtuvimos células A549/D3 infectadas en forma persistente con la cepa 47832c perteneciente al subtipo 3c, predominante en Europa [126]. Con dichas células, se implementó y optimizó un protocolo de inmunofluorescencia indirecta (IFI).

Brevemente, se crecieron $1x10^4$ células A549/D3 infectadas persistente y no-infectadas en placas de 96 *wells* y se fijaron con una solución de acetona-metanol 1:1, se bloquearon con PBS-BSA 1% y posteriormente se incubaron con un anticuerpo primario (Ac 1°) mouse anti-HEV ORF2 monoclonal (ab233244) (abcam, UK) por 1 hr a temperatura ambiente y con un anticuerpo secundario (Ac 2°) conjugado a FITC- Goat Anti-Mouse IgG H&L (ab6785) (abcam, UK) por 1 hr a temperatura ambiente. Para ello, se evaluaron cuatro condiciones de diluciones de anticuerpo primario y secundario, según los rangos recomendados por los fabricantes.

Condición 1: Ac 1°-- 1/50 | Ac 2° -- 1/100

Condición 2: Ac 1°-- 1/50 | Ac 2° -- 1/500

Condición 3: Ac 1°-- 1/100 | Ac 2° -- 1/100

Condición 4: Ac 1°-- 1/100 | Ac 2° -- 1/500

Para teñir los núcleos celulares se utilizó 4',6-Diamidino-2'-fenilindol (DAPI) (1µg/ml) (Sigma-Aldrich, USA).

Los focos fluorescentes se visualizaron en un microscopio ZOE Fluorescent Cell Imager-Bio-Rad (Facultad de Ciencias).

El protocolo de IFI obtenido fue implementado para la visualización de focos en las infecciones realizadas con las cepas HEV_C1_Uy y HEV-7_uy, con el propósito de implementar a futuro un sistema de cuantificación de partículas virales infecciosas mediante unidades formadoras de foco fluorescentes (FFU), el cual es frecuentemente empleado para aquellos virus que no

desarrollan un efecto citopático evidente y no es posible titularlos por formación de placas de lisis.

6.4.4. Cultivo primario de hepatocitos de jabalí

Con el objetivo de estudiar la biología viral de las cepas de HEV3 en un contexto biológico más realista y comparar los resultados obtenidos de la infección en células A549/D3, se planteó la posibilidad de implementar un sistema de aislamiento *in vitro* en cultivo primario de hepatocitos de jabalíes. Para ello, se prepararon cultivos primarios de tres hepatocitos de jabalíes, a partir de hígados obtenidos de actividades de caza de la Fiesta Nacional del Jabalí, Aiguá-Maldonado. Los hígados se transportaron refrigerados hasta su procesado en el laboratorio.

El procedimiento se basó en el descrito para hepatocitos de rata en mi Tesis de Maestría, el cual consistió en disgregar los hígados mecánicamente y enzimáticamente por medio de material quirúrgico estéril y homogeneizador en solución de tripsina 0,25% e incubándose en agitación por 15 min, 100 RPM a 37 °C. Posteriormente, se centrifugó el homogeneizado durante 10 min a 2000 RPM. El sobrenadante obtenido se plaqueó en placas de 60mm para cultivo celular en medio de crecimiento, incubándose a 37°C con 5% CO_2 en ambiente húmedo. El medio de crecimiento consistió en DMEM/F-12 con L-Glutamina (Capricorn, Scientific), suplementado con 15% de suero fetal bovino (SFB) (Gibco™, Thermo Scientific), 100U/ml penicilina G, 100µg/ml estreptomicina, 2.5µg/ml anfotericina B (Thermo Scientific), 3,0 g/L de caldo sulfato de triptosa estéril (Sigma Aldrich, Merck) y 10 mg/ml de insulina (Sigma-Aldrich).

A continuación, se analizaron los sueros correspondientes a los tres jabalíes por medio del kit de ELISA HEV Ab (Dia.Pro Diagnostic Bioprobs, Italia) y por RT-PCR según [92] para descartar la presencia de una infección activa por HEV.

6.4.5. Ensayos de citotoxicidad de RBV *in vitro*

La toxicidad de RBV *in vitro* en la línea A549/D3 se evaluó mediante el método de concentración citotóxica 50% (CC50%) [127], empleando el reactivo sal de bromuro 3-(4,5-dimetiltiazol-2-il)-2,5-difenil tetrazolio (MTT), el cual se basa en una reacción colorimétrica

debido a que este reactivo es reducido en las células viables produciendo un producto que es medido por absorbancia en espectrofotómetro [128].

Para ello, se sembraron $5x10^4$ células A549/D3 en placas de 96 *wells*, incubándolas con distintas diluciones en base 2 de RBV en un rango de concentraciones de 3,9µM a 1000 µM por triplicado. A las 48 hs se removieron las diluciones de RBV de las células y se añadió 5mg/ml del reactivo MTT, el cual se incubó por 3 hs a 37°C. Luego, se solubilizaron los cristales formados con DMSO y se midió su absorbancia a 540 nm.

Además, se incluyeron controles negativos de células sin tratamiento con RBV y controles positivos incubando las células con peróxido de hidrógeno.

6.4.6. Determinación de la concentración inhibitoria 50 (IC50) de RBV

El valor de IC50 de una droga antiviral es uno de los métodos más utilizados para identificar la concentración necesaria para disminuir el título viral en un 50% [129].

Se realizó el ensayo de IC50 en células A549/D3 infectadas persistentemente con la cepa de HEV 47832c. En placas de 96 *wells* se crecieron $4x10^4$ células y se trataron por triplicado con diluciones en base 2 de RBV en un rango de concentraciones de 3,9 µM a 62,5 µM, incubándose 72 hs. Se seleccionó este rango de concentraciones debido a los valores de IC50 de HEV reportados previamente por otros autores [129].

Se incluyó como control negativo células infectadas en ausencia de droga antiviral.

Se realizo la extracción del ARN total de los *pellets* celulares y detección de HEV mediante RT-qPCR como se describió en la sección 6.4.3.

Se calculó el valor de IC50 mediante regresión-no lineal (inhibición/dosis-respuesta) en GraphPad Prism v5.

6.4.7. Ensayo de resistencia a RBV *in vitro*

Se evaluó si la cepa HEV_C1_Uy presentaba resistencia a RBV. De esta manera, a partir del aislamiento obtenido se crecieron $5x10^4$ células A549/D3 infectadas en placas de 24 *wells* y se incubaron con distintas diluciones de la droga, realizando subcultivos cada 72 hs, en 3 condiciones como se describe a continuación (Figura 12).

Se extrajo el ARN total de los *pellets* celulares colectados de cada condición con el Quick-RNA Miniprep Kit (Zymo Research, USA) y se analizó por RT-qPCR como mencionado en los puntos anteriores. Se calculó el valor de IC50 como se describió en el punto anterior.

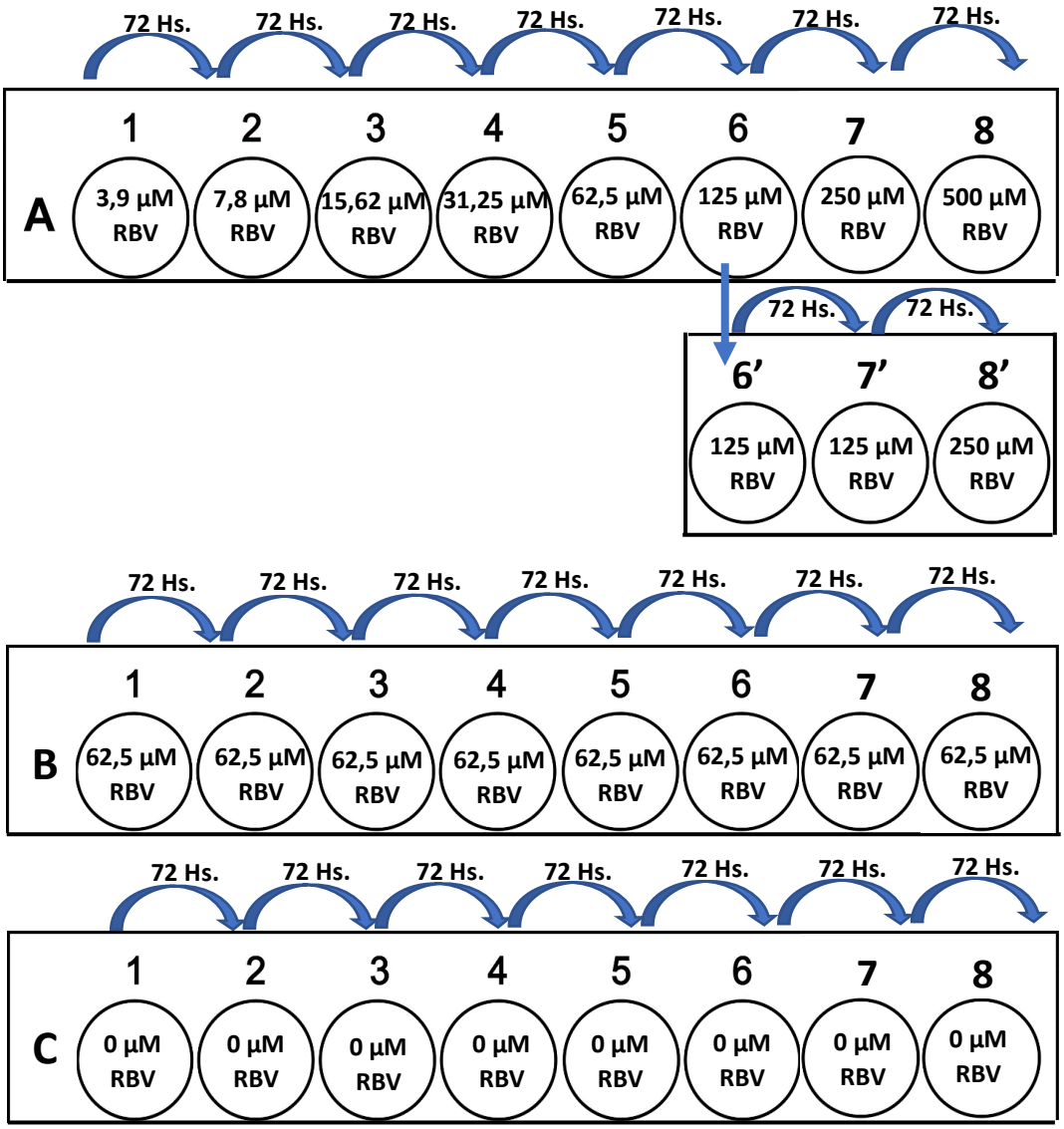

Figura 12. Esquema de ensayo de resistencia a RBV *in vitro*. Se indican las 3 condiciones del experimento en células A549/D3 infectadas con la cepa HEV_C1_Uy realizando subcultivos cada 72 hrs. **A.** Diluciones seriadas en base 2 de RBV en un rango de concentración creciente de 3,9 µM a 500 µM. **B.** Tratamiento con la droga a concentración fija de 62,5 µM (concentración inhibitoria para la cepa HEV 47832c testeada). **C.** Control de células infectadas sin tratamiento de RBV.

6.4.8. *Array* de perfil de proteoma

Se evaluaron los niveles de expresión relativa de distintas proteínas mediante kits comerciales de Proteome Profiler™ Antibody Arrays - R&D Systems, siguiendo las instrucciones del fabricante. El principio del ensayo se ilustra en la Figura 13.

En todos los casos se compararon simultáneamente tres condiciones, a) células A549/D3 infectadas con la cepa HEV_C1_Uy, b) células A549/D3 infectadas con la cepa HEV 47832c y c) células A549/D3 sin infectar.

Para ello, se utilizaron 3 kits, en los cuales se analizaron:

1. 36 citoquinas y quimioquinas humanas a partir de 1,5 ml de sobrenadante celular.
2. 35 proteínas relacionadas a apoptosis a partir de 600 µg de proteínas totales.
3. 41 proteínas y 4 sitios de fosforilación de serinas o tirosinas pertenecientes a la vía NFkB a partir de 700 µg de proteínas totales.

A partir de aproximadamente 1 x 10^7 células, se llevó a cabo la lisis celular para los kits de array 2 y 3 utilizando 450 µl de buffer de lisis incluidos en los respectivos kits, añadiéndole 1X de *cocktail* inhibidor de proteasas (Sigma) y 1X de inhibidor de fosfatasas (Pierce Phosphatase Inhibitor, mini tablets Thermo Scientific™).

La cuantificación de la concentración proteica se realizó mediante el método colorimétrico de Bradford, utilizando una curva de calibración conteniendo las concentraciones de 0,2; 0,4: 0,6: 0,8; 1 mg/ml de BSA y midiéndose en espectrofotómetro a 595 nm (Varioskan, Thermo Scientific™).

Las 3 membranas se revelaron mediante 10 min de exposición en un equipo G-Box, Syngene. El análisis de datos se realizó con el *software* libre Image J, midiéndose la densidad de pixel de cada *spot* y promediándose los duplicados para cada analito. La corrección de los valores de cada analito se realizó sustrayendo la medida de los *spots* correspondientes al control negativo. El experimento fue validado al observarse señal de los controles positivos de referencia incluidos en el kit.

Los análisis gráficos y estadísticos fueron realizados con el software GraphPad Prism v6 (GraphPad Software Inc., San Diego, CA, USA). Los resultados obtenidos de los kits de *array*

fueron analizados con el test de varianza ANOVA-dos factores y el test *post-hoc* de Bonferroni para determinar si existe diferencia estadísticamente significativa entre las 3 condiciones para cada caso.

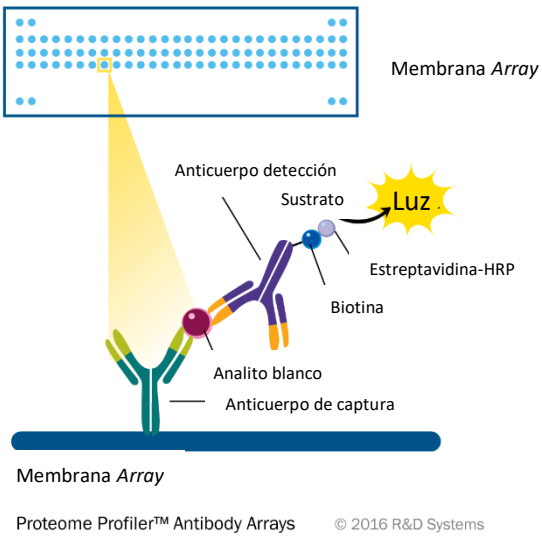

Figura 13. Principio del ensayo de perfil de proteoma mediante *arrays* de anticuerpo. Los anticuerpos de captura se encuentran fijados por duplicado en una membrana de nitrocelulosa, los analitos blancos se unen a estos anticuerpos de captura, que son luego detectados utilizando un anticuerpo de detección conjugado a biotina. Posteriormente, los anticuerpos biotinilados reaccionan con el sustrato de estreptavidina-HRP incubándose con un reactivo quimioluminiscente, produciendo una señal de luz proporcional a la cantidad de analito. Extraído y adaptado de [130]. https://www.rndsystems.com/products/proteome-profiler-antibody-arrays.

6.5. Resultados

6.5.1. Curva de ARN para cuantificación por RT-qPCR de HEV

Se validó una curva de ARN para la cuantificación absoluta de HEV mediante RT-qPCR, para lo cual se evaluó su desempeño en tres equipos diferentes: ABI 7500 (Applied Biosystems-Thermo scientific), Rotor Gene Q (Qiagen) y MIC (Biomolecular Systems).

Para los 3 casos se observó un rango dinámico lineal entre $4x10^8$-$4x10^3$ copias de ARN/µl (Figura 14), perdiendo el comportamiento lineal para concentraciones menores ($4x10^2$ y $4x10^1$). Los valores de eficiencia ($E= (10^{(-1/k)} - 1)$, k: pendiente de la curva) y coeficiente de determinación (R^2) obtenidos fueron considerados satisfactorios. Los valores de E deben encontrarse entre 90-110% y para R^2 deben ser mayor a 0,98 para considerarse aceptables.

Los parámetros analizados para la validación de la curva se muestran en la Tabla 7.

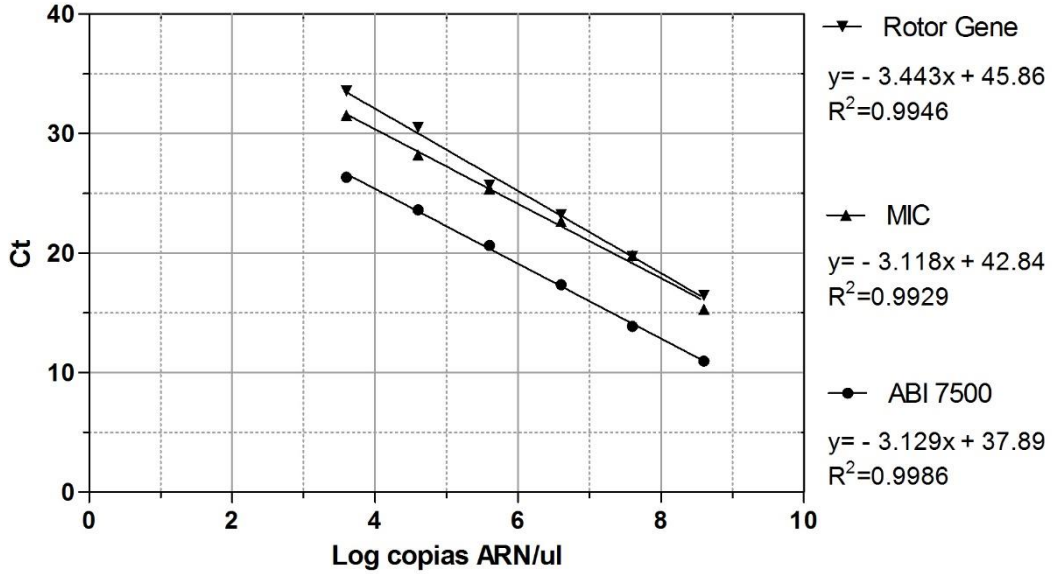

Figura 14. Curva estándar de cuantificación absoluta por RT-qPCR para HEV. Se muestran los resultados obtenidos de la curva de regresión lineal para los tres equipos evaluados.

Tabla 7. Resultados obtenidos para los parámetros de eficiencia (E) y coeficiente de determinación (R^2) para validación de la curva de RT-qPCR de HEV en tres equipos diferentes.

Equipo	Eficiencia (%)	Coeficiente de determinación (R^2)
ROTOR GENE	95	0,9946
MIC	109	0,9929
ABI 7500	109	0,9986

6.5.2. Aislamiento de HEV *in vitro.*

En primer lugar, no se detectó la presencia de *Mycoplasma sp*. por la técnica de PCR en las líneas celulares A549 y A549/D3 empleadas.

6.5.2.1. Infección en la línea A549

No se detectó infección por RT-qPCR en las células A549 a partir de las cepas HEV_C1_Uy y HEV-7_uy en ninguna de las condiciones evaluadas.

6.5.2.2. Infección en la línea A549/D3

Sin embargo, si se confirmó el aislamiento *in vitro* de HEV_C1_Uy en las células A549/D3 a los 17 días post-infección (dpi) por RT-qPCR recuperándose un título viral de $4{,}17x10^5$ copias ARN/µl y $6{,}94x10^4$ copias ARN/µl para las monocapas celulares que fueron infectadas con los inóculos de $9.0x10^6$ y $6.7x10^6$ copias ARN HEV totales, respectivamente (provenientes de un inóculo de $7{,}7x10^4$ copias ARN/µl). Los inóculos debieron ser incubados por 1 hora ya que a mayor tiempo se observó un desprendimiento de las células.

El aislamiento de HEV_C1_Uy mantuvo un título viral estable durante el período que se mantuvieron los cultivos viables mediante subcultivos cada 72 hrs.

Además, la replicación de HEV_C1_Uy fue confirmada por el método de IFI (Figura 15), obteniéndose los mejores resultados para la condición 1 (Ac 1°-- 1/50 | Ac 2° -- 1/100).

Contrariamente, los inóculos de $1.3x10^7$ y $2.7x10^7$ copias ARN totales de HEV_C1_Uy resultaron ser muy tóxicos para las células provocando un desprendimiento total de las monocapas celulares a los pocos minutos.

Por otro lado, no fue posible aislar la cepa HEV-7_uy.

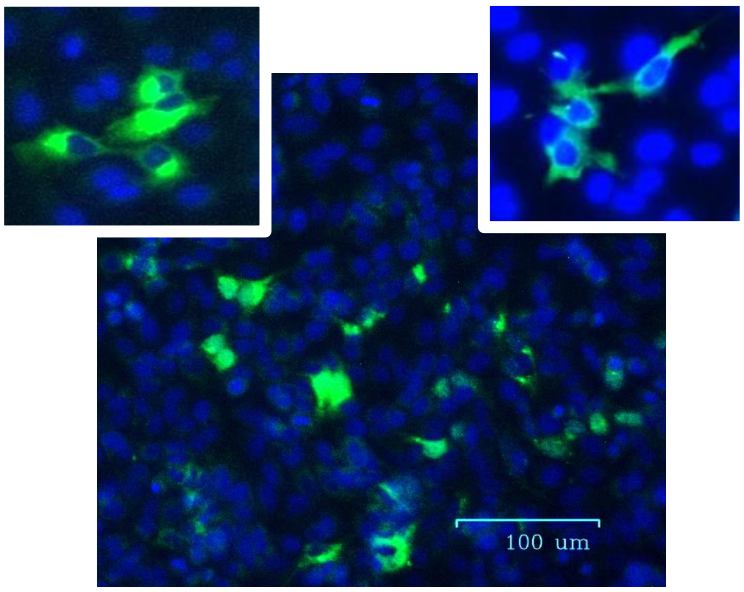

Figura 15. Ensayo de inmunofluorescencia en células A549/D3 infectadas con la cepa HEV_C1_Uy. Se observa la señal de fluorescencia para Ac-anti ORF2-FITC en los citoplasmas celulares y los núcleos teñidos de azul con DAPI.

6.5.3 Obtención de cultivos primarios de hepatocitos de jabalí.

Luego de realizada la disgregación celular del tejido hepático de los 3 jabalíes, a los 2 días post plaqueo se observó adhesión de las células a las placas de cultivo (Figura 16) pero no se obtuvo un crecimiento confluente en monocapa celular. A los 30 días post plaqueo se decidió realizar el primer subcultivo, sin embargo, a los pocos días el cultivo no permaneció viable, por lo que no fue posible llevar a cabo ensayos de aislamiento viral.

En paralelo, se realizó el test de ELISA (Anti-HEV total) para los sueros obtenidos de los 3 jabalíes, resultando positivo para 2 de ellos. Posteriormente, se extrajo el ARN total de los sueros y los mismos fueron analizados por RT-PCR arrojando resultados negativos para los 3 casos, descartando así una infección activa.

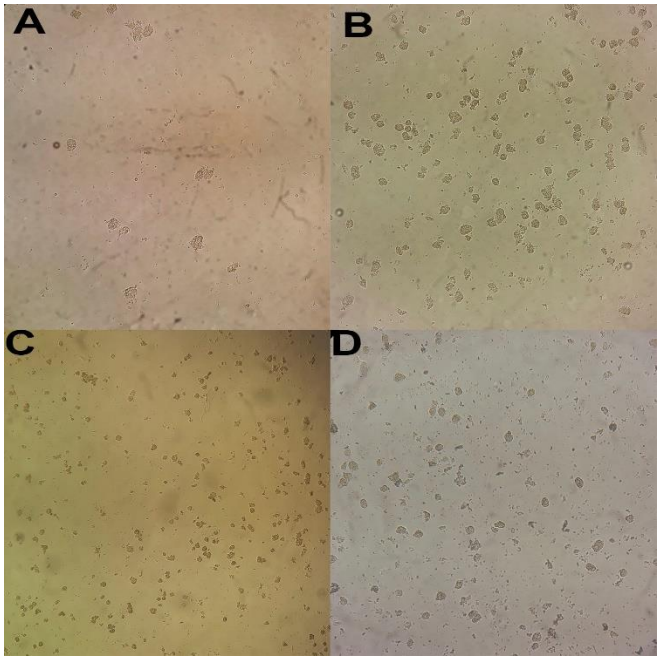

Figura 16. Imágenes de cultivo primario de hepatocitos de jabalí obtenidas por microscopio óptico invertido.
A. Células adheridas a los 2 días post plaqueo (20X). **B.** Células a los 12 días post plaqueo (20x) y **C** (10x).
D. Primer pasaje celular a los 30 días post plaqueo (20X).

6.5.4 Ensayo de resistencia a RBV *in vitro*.

En primer lugar, se obtuvo una viabilidad celular del 100% para las células A549/D3 sin infectar tratadas con RBV en el rango de concentración evaluado de 3,9 µM a 1000 µM por el

método de MTT. No se obtuvo el valor de CC50% al representar concentraciones no citotóxicas.

Para el caso de la infección con la cepa HEV_47832c tratada con RBV, se observó una marcada disminución del título viral a partir de la concentración de 15,62 µM y no se detectó ARN viral para la concentración de 62,5 µM (Figura 17).

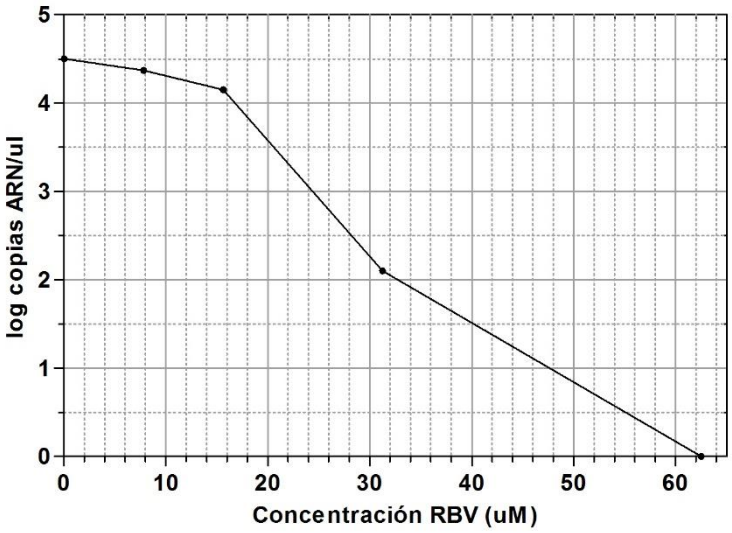

Figura 17. Gráfico de concentración viral de la cepa HEV 47832c en células A549/D3 tratadas con RBV. Se obtuvieron los valores de copias de log ARN/µl mediante RT-qPCR. Se incluyeron los puntos de 7,8 a 62,5 µM de RBV.

Por otro lado, el tratamiento de la droga RBV en células A549/D3 infectadas con HEV_C1_Uy mostró que a partir de la concentración de 250 µM no se detectó ARN de HEV por RT-qPCR (Figura 18A). El control realizado de tratamiento a concentración fija de 62,5 µM evidenció que a partir del séptimo día del ensayo no hubo presencia del genoma viral (Figura 18B).

Además, el control de células infectadas sin tratamiento de RBV permitió validar el estudio ya que se detectó título viral entre los 20 a 45 dpi de duración del ensayo (Figura 18C).

Por otro lado, el análisis de los 3 subcultivos realizados en paralelo (a 125 µM, 125 µM y 250 µM) a partir del pasaje inicial con 125 µM, con el objetivo de ejercer una presión selectiva de resistencia, dio negativo por RT-qPCR para los 3 casos.

Se obtuvieron los valores de IC50 de RBV para la cepa HEV 47832c (30,45 µM) de infección persistente y para la cepa HEV_C1_Uy (127,50 µM), determinados mediante RT-qPCR (Figura 19).

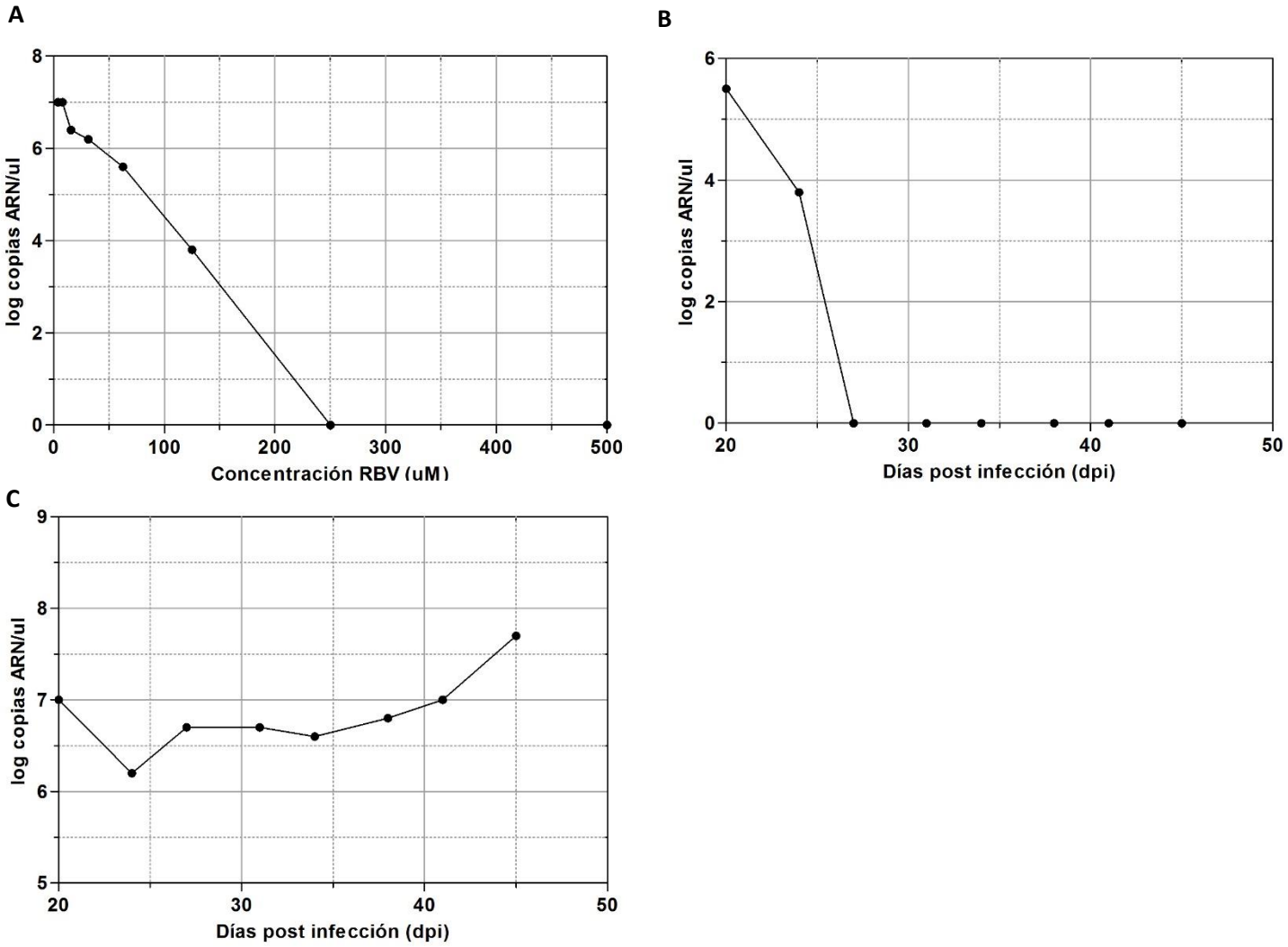

Figura 18. Resultados de concentración viral de la cepa HEV_C1_Uy en células A549/D3 tratadas con RBV. **A**. Log copias ARN/µl en función de la concentración de RBV en el rango comprendido entre 3,9 µM a 500 µM. **B.** Log copias ARN/µl vs concentración fija de RBV a 62,5 µM (concentración inhibitoria para la cepa HEV_47832c testeada) entre los 20 y 45 dpi. **C**. Control de células infectadas sin tratamiento de RBV entre los 20 y 45 dpi.

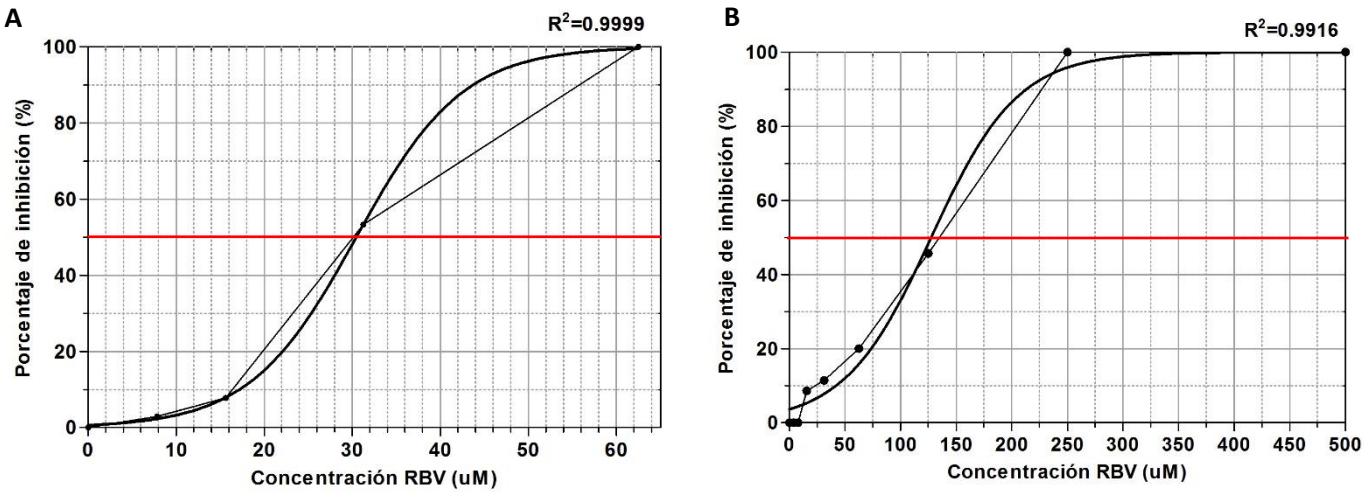

	HEV_47832c	HEV_C1_Uy
IC50	30,45 µM	127,50 µM

Figura 19. Gráficos de IC50 de RBV. En el eje Y se incluyeron los porcentajes de inhibición para la concentración viral de HEV y se calcularon los valores de IC50 por regresión no-lineal (inhibición/dosis-respuesta) para **A**: HEV_47832c y **B**: HEV_C1_Uy. Se indica el coeficiente de determinación (R^2) en la esquina superior de cada gráfico y se muestra la intersección del porcentaje de inhibición correspondiente al 50% mediante una línea roja.

6.5.5 *Array* de perfil de proteoma

En primer lugar, se validaron los 3 ensayos de *array* al registrarse señal de los *spots* de referencia y no observarse señal en los *spots* de control negativo.

Se identificó expresión diferencial de numerosas proteínas relacionadas a apoptosis, a la vía de señalización NFκB y citoquinas con significancia estadística entre las distintas condiciones evaluadas (Figura 20). Particularmente, se observó una expresión diferencial entre las cepas pertenecientes a distintos subtipos de HEV3 (HEV_C1_Uy - nuevo subtipo 3o; HEV_47832c – subtipo 3c).

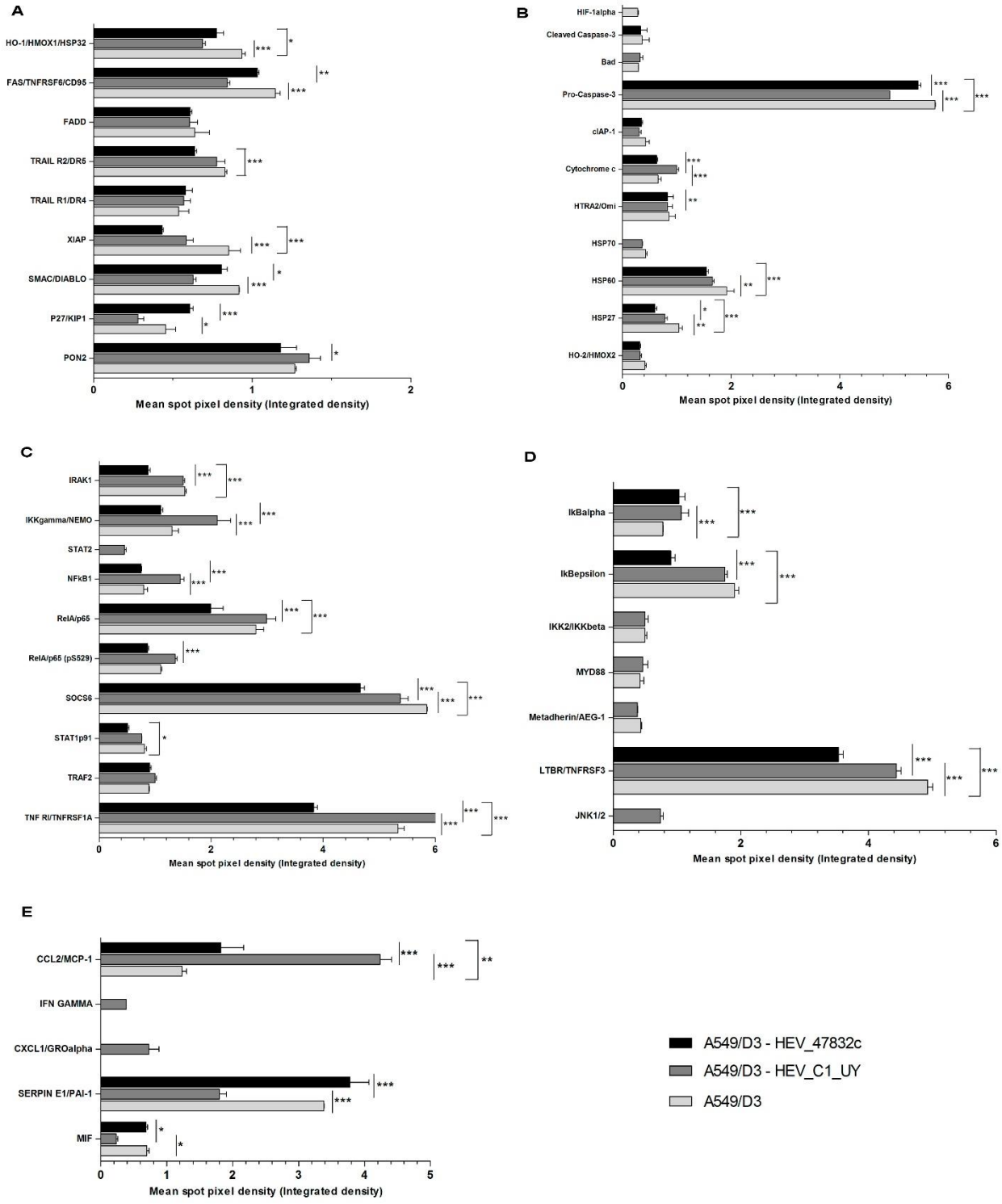

Figura 20. Perfil de expresión relativa de proteínas en A549/D3 infectadas con la cepa HEV_C1_Uy o HEV_47832c y células control. A y B. Perfil de expresión de proteínas relacionadas a apoptosis. **C y D**. Perfil de expresión de proteínas pertenecientes a la vía de señalización NFκB. **E.** Perfil de expresión de citoquinas solubles. Se muestra el valor promedio ± desvío estándar. Los análisis estadísticos fueron realizados con el test de varianza ANOVA-dos factores y el test *post-hoc* de Bonferroni. (*) $p < 0.05$, (**) $p < 0.01$, (***) $p < 0.001$.

7. Discusión global

La información sobre la epidemiología de hepatitis E en el mundo y particularmente en Latinoamérica es aún muy escasa [52]. Es claro que el virus tiene un rango de reservorios animales que está en constante expansión y no está definido cuál es el rol que cumplen en la amplificación de la infección. En Uruguay, además, la elevada seroprevalencia en la población donante de sangre (10%) [71] sugiere que el virus circula en forma críptica, con casos en seres humanos mayormente asintomáticos, y muy probablemente empleando diversos mecanismos de transmisión en forma simultánea.

Es crucial comprender mejor estos procesos y descifrar las claves que permitan entender la dinámica viral de HEV en la interfase animal-humano-medioambiente con un enfoque de Una Salud.

El ciervo Axis (*Axis axis*) es un cérvido exótico, introducido desde Asia a principios del 1900 con fines cinegéticos. Se ha constatado una significativa sobrepoblación de esta especie desde los 2000, con un aumento concomitante en el impacto de pérdidas de cultivos y degradación de hábitat. Por lo tanto, ha sido clasificado como prioridad para establecer medidas de control poblacional mediante la caza [131].

Asimismo, debido a su abundancia, el ciervo Axis cohabita con ganado y grandes poblaciones de jabalíes silvestres (*Sus scrofa*), otra especie exótica ampliamente distribuida en nuestro país. Los cérvidos comparten diversos patógenos y agentes etiológicos con los bovinos y ovinos, lo que podría favorecer la transmisión de enfermedades endémicas o incluso exóticas entre ambas especies [132].

Los datos obtenidos de relevamiento serológico y molecular en ciervos Axis silvestres en esta Tesis indican que esta especie de cérvido puede infectarse con cepas de HEV3 y posiblemente transmitirlo a sus congéneres y otras potenciales especies susceptibles a través de la ruta fecal-oral. HEV es altamente prevalente en jabalíes en Uruguay, por lo tanto, el estrecho y frecuente contacto de estos animales con ciervos Axis, puede promover eventos de "*spill-over*" [133], explotando circuitos no especie-específicos de diseminación viral en la naturaleza. De hecho, la presencia de ARN de HEV en una de las cañadas naturales donde ambas especies comparten puede implicar una potencial fuente adicional de infección de HEV y otros agentes etiológicos.

Estos resultados demuestran, por primera vez, que las cepas zoonóticas de HEV3 junto con variantes de HEV-*like* sin clasificar co-circulan entre ciervos Axis silvestres de dicha población. Interesantemente, estas variantes HEV-*like* podrían corresponder a cepas restringidas a los *Cervidae*, ya que están más cercanamente relacionadas a secuencias de HEV reportadas en alces suecos (*Paslahepevirus alci*) [134], con un valor de p-distancia de 0,103-0,126.

Para profundizar en la caracterización viral de estas cepas HEV-*like*, actualmente estamos trabajando en el diseño de nuevas estrategias para la obtención de genomas completos de HEV de ciervos Axis. Además, para confirmar si los ciervos Axis pueden actuar como reservorios verdaderos de HEV o si se trata de eventos accidentales de "*spill-over*", es necesario expandir el estudio de la presencia de HEV para poblaciones de otras zonas geográficas del país.

Como se mencionó anteriormente, HEV tiene un rango de hospederos en constante expansión. Precisamente, los estudios serológicos realizados en este trabajo evidenciaron la presencia de anticuerpos anti-HEV en venados y ovinos, indicando una posible circulación viral en estas especies, para los cuales existen escasos o nulos reportes [135, 136].

Cabe destacar también, que se reportó la primera secuencia completa de HEV de Sudamérica (HEV_C1_Uy), correspondiente a un paciente con trasplante de hígado infectado crónicamente con HEV3 y la primera proveniente de cerdo (HEV-8_Uy). A raíz de estos resultados, fue posible implementar análisis filogenéticos para genomas completos y parciales de HEV3, los cuales revelaron que las secuencias identificadas en el país de diversas matrices (casos humanos y reservorios animales) presentan escasa divergencia evolutiva y un muy elevado porcentaje de identidad nucleotídica a lo largo de todo el genoma, formando un *cluster* monofilético. Asimismo, este *cluster* presenta una importante divergencia con el resto de los subtipos de HEV3 reportados, encontrándose por encima del valor *cut-off*, suficiente como para ser clasificado según los criterios establecidos como un nuevo subtipo. Esta hipótesis fue confirmada mediante una comunicación directa con el Dr. Donald B. Smith, miembro del grupo de clasificación taxonómica viral (ICTV) de *Hepeviridae*. Por lo tanto, proponemos clasificar al *cluster* de secuencias identificadas en el país como subtipo 3o.

Además, estos resultados indican que la vía zoonótica es probablemente la principal vía de transmisión hacia humanos en el país, surgiendo entonces la hipótesis de que este proceso

pueda ocurrir a través del consumo de alimentos, aunque no puede descartarse que existan otros circuitos de amplificación viral.

Durante el transcurso de escritura de esta Tesis fue publicado un trabajo de Brasil con dos genomas completos de cerdo HEV3 (PRsw1- OQ433914 y RJsw1 - OQ433915), siendo los más cercanamente relacionados a los dos genomas completos uruguayos (valores de p-distancia: 0,117 a 0,124 y valores de identidad nucleotídica: 84,7% a 88,1%) [137]. En dicho artículo, los autores sugieren que estas cuatro secuencias representan un nuevo subtipo, sin embargo, en base a los valores de p-distancia obtenidos, los cuales superan el valor *cut-off* establecido, más genomas completos son necesarios para confirmar si las secuencias brasileras pertenecen al mismo nuevo subtipo que las uruguayas.

Por otro lado, los estudios *in silico* de caracterización de la cepa HEV_C1_Uy, particularmente su RdRp, permitieron brindar información sobre la interacción molecular de esta proteína con el antiviral RBV, determinándose su posible bolsillo de unión.

Interesantemente, la comparación de secuencia entre HEV_C1_Uy con los genotipos de HEV y subtipos de HEV3 revelaron varias diferencias, observándose una sustitución única (V/I1220A) y algunas infrecuentes (T/A1608V, V1659A y Q1700H).

Adicionalmente, HEV_C1_Uy RdRp presentó la sustitución F1439Y (F233Y en HEV_C1_Uy RdRp), asociada significativamente a casos de falla hepática fulminante [138] y V1479I (V273I). Sin embargo, aunque el paciente infectado crónicamente con HEV había sido tratado con RBV por 9 meses, no se observaron mutaciones asociadas a resistencia. Esto sugiere que la resistencia a RBV puede no ser fácilmente alcanzada en algunos pacientes.

A su vez, con el fin de caracterizar la cepa HEV_C1_Uy a nivel *in vitro*, se obtuvo un aislamiento exitoso con títulos virales estables en el tiempo en las células A549/D3, contribuyendo así a la comprensión de la biología viral de HEV permitiendo el estudio de la interacción virus-célula a nivel proteómico.

Sin embargo, no fue posible aislar la cepa HEV-7_uy (proveniente de cerdo con HEV3). La eficiencia del aislamiento parece depender en gran medida de las características específicas de la cepa, ya que se ha reportado que ciertas sustituciones en el genoma viral son necesarias para la adaptación al cultivo celular [55].

Los ensayos de resistencia a RBV, revelaron que si bien no se detectó resistencia fenotípica *in vitro* para las infecciones con las cepas HEV_C1_Uy y HEV_47832c, si se identificó un aumento

en el valor de IC50 para la cepa HEV_C1_Uy (127,50 µM) en comparación con la cepa HEV_47832c (30,45 µM), sugiriendo que quizás algunas características particulares en la secuencia de HEV_C1_Uy (subtipo 3o), la cual comparte 83,2% de identidad nucleotídica con la cepa HEV_47832c (subtipo 3c), podrían estar implicados en este comportamiento. Son muy escasos los estudios *in vitro* que buscan determinar el valor de IC50 de RBV para HEV, empleando mayormente replicones. En un trabajo realizado a partir de distintos constructos para cepas de HEV1 (HEVSar55/S17) y HEV3 (HEVp6, HEVp6-G1634R, HEV 83-2), los autores reportaron diferencias en el valor de IC50 en un rango de 8,16 µM a 43,08 µM de RBV a las 24 hrs post-transfección y un rango de IC50 de 6,90 µM a 62,48 µM de RBV a las 42 hrs post-transfección [129], observándose los mayores valores de IC50 para el clon de HEV1 cepa Sar55 conteniendo el gen ribosomal humano S17 (insertado experimentalmente) a lo cual los autores no atribuyen una razón específica, pudiendo estar asociado a la mayor adaptación al crecimiento *in vitro* producto de esta inserción [129]. De todas formas, no resulta sencillo realizar una comparación directa *a priori* entre ambos trabajos, ya que en esta publicación no se realizó la infección *in vitro* mediante partículas de HEV completamente infectivas provenientes de la muestra biológica, siendo el caso de esta Tesis.

Actualmente, en el marco de un proyecto CSIC, recientemente financiado del cual soy responsable (CSIC INI 2021), se están llevando a cabo estudios funcionales por genética reversa, determinando el efecto en la replicación viral y resistencia a RBV de las sustituciones no-sinónimas únicas identificadas en la RdRp de HEV_C1_Uy, comparándolo a la cepa HEV_47832c adaptada al crecimiento *in vitro* (cedida por el Dr. Reimar Johne) que no presenta esas sustituciones. Dicho proyecto en curso busca complementar los resultados *in silico* recientemente publicados de *docking* molecular de esta Tesis, así como también pretende profundizar los resultados obtenidos a nivel *in vitro.*

Interesantemente, los análisis de perfil de expresión de proteínas revelaron la presencia de varias proteínas diferencialmente expresadas con significancia estadística entre las condiciones evaluadas. Cabe destacar que se observó una expresión diferencial entre las cepas HEV_47832c y HEV_C1_Uy, esta diferencia podría deberse al hecho de que las cepas pertenecen a distintos subtipos 3c y 3o, respectivamente, a que la cepa HEV_47832c es una cepa adaptada al crecimiento *in vitro* con una inserción en la región HVR (ORF1) derivada de la región 3' de ORF1; o puede deberse a otra razón biológica.

Hasta el momento se desconoce si el subtipo de HEV3 juega un rol en la severidad del cuadro de hepatitis E aguda, sin embargo, un estudio realizado en Francia ha sugerido que pacientes inmunocompetentes infectados con HEV3 3f requerirían hospitalización más frecuente debido a una evolución más severa en comparación a los infectados con HEV3 3c. [139]. Asimismo, se ha reportado para una población de pacientes alemanes con infección aguda por HEV3 3efg una mayor frecuencia de hospitalizaciones y cuadro graves, en comparación con los pacientes infectados con 3abchijklm. [140]. Por el contrario, otro trabajo mostró ausencia de asociación entre la severidad del cuadro y la infección por subtipos 3cef [141].

Actualmente, son muy escasos los estudios de proteoma (o de expresión de proteínas) de la infección por HEV (*punto 1.7*. de la sección *Introducción*), por lo que no es posible realizar amplios estudios comparativos. Entre ellos, se han publicado reportes sobre las alteraciones funcionales *in vivo* en la mitocondria de hepatocitos de roedores gerbiles de Mongolia (*Meriones unguiculatus*) infectados por HEV4, destacándose particularmente, un aumento en la expresión de los niveles de las proteínas Bax (pro-apoptótica) y Bcl-2 (anti-apoptótica) [142], las cuales no fueron detectadas en esta Tesis pero si se encontraban incluidas en el kit de *array* utilizado. Conjuntamente, en dicha publicación se reportó una disminución de los niveles de citocromo-c en la mitocondria de los hepatocitos y un aumento de la proteína en el citoplasma celular, sugiriendo que HEV activa la vía apoptótica mitocondrial. Por otro lado, estos autores reportaron que la proteína caspasa-3 se encontraba muy aumentada en el grupo de animales inoculados, probablemente como producto de la liberación del citocromo-c de la mitocondria y posterior activación de la cascada de caspasas. Para el caso de la infección *in vitro* con la cepa HEV_C1_Uy si se detectó un incremento significativo en la expresión de citocromo-c en comparación a la condición control (células no infectadas) y a la cepa HEV_47832c, pero sin embargo, se observó una disminución en los niveles de pro-caspasa 3 y la caspasa-3 en su forma clivada no fue detectada.

Por otra parte, la sobre-expresión de ORF2 de HEV1 en células Huh7 reveló un aumento en la expresión de proteínas chaperonas como Hsp72, Hsp70B' (de la familia Hsp70) y la co-chaperona Hsp40 mediante análisis de *microarray* [143]. Contrariamente, la infección con la cepa HEV_C1_Uy mostró una disminución de proteínas chaperonas como Hsp70, Hsp60 y Hsp27 e interesantemente, Hsp70 no fue detectada en la infección por la cepa HEV_47832c. De todas formas, las proteínas Hsp72 y Hsp40 no se encontraban disponibles en el kit

utilizado. Estudios sugieren que la chaperona Hsc70 (de la familia de las Hsp70) es una de las proteínas que interacciona con la cápside de HEV participando en su ingreso a la célula [114]. Además, un estudio reportó el análisis de perfil de expresión de genes relacionados a la respuesta inmune en hígados de monos rhesus infectados experimentalmente con cepas de HEV1 y HEV3. Si bien no es posible realizar una comparación directa entre expresión a nivel de genes y expresión proteica, en la mencionada publicación se detectaron un gran número de genes con expresión diferencial entre los monos inoculados y los no-inoculados, entre los cuales algunos de ellos se correlacionan con las proteínas alteradas por la infección con HEV_C1_Uy (DIABLO, MYD88, STAT1, STAT2, TNFRI, FADD, CCL2) [57].

Particularmente, las proteínas STAT2, IFNγ, IKKβ y MYD88 se encontraron presentes solamente en la infección con la cepa HEV_C1_Uy. Además, se observó una sobreexpresión de la proteína IKKγ en las células infectadas por esta cepa. Se ha propuesto que estas proteínas pertenecen a la vía de activación de la respuesta inmune innata ante una infección por HEV (Figura 10). Por otro lado, la proteína SOCS6, un regulador negativo de la vía JAK/STAT, se encontró subexpresado para la infección por ambas cepas en comparación a las células sin infectar.

Estos resultados sugieren la inducción de un estado antiviral producto de la infección por HEV, mostrando diferencias de expresión de proteínas entre la infección por HEV_C1_Uy y HEV_47832c.

Similarmente, reportes anteriores han demostrado que los genes de la vía JAK/STAT activados por IFN se encuentran desregulados durante la infección por HEV [144].

Interesantemente, en mi Tesis de Maestría, se observó una sobreexpresión de genes IFI6, IFI16 y concomitantemente los genes de la vía JAK/STAT activados por IFN como JAK3, STAT2, STAT6, IRF7 y una subexpresión de los genes SOCS2 y SOCS3 mediante análisis transcriptómicos en células A549 infectadas con HEV3 (proveniente de un caso agudo [70]) y células no infectadas.

En conclusión, en esta Tesis, mediante metodologías que se desarrollaron y optimizaron específicamente para este proyecto, se presenta información novedosa que contribuye a profundizar aspectos de la epidemiología molecular en el país, así como en la respuesta celular ante la infección por HEV. Los datos obtenidos podrían llegar a brindar

valiosas herramientas para el diseño de potenciales políticas sanitarias para la prevención de la transmisión e infección por HEV.

8. Conclusiones

- Se identificó por primera vez la circulación de cepas de HEV3 y HEV-*like* en ciervos Axis silvestres, sugiriendo que esta especie podría actuar como un reservorio/hospedero para cepas zoonóticas.

- Se obtuvieron los primeros genomas completos de HEV3 de Sudamérica.

- Se encontraron evidencias serológicas de circulación de HEV en fauna silvestre y doméstica.

- Las cepas de HEV3 uruguayas representarían un nuevo subtipo, el cual proponemos nombrar como nuevo 3o.

- Se obtuvo un modelo 3D *in silico* para la RdRp de HEV y se identificó el posible sitio de unión entre RBV y esta proteína.

- Se aisló de forma exitosa la cepa HEV_C1_Uy en células A549/D3.

- Se detectó una resistencia parcial a RBV por la cepa HEV_C1_Uy (IC50: 127,50 µM) en comparación a HEV_47832c (IC50: 30,45 µM).

- Se observó expresión diferencial de proteínas relacionadas a apoptosis, citoquinas y de la vía NFκB entre células A549/D3 infectadas con las cepas HEV_C1_Uy, HEV_47832c y células sin infectar, sugiriendo la inducción de un estado antiviral producto de la infección.

- Los resultados obtenidos podrían ser útiles para colaborar en la prevención de la infección por HEV.

En suma, se generaron e implementaron diversas metodologías para la detección de cepas de *Hepeviridae,* cuantificación, obtención de genomas completos y aislamiento *in vitro.* Varias de estas técnicas y protocolos fueron transferidas a distintos grupos de investigación de Sudamérica, con lo cuales realizamos colaboraciones y capacitaciones.

9. Perspectivas

El trabajo realizado en esta Tesis permitirá el desarrollo de nuevas líneas que contribuirán a profundizar los resultados obtenidos.

- Optimizar e implementar un protocolo de amplificación y cuantificación absoluta de HEV por el sistema de PCR digital QIAcuity (dPCR, Qiagen™) con el fin de compararlo con los resultados obtenidos por RT-qPCR. Los ensayos se llevarán a cabo en un equipo Qiagen de Facultad de Veterinaria, UdelaR.

- Profundizar los estudios de resistencia a RBV mediante técnicas de genética reversa, determinando el efecto en la replicación viral y resistencia antiviral de las sustituciones identificadas en la RdRp de HEV_C1_Uy (V1220A y V1479I) comparándolo con la cepa HEV_47832c. Este punto está siendo abordado en un proyecto CSIC INI, del cual soy responsable.

- A partir del protocolo de IFI optimizado en esta Tesis, implementar un sistema de cuantificación de partículas virales infecciosas mediante FFU para determinar la infectividad específica de HEV en ARN/FFU en los cultivos celulares tratados con RBV. Este punto también será llevado a cabo en el marco del proyecto CSIC INI.

- Identificar las eventuales mutaciones mayoritarias y minoritarias presentes en la región RdRp de la cepa HEV_C1_Uy como consecuencia del tratamiento *in vitro* con RBV, mediante secuenciación masiva de productos de PCR.

- Obtener genomas completos de cepas HEV-*like* de ciervos.

- Evaluar la posibilidad de aislar la muestra Axis_71_uy HEV-*like* de ciervos en células A549/D3 para determinar su infectividad.

- Visualizar partículas virales de HEV-*like* en materia fecal mediante microscopía electrónica de transmisión utilizando el protocolo optimizado en esta Tesis.

- Continuar optimizando el sistema de cultivo primario de hepatocitos de jabalíes con el propósito de obtener un cultivo más estable en el tiempo.

- Desarrollar una estrategia de inoculación oral de cerdos con la cepa 71 HEV-*like* de ciervos para determinar su capacidad de infección y transmisión por contacto directo entre cerdos [145], comparando con el sistema *in vitro*. Este trabajo se realizará en conjunto con la Facultad de Veterinaria, UdelaR.

- Estudiar la presencia de HEV para otras poblaciones de ciervos *Axis axis*.

- Realizar un relevamiento serológico y molecular de HEV a otras especies de animales silvestres y domésticos del país.

10. REFERENCIAS

1. **Sayed IM, Meuleman P**. Updates in Hepatitis E virus (HEV) field; lessons learned from human liver chimeric mice. *Rev Med Virol* 2019;e2086.

2. **Webb GW, Dalton HR**. Hepatitis E: an underestimated emerging threat. *Ther Adv Infect Dis* 2019;6:2049936119837162.

3. **Aslan AT, Balaban HY**. Hepatitis E virus: Epidemiology, diagnosis, clinical manifestations, and treatment. *World J Gastroenterol* 2020;26:5543–5560.

4. **Tam AW, Smith MM, Guerra ME, Huang CC, Bradley DW, *et al.*** Hepatitis E virus (HEV): molecular cloning and sequencing of the full-length viral genome. *Virology* 1991;185:120–131.

5. **Ji H, Chen S, He Q, Wang W, Gong S, *et al.*** The different replication between nonenveloped and quasi-enveloped hepatitis E virus. *J Med Virol* 2021;93:6267–6277.

6. **Guu TSY, Liu Z, Ye Q, Mata DA, Li K, *et al.*** Structure of the hepatitis E virus-like particle suggests mechanisms for virus assembly and receptor binding. *Proc Natl Acad Sci U S A* 2009;106:12992–12997.

7. **van der Heijden MW, Bol JF**. Composition of alphavirus-like replication complexes: involvement of virus and host encoded proteins. *Arch Virol* 2002;147:875–898.

8. **Yin X, Ambardekar C, Lu Y, Feng Z**. Distinct Entry Mechanisms for Nonenveloped and Quasi-Enveloped Hepatitis E Viruses. *J Virol* 2016;90:4232–4242.

9. **Kumar S, Subhadra S, Singh B, Panda BK**. Hepatitis E virus: the current scenario. *Int J Infect Dis* 2013;17:e228-33.

10. **Nan Y, Zhang Y-J**. Molecular Biology and Infection of Hepatitis E Virus. *Front Microbiol* 2016;7:1419.

11. **Paliwal D, Panda SK, Kapur N, Varma SPK, Durgapal H**. Hepatitis E virus (HEV) protease: a chymotrypsin-like enzyme that processes both non-structural (pORF1) and capsid (pORF2) protein. *J Gen Virol* 2014;95:1689–1700.

12. **Parvez MK**. Molecular characterization of hepatitis E virus ORF1 gene supports a papain-like cysteine protease (PCP)-domain activity. *Virus Res* 2013;178:553–556.

13. **Perttilä J, Spuul P, Ahola T**. Early secretory pathway localization and lack of processing for hepatitis E virus replication protein pORF1. *J Gen Virol* 2013;94:807–816.

14. **Suppiah S, Zhou Y, Frey TK**. Lack of processing of the expressed ORF1 gene product of hepatitis E virus. *Virol J* 2011;8:245.

15. **Koonin E V, Gorbalenya AE, Purdy MA, Rozanov MN, Reyes GR, *et al.*** Computer-assisted assignment of functional domains in the nonstructural polyprotein of hepatitis E virus: delineation of an additional group of positive-strand RNA plant and animal viruses. *Proc Natl Acad Sci U S A* 1992;89:8259–8263.

16. **Zhao M, Li X-J, Tang Z-M, Yang F, Wang S-L, *et al.*** A Comprehensive Study of Neutralizing Antigenic Sites on the Hepatitis E Virus (HEV) Capsid by Constructing, Clustering, and Characterizing a Tool Box. *J Biol Chem* 2015;290:19910–19922.

17. **Ding Q, Heller B, Capuccino JM V, Song B, Nimgaonkar I, *et al.*** Hepatitis E virus ORF3 is a functional ion channel required for release of infectious particles. *Proc Natl Acad Sci U S A* 2017;114:1147–1152.

18. **Purdy MA, Drexler JF, Meng X-J, Norder H, Okamoto H, *et al.*** ICTV Virus Taxonomy Profile: Hepeviridae 2022. *J Gen Virol*;103. Epub ahead of print September 2022. DOI: 10.1099/jgv.0.001778.

19. **Batts W, Yun S, Hedrick R, Winton J**. A novel member of the family Hepeviridae from cutthroat trout (Oncorhynchus clarkii). *Virus Res* 2011;158:116–123.

20. **Lin J, Norder H, Uhlhorn H, Belák S, Widén F**. Novel hepatitis E like virus found in Swedish moose. *J Gen Virol* 2014;95:557–570.

21. **Smith DB, Simmonds P, Jameel S, Emerson SU, Harrison TJ, *et al.*** Consensus proposals for classification of the family Hepeviridae. *J Gen Virol* 2014;95:2223–2232.

22. **Tsarev SA, Emerson SU, Reyes GR, Tsareva TS, Legters LJ, *et al.*** Characterization of a prototype strain of hepatitis E virus. *Proc Natl Acad Sci U S A* 1992;89:559–563.

23. **Velavan TP, Pallerla SR, Johne R, Todt D, Steinmann E, *et al.*** Hepatitis E: An update on One Health and clinical medicine. *Liver Int Off J Int Assoc Study Liver* 2021;41:1462–1473.

24. **Li P, Liu J, Li Y, Su J, Ma Z, *et al.*** The global epidemiology of hepatitis E virus infection: A systematic review and meta-analysis. *Liver Int* 2020;40:1516–1528.

25. **Lee G-H, Tan B-H, Teo EC-Y, Lim S-G, Dan Y-Y, *et al.*** Chronic Infection With Camelid Hepatitis E Virus in a Liver Transplant Recipient Who Regularly Consumes Camel Meat and Milk. *Gastroenterology* 2016;150:355–7.e3.

26. **Emerson SU, Clemente-Casares P, Moiduddin N, Arankalle VA, Torian U, *et al.*** Putative neutralization epitopes and broad cross-genotype neutralization of Hepatitis E virus confirmed by a quantitative cell-culture assay. *J Gen Virol* 2006;87:697–704.

27. **Okamoto H**. Genetic variability and evolution of hepatitis E virus. *Virus Res* 2007;127:216–228.

28. **Smith DB, Izopet J, Nicot F, Simmonds P, Jameel S, *et al.*** Update : proposed reference sequences for subtypes of hepatitis E virus (species Orthohepevirus A). 2020;1–7.

29. **Treagus S, Wright C, Baker-Austin C, Longdon B, Lowther J**. The Foodborne Transmission of Hepatitis E Virus to Humans. *Food Environ Virol* 2021;13:127–145.

30. **Ruggeri FM, Di Bartolo I, Ponterio E, Angeloni G, Trevisani M, *et al.*** Zoonotic transmission of hepatitis E virus in industrialized countries. *New Microbiol* 2013;36:331–344.

31. **Ahmed R, Nasheri N**. Animal reservoirs for hepatitis E virus within the Paslahepevirus genus. *Vet Microbiol* 2023;278:109618.

32. **Li Y, Qu C, Spee B, Zhang R, Penning LC, *et al.*** Hepatitis E virus seroprevalence in pets in the Netherlands and the permissiveness of canine liver cells to the infection. *Ir Vet J* 2020;73:6.

33. **Mirazo S, Gardinali NR, Cecilia D, Verger L, Ottonelli F, *et al.*** Serological and virological survey of hepatitis E virus (HEV) in animal reservoirs from Uruguay reveals elevated prevalences and a very close phylogenetic relationship between swine and human strains. *Vet Microbiol* 2018;213:21–27.

34. **Ferreiro I, Herrera ML, González I, Cancela F, Leizagoyen C, *et al.*** Hepatitis E Virus (HEV) infection in captive white-collared peccaries (Pecari tajacu) from Uruguay. *Transbound Emerg Dis*. Epub ahead of print August 2020. DOI: 10.1111/tbed.13790.

35. **Sridhar S, Lau SKP, Woo PCY**. Hepatitis E: A disease of reemerging importance. *J Formos Med Assoc* 2015;114:681–690.

36. **Grierson S, Heaney J, Cheney T, Morgan D, Wyllie S, *et al.*** Prevalence of Hepatitis E Virus Infection in Pigs at the Time of Slaughter, United Kingdom, 2013. *Emerg Infect Dis* 2015;21:1396–1401.

37. **Sooryanarain H, Heffron CL, Hill DE, Fredericks J, Rosenthal BM, *et al.*** Hepatitis E Virus in Pigs from Slaughterhouses, United States, 2017-2019. *Emerg Infect Dis* 2020;26:354–357.

38. **Renou C, Cadranel J-F, Bourlière M, Halfon P, Ouzan D, *et al.*** Possible zoonotic transmission of hepatitis E from pet pig to its owner. *Emerg Infect Dis* 2007;13:1094–1096.

39. **Meng X-J**. Zoonotic and foodborne transmission of hepatitis E virus. *Semin Liver Dis* 2013;33:41–49.

40. **Galiana C, Fernández-Barredo S, García A, Gómez MT, Pérez-Gracia MT**. Occupational exposure to hepatitis E virus (HEV) in swine workers. *Am J Trop Med Hyg* 2008;78:1012–1015.

41. **Christensen PB, Engle RE, Hjort C, Homburg KM, Vach W, *et al.*** Time trend of the prevalence of hepatitis E antibodies among farmers and blood donors: a potential zoonosis in Denmark. *Clin Infect Dis an Off Publ Infect Dis Soc Am* 2008;47:1026–1031.

42. **Mitsui T, Tsukamoto Y, Yamazaki C, Masuko K, Tsuda F, *et al.*** Prevalence of hepatitis E virus infection among hemodialysis patients in Japan: evidence for infection with a genotype 3 HEV by blood transfusion. *J Med Virol* 2004;74:563–572.

43. **Satake M, Matsubayashi K, Hoshi Y, Taira R, Furui Y, *et al.*** Unique clinical courses of transfusion-transmitted hepatitis E in patients with immunosuppression. *Transfusion* 2017;57:280–288.

44. **Hewitt PE, Ijaz S, Brailsford SR, Brett R, Dicks S, *et al.*** Hepatitis E virus in blood components: a prevalence and transmission study in southeast England. *Lancet (London, England)* 2014;384:1766–1773.

45. **Boland F, Martinez A, Pomeroy L, O'Flaherty N**. Blood Donor Screening for Hepatitis e Virus in the European Union. *Transfus Med Hemotherapy* 2019;46:95–103.

46. **Cancela F, Noceti O, Arbiza J, Mirazo S**. Structural aspects of hepatitis E virus. *Arch Virol* 2022;167:2457–2481.

47. **Lhomme S, Marion O, Abravanel F, Izopet J, Kamar N**. Clinical Manifestations, Pathogenesis and Treatment of Hepatitis E Virus Infections. *J Clin Med*;9. Epub ahead of print January 2020. DOI: 10.3390/jcm9020331.

48. **Kumar A, Saraswat VA**. Hepatitis E and Acute-on-Chronic Liver Failure. *J Clin Exp Hepatol* 2013;3:225–230.

49. **Hepatology TLG**. Hepatitis E: a neglected virus. *The lancet. Gastroenterology & hepatology* 2016;1:261.

50. **Nimgaonkar I, Ding Q, Schwartz RE, Ploss A**. Hepatitis E virus: advances and challenges. *Nat*

Rev Gastroenterol Hepatol 2018;15:96–110.

51. **Tanaka T, Takahashi M, Kusano E, Okamoto H**. Development and evaluation of an efficient cell-culture system for Hepatitis E virus. *J Gen Virol* 2007;88:903–911.

52. **Fu RM, Decker CC, Dao Thi VL**. Cell Culture Models for Hepatitis E Virus. *Viruses*;11. Epub ahead of print July 2019. DOI: 10.3390/v11070608.

53. **Shukla P, Nguyen HT, Faulk K, Mather K, Torian U, *et al.*** Adaptation of a genotype 3 hepatitis E virus to efficient growth in cell culture depends on an inserted human gene segment acquired by recombination. *J Virol* 2012;86:5697–5707.

54. **Nguyen HT, Torian U, Faulk K, Mather K, Engle RE, *et al.*** A naturally occurring human/hepatitis e recombinant virus predominates in serum but not in faeces of a chronic hepatitis E patient and has a growth advantage in cell culture. *J Gen Virol* 2012;93:526–530.

55. **Johne R, Reetz J, Ulrich RG, Machnowska P, Sachsenröder J, *et al.*** An ORF1-rearranged hepatitis e virus derived from a chronically infected patient efficiently replicates in cell culture. *J Viral Hepat* 2014;21:447–456.

56. **Shukla P, Nguyen HT, Torian U, Engle RE, Faulk K, *et al.*** Cross-species infections of cultured cells by hepatitis E virus and discovery of an infectious virus – host recombinant. *Proc Natl Acad Sci U S A* 2011;108:1–6.

57. **Choi YH, Zhang X, Tran C, Skinner B**. Expression profiles of host immune response-related genes against HEV genotype 3 and genotype 1 infections in rhesus macaques. *J Viral Hepat* 2018;25:986–995.

58. **Shen Q, Pu Y, Fu X, Xie Y, Bian X, *et al.*** Changes in the cellular proteins of A549 infected with Hepatitis E virus by proteomics analysis. *BMC Vet Res* 2014;10:1–8.

59. **Rogée S, Le Gall M, Chafey P, Bouquet J, Cordonnier N, *et al.*** Quantitative Proteomics Identifies Host Factors Modulated during Acute Hepatitis E Virus Infection in the Swine Model. *J Virol* 2015;89:129–143.

60. **Wu J, Xu Y, Cui Y, Bortolanza M, Wang M, *et al.*** Dynamic changes of serum metabolites associated with infection and severity of patients with acute hepatitis E infection. *J Med Virol* 2022;94:2714–2726.

61. **Jagya N, Varma SPK, Thakral D, Joshi P, Durgapal H, *et al.*** RNA-seq based transcriptome analysis of hepatitis E virus (HEV) and hepatitis B virus (HBV) replicon transfected Huh-7 cells. *PLoS One* 2014;9:e87835.

62. **Xu K, Guo S, Zhao T, Zhu H, Jiao H, *et al.*** Transcriptome Analysis of HepG2 Cells Expressing ORF3 from Swine Hepatitis E Virus to Determine the Effects of ORF3 on Host Cells. *Biomed Res Int* 2016;2016:1648030.

63. **Kamar N, Garrouste C, Haagsma EB, Garrigue V, Pischke S, *et al.*** Factors associated with chronic hepatitis in patients with hepatitis E virus infection who have received solid organ transplants. *Gastroenterology* 2011;140:1481–1489.

64. **Pischke S, Hardtke S, Bode U, Birkner S, Chatzikyrkou C, *et al.*** Ribavirin treatment of acute and chronic hepatitis E: a single-centre experience. *Liver Int* 2013;33:722–726.

65. **Kamar N, Izopet J, Tripon S, Bismuth M, Hillaire S, *et al.*** Ribavirin for chronic hepatitis E virus infection in transplant recipients. *N Engl J Med* 2014;370:1111–1120.

66. **Debing Y, Ramiere C, Dallmeier K, Piorkowski G, Trabaud M-A, *et al.*** Hepatitis E virus mutations associated with ribavirin treatment failure result in altered viral fitness and ribavirin sensitivity. *J Hepatol* 2016;65:499–508.

67. **Kamar N, Chatelut E, Manolis E, Lafont T, Izopet J, *et al.*** Ribavirin pharmacokinetics in renal and liver transplant patients: evidence that it depends on renal function. *Am J kidney Dis Off J Natl Kidney Found* 2004;43:140–146.

68. **Blasco-Perrin H, Abravanel F, Blasco-Baque V, Peron JM**. Hepatitis E, the neglected one. *Liver Int* 2016;36 Suppl 1:130–134.

69. **Azman AS, Ciglenecki I, Wamala JF, Lynch J, Aggarwal R, *et al.*** Hepatitis E should be considered a neglected tropical disease. *PLoS Negl Trop Dis* 2019;13:e0007453.

70. **Mirazo S, Ramos N, Russi JC, Gagliano G, Arbiza J**. Detection and molecular characterization of sporadic cases of acute human hepatitis E virus infection in Uruguay. *Arch Virol* 2011;156:1451–1454.

71. **Bangueses F, Abin-Carriquiry JA, Cancela F, Curbelo J, Mirazo S**. Serological and molecular prevalence of hepatitis E virus among blood donors from Uruguay. *J Med Virol*. Epub ahead of print 2020. DOI: 10.1002/jmv.26231.

72. **Mirazo S, Mainardi V, Ramos N, Gerona S, Rocca A, *et al.*** Indigenous hepatitis E virus genotype 1 infection, Uruguay. *Emerging infectious diseases* 2014;20:171–173.

73. **MSP**. DIRECCIÓN GENERAL DE LA SALUD DIVISIÓN EPIDEMIOLOGÍA Departamento de Vigilancia en Salud.

74. **Mainardi V, Gerona S, Ardao G, Ferreira N, Ramirez G, *et al.*** Locally Acquired Chronic Hepatitis E Followed by Epstein-Barr Virus Reactivation and Burkitt Lymphoma as a Suspected Extrahepatic Manifestation in a Liver Transplant Recipient. *Am J Case Rep* 2019;20:1016–1021.

75. **Mainardi V, Ardao G, Mirazo S, Cecilia D, Galbisso R, *et al.*** Primer caso de falla hepática por el virus de la hepatitis E en Uruguay. *Arch Med Interna* 2014;36:111–114.

76. **Cancela F**. *Aproximación al estudio de la replicación in vitro del Virus de la Hepatitis E (HEV) a través de análisis proteómicos y transcriptómicos.* Universidad de la República; 2018.

77. **Gebreyes WA, Dupouy-Camet J, Newport MJ, Oliveira CJB, Schlesinger LS, *et al.*** The Global One Health Paradigm: Challenges and Opportunities for Tackling Infectious Diseases at the Human, Animal, and Environment Interface in Low-Resource Settings. *PLoS Negl Trop Dis*;8. Epub ahead of print 2014. DOI: 10.1371/journal.pntd.0003257.

78. **Glud HA, George S, Skovgaard K, Larsen LE**. Zoonotic and reverse zoonotic transmission of viruses between humans and pigs. *Apmis* 2021;129:675–693.

79. **Smith DB, Ijaz S, Tedder RS, Hogema B, Zaaijer HL, *et al.*** Variability and pathogenicity of hepatitis E virus genotype 3 variants. *J Gen Virol* 2015;96:3255–3264.

80. **Nicot F, Dimeglio C, Migueres M, Jeanne N, Latour J, *et al.*** Classification of the Zoonotic Hepatitis E Virus Genotype 3 Into Distinct Subgenotypes. *Front Microbiol* 2021;11:1–8.

81. **Ibarbalz FM, Pérez MV, Figuerola ELM, Erijman L**. The bias associated with amplicon sequencing does not affect the quantitative assessment of bacterial community dynamics. *PLoS One* 2014;9:e99722.

82. **Davis CA, Haywood B, Vattipally S, Da Silva Filipe A, AlSaeed M, *et al.*** Hepatitis E virus: Whole genome sequencing as a new tool for understanding HEV epidemiology and phenotypes. *J Clin Virol* 2021;139:104738.

83. **Baylis SA, Blümel J, Mizusawa S, Matsubayashi K, Sakata H, *et al.*** World Health Organization International Standard to harmonize assays for detection of hepatitis E virus RNA. *Emerg Infect Dis* 2013;19:729–735.

84. **Baylis SA, Hanschmann K-MO, Matsubayashi K, Sakata H, Roque-Afonso A-M, *et al.*** Development of a World Health Organization International Reference Panel for different genotypes of hepatitis E virus for nucleic acid amplification testing. *J Clin Virol Off Publ Pan Am Soc Clin Virol* 2019;119:60–67.

85. **Houldcroft CJ, Beale MA, Breuer J**. Clinical and biological insights from viral genome sequencing. *Nat Rev Microbiol* 2017;15:183–192.

86. **Yang J, Yang F, Ren L, Xiong Z, Wu Z, *et al.*** Unbiased parallel detection of viral pathogens in clinical samples by use of a metagenomic approach. *J Clin Microbiol* 2011;49:3463–3469.

87. **Kleiner M, Hooper L V, Duerkop BA**. Evaluation of methods to purify virus-like particles for metagenomic sequencing of intestinal viromes. *BMC Genomics* 2015;16:7.

88. **Li D, Li Z, Zhou Z, Li Z, Qu X, *et al.*** Direct next-generation sequencing of virus-human mixed samples without pretreatment is favorable to recover virus genome. *Biol Direct* 2016;11:3.

89. **Goya S, Valinotto LE, Tittarelli E, Rojo GL, Nabaes Jodar MS, *et al.*** An optimized methodology for whole genome sequencing of RNA respiratory viruses from nasopharyngeal aspirates. *PLoS One* 2018;13:e0199714.

90. Shotgun sequencing. https://www.genome.gov/genetics-glossary/Shotgun-Sequencing.

91. **Legrand-Abravanel F, Mansuy JM, Dubois M, Kamar N, Peron JM, *et al.*** Hepatitis E virus genotype 3 diversity, France. *Emerg Infect Dis* 2009;15:110–114.

92. **Mirazo S, Ramos N, Russi JC, Arbiza J**. Genetic heterogeneity and subtyping of human Hepatitis E virus isolates from Uruguay. *Virus Res* 2013;173:364–370.

93. **Cameron CE, Castro C**. The mechanism of action of ribavirin: Lethal mutagenesis of RNA virus genomes mediated by the viral RNA-dependent RNA polymerase. *Curr Opin Infect Dis* 2001;14:757–764.

94. **Feld JJ, Hoofnagle JH**. Mechanism of action of interferon and ribavirin in treatment of hepatitis C. *Nature* 2005;436:967–972.

95. **Ferrer-Orta C, Arias A, Pérez-Luque R, Escarmis C, Domingo E, *et al.*** Sequential structures provide insights into the fidelity of RNA replication. *Proc Natl Acad Sci U S A* 2007;104:9463–9468.

96. **Hodos RA, Kidd BA, Shameer K, Readhead BP, Dudley JT**. In silico methods for drug repurposing and pharmacology. *Wiley Interdiscip Rev Syst Biol Med* 2016;8:186–210.

97. **Salum LB, Polikarpov I, Andricopulo AD**. Structure-based approach for the study of estrogen receptor binding affinity and subtype selectivity. *J Chem Inf Model* 2008;48:2243–2253.

98. **Kalyaanamoorthy S, Chen Y-PP**. Structure-based drug design to augment hit discovery. *Drug Discov Today* 2011;16:831–839.

99. **Ferreira LG, Dos Santos RN, Oliva G, Andricopulo AD**. *Molecular docking and structure-based drug design strategies*. 2015. Epub ahead of print 2015. DOI: 10.3390/molecules200713384.

100. **El AA**. Ribavirin , Remdesivir , Sofosbuvir , Galidesivir , and Tenofovir against SARS- CoV-2 RNA dependent RNA polymerase (RdRp): A molecular docking study. 253. Epub ahead of print 2020. DOI: 10.1016/j.lfs.2020.117592.

101. **Elfiky AA, Ismail AM**. Molecular docking revealed the binding of nucleotide/side inhibitors to Zika viral polymerase solved structures. *SAR QSAR Environ Res* 2018;29:409–418.

102. **Okamoto H**. Culture systems for hepatitis E virus. *J Gastroenterol* 2013;48:147–158.

103. **Emerson SU, Arankalle VA, Purcell RH**. Thermal stability of hepatitis E virus. *J Infect Dis* 2005;192:930–933.

104. **Johne R, Trojnar E, Filter M, Hofmann J**. Thermal Stability of Hepatitis E Virus as Estimated by a Cell Culture Method. *Appl Environ Microbiol* 2016;82:4225–4231.

105. **Huang R, Li D, Wei S, Li Q, Yuan X, *et al.*** Cell culture of sporadic hepatitis E virus in China. *Clin Diagn Lab Immunol* 1999;6:729–733.

106. **Yamada K, Takahashi M, Hoshino Y, Takahashi H, Ichiyama K, *et al.*** Construction of an infectious cDNA clone of hepatitis E virus strain JE03-1760F that can propagate efficiently in cultured cells. *J Gen Virol* 2009;90:457–462.

107. **Takahashi M, Tanaka T, Takahashi H, Hoshino Y, Nagashima S, *et al.*** Hepatitis E Virus (HEV) strains in serum samples can replicate efficiently in cultured cells despite the coexistence of HEV antibodies: characterization of HEV virions in blood circulation. *J Clin Microbiol* 2010;48:1112–1125.

108. **Schemmerer M, Apelt S, Trojnar E, Ulrich RG, Wenzel JJ, *et al.*** Enhanced replication of hepatitis E virus strain 47832C in an A549-derived subclonal cell line. *Viruses*;8. Epub ahead of print 2016. DOI: 10.3390/v8100267.

109. **Lhomme S, Garrouste C, Kamar N, Saune K, Abravanel F, *et al.*** Influence of polyproline region and macro domain genetic heterogeneity on HEV persistence in immunocompromised patients. *J Infect Dis* 2014;209:300–303.

110. **Bruenn JA**. A structural and primary sequence comparison of the viral RNA-dependent RNA polymerases. *Nucleic Acids Res* 2003;31:1821–1829.

111. **Debing Y, Gisa A, Dallmeier K, Pischke S, Bremer B, *et al.*** A mutation in the hepatitis E virus RNA polymerase promotes its replication and associates with ribavirin treatment failure in organ transplant recipients. *Gastroenterology* 2014;147:1006–1008.

112. **Young K, Lindsay KL, Lee K, Liu W, He J, *et al.*** Identification of a Ribavirin-Resistant NS5B Mutation of Hepatitis C Virus During Ribavirin Monotherapy. Epub ahead of print 2011. DOI: 10.1053/jhep.2003.50445.

113. **Severson WE, Schmaljohn CS, Javadian A, Jonsson CB**. Ribavirin causes error catastrophe during Hantaan virus replication. *J Virol* 2003;77:481–488.

114. **Devhare P, Madiyal M, Mukhopadhyay C, Shetty S, Shastry S**. Interplay between hepatitis E virus and host cell pattern recognition receptors. *Int J Mol Sci*;22. Epub ahead of print 2021. DOI: 10.3390/ijms22179259.

115. **Aggarwal R, Goel A**. Advances in hepatitis E - I: virology, pathogenesis and diagnosis. *Expert Rev Gastroenterol Hepatol* 2016;10:1053–1063.

116. **Guidotti LG, Chisari F V**. Noncytolytic control of viral infections by the innate and adaptive immune response. *Annu Rev Immunol* 2001;19:65–91.

117. **Liu C, Chu D, Kalantar-Zadeh K, George J, Young HA, *et al.*** Cytokines: From Clinical Significance to Quantification. *Adv Sci (Weinheim, Baden-Wurttemberg, Ger* 2021;8:e2004433.

118. **Griffith JW, Sokol CL, Luster AD**. Chemokines and chemokine receptors: positioning cells for host defense and immunity. *Annu Rev Immunol* 2014;32:659–702.

119. **Kumar A, Devi SG, Kar P, Agarwal S, Husain SA, *et al.*** Association of cytokines in hepatitis E with pregnancy outcome. *Cytokine* 2014;65:95–104.

120. **Saravanabalaji S, Tripathy AS, Dhoot RR, Chadha MS, Kakrani AL, *et al.*** Viral load, antibody titers and recombinant open reading frame 2 protein-induced TH1/TH2 cytokines and cellular immune responses in self-limiting and fulminant hepatitis e. *Intervirology* 2009;52:78–85.

121. **Devhare PB, Chatterjee SN, Arankalle VA, Lole KS**. Analysis of Antiviral Response in Human Epithelial Cells Infected with Hepatitis E Virus. *PLoS One*;8. Epub ahead of print 2013. DOI: 10.1371/journal.pone.0063793.

122. **Moin SM, Panteva M, Jameel S**. The hepatitis E virus Orf3 protein protects cells from mitochondrial depolarization and death. *J Biol Chem* 2007;282:21124–21133.

123. **Uphoff CC, Drexler HG**. Detection of Mycoplasma contamination in cell cultures. *Curr Protoc Mol Biol* 2014;106:28.4.1-28.4.14.

124. **Uphoff CC, Drexler HG**. Detecting Mycoplasma contamination in cell cultures by polymerase chain reaction. *Methods Mol Med* 2004;88:319–326.

125. **Jothikumar N, Cromeans TL, Robertson BH, Meng XJ, Hill VR**. A broadly reactive one-step real-time RT-PCR assay for rapid and sensitive detection of hepatitis E virus. *J Virol Methods* 2006;131:65–71.

126. **Scholz J, Bächlein C, Gadicherla AK, Falkenhagen A, Tausch SH, *et al.*** Establishment of a plasmid-based reverse genetics system for the cell culture-adapted hepatitis e virus genotype 3c strain 47832c. *Pathogens*;9. Epub ahead of print 2020. DOI: 10.3390/pathogens9030157.

127. **Faral-Tello P, Mirazo S, Dutra C, Perez A, Geis-Asteggiante L, *et al.*** Cytotoxic, virucidal, and antiviral activity of South American plant and algae extracts. *ScientificWorldJournal* 2012;2012:174837.

128. **Präbst K, Engelhardt H, Ringgeler S, Hübner H**. Basic Colorimetric Proliferation Assays: MTT, WST, and Resazurin. *Methods Mol Biol* 2017;1601:1–17.

129. **Todt D, Moeller N, Praditya D, Kinast V, Friesland M, *et al.*** The natural compound silvestrol inhibits hepatitis E virus (HEV) replication in vitro and in vivo. *Antiviral Res* 2018;157:151–158.

130. Proteome profiler array. www.rndsystems.com/products/proteome-profiler-antibody-arrays.

131. Informe Comité de Especies Exóticas Invasoras (CEEI): Especies exóticas invasoras de Uruguay: distribución, impactos socioambientales y estrategias de gestión. C. XII, p.

Montevideo; 2021.

132. **Crispell J, Cassidy S, Kenny K, McGrath G, Warde S, *et al.*** Mycobacterium bovis genomics reveals transmission of infection between cattle and deer in Ireland. *Microb genomics*;6. Epub ahead of print August 2020. DOI: 10.1099/mgen.0.000388.

133. **Anheyer-Behmenburg HE, Szabo K, Schotte U, Binder A, Klein G, *et al.*** Hepatitis E Virus in Wild Boars and Spillover Infection in Red and Roe Deer, Germany, 2013-2015. *Emerg Infect Dis* 2017;23:130–133.

134. **Lin J, Karlsson M, Olofson AS, Belák S, Malmsten J, *et al.*** High prevalence of hepatitis E virus in Swedish moose - A phylogenetic characterization and comparison of the virus from different regions. *PLoS One* 2015;10:1–14.

135. **Sarchese V, Di Profio F, Melegari I, Palombieri A, Sanchez SB, *et al.*** Hepatitis E virus in sheep in Italy. *Transbound Emerg Dis* 2019;66:1120–1125.

136. **Doceul V, Bagdassarian E, Demange A, Pavio N**. Zoonotic Hepatitis E Virus: Classification, Animal Reservoirs and Transmission Routes. *Viruses*;8. Epub ahead of print October 2016. DOI: 10.3390/v8100270.

137. **Dos Santos DRL, Durães-Carvalho R, Gardinali NR, Machado LC, de Paula VS, *et al.*** Uncovering neglected subtypes and zoonotic transmission of Hepatitis E virus (HEV) in Brazil. *Virol J* 2023;20:83.

138. **Smith DB, Simmonds P**. Hepatitis E virus and fulminant hepatitis--a virus or host-specific pathology? *Liver Int Off J Int Assoc Study Liver* 2015;35:1334–1340.

139. **Abravanel F, Dimeglio C, Castanier M, Péron JM, Kamar N, *et al.*** Does HEV-3 subtype play a role in the severity of acute hepatitis E? *Liver Int* 2020;40:333–337.

140. **Schemmerer M, Wenzel JJ, Stark K, Faber M**. Molecular epidemiology and genotype-specific disease severity of hepatitis E virus infections in Germany, 2010–2019. *Emerg Microbes Infect* 2022;11:1754–1763.

141. **Minosse C, Biliotti E, Lapa D, Rianda A, Marchili M, *et al.*** Clinical characteristics of acute hepatitis E and their correlation with HEV genotype 3 subtypes in Italy. *Pathogens* 2020;9:1–22.

142. **Yang Y, Shi R, Soomro MH, Hu F, Du F, *et al.*** Hepatitis E virus induces hepatocyte apoptosis via mitochondrial pathway in Mongolian gerbils. *Front Microbiol*;9. Epub ahead of print 2018. DOI: 10.3389/fmicb.2018.00460.

143. **John L, Thomas S, Herchenröder O, Pützer BM, Schaefer S**. Hepatitis E virus ORF2 protein activates the pro-apoptotic gene CHOP and anti-apoptotic heat shock proteins. *PLoS One* 2011;6:e25378.

144. **Trehanpati N, Sukriti S, Geffers R, Hissar S, Riese P, *et al.*** Gene expression profiles of T cells from hepatitis e virus infected patients in acute and resolving phase. *J Clin Immunol* 2011;31:498–508.

145. **Casas M, Pina S, de Deus N, Peralta B, Martín M, *et al.*** Pigs orally inoculated with swine hepatitis E virus are able to infect contact sentinels. *Vet Microbiol* 2009;138:78–84.

146. **Kamar N, Bendall R, Legrand-Abravanel F, Xia NS, Ijaz S, *et al.*** Hepatitis e. *Lancet* 2012;379:2477–2488.

147. **Himmelsbach K, Bender D, Hildt E**. Life cycle and morphogenesis of the hepatitis E virus. *Emerg Microbes Infect*;7. Epub ahead of print 2018. DOI: 10.1038/s41426-018-0198-7.

148. **Hoofnagle JH, Nelson KE, Purcell RH**. Hepatitis E. *N Engl J Med* 2012;367:1237–1244.

11. ANEXO I

ARTÍCULOS PUBLICADOS VINCULADOS AL TEMA DE TESIS

11.1. Ferreiro I, Herrera ML, González I, **Cancela F**, Leizagoyen C, Loureiro M, Arellano H, Echaides C, Bon B, Castro G, Arbiza J, Mirazo S. Hepatitis E Virus (HEV) infection in captive white-collared peccaries (*Pecari tajacu*) from Uruguay. Transbound Emerg Dis. 2021. 68(3):1040-1045. doi: 10.1111/tbed.13790.

11.2. Bangueses F, Abin-Carriquiry JA, **Cancela F**, Curbelo J, Mirazo S. Serological and molecular prevalence of hepatitis E virus among blood donors from Uruguay. J Med Virol. 2021. 93(6):4010-4014. doi: 10.1002/jmv.26231.

Received: 7 June 2020 | Revised: 3 August 2020 | Accepted: 10 August 2020

DOI: 10.1111/tbed.13790

RAPID COMMUNICATION

Transboundary and Emerging Diseases WILEY

Hepatitis E Virus (HEV) infection in captive white-collared peccaries (*Pecari tajacu*) from Uruguay

Irene Ferreiro[1] | María Laura Herrera[1] | Ignacio González[1] | Florencia Cancela[1] | Carmen Leizagoyen[2] | Matías Loureiro[3] | Hugo Arellano[3] | César Echaides[2] | Brenda Bon[3] | Gustavo Castro[4] | Juan Arbiza[1] | Santiago Mirazo[1]

[1]Sección Virología, Facultad de Ciencias, Universidad de la República, Montevideo, Uruguay

[2]Parque Lecocq, Intendencia Municipal de Montevideo, Montevideo, Uruguay

[3]Estación de Cría de Fauna Autóctona de Pan de Azúcar, Municipio de Maldonado, Maldonado, Uruguay

[4]Area Suinos, Facultad de Veterinaria, Universidad de la República, Montevideo, Uruguay

Correspondence
Santiago Mirazo, Iguá 4225, PC 11400 Montevideo, Uruguay.
Email: smirazo@fcien.edu.uy

Funding information
Comisión Sectorial de Investigación Científica.; Ministerio de Educación y Cultura. Fondo Vaz Ferreira.; Fondo Vaz Ferreira

Abstract

Hepatitis E virus (HEV) infection is a major cause of acute hepatitis worldwide. Clinical presentation of hepatitis E mainly occurs as an acute and self-limited disease, though chronic cases are now being commonly reported in immunocompromised individuals. In high-income developed areas and non-endemic regions, HEV is mainly transmitted by the zoonotic route through direct contact with infected animals or by consumption of contaminated meat products. Although pigs and wild boars are the main reservoirs of the disease, HEV can also infect deer, camels, and rats and seems to have an ever-expanding host range. Peccaries (*Tayassuidae* family, superfamily Suoidea), the 'new world pigs', share susceptibility to several pathogens with domestic pigs and wild boars. Herein, we performed a serological and molecular survey of two captive populations of white-collared peccaries (*Pecari tajacu*) from Uruguay, with the aim to assess the role of the species as an HEV reservoir. One-hundred and one serum samples were analysed for anti-HEV antibodies. Further evidences of active HEV infection were investigated in stool by RT-nested PCR. Animals from both wildlife reserves were exposed to HEV with an overall prevalence of 24.7%. Moreover, HEV RNA could be detected in peccaries' stool samples from one of the reserves. Phylogenetic analysis clustered the strains within HEV-3, closely related to both human and swine isolates. Our work provides the first evidences supporting the notion that white-collared peccaries are susceptible to HEV. However, these data should not be overinterpreted. Further research is needed concerning the role of peccaries in the transmission of HEV.

KEYWORDS
Hepatitis E virus, *Pecari tajacu*, survey

1 | INTRODUCTION

Hepatitis E virus (HEV) is a major cause of acute hepatitis worldwide with 3.3 million symptomatic cases per year and about 70.000 deaths (World Health Organization, 2017). In high-income countries and non-endemic regions, Hepatitis E is regarded as an emerging disease of increasing concern. In this setting, cases are mainly sporadic and autochthonous, and infection seems to occur zoonotically by direct contact or through the consumption of raw or undercooked meat from reservoir animals (Colson & Decoster, 2019). HEV belongs

FIGURE 1 Captive white-collared peccaries (*Pecari tajacu*) from Estación de Cría de Fauna Autóctona (ECFA) (a). View from the entrance of the peccaries' captivity breeding area within ECFA (b). Images taken by the authors

to the *Orthohepevirus A* genus within Hepevirus family and is classified into 8 genotypes (HEV-1 to HEV-8). At least three zoonotic genotypes, HEV-3, HEV-4 and HEV-7 can infect both humans and other mammals, mainly domestic pigs and wild boars (Primadharsini, Nagashima, & Okamoto, 2019).

In immunocompetent individuals, Hepatitis E is commonly an acute and self-limiting disease. However, novel concerning aspects regarding HEV infection have been recently uncovered in high-income countries such as a severe clinical presentation with a wide range of extrahepatic manifestations and the possibility of the disease to become chronic, particularly in immunocompromised individuals and solid organ transplant recipients (Narayanan, Abutaleb, Sherman, & Kottilil, 2019).

Domestic pigs and wild boars are the main reservoirs of HEV, and they are highly exposed to the virus. During the last decade, several studies revealed elevated seroprevalence and infection rates in those animals, possessing a considerable zoonotic risk for human population (Doceul, Bagdassarian, Demange, & Pavio, 2016). Besides, HEV seems to have an ever-expanding host range, and evidence of viral infection has been reported in deers, rodents, ferrets, sheeps and camels (Kenney, 2019).

Peccaries are members of the family Tayassuidae and include three species: collared peccary (*Pecari tajacu*), Chacoan peccary (*Catagonus wagneri*) and the white-lipped peccary (*Tayassu pecari*). Tayassuidae and Suidae family, which comprises pigs and wild boars (*Sus scrofa)*, belong together to the superfamily Suoidea (Frantz et al., 2016).

Peccaries are all confined to the American continent and are distributed throughout a wide range of ecosystems from the south United States to northern Argentina (Briceño-Méndez, Reyna-Hurtado, Calmé, & García-Gil, 2014; Desbiez, Santos, Keuroghlian, & Bodmer, 2009; Frantz et al., 2016). In Uruguay, the collared peccary (*Pecari tajacu*) was abundant until 150–200 years ago, when it got extinct (Achával, Clara, & Olmos, 2004). However, during the last decade, several ambitious government-leaded captive breeding programs for recovering the species have been carried out (Soutullo, Clavijo, & Martínez-Lanfranco, 2013).

Surveillance of pathogens in wild animals is crucial to understand the epidemiology of infectious diseases which can impact in both human and livestock health. Notably, peccaries and swine (domestic pigs and wild boars) share susceptibility to several important infectious agents as Classical Swine Fever virus and *Leptospira* (de Castro et al., 2014; Corn, Lee, Erickson, & Murphy, 1987; Montenegro et al., 2018). HEV, which is widely distributed in swine populations worldwide, has never been reported to infect peccaries. Herein, we performed a detailed serological and molecular survey of two captive populations of collared peccaries (*Pecari tajacu*) from Uruguay, with the aim to identify evidences of HEV infection in this species and to explore its likely role as an active reservoir for the disease.

2 | MATERIALS AND METHODS

2.1 | Animals and sample collection

In this study, were included captive populations of collared peccaries (*Pecari tajacu*) (Figure 1) coming from two wildlife reserves that breed this locally extinct species to be reintroduced into its natural habitat. Estación de Cría de Fauna Autóctona de Pan de Azúcar (ECFA) (34°48′00″S 55°13′00″O) is located in eastern Uruguay and houses 40 animals, whereas Parque Lecocq (34°47′30″S 56°20′03″O), situated in southern Uruguay, has a population of 160 individuals.

Blood samples were obtained from 20 and 81 adult collared peccaries from ECFA and Parque Lecocq, respectively (50% of each

adult population). To this, each animal was chemically immobilized with 2,4–3 mg/kg of tiletamine–zolazepam and 4–6 mg/kg of xylazine, applied by an anaesthetic dart gun. Two millilitres of blood was aseptically collected by vein puncture by trained personnel, and after clottiing, sera samples were kept at −70°C until use.

Additionally, 21 fresh stool samples (25–40 gr) from Parque Lecocq and 4 from ECFA were collected in sterile bags that were kept on ice until processing in the laboratory in the following 3 hr. In both reserves, peccaries use communal latrine areas to defecate and urinate, and animals' faeces are naturally pooled. Therefore, the stool samples were taken from 25 different sites and did not correspond to individual animals.

2.2 | ELISA testing

Detection of anti-HEV IgG/IgM antibodies in the 101 samples was performed using 100 μl of serum by HEV Ab IgG, IgM, IgA version ULTRA (Dia.Pro Diagnostic Bioprobs), in quadruplicate according to the manufacturer's specifications. The assay configuration allows this kit to be used in testing total antibodies against HEV in serum from non-human recipients. For each tested sample, the OD (optical density)/cut-off ratio was calculated. Samples with a ratio >1.1 were considered positive, samples with a ratio <0.9 were considered negative, and samples with a ratio 0.9–1.1 were considered equivocal.

2.3 | RNA extraction and reverse transcription-nested PCR

Stool samples ($N = 21$) from Parque Lecocq were further divided into 6 groups of 3–4 samples each. RNA from these 6 groups and the 4 pools from ECFA were purified from the supernatant of a previously homogenized 10% suspension in phosphate buffer saline (PBS) with TRIzol® (ThermoFisher Scientific) according to manufacturer's instructions. The purified RNA was stored at −70°C.

Reverse transcription was performed in 20 μl volume with random hexamer primers (Life Technologies) and Revert Aid™ (ThermoFisher Scientific) enzyme, following the supplier's recommendations.

HEV RNA detection was accomplished by nested PCR amplification of a 287-bp region within the 5′ end of the ORF1 as previously described (Mirazo, Ramos, Russi, & Arbiza, 2013). A plasmid containing the complete genome of the HEV-1 Hyderabad strain kindly provided by Dr. Shahid Jameel was used as positive control. Several no template control (NTC) were included in each stage.

For phylogenetic analysis, nested PCR amplification of a 330-bp region within ORF2 was carried out according to Meng et al. (1997).

2.4 | Sequencing and phylogenetic analysis

PCR products were sequenced directly in both directions by Macrogen automatic sequencing service (South Korea) and Institut Pasteur de Montevideo, Uruguay. Sequence analysis was performed with Clustal W software, and identity matrices were constructed with BioEdit v7.0.5 software. Phylogenetic tree was reconstructed by the neighbour-joining method with Kimura-2 parameters as the substitution method by using Molecular Evolutionary Genetics Analysis (MEGA) v6.0 software. Reference sequences of each genotype were retrieved from Genbank and included in the analysis (Smith et al., 2016). The substitution model that best fitted the data was obtained with ModelTest tool. Bootstrap values for providing significant evidence for phylogenetic grouping were determined with 1,000 resampling of the data sets.

TABLE 1 Anti-HEV antibodies prevalence and RNA detection in captive peccaries ($N = 101$) from two wildlife reserves in Uruguay

Reserve	*N* of animals	Anti-HEV+ % (*N*)	HEV-RNA+[a], *N* (genotype)
ECFA	20	5% (1)	-
Parque Lecocq	81	29.6% (24)	2 (HEV-3)
Total	101	24.7% (25)	2 (HEV-3)

Abbreviation: ECFA, Estación de Cría de Fauna Autóctona.
[a]Viral RNA detection in stool samples.

3 | RESULTS AND DISCUSSION

ELISA testing for HEV was performed in 101 serum samples from captive adult peccaries held in two reserves. Of note, the ELISA kit used in this study has been extensively used for the detection of anti-HEV antibodies in human and non-human reservoirs (Mirazo et al., 2018; Pankovics et al., 2020; Pisano et al., 2019). Specific anti-HEV antibodies were found in animals from both enclosures with an overall prevalence of 24.7% (25/101). The estimated anti-HEV seroprevalence in Parque Lecocq was 29.6% (24/81) whereas in ECFA, it was 5% (1/20), respectively (Table 1). Several factors could explain this difference. First, given that HEV infection among animals is mainly transmitted by the faecal–oral route (Bouwknegt, Teunis, Frankena, de Jong, & de Roda Husman, 2011), it is possible that the animals from Parque Lecocq are more exposed to contaminated faeces or waste and/or recreational water because the animal density is higher than in ECFA. Second, the existence of co-infections with unrecognized immunosuppressive viruses could lead to chronic HEV infection, thus increasing the duration of viral spreading among peccaries' populations. This effect has been reported in swine herds, where HEV-infected animals co-infected with PRRSV increased the quantity of virus particles shed and extended the shedding period (Salines, Andraud, & Rose, 2017). Therefore, this possibility and the existence of these immunosuppressive pathogens should be further investigated. Additionally, *Pecari tajacu* seems to be susceptible to PRRSV infection, and this is an important point, since this pathogen is widely distributed in Uruguay, at least in pigs (Molina-Barrios et al., 2018; Ramos et al., 2018). And third, given that animal populations were closed, and individuals were not routinely extracted

nor introduced in the enclosures until this work ended, which may have affected the dynamics of the disease, the different source (e.g. genetic background) of the founding individuals of the reserve may have likely played a role in the differential levels of viral susceptibility and spreading. An interesting study performed with 90 domestic pig farms in France suggested that maternal genetic background was likely associated with the risk of HEV infection and level of viral dispersion in the farm. Inherited immunological characteristics and genetic resistance to swine diseases were proposed to be involved (Walachowski et al., 2014).

In concordance with the serological data, obtained by using a non-species-specific assay, viral RNA was detected by nested PCR of 5′ ORF1 in two of the six analysed groups of stool samples from Parque Lecocq, whereas it was not amplified in any of the four faecal pooled samples from ECFA (Table 1). For further phylogenetic analysis, the region within ORF2 was subsequently amplified and sequenced from the two positive groups of samples. Phylogenetic tree reconstruction of HEV genotypes and the two strains detected in this study, named He_Uy_Pc1 and He_Uy_Pc2 (GenBank accession numbers MT497902 and MT497901), showed that they clustered with swine and human strains from HEV-3 genotype, clade 3chi (Figure 2). As expected, the strains detected in samples collected in the same enclosure were identical at both nucleotide and amino acid level. Notably, sequence analysis revealed a high percentage of nucleotide identity (91.4%–99.6%) with human and swine strains detected in Uruguay in the period 2012–2017 (Mirazo et al., 2013, 2018). Furthermore, the He_Uy_Pc1 and He_Uy_Pc2 strains were 100% identical to an HEV sequence recently isolated from a patient chronically infected with HEV (MT497903; Mainardi et al., 2019). This high similarity detected at the nucleotide level is not surprising as the same observation is very frequently reported when comparing both human and swine (domestic pigs and wild boars) HEV strains from a given geographical region (Doceul et al., 2016; Jemeršić et al., 2019). On the other hand, it should be noted that both HEV partial genetic regions selected for molecular analysis are relatively conserved among HEV genotypes. Thus, a much deeper phylogenetic study with complete genomes will be necessary to obtain a more reliable picture of the evolutive relationships between peccary strains and those isolated from human and swine.

Evidently, all these results should not be overinterpreted since much more research is needed, and additional laboratory and epidemiological data are required. For instance, infectious virus could not be successfully isolated in cell culture from none of the HEV-positive samples detected in this work (data not shown). Therefore, it remains unclear if peccaries could indeed transmit HEV to other reservoirs or host including humans; a possibility that should be carefully assessed.

Peccaries are extinct in Uruguay since the 19th century, and in light of the ongoing programs aimed to reintroduce the species into the wild, it should be borne in mind that translocation of wild species as a management strategy in conservation biology is not exempt for risks and carry additional concerns for both the introduced species and the local wild and domestic animal communities.

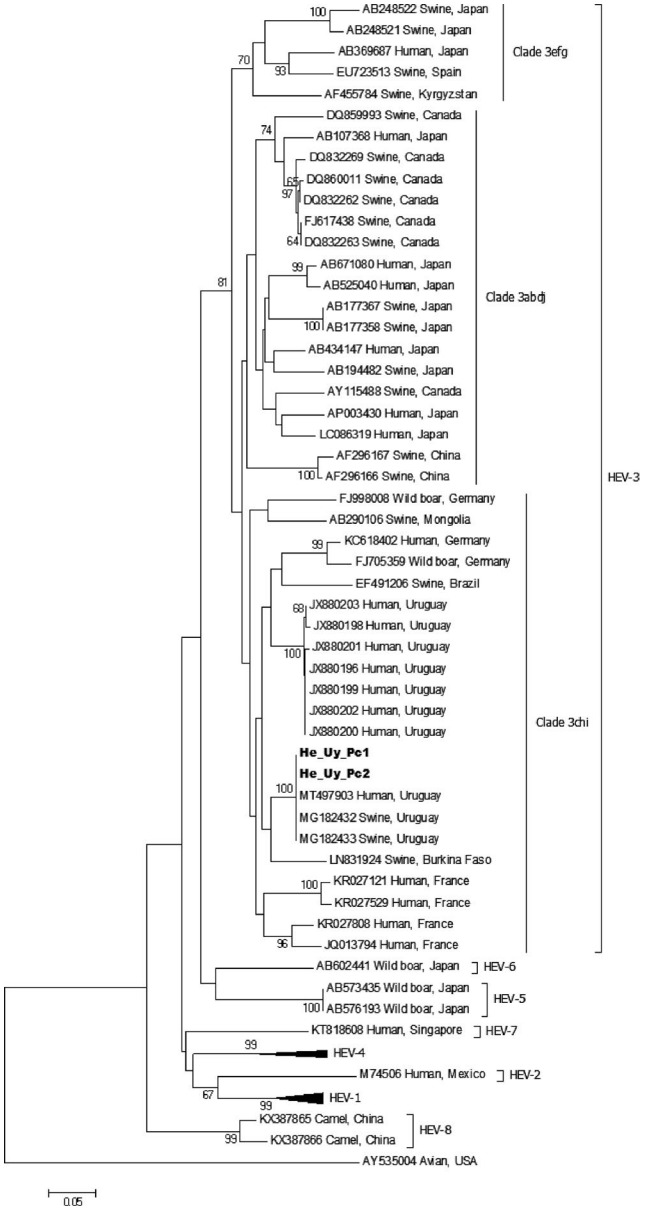

FIGURE 2 Phylogenetic reconstruction of HEV genotypes (HEV-1 to 8) based on the partial 330-nt region within the ORF2. The tree was generated with the neighbour-joining algorithm using Kimura-2 parameters method (as the best substitution model, tested by ModelTest v3.7 tool). Robustness of the tree was determined by bootstrap for 1,000 replicates. Only values ≥60% are shown. Strains He_Uy_Pc1 and He_Uy_Pc2 detected in this study are highlighted in bold

In summary, our work provides the first evidences supporting the notion that white-collared peccaries (*Pecari tajacu*) can be infected by HEV. Results presented herein raise questions regarding the evolutionary history of HEV in non-Sus members of the superfamily Suoidea and offer novel insights on the ever-expanding range of potential reservoirs of the virus.

ACKNOWLEDGMENTS

This work was founded by grants from Fondo Vaz Ferreira, Ministerio de Educación y Cultura and Comisión Sectorial de Investigación

Científica. Authors would like to thank Programa de Desarrollo de las Ciencias Básicas and Agencia Nacional de Investigación e Innovación.

CONFLICT OF INTEREST

The authors declare that they have no conflicts of interest.

ETHICAL APPROVAL

The authors confirm that the ethical policies of the journal, as noted on the journal's author guidelines page, have been adhered to, and the appropriate ethical review committee approval has been received. The experimental procedures and protocols were approved by Comisión Honoraria de Experimentación Animal from Facultad de Ciencias, Universidad de la República (protocol #951, resolution 240011-001479-19). This study did not include any experiments or trials.

DATA AVAILABILITY STATEMENT

The data that support the findings of this study are available from the corresponding author upon reasonable request.

ORCID

Santiago Mirazo https://orcid.org/0000-0003-0121-5268

REFERENCES

Achával, F., Clara, M., & Olmos, A. (2004). *Mamíferos de la República Oriental del Uruguay* (1st ed.). Montevideo, Uruguay: Imprimex.

Bouwknegt, M., Teunis, P. F. M., Frankena, K., de Jong, M. C. M., & de Roda Husman, A. M. (2011). Estimation of the likelihood of fecal-oral HEV transmission among pigs. *Risk Analysis: An Official Publication of the Society for Risk Analysis*, *31*(6), 940–950. https://doi.org/10.1111/j.1539-6924.2010.01546.x

Briceño-Méndez, M., Reyna-Hurtado, R., Calmé, S., & García-Gil, G. (2014). Preferencias de hábitat y abundancia relativa de Tayassu pecari en un área con cacería en la región de Calakmul, Campeche. *México. Revista Mexicana de Biodiversidad*, *85*(1), 242–250. https://doi.org/10.7550/rmb.31937

Colson, P., & Decoster, C. (2019). Recent data on hepatitis E. *Current Opinion in Infectious Diseases*, *32*(5), 475–481. https://doi.org/10.1097/QCO.0000000000000590

Corn, J. L., Lee, R. M., Erickson, G. A., & Murphy, C. D. (1987). Serologic survey for evidence of exposure to vesicular stomatitis virus, pseudorabies virus, brucellosis and leptospirosis in collared peccaries from Arizona. *Journal of Wildlife Diseases*, *23*(4), 551–557. https://doi.org/10.7589/0090-3558-23.4.551

de Castro, A. M. M. G., Brombila, T., Bersano, J. G., Soares, H. S., Silva, S. O., Minervino, A. H. H., … Richtzenhain, L. J. (2014). Swine infectious agents in *Tayassu pecari* and *Pecari tajacu* tissue samples from Brazil. *Journal of Wildlife Diseases*, *50*(2), 205–209. https://doi.org/10.7589/2013-01-021

Desbiez, A. L. J., Santos, S. A., Keuroghlian, A., & Bodmer, R. E. (2009). Niche partitioning among white-lipped peccaries (*Tayassu pecari*), collared peccaries (*Pecari tajacu*), and feral pigs (*Sus Scrofa*). *Journal of Mammalogy*, *90*(1), 119–128. https://doi.org/10.1644/08-mamm-a-038.1

Doceul, V., Bagdassarian, E., Demange, A., & Pavio, N. (2016). Zoonotic hepatitis E virus: Classification, animal reservoirs and transmission routes. *Viruses*, *8*(10), 270. https://doi.org/10.3390/v8100270

Frantz, L., Meijaard, E., Gongora, J., Haile, J., Groenen, M. A. M., & Larson, G. (2016). The evolution of Suidae. *Annual Review of Animal Biosciences*, *4*, 61–85. https://doi.org/10.1146/annurev-animal-021815-111155

Jemeršić, L., Prpić, J., Brnić, D., Keros, T., Pandak, N., & Rode, O. D. (2019). Genetic diversity of hepatitis E virus (HEV) strains derived from humans, swine and wild boars in Croatia from 2010 to 2017. *BMC Infectious Diseases*, *19*, 269. https://doi.org/10.1186/s12879-019-3906-6

Kenney, S. P. (2019). The current host range of hepatitis E viruses. *Viruses*, *11*(5), 452. https://doi.org/10.3390/v11050452

Mainardi, V., Gerona, S., Ardao, G., Ferreira, N., Ramirez, G., Arbiza, J., & Mirazo, S. (2019). Locally acquired chronic hepatitis E followed by Epstein-Barr virus reactivation and Burkitt lymphoma as a suspected extrahepatic manifestation in a liver transplant recipient. *The American Journal of Case Reports*, *20*, 1016–1021. https://doi.org/10.12659/AJCR.916253

Meng, X. J., Purcell, R. H., Halbur, P. G., Lehman, J. R., Webb, D. M., Tsareva, T. S., … Emerson, S. U. (1997). A novel virus in swine is closely related to the human hepatitis E virus. *Proceedings of the National Academy of Sciences of the United States of America*, *94*(18), 9860–9865. https://doi.org/10.1073/pnas.94.18.9860

Mirazo, S., Gardinali, N. R., Cecilia, D. A., Verger, L., Ottonelli, F., Ramos, N., … Arbiza, J. (2018). Serological and virological survey of hepatitis E virus (HEV) in animal reservoirs from Uruguay reveals elevated prevalences and a very close phylogenetic relationship between swine and human strains. *Veterinary Microbiology*, *213*, 21–27. https://doi.org/10.1016/j.vetmic.2017.11.013

Mirazo, S., Ramos, N., Russi, J. C., & Arbiza, J. (2013). Genetic heterogeneity and subtyping of human Hepatitis E virus isolates from Uruguay. *Virus Research*, *173*(2), 364–370. https://doi.org/10.1016/j.virusres.2013.01.005

Molina-Barrios, R., Luevano-Adame, J., Henao-Díaz, Y. A., Giménez-Lirola, L., Piñeyro, P., Magtoto, R., … Zimmerman, J. (2018). Collared peccary (Pecari tajacu) are susceptible to porcine reproductive and respiratory syndrome virus (PRRSV). *Transboundary and Emerging Diseases*, *65*(6), 1712–1719. https://doi.org/10.1111/tbed.12944

Montenegro, O. L., Roncancio, N., Soler-Tovar, D., Cortés-Duque, J., Contreras-Herrera, J., Sabogal, S., … Navas-Suárez, P. E. (2018). Serologic survey for selected viral and bacterial swine pathogens in Colombian collared peccaries (*Pecari tajacu*) and feral pigs (*Sus scrofa*). *Journal of Wildlife Diseases*, *54*(4), 700–707. https://doi.org/10.7589/2017-09-236

Narayanan, S., Abutaleb, A., Sherman, K. E., & Kottilil, S. (2019). Clinical features and determinants of chronicity in hepatitis E virus infection. *Journal of Viral Hepatitis*, *26*(4), 414–421. https://doi.org/10.1111/jvh.13059

Pankovics, P., Némethy, O., Boros, Á., Pár, G., Szakály, P., & Reuter, G. (2020). Four-year long (2014–2017) clinical and laboratory surveillance of hepatitis E virus infections using combined antibody, molecular, antigen and avidity detection methods: Increasing incidence and chronic HEV case in Hungary. *Journal of Clinical Virology*, *124*, 104284. https://doi.org/10.1016/j.jcv.2020.104284

Pisano, M. B., Winter, M., Raimondo, N., Martínez-Wassaf, M. G., Abate, S. D., & Ré, V. E. (2019). New pieces in the transmission cycle of the hepatitis E virus in South America: First viral detection in wild boars from Argentina. *Transactions of the Royal Society of Tropical Medicine and Hygiene*, *113*(8), 497–499. https://doi.org/10.1093/trstmh/trz034

Primadharsini, P. P., Nagashima, S., & Okamoto, H. (2019). Genetic variability and evolution of hepatitis E virus. *Viruses*, *11*(5), 456. https://doi.org/10.3390/v11050456

Ramos, N., Mirazo, S., Castro, G., Cabrera, K., Osorio, F., & Arbiza, J. (2018). First-time detection of porcine reproductive and respiratory syndrome virus (PRRSV) infection in Uruguay. *Transboundary*

and Emerging Diseases, *65*(2), 352–356. https://doi.org/10.1111/tbed.12813

Salines, M., Andraud, M., & Rose, N. (2017). From the epidemiology of hepatitis E virus (HEV) within the swine reservoir to public health risk mitigation strategies: A comprehensive review. *Veterinary Research*, *48*(1), 31. https://doi.org/10.1186/s13567-017-0436-3

Smith, D. B., Simmonds, P., Izopet, J., Oliveira-Filho, E. F., Ulrich, R. G., Johne, R., … Purdy, M. A. (2016). Proposed reference sequences for hepatitis E virus subtypes. *The Journal of General Virology*, *97*(3), 537–542. https://doi.org/10.1099/jgv.0.000393

Soutullo, A., Clavijo, S., & Martínez-Lanfranco, J. (2013). *Especies prioritarias para la conservación en Uruguay-Vertebrados, moluscos continentales y plantas vasculares*. Montevideo, Uruguay.

Walachowski, S., Dorenlor, V., Lefevre, J., Lunazzi, A., Eono, F., Merbah, T., … Rose, N. (2014). Risk factors associated with the presence of hepatitis E virus in livers and seroprevalence in slaughter-age pigs: A retrospective study of 90 swine farms in France. *Epidemiology and Infection*, *142*(9), 1934–1944. https://doi.org/10.1017/S0950268813003063

World Health Organization. (2017). *Global hepatitis report*.

How to cite this article: Ferreiro I, Herrera ML, González I, et al. Hepatitis E Virus (HEV) infection in captive white-collared peccaries (*Pecari tajacu*) from Uruguay. *Transbound Emerg Dis*. 2020;00:1–6. https://doi.org/10.1111/tbed.13790

Received: 21 May 2020 | Accepted: 25 June 2020

DOI: 10.1002/jmv.26231

SHORT COMMUNICATION

JOURNAL OF MEDICAL VIROLOGY WILEY

Serological and molecular prevalence of hepatitis E virus among blood donors from Uruguay

Fernanda Bangueses[1] | Juan A. Abin-Carriquiry[2] | Florencia Cancela[3] | Jorge Curbelo[1] | Santiago Mirazo[3]

[1]Hemocentro, Maldonado, Uruguay

[2]ATGen, Montevideo, Uruguay

[3]Sección Virología, Departamento de Biología Celular y Molecular, Facultad de Ciencias, Universidad de la República, Montevideo, Uruguay

Correspondence
Santiago Mirazo, Iguá 4225 PC, 11400 Montevideo, Uruguay.
Email: smirazo@fcien.edu.uy

Abstract

Hepatitis E virus (HEV) infection is considered a neglected disease of major concern in developed countries. Clinically, HEV occurs as an acute and self-limited disease, though chronic cases mostly associated to HEV-3 are now being commonly reported in immunocompromised individuals and solid organ transplant recipients. Transmission of HEV through blood and derivatives have been increasingly described in the last years, highlighting the importance of including this agent on the screening programs. Since 2010 both acute and chronic hepatitis E cases have been frequently reported in Uruguay. However, updated prevalence data among different population groups are lacking and HEV is not currently screened in blood banks. Herein, we report a seroprevalence and molecular survey of HEV in 400 plasma samples from blood donors. Overall, our results showed an HEV seroprevalence rate of 10% (40/400); almost 10-fold higher than 20 years ago. Total anti-HEV immunoglobulin antibodies were found to increase with age. Moreover, we reported an RNA detection rate of at least 0.75%, and two strains were sequenced. Phylogenetic analysis grouped them with human and swine HEV-3 strains from Uruguay. Data presented here should prompt public health policies of HEV screening in blood banks to minimize the risk of transfusion-transmitted hepatitis E.

KEYWORDS

blood donors, hepatitis E, serologic and molecular prevalence, Uruguay

1 | INTRODUCTION

Globally, hepatitis E virus (HEV) is considered a major cause of acute viral hepatitis. About 20 million people worldwide become infected each year, mostly in developing and resource-poor areas.[1] Furthermore, 3.3 million of these cases are symptomatic that produce 70 000 deaths.[1,2] HEV belongs to the *Orthohepevirus A* genus within *Hepeviridae* family and is classified into eight genotypes (HEV-1 to HEV-8).[3] In developed areas, the majority of cases are sporadic and autochthonous associated to HEV-3, and infection is linked to the consumption of contaminated food, including meat products derived from pigs and wild boars, the main animal reservoirs of the disease.[3] More importantly, HEV can also be a transfusion-transmitted agent, since blood transfusion is considered a source of infection through contaminated blood products or organs derived from asymptomatic HEV-infected individuals.[4] Hepatitis E is typically an acute and self-limiting disease in immunocompetent individuals.[5] However, it has been recently shown that particularly HEV-3 infection may become into a chronic state in immunocompromised individuals as solid organ transplant recipients, frequently displaying a wide range of extrahepatic manifestations, including renal, neurological, and hematological disorders.[5]

In Uruguay, hepatitis E is an important public health problem, and cases are mostly associated with HEV-3.[6] Moreover, the virus is widely spread among domestic pig and wild boars and zoonotic HEV strains have been recently detected.[7] However, updated prevalence data from human population is not currently available since the last

serologic survey was published in 1990s and no further study was performed.[8]

Here, we aimed to investigate the HEV seroprevalence and RNA frequency among blood donors from Uruguay.

2 | MATERIALS AND METHODS

2.1 | Study population and enzyme-linked immunosorbent assay testing

Four-hundred plasma samples were collected during 2017 to 2018 from anonymous blood donors at the Hemocentro from Maldonado city, Uruguay.

Donors were grouped by age range in three groups: 18 to 30, 31 to 50, and ≥51 years old (yo). Total anti-HEV immunoglobulin (Ig) antibodies (Abs) were tested with HEV Ab (Dia.Pro Diagnostic Bioprobs, Italy) and positive samples were further screened for specific anti-HEV immunoglobulin M (IgM) Abs with HEV Ab IgM (Dia.Pro Diagnostic Bioprobs). Test results were interpreted as the ratio of absorbance of the sample and the cutoff. Samples with a ratio greater than 1.1 were considered positive, samples with a ratio less than 0.9 were considered negative, and samples with a ratio of 0.9 to 1.1 were considered equivocal.

2.2 | Reverse-transcription nested polymerase chain reaction

RNA extraction was performed from 140 μL of anti-HEV IgG/IgM positive and negative serum samples with QIAamp Viral RNA Mini Kit (QIAGEN), according to the manufacturer's instructions.

Reverse transcription (RT) was performed in 20 μL volume with random hexamer primers (Life Technologies) and RevertAid (Thermo Fisher Scientific) enzyme.

HEV-RNA detection was accomplished by nested-polymerase chain reaction (PCR) amplification of a region within the 5′-end of the ORF1 as previously reported.[6]

2.3 | Sequencing and phylogenetic analysis

PCR products were sequenced directly in both directions by Macrogen Inc, South Korea, automatic sequencing service. The phylogenetic tree was reconstructed by the neighbor-joining method with Tamura-Nei as the substitution method by using molecular evolutionary genetics analysis v6.0 software. Reference sequences of each HEV genotypes and selected HEV-3 reference subtypes[9] were included in the analysis. The substitution model that best fitted the data was obtained with the ModelTest tool.

2.4 | Statistical analysis

Statistical analysis was performed with Fisher's exact test to determine significant differences between age groups and seropositive results. $P < .05$ in this test was considered statistically significant.

HEV IgG/IgM seroprevalence was determined with 95% confidence intervals (CIs) calculation.

2.5 | Ethical considerations

All participants signed written informed consent and agreed to provide study samples. Samples were processed in accordance with the requirements of the Ministry of Public Health of Uruguay and complied with the ethical standards of the Helsinki Declaration (1964, amended in 2008) of the World Medical Association.

3 | RESULTS

Four-hundred blood donor plasma samples were grouped in three age categories: 18 to 30 yo, 135 samples (33.7%); 31 to 50 yo, 196 samples (49%), and ≥51 yo, 69 samples (17.3%). Overall, 10% (40/400) of samples had specific anti-HEV Ig Abs. These reactive samples grouped as follows: 13 (18.8% [95% CI, 11.3-29.6] of the total from each age category) ≥51 yo, 19 (9.7% [95% CI, 6.3-14.6]) in the 31 to 50, and 8 (5.9% [95% CI, 3.0-11.2]) in blood donors under 30 yo (Table 1). A statistically significant difference in the anti-HEV Ig seroprevalence rate was observed between 18 to 30 and greater than 51 yo groups ($P = .0065$).

Forty anti-HEV IgG positive samples were further tested for anti-HEV IgM, resulting in 19 (4.75% of the total) positive samples: 9 in the 31 to 50 yo group (3.7% [95% CI, 1.6-8.4]) and 5 in each of the other two age categories, 18 to 30 yo group (4.6% [95% CI, 2.4-8.5]), and ≥51 yo group (7.2% [95% CI, 3.1-15.9]).

TABLE 1 Anti-HEV IgG/IgM and RNA detection frequencies in 400 blood donors

Age, y	N (%)	IgG/IgM, N (% [CI, 95%])	IgM, N (% [CI, 95%])	HEV-RNA, N (%)
18-30	135 (33.7)	8 (5.9 [3.0-11.2])*	5 (3.7 [1.6-8.4])	1 (0.74)
31-50	196 (49)	19 (9.7 [6.3-14.6])	9 (4.6 [2.4-8.5])	2 (1)
≥51	69 (17.3)	13 (18.8 [11.3-29.6])*	5 (7.2 [3.1-15.9])	0 (0)
Total	400 (100)	40 (10)[a]	19 (4.75)[b]	3 (0.75)[c,d]

Abbreviations: CI, confidence interval; HEV, hepatitis E virus; IgG, immunoglobulin G.

*Statistically significant difference, $P = .0065$.

[a,b,c]Overall prevalence.

[d]All IgG/IgM+ serum samples and 20 seronegative samples were tested.

HEV-RNA was further investigated in all 40 samples with anti-HEV Ig Abs and in 20 randomly selected seronegative samples. Viral RNA was detected in three HEV IgM+ samples. Sequencing and phylogenetic analyses performed with the 287-base pair ORF1 region grouped two of these strains BD1 and BD2 (Genbank accession numbers MT430885 and MT430886) within HEV-3, very closely related to previously reported human and swine strains from Uruguay (Figure 1). One sample could not be sequenced. On the other hand, viral RNA was detected in none of the seronegative samples.

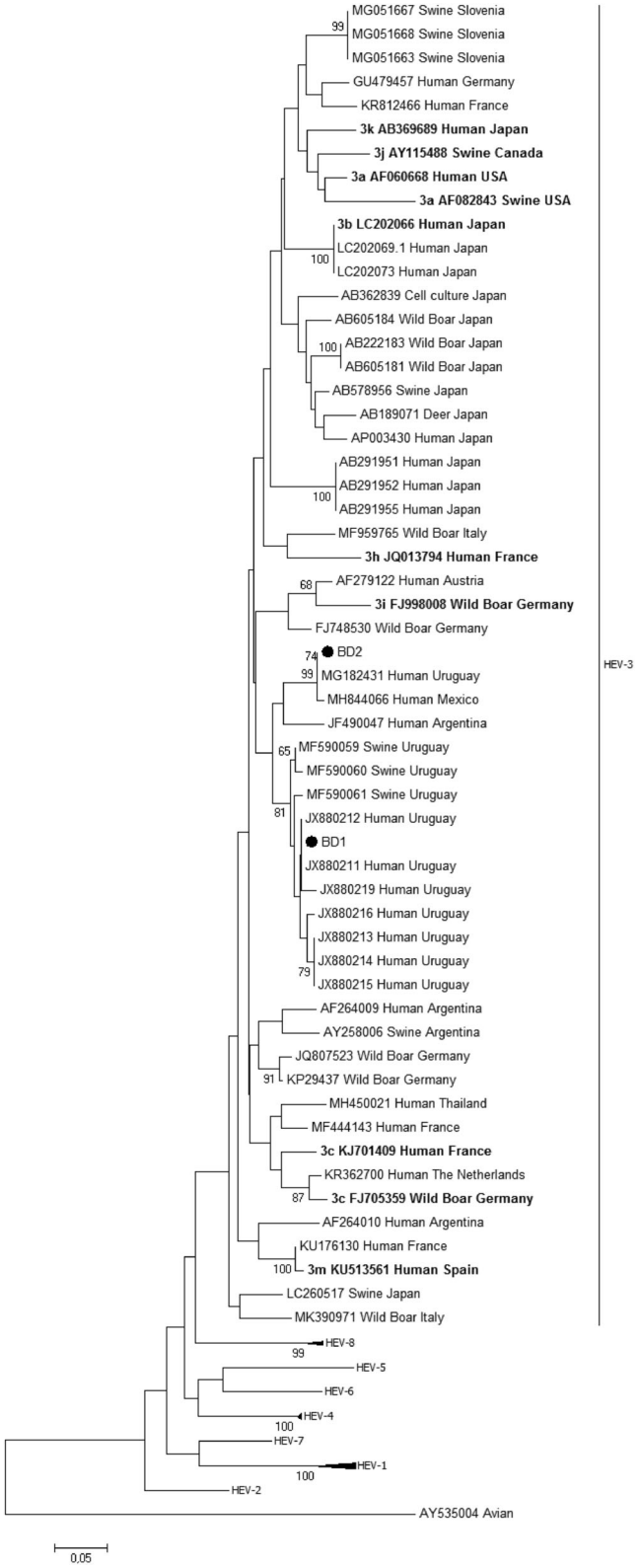

4 | DISCUSSION

Hepatitis E is an emerging disease of increasing concern in the developed world and nonendemic regions. HEV infection is a frequent cause of enteric transmitted acute viral hepatitis worldwide and has recently been recommended to the World Health Organization to be considered a neglected disease.[10]

Even though the parenteral transmission is probably not the main route of transmission of HEV, in 2004, HEV was acknowledged as a transfusion transmissible agent that could consequently jeopardize the blood and organs bank centers.[11]

Screening of blood, blood-derived products, and organs from donors is now becoming necessary, as elevated seroprevalence rates of HEV are being reported in nonendemic regions.[12] Though serologic tests have demonstrated to be useful, particularly those that detect specific anti-IgM-type Abs, RNA detection by RT-PCR is yet considered the gold standard to effectively reduce the risk of HEV transmission to blood and organ transplant recipients.[13] Fortunately, it has been suggested that not all patients receiving transfusions can become infected as shown in one study where the HEV infectivity in blood-contaminated products was 50%,[14] allegedly depending on the viral load and on the presence of Abs in the components.[15] Thus, the simultaneous use of both serologic and molecular tests to screen pooled blood might be appropriate to decide in the critical setting of blood scant in banks, where cost-effectiveness should be evaluated.

In South American countries, HEV is not currently screened in blood banks and the epidemiology of the virus is poorly known.

Herein, to shed some light on this issue, we performed a serologic survey for HEV in Uruguayan blood donors, aimed to update prevalence data. More importantly, this study constitutes a new report in the region describing the frequency of viremia individuals among HEV-seropositive blood donors.

In the last serological survey performed in Uruguay in 1997, 252 blood donors samples from the Montevideo National Blood Bank were analyzed for total HEV Abs and 3 were found positive (1.2%).[8] In our study, the 10% overall rate detected evidence that HEV

FIGURE 1 Phylogenetic tree based on the partial 287-nucleotide region within the ORF1. Reconstruction was generated by using the neighbor-joining algorithm using Tamura-Nei as the best substitution model as tested by the ModelTest v3.7 tool. The robustness of the tree was determined by bootstrap for 1000 replicates. Only values ≥60% are shown. HEV-3 strain BD1 and BD2 detected in this study (GenBank accession numbers MT430885 and MT430886, respectively) are indicated. Reference sequences for HEV-3 subtypes[9] are shown in bold. HEV, hepatitis E virus

prevalence had a 10-fold increase in 20 years among this population. Similar HEV-seropositive rates among blood donors were described in the region in the last 2 years. Very recently, studies from southern Brazil and northern Argentina have reported seroprevalence rates of 7% to 10%, and 9%, respectively.[16,17] In addition, anti-HEV Ig prevalence in blood donors from this study was found to increase with age, a finding that is in concordance with previous data published elsewhere.[16,18]

On the other hand, it may be noted that severe discrepancies and the existence of wide variability in terms of sensitivity and specificity have been reported for commercially available serologic tests.[3] The enzyme-linked immunosorbent assay used in this study is the same of that employed in the two reports from Argentina. This observation should be carefully taken into account when comparing this kind of data from an epidemiological perspective.

In high-income countries, seroprevalence rates varies greatly, from 6% in Canada to 15% in Hong Kong, and 2% to 20% across Europe.[19] Furthermore, some European regions, for example, Southwestern France have shown much higher rates, up to 52%.[18] Hence, given the increased prevalence of HEV in Europe observed in the last decade, partially due to increased awareness and improvement of diagnostic tools, Ireland, UK, Holland, France, Germany, Spain, Austria, and Luxembourg have implemented HEV-RNA screening programs in blood donations.[20]

HEV-RNA detection rate in European blood donors ranges from 0.01% to 0.13%.[20] Here, we report an RNA detection rate of at least 0.75%, considering that all IgG and/or IgM positive samples and some negative samples were tested. All these three positive samples had both anti-IgG- and anti-IgM-specific Abs. Unfortunately, in South America, only the study from Southern Brazil[16] had performed both Abs and RNA detection in blood donors, thus limiting the robustness of any comparative analysis in the region concerning HEV epidemiology in this group. Though higher than most of the European countries, the overall RNA detection rate in blood donors from Brazil is still quite lower than the one reported in this study (0.3% vs a minimum of 0.75%).

HEV-RNA was not detected in the seronegative samples analyzed, which is in agreement with a previous study from Brazil.[16] In fact, the HEV-RNA prevalence rate even among seropositive individuals can be relatively low.[21] Nevertheless, some studies from European countries have reported the presence of HEV-RNA in seronegative samples from blood donors,[22] supporting the notion that molecular tests might be a more reliable approach to screen HEV in blood banks.

Phylogenetic analysis showed that the viral strains detected in blood donors from Uruguay are highly related to previously reported HEV-3 sequences from human (acute and chronic cases) and swine in the country, some of them reported 9 years ago.[6,7] This finding is interesting and suggests a low degree of sequence diversity in the country at the viral 5′ORF1 level, an observation that should be further investigated with genetic analysis involving larger regions.

Altogether, data presented in this study should augment the awareness of hepatitis E as a public health concern, since detection of HEV in blood banks is still not currently settled in most of the developing and nonendemic high-income countries. The serological and molecular detection rates observed among blood donors suggest that intensive and countrywide HEV screening programs should be performed in Uruguay, aimed to reduce the risk of transfusion-transmitted hepatitis E.

CONFLICT OF INTERESTS

The authors declare that there are no conflict of interests.

ORCID

Santiago Mirazo http://orcid.org/0000-0003-0121-5268

REFERENCES

1. World Health Organization. *Global Hepatitis Report*. Geneva, Switzerland: WHO, 2017.
2. Primadharsini PP, Nagashima S, Okamoto H. Genetic variability and evolution of hepatitis E virus. *Viruses*. 2019;11(5):456. https://doi.org/10.3390/v11050456
3. Colson P, Decoster C. Recent data on hepatitis E. *Curr Opin Infect Dis*. 2019;32(5):475-481. https://doi.org/10.1097/QCO.0000000000000590
4. Gallian P, Pouchol E, Djoudi R, et al. Transfusion-transmitted hepatitis E virus infection in France. *Transfus Med Rev*. 2019;33(3):146-153. https://doi.org/10.1016/j.tmrv.2019.06.001
5. Narayanan S, Abutaleb A, Sherman KE, Kottilil S. Clinical features and determinants of chronicity in hepatitis E virus infection. *J Viral Hepat*. 2019;26(4):414-421. https://doi.org/10.1111/jvh.13059
6. Mirazo S, Ramos N, Russi JC, Arbiza J. Genetic heterogeneity and subtyping of human hepatitis E virus isolates from Uruguay. *Virus Res*. 2013;173(2):364-370. https://doi.org/10.1016/j.virusres.2013.01.005
7. Mirazo S, Gardinali NR, Cecilia DA, et al. Serological and virological survey of hepatitis E virus (HEV) in animal reservoirs from Uruguay reveals elevated prevalences and a very close phylogenetic relationship between swine and human strains. *Vet Microbiol*. 2018;213:21-27. https://doi.org/10.1016/j.vetmic.2017.11.013
8. Cruells MR, Mescia G, Gaibisso R, et al. Epidemiological study of hepatitis A and E viruses in different populations in Uruguay. *Gastroenterol Hepatol*. 1997;20(6):295-298.
9. Smith DB, Izopet J, Nicot F, et al. Update: proposed reference sequences for subtypes of hepatitis E virus (species *Orthohepevirus A*). *J Gen Virol*. 2020. https://doi.org/10.1099/jgv.0.001435
10. Azman AS, Ciglenecki I, Wamala JF, et al. Hepatitis E should be considered a neglected tropical disease. *PLoS Negl Trop Dis*. 2019;13(7):e0007453. https://doi.org/10.1371/journal.pntd.0007453
11. Mitsui T, Tsukamoto Y, Yamazaki C, et al. Prevalence of hepatitis E virus infection among hemodialysis patients in Japan: evidence for infection with a genotype 3 HEV by blood transfusion. *J Med Virol*. 2004;74(4):563-572. https://doi.org/10.1002/jmv.20215
12. Sauleda S, Ong E, Bes M, et al. Seroprevalence of hepatitis E virus (HEV) and detection of HEV RNA with a transcription-mediated amplification assay in blood donors from Catalonia (Spain). *Transfusion*. 2015;55(5):972-979. https://doi.org/10.1111/trf.12929
13. Vollmer T, Knabbe C, Dreier J. Comparison of real-time PCR and antigen assays for detection of hepatitis E virus in blood donors. *J Clin Microbiol*. 2014;52(6):2150-2156. https://doi.org/10.1128/JCM.03578-13
14. Satake M, Matsubayashi K, Hoshi Y, et al. Unique clinical courses of transfusion-transmitted hepatitis E in patients with immunosuppression. *Transfusion*. 2017;57(2):280-288. https://doi.org/10.1111/trf.13994
15. Hewitt PE, Ijaz S, Brailsford SR, et al. Hepatitis E virus in blood components: a prevalence and transmission study in southeast England. *Lancet*. 2014;384(9956):1766-1773. https://doi.org/10.1016/S0140-6736(14)61034-5

16. Moss da Silva C, Oliveira JM, Mendoza-Sassi RA, et al. Detection and characterization of hepatitis E virus genotype 3 in HIV-infected patients and blood donors from southern Brazil. *Int J Infect Dis*. 2019;86:114-121. https://doi.org/10.1016/j.ijid.2019.06.027
17. Arce LP, Müller MF, Martinez A, et al. A novel in-house enzyme-linked immunosorbent assay for genotype 3 hepatitis E virus reveals high seroprevalence in blood donors in Northern Argentina. *Front Microbiol*. 2019;10:2481. https://doi.org/10.3389/fmicb.2019.02481
18. Mansuy J-M, Bendall R, Legrand-Abravanel F, et al. Hepatitis E virus antibodies in blood donors, France. *Emerg Infect Dis*. 2011;17(12):2309-2312. https://doi.org/10.3201/eid1712.110371
19. Al-Sadeq DW, Majdalawieh AF, Nasrallah GK. Seroprevalence and incidence of hepatitis E virus among blood donors: a review. *Rev Med Virol*. 2017;27(5):1-10. https://doi.org/10.1002/rmv.1937
20. Boland F, Martinez A, Pomeroy L, O'Flaherty N. Blood donor screening for hepatitis E virus in the European Union. *Transfus Med Hemother*. 2019;46(2):95-103. https://doi.org/10.1159/000499121
21. Tissera G, Lardizabal MC, Torres SB, et al. Hepatitis E virus infection in pregnant women, Argentina. *BMC Infect Dis*. 2020;20:368. https://doi.org/10.1186/s12879-020-05087-3
22. Riveiro-Barciela M, Rando-Segura A, Barreira-Díaz A, et al. Unexpected long-lasting anti-HEV IgM positivity: is HEV antigen a better serological marker for hepatitis E infection diagnosis? *J Viral Hepat*. 2020;27:747-753. https://doi.org/10.1111/jvh.13285

How to cite this article: Bangueses F, Abin-Carriquiry JA, Cancela F, Curbelo J, Mirazo S. Serological and molecular prevalence of hepatitis E virus among blood donors from Uruguay. *J Med Virol*. 2020;1–5. https://doi.org/10.1002/jmv.26231

12. ANEXO II

OTROS ARTÍCULOS PUBLICADOS DURANTE EL DOCTORADO

12.1. **Cancela F**, Marandino A, Panzera Y, Betancour G, Mirazo S, Arbiza J, Ramos N. A combined approach of rolling-circle amplification-single site restriction endonuclease digestion followed by next generation sequencing to characterize the whole genome and intra-host variants of human Torque teno virus. Virus Res. 2022. doi: 10.1016/j.virusres.2022.198974.

12.2. **Cancela F**, Ramos N, Smyth DS, Etchebehere C, Berois M, Rodríguez J, Rufo C, Alemán A, Borzacconi L, López J, González E, Botto G, Thornhill SG, Mirazo S, Trujillo M. Wastewater surveillance of SARS-CoV-2 genomic populations on a country-wide scale through targeted sequencing. PLoS One. 2023. doi: 10.1371/journal.pone.0284483.

12.3. Panzera Y, Mirazo S, Baz M, Techera C, Grecco S, **Cancela F**, Fuques E, Condon E, Calleros L, Camilo N, Fregossi A, Vaz I, Pessina P, Deshpande N, Pérez R, Benech A. Detection and genome characterisation of SARS-CoV-2 P.6 lineage in dogs and cats living with Uruguayan COVID-19 patients. Mem Inst Oswaldo Cruz. 2023. doi: 10.1590/0074-02760220177.

Virus Research 323 (2023) 198974

Contents lists available at ScienceDirect

Virus Research

journal homepage: www.elsevier.com/locate/virusres

Short communication

A combined approach of rolling-circle amplification-single site restriction endonuclease digestion followed by next generation sequencing to characterize the whole genome and intra-host variants of human Torque teno virus

Florencia Cancela [a], Ana Marandino [b], Yanina Panzera [b], Gabriela Betancour [a], Santiago Mirazo [a,c], Juan Arbiza [a], Natalia Ramos [a,*]

[a] Sección Virología, Instituto de Biología e Instituto de Química Biológica, Facultad de Ciencias, Universidad de la República, Montevideo, Uruguay
[b] Sección Genética Evolutiva, Instituto de Biología, Facultad de Ciencias, Universidad de la Republica, Montevideo, Uruguay
[c] Departamento de Bacteriología y Virología, Instituto de Higiene, Facultad de Medicina, Universidad de la Republica, Montevideo, Uruguay

ARTICLE INFO

Keywords:
Torque Teno Virus
Whole genome
Rolling circle-amplification
Restriction endonuclease digestion
Next generation sequencing
Intra-host variants

ABSTRACT

Torque Teno Virus (TTV) was initially associated with post-transfusion hepatitis, but growing evidence of its ubiquity in humans is compatible to no apparent clinical significance. TTV is a small non-enveloped virus with a circular single-negative-stranded DNA genome, belonging to the *Anelloviridae* family. Currently, TTVs are divided in seven phylogenetic groups and are further classified into 21 species. Studies about diversity of TTV in different conditions are receiving increasing interest and in this sense, sequencing of whole genomes for better genetic characterization becomes even more important. Since its discovery in 1997, few TTV complete genomes have been reported worldwide. This is probably due, among other reasons, to the great genetic heterogeneity among TTV strains that prevents its amplification and sequencing by conventional PCR and cloning methods. In addition, although metagenomics approach is useful in these cases, it remains a challenging tool for viromic analysis. With the aim of contributing to the expansion of the TTV whole genomes dataset and to study intra-host variants, we employed a methodology that combined a rolling-circle amplification approach followed by EcoRI digestion, generating a DNA fragment of ~4Kb consistent with TTV genome length which was sequenced by Illumina next generation sequencing. A genogroup 3 full-length consensus TTV genome was obtained and co-infection with other species (at least those with a single EcoRI cleavage site) was not identified. Additionally, bioinformatics analysis allowed to identify the spectrum of TTV intra-host variants which provides evidence of a complex evolution dynamics of these DNA circular viruses, similarly to what occurs with RNA viruses.

Torque Teno Virus (TTV) was first discovered in 1997 in a Japanese patient with acute post-transfusion hepatitis of unknown etiology (Nishizawa et al., 1997). Currently, TTV is globally spread with very high prevalence in human population and has not been associated to a clinical disease so far, being its role in pathogenesis largely unknown (Bendinelli et al., 2001; Okamoto, 2009). In fact, its widespread detection in the intestine, skin, oral and nasal cavities, pharynx, saliva, urine and blood, and the identification of viremic individuals independently of age group or health status, are hardly compatible with the concept of pathogenicity, unless associations of viral loads or genetic variants with particular conditions are specified (Lolomadze and Rebrikov, 2020). Interestingly, TTV loads have been recently proposed to be employed as an endogenous marker for the human immune status after solid organ transplantation (Rezahosseini et al., 2019; Schmidt et al., 2021). Additionally, TTV species in the follow-up of kidney transplantation have been analyzed by a metagenomic approach showing differences in diversity between recipients and donors (Kulifaj et al., 2020).

TTV is a small (30–50 nm), icosahedral non-enveloped virus with a circular single-stranded DNA (ssDNA) genome of negative polarity and is classified in the *Anelloviridae* family (Nishizawa et al., 1997). This viral family includes 30 genera but only *Alphatorquevirus* (TTV), *Betatorquevirus* (Torque teno Mini virus) and *Gammatorquevirus* (Torque teno

* Corresponding author.
E-mail address: nramos@fcien.edu.uy (N. Ramos).

https://doi.org/10.1016/j.virusres.2022.198974
Received 7 September 2022; Received in revised form 17 October 2022; Accepted 18 October 2022
Available online 19 October 2022

PLOS ONE

RESEARCH ARTICLE

Wastewater surveillance of SARS-CoV-2 genomic populations on a country-wide scale through targeted sequencing

Florencia Cancela[1], Natalia Ramos[1], Davida S. Smyth[2], Claudia Etchebehere[3], Mabel Berois[1], Jesica Rodríguez[4], Caterina Rufo[4], Alicia Alemán[5], Liliana Borzacconi[6], Julieta López[7], Elizabeth González[7], Germán Botto[8], Starla G. Thornhill[2], Santiago Mirazo[1,9]*, Mónica Trujillo[10]*

1 Sección Virología, Instituto de Química Biológica, Facultad de Ciencias, Universidad de la República, Montevideo, Uruguay, **2** Department of Life Sciences, Texas A&M University-San Antonio, San Antonio, Texas, United States of America, **3** Departamento de Bioquímica y Genómica Microbiana, Instituto de Investigaciones Biológicas Clemente Estable, Ministerio de Educación y Cultura, Montevideo, Uruguay, **4** Laboratorio de Alimentos y Nutrición, Polo Tecnológico de Pando, Facultad de Química, Universidad de la República, Montevideo, Uruguay, **5** Departamento de Medicina Preventiva, Facultad de Medicina, Universidad de la República, Montevideo, Uruguay, **6** Instituto de Ingeniería Química, Facultad de Ingeniería, Universidad de la República, Montevideo, Uruguay, **7** Departamento de Ingeniería Ambiental, Facultad de Ingeniería, Universidad de la República, Montevideo, Uruguay, **8** Departamento de Métodos Cuantitativos, Facultad de Medicina, Universidad de la República, Montevideo, Uruguay, **9** Departamento de Bacteriología y Virología, Instituto de Higiene, Facultad de Medicina, Universidad de la República, Montevideo, Uruguay, **10** Department of Biological Sciences and Geology, Queensborough Community College of The City University of New York, Queens, New York, United States of America

* mtrujillo@qcc.cuny.edu (MT); smirazo@higiene.edu.uy (SM)

OPEN ACCESS

Citation: Cancela F, Ramos N, Smyth DS, Etchebehere C, Berois M, Rodríguez J, et al. (2023) Wastewater surveillance of SARS-CoV-2 genomic populations on a country-wide scale through targeted sequencing. PLoS ONE 18(4): e0284483. https://doi.org/10.1371/journal.pone.0284483

Editor: Nagarajan Raju, Emory University, UNITED STATES

Received: November 19, 2022

Accepted: March 31, 2023

Published: April 21, 2023

Peer Review History: PLOS recognizes the benefits of transparency in the peer review process; therefore, we enable the publication of all of the content of peer review and author responses alongside final, published articles. The editorial history of this article is available here: https://doi.org/10.1371/journal.pone.0284483

Data Availability Statement: The raw sequence data has been deposited in the NCBI-SRA database under the BioSample accession numbers

Abstract

SARS-CoV-2 surveillance of viral populations in wastewater samples is recognized as a useful tool for monitoring epidemic waves and boosting health preparedness. Next generation sequencing of viral RNA isolated from wastewater is a convenient and cost-effective strategy to understand the molecular epidemiology of SARS-CoV-2 and provide insights on the population dynamics of viral variants at the community level. However, in low- and middle-income countries, isolated groups have performed wastewater monitoring and data has not been extensively shared in the scientific community. Here we report the results of monitoring the co-circulation and abundance of variants of concern (VOCs) of SARS-CoV-2 in Uruguay, a small country in Latin America, between November 2020—July 2021 using wastewater surveillance. RNA isolated from wastewater was characterized by targeted sequencing of the Receptor Binding Domain region within the spike gene. Two computational approaches were used to track the viral variants. The results of the wastewater analysis showed the transition in the overall predominance of viral variants in wastewater from No-VOCs to successive VOCs, in agreement with clinical surveillance from sequencing of nasal swabs. The mutations K417T, E484K and N501Y, that characterize the Gamma VOC, were detected as early as December 2020, several weeks before the first clinical case was reported. Interestingly, a non-synonymous mutation described in the Delta VOC, L452R, was detected at a very low frequency since April 2021 when using a recently described sequence analysis tool (SAM Refiner). Wastewater NGS-based surveillance of

Detection and genome characterisation of SARS-CoV-2 P.6 lineage in dogs and cats living with Uruguayan COVID-19 patients

Yanina Panzera[1]/+, Santiago Mirazo[2,3], Mariana Baz[4], Claudia Techera[1], Sofía Grecco[1], Florencia Cancela[2], Eddie Fuques[1], Emma Condon[1], Lucía Calleros[1], Natalia Camilo[5], Andrea Fregossi[5], Inés Vaz[5], Paula Pessina[6], Nikita Deshpande[4], Ruben Pérez[1], Alejandro Benech[5]

[1]Universidad de la República, Facultad de Ciencias, Instituto de Biología, Departamento de Biología Animal, Sección Genética Evolutiva, Montevideo, Uruguay
[2]Universidad de la República, Facultad de Ciencias, Sección Virología, Montevideo, Uruguay
[3]Universidad de la República, Facultad de Medicina, Instituto de Higiene, Departamento de Bacteriología y Virología, Montevideo, Uruguay
[4]WHO Collaborating Centre for Reference and Research on Influenza, Peter Doherty Institute, Melbourne, Victoria, Australia
[5]Universidad de la República, Facultad de Veterinaria, Unidad de Clínica y Hospital Veterinario, Montevideo, Uruguay
[6]Universidad de la República, Facultad de Veterinaria, Laboratorio Clínico del Hospital Veterinario, Montevideo, Uruguay

BACKGROUND Severe acute respiratory syndrome coronavirus 2 (SARS-CoV-2) infections in domestic animals have occurred from the beginning of the pandemic to the present time. Therefore, from the perspective of One Health, investigating this topic is of global scientific and public interest.

OBJECTIVES The present study aimed to determine the presence of SARS-CoV-2 in domestic animals whose owners had coronavirus disease 2019 (COVID-19).

METHODS Nasopharyngeal and faecal samples were collected in Uruguay. Using quantitative polymerase chain reaction (qPCR), we analysed the presence of the SARS-CoV-2 genome. Complete genomes were obtained using ARTIC enrichment and Illumina sequencing. Sera samples were used for virus neutralisation assays.

FINDINGS SARS-CoV-2 was detected in an asymptomatic dog and a cat. Viral genomes were identical and belonged to the P.6 Uruguayan SARS-CoV-2 lineage. Only antiserum from the infected cat contained neutralising antibodies against the ancestral SARS-CoV-2 strain and showed cross-reactivity against the Delta but not against the B.A.1 Omicron variant.

MAIN CONCLUSIONS Domestic animals and the human SARS-CoV-2 P.6 variant comparison evidence a close relationship and gene flow between them. Different SARS-CoV-2 lineages infect dogs and cats, and no specific variants are adapted to domestic animals. This first record of SARS-CoV-2 in domestic animals from Uruguay supports regular surveillance of animals close to human hosts.

Key words: SARS-CoV-2 – domestic animals – next-generation sequencing – serology – One Health

Coronaviruses (subfamily *Orthocoronavirinae*, family *Coronaviridae*, order *Nidovirales*) are a recognised cause of disease in humans and animals. They are classified into four genera based on their genetic and antigenic properties: *Alpha*, *Beta*, *Gamma* and *Deltacoronavirus*. *Alpha* and *Betacoronavirus* infect mammals, while Gamma and *Deltacoronavirus* infect mainly birds.[1]

Betacoronavirus includes the severe acute respiratory syndrome coronavirus 2 (SARS-CoV-2), the causative agent for the coronavirus disease 2019 (COVID-19) in humans.[2] Since March 2020, SARS-CoV-2 (subgenus *Sarbercovirus*) has been the most significant public health crisis, devastatingly affecting the global economy.

SARS-CoV-2, like other coronaviruses, has a relatively large single-stranded positive-sense RNA genome (~ 30 kb) with well-characterised open reading frames (ORFs) coding for proteins engaged in viral replication and transcription (nsp1-16) and the structure of the virion (spike, matrix, small envelope and nucleocapsid). The genome also contains ORFs for accessory proteins (3a, 6, 7a, 7b, 8 and 10) that modulate the infection process in the natural host.[3,4]

The coronavirus genome has fast evolution and high plasticity driven by point mutations, deletions and insertions (indels) and recombination. This feature contributes to the rapid transmission and global spread of SARS-CoV-2 and the emergence of new strains with new biological properties.[5,6]

SARS-CoV-2 has an ancestral zoonotic origin from bats and probably includes a hitherto unknown intermediate host.[7] The initial outbreak in the human population occurred in December 2019 in China, and from then, the virus spread worldwide by interpersonal transmission.[8-10] The possible anthroponotic transmission between humans and animals (production, recreation animals and domestic animals) raises awareness and concerns. It alerts health authorities to take significant measures to identify receptive species and avoid transmission cycles.[11]

doi: 10.1590/0074-02760220177
Financial support: CSIC (grant: Equipment, Genomic Platform, Faculty of Science and "Specialised knowledge to face the emergency posed by COVID-19 and its impacts").
+ Corresponding author: ypanzera@fcien.edu.uy
https://orcid.org/0000-0002-7459-7810
Received 04 August 2022
Accepted 07 November 2022